

PIK Report

No. 77

LARGE-SCALE HYDROLOGICAL MODELLING
IN THE SEMI-ARID NORTH-EAST OF BRAZIL

Andreas Güntner



POTSDAM INSTITUTE
FOR
CLIMATE IMPACT RESEARCH (PIK)

Submitted as Ph. D. thesis to the Faculty of Mathematics and Sciences
at the University of Potsdam in March 2002

Author:

Dr. Andreas Güntner

Potsdam Institute for Climate Impact Research

P.O. Box 60 12 03, D-14412 Potsdam, Germany

Phone: +49-331-288-2693

Fax: +49-331-288-2695

E-mail: Andreas.Guentner@pik-potsdam.de

Herausgeber:

Dr. F.-W. Gerstengarbe

Technische Ausführung:

U. Werner

POTSDAM-INSTITUT
FÜR KLIMAFOLGENFORSCHUNG
Telegrafenberg
Postfach 60 12 03, 14412 Potsdam
GERMANY

Tel.: +49 (331) 288-2500

Fax: +49 (331) 288-2600

E-mail-Adresse: pik@pik-potsdam.de

Abstract

Semi-arid areas are characterized by small water resources. An increasing water demand due to population growth and economic development as well as a possible decreasing water availability in the course of climate change may aggravate water scarcity in future in these areas. The quantitative assessment of the water resources is a prerequisite for the development of sustainable measures of water management. For this task, hydrological models within a dynamic integrated framework are indispensable tools.

The main objective of this study is to develop a hydrological model for the quantification of water availability over a large geographic domain of semi-arid environments. The study area is the Federal State of Ceará in the semi-arid north-east of Brazil. Surface water from reservoirs provides the largest part of water supply. The area has recurrently been affected by droughts which caused serious economic losses and social impacts like migration from the rural regions.

The hydrological model WASA (Model of Water Availability in Semi-Arid Environments) developed in this study is a deterministic, spatially distributed model. Water availability is determined in terms of river discharge, storage volumes in reservoirs and soil moisture. Specific model formulations applicable for hydrological processes under semi-arid conditions are used. Temporal and spatial scaling approaches are applied to link the process scales with the scales of interest for model application. Modelling units are defined by similarity of landscape characteristics with regard to both lateral and vertical hydrological processes.

Model applications of WASA generally result in a good model performance when compared to observed historical time series of river discharge and reservoir storage volumes. An appropriate process representation is shown to be the basis for reliable simulation results. However, the results are characterized by large uncertainties, mainly due to uncertainties of the input data in view of the low data availability. This refers in particular to rainfall data and soil parameters. Results of model simulations for climate scenarios until the year 2050 show that a possible future change in precipitation volumes causes a larger percentage change in runoff volumes by a factor of two to three. In the case of a decreasing precipitation trend, the efficiency of new reservoirs for securing water availability tends to decrease in the study area because of the interaction of the large number of reservoirs in retaining the overall decreasing runoff volumes.

Preface

This study has been developed within the joint Brazilian-German research project WAVES (Water Availability and Vulnerability of Ecosystems and Society in the North-East of Brazil), funded by the German Ministry for Education and Research (Bundesministerium für Bildung und Forschung - BMBF) and by the Brazilian National Council for the Scientific and Technological Development (Conselho Nacional de Desenvolvimento Científico e Tecnológico - CNPq). The results obtained here in the sub-project on large-scale hydrological modelling, carried out at the Potsdam Institute for Climate Impact Research (PIK) in Potsdam, Germany, have been included into the interdisciplinary analysis of social and natural systems in areas of limited water resources of north-eastern Brazil within the WAVES project.

At first, I would like to express my sincere thanks to my main supervisor, Prof. Dr. Axel Bronstert, who supported the work on this thesis in every respect. My thanks to him are not only for many helpful discussions which accompanied and improved this research, but also for providing very agreeable background conditions under which this work could arise, as in raising the financial support, in granting me freedom in the scientific work and in showing confidence in my way of proceeding.

I would also like to thank the colleagues at the Potsdam Institute for Climate Impact Research and at several other institutions in Germany and Brazil, who contributed to the WAVES project and thus supported this work with their experience, with critical questions on its concepts and with data. Beside of the professional value, I am grateful to them for the common time in which they introduced me, or in which we got known together, to the fascinating people, nature and culture of north-eastern Brazil. In particular, my

thanks to Dr. Maarten Krol from PIK, to Maike Hauschild, Dr. Mario Mendiondo and Dr. Petra Döll from the University of Kassel, to Dr. Thomas Gaiser and Dr. Dietrich Halm from the University of Hohenheim, to Andreas Printz from the Technical University of Munich, to Prof. Dr. José Nilson Campos and Dr. Eduardo Sávio Martins from FUNCEME in Fortaleza, to Claudio Pacheco from COGERH in Fortaleza, to Dr. João Suassuna from FUNDAJ in Recife and to Dr. Cíntia Bertacchi Uvo.

My special thanks in the above respect to Prof. José Carlos de Araújo from the Federal University of Ceará in Fortaleza for the close co-operation, for his untiring efforts in organizing data and opening doors to institutions in Ceará, for the excursions with him and others of his team which were very inspiring to get known to the field of water resources in the study area, and, last but not least, for several pleasant evenings he organized where we quickly got ideas of our host country beyond hydrology.

I would also like to thank Dr. Jonas Olsson, who was at Kyushu University in Japan at that time, for facilitating my access to the field of rainfall disaggregation and for the intensive and fruitful common work on this subject.

Many thanks to Dr. Eric Cadier from IRD (ORSTOM) in France, who gave, at the onset of this study, a very valuable introduction into the hydrology of north-eastern Brazil and provided data of the small-scale studies. My thanks also to Dr. Kirk Haselton from Potsdam University to support the work on rainfall estimation from remote sensing data.

Finally, I am deeply grateful to Annette, who helped me to get over sleepless nights and similar side effects of this thesis with a lot of sympathy, patience and encouragement.

Andreas Güntner

Potsdam, March 2002

Contents

List of Figures	XI
List of Tables	XV
Summary	XVII
Zusammenfassung	XIX
Introduction	1
1.1 Background and Motivation	1
1.2 Objectives	2
1.3 Structure of this Study	2
Study Area	3
2.1 Federal State of Ceará, Brazil	3
2.1.1 Location and overview	3
2.1.2 Climate	3
2.1.3 Vegetation	5
2.1.4 Geology and soils	5
2.1.5 Hydrology and water resources	6
2.1.6 Available data	6
2.1.6.1 Spatial physiographic data	6
2.1.6.2 Climate data	6
2.1.6.3 Discharge and reservoir storage time series	8
2.2 Small-scale Basin Tauá	9
Processes and Models of Semi-Arid Hydrology	11
3.1 Precipitation	11
3.1.1 Process overview	11
3.1.2 Rainfall models	13
3.1.3 Cascade-based model for temporal rainfall disaggregation	13
3.2 Evapotranspiration	14
3.2.1 Process overview	14
3.2.2 Interception models	15
3.2.3 Soil evaporation models	16
3.2.4 Evapotranspiration models	16
3.3 Runoff Generation	19
3.3.1 Process overview	19

3.3.1.1	Infiltration and infiltration-excess runoff	19
3.3.1.2	Saturation-excess runoff	20
3.3.1.3	Lateral redistribution	20
3.3.2	Modelling approaches	22
3.3.2.1	Models for infiltration and vertical soil water movement	22
3.3.2.2	Models for lateral flow processes	23
3.4	Watershed Models	24
3.4.1	Scale and variability	24
3.4.2	Watershed models for semi-arid areas	25
3.4.3	Watershed models for the assessment of climate change impacts	27
3.5	Conclusions on a Modelling Concept in this Study	29
3.5.1	General aspects	29
3.5.2	Model type, calibration, validation and uncertainty	29
3.5.3	Process representation	31
3.5.4	Spatial model structure	32
Model Description		33
4.1	Model Structure	33
4.1.1	General features	33
4.1.2	Structure of spatial modelling units	33
4.1.3	Temporal sequence of process modelling	36
4.2	Process Representation	37
4.2.1	Interception model	37
4.2.2	Evapotranspiration model	38
4.2.3	Infiltration model	41
4.2.4	Soil water model	42
4.2.5	Lateral redistribution among spatial units	43
4.2.5.1	Redistribution between soil-vegetation components	44
4.2.5.2	Redistribution between terrain components	44
4.2.6	Deep groundwater	45
4.2.7	Reservoir storage	46
4.2.7.1	Small and medium-sized reservoirs	46
4.2.7.2	Large reservoirs	48
4.2.8	River network routing	48
4.2.9	Water use	49
4.3	Derivation of Modelling Units and Parameters	50
4.3.1	Derivation of soil-vegetation components	50
4.3.2	Soil and terrain parameters	51
4.3.3	Vegetation parameters	52
Model Applications		55
5.1	Rainfall Disaggregation	55
5.2	Small-Catchment-Scale Application	58
5.2.1	Caldeirão basin	58
5.2.2	Tauá basin	61
5.3	Sensitivity Analysis at the Regional Scale	65
5.3.1	Model sensitivity to precipitation input	65
5.3.1.1	Temporal rainfall characteristics	65
5.3.1.2	Spatial rainfall variability	68
5.3.1.3	Mean rainfall volume	69
5.3.2	Sensitivity to model structure	72

5.3.2.1	Spatial structure of modelling units	72
5.3.2.2	Lateral redistribution of runoff	73
5.3.2.3	Temporal scale in evapotranspiration modelling	75
5.3.3	Sensitivity to model parameters	76
5.3.3.1	Soil and terrain parameters	76
5.3.3.2	Vegetation parameters	79
5.4	Results for the Historical Period at the Regional Scale	81
5.4.1	General results on runoff and soil moisture	81
5.4.2	Effect of reservoirs and water use	82
5.4.3	Model validation	83
5.4.3.1	General aspects and criteria	83
5.4.3.2	Results for discharge	84
5.4.3.3	Results for reservoir storage volumes	87
5.5	Scenario Simulations	89
5.5.1	Climate scenarios	89
5.5.2	Results	90
Conclusions and Perspectives		97
6.1	General Discussion and Conclusions	97
6.1.1	Modelling concept	97
6.1.2	Spatial structure and lateral fluxes	97
6.1.3	Temporal resolution, rainfall characteristics and runoff generation	99
6.1.4	Model performance and uncertainty	100
6.2	Perspectives	102
References		105
Appendix		121

Figures

Fig. 2.1	Location of the study area (Federal State of Ceará, Brazil)	3
Fig. 2.2	Scheme of the large-scale circulation patterns over the tropical Atlantic Ocean, causing (a) dry and (b) wet conditions in north-eastern Brazil	3
Fig. 2.3	Spatial distribution of (a) mean annual precipitation and of (b) the coefficient of variation of annual precipitation in Ceará, period 1960-1998	4
Fig. 2.4	Annual rainfall and monthly distribution in the interior of Ceará, example for the watershed of reservoir Várzea do Boi (1400 km ²), period 1960-98	5
Fig. 2.5	Number of stations in Ceará with complete annual time series of daily rainfall data for the years in the period 1960-1998	7
Fig. 2.6	Major river basins of the study area (State of Ceará, Brazil); discharge gauging stations and large reservoirs with time series used for model validation	8
Fig. 2.7	Location of the Tauá basin (194 km ² at station Pirangi) and Caldeirão research basin (0.77 km ²)	9
Fig. 3.1	(a) Rainfall patterns in the study area of Ceará (red line), three examples from Jan/Feb 1994 derived from SSM/I satellite data, grid resolution 10x10 km, (b) Mean variogram of rainfall intensities derived from 17 SSM/I satellite images covering the entire study area in the period Jan/Feb 1994	12
Fig. 3.2	(a) Frequency of rainfall events of certain duration as fraction of all events, (b) Auto-correlation of hourly precipitation time series. 3-year time series for stations in a semi-arid climate (Tauá, north-eastern Brazil) and a humid temperate climate (Tweed, southern Scotland).	12
Fig. 3.3	Exemplary scheme of the cascade process used in the temporal disaggregation model	14
Fig. 3.4	Schematic description of Soil-Vegetation-Atmosphere-Transfer models. (a) One-source model (<i>PENMAN-MONTEITH</i>), (b) One-compartment, two-layer model (<i>SHUTTLEWORTH & WALLACE</i>), (c) Two-compartment model with interaction, (d) Two-compartment model without interaction (mosaic approach)	17
Fig. 3.5	Characteristic toposequence in the Juatama basin, Ceará, north-eastern Brazil, and its effect on runoff generation characteristics	20
Fig. 4.1	Hierarchical multi-scale disaggregation scheme for structuring river basins into modelling units	34
Fig. 4.2	Air-borne radar image of the Itatira region, Ceará, north-eastern Brazil, with delimitation and parametrization of landscape units with similar topography	35
Fig. 4.3	Example for the distribution function of soil water storage capacity in a soil-vegetation component	36
Fig. 4.4	Scheme of surface and aerodynamic resistances in the S&W-model	38
Fig. 4.5	Scheme of the structure terrain components and soil-vegetation components within a landscape unit.	43
Fig. 4.6	Simplified scheme of lateral redistribution of water fluxes among soil-vegetation components within a terrain component	44
Fig. 4.7	Simplified scheme of lateral redistribution of surface water fluxes between terrain components	45

Fig. 4.8	Cascade scheme for runoff retention and routing between small and medium-sized reservoirs in each sub-basin or municipality in <i>WASA</i>	47
Fig. 4.9	Scheme of the linear response function for runoff routing in the river network	49
Fig. 4.10	Scheme for derivation of soil-vegetation components	50
Fig. 4.11	Relationship between leaf biomass ml and leaf area index derived from various vegetation types	53
Fig. 4.12	Scheme of the seasonal distribution of vegetation parameters in <i>WASA</i>	53
Fig. 5.1	Comparison of the distributions of validation variables for observed and disaggregated 1-hour data, example for station Picos in north-eastern Brazil, period 05/95-93/99	57
Fig. 5.2	Caldeirão basin (0.77 km ²), period 10/80-09/88, daily time series of (a) precipitation, (b) measured discharge, and (c)-(f) simulated discharge, for different daily and hourly versions of <i>WASA</i>	60
Fig. 5.3	Distribution of daily runoff volumes, basin Caldeirão, period 10/80-09/88, observation and simulations	61
Fig. 5.4	Tauá basin (194 km ²), period 10/78-09/88, daily time series of (a) precipitation, (b) measured discharge, and (c) simulated discharge with <i>WASA</i>	62
Fig. 5.5	Storage volume relative to storage capacity for the 5 reservoir classes in Pirangi	63
Fig. 5.6	Plant-available soil moisture in the root zone for both terrain components in the Tauá basin	64
Fig. 5.7	Distributions of (a) daily rainfall volumes and (b) event duration of different grid-based daily rainfall times series P1-P4, averaged for the 1460 grid cells of the study area and the period 1960-98	66
Fig. 5.8	Ratio of daily rainfall volumes of station-based time series (P4) to daily volumes of interpolated time series with ordinary kriging (P1). Mean of period 1960-98.	67
Fig. 5.9	Relationship between ratios of mean daily rainfall intensities and mean annual interception evaporation for simulation with rainfall time series P1 (interpolated) and P4 (station-based)	67
Fig. 5.10	Mean annual runoff (mm) of the 118 sub-basin of the study area for simulations P5-P7 with different spatial variability of rainfall, period 1960-98.	68
Fig. 5.11	Monthly coefficients of variation (cv) of soil moisture to a depth of 1 m within sub-basins of the study area with an area of more than 500km ²	69
Fig. 5.12	Effect of variation in rainfall input between simulations P8 and P5 on (a) simulated runoff and (b) simulated plant-available soil moisture to a soil depth of 1 m	70
Fig. 5.13	Difference in mean annual rainfall at the scale of municipalities between the rainfall data sets of simulations P10 and P9, period 1960-98	71
Fig. 5.14	Effect of variation in rainfall input between simulations P10 and P9 on simulated runoff for the 184 municipalities of the study area, period 1960-98.	71
Fig. 5.15	Percentage difference in mean annual runoff (period 1960-98) for (a) 1460 grid cells in Ceará, difference simulations S2-S1, (b) 137 sub-basins in Ceará, difference S2-S1, (c) sub-basins, difference S3-S1.	72
Fig. 5.16	Ratio of contributing basin area and of simulated mean annual discharge between simulation S4 (based on municipalities) and simulation S1 (based on cells and sub-basins).	73
Fig. 5.17	Differences in simulated mean annual runoff between simulations L2 and L1 without and with lateral redistribution, period 1960-98.	74
Fig. 5.18	Difference in actual evapotranspiration, plant-available soil moisture to a profile depth of 1 m during the rainy period, months Feb-May, and runoff between simulations with mean daily evapotranspiration modelling and with separate day-night calculations	75
Fig. 5.19	Sensitivity analysis for soil and terrain parameters in <i>WASA</i>	77
Fig. 5.20	Sensitivity analysis for vegetation parameters in <i>WASA</i>	79
Fig. 5.21	Scaling relationship for surface resistance from the leaf to the canopy scale for two different values of leaf stomatal resistance	80

Fig. 5.22	Results of model application for the state of Ceará, mean annual values for the period 1960-1998	81
Fig. 5.23	Plant available soil moisture to a depth of 1 m for the months February-May	82
Fig. 5.24	Simulation results for Ceará on the effect of reservoirs and water use on water availability; mean annual values for period 1960-98.	83
Fig. 5.25	Model performance of <i>WASA</i> , validated against observed discharge at 23 stations in Ceará.	86
Fig. 5.26	Examples of model validation for mean monthly runoff.	87
Fig. 5.27	Example of model validation for monthly discharge at station Peixe Gordo, Jaguaribe River.	87
Fig. 5.28	Observed versus simulated mean reservoir storage volume at the end of the rainy period (June) for 22 reservoirs in Ceará.	88
Fig. 5.29	Examples of model validation for monthly storage volumes in large reservoirs.	88
Fig. 5.30	Annual precipitation in Ceará for the historical time series (1921-1998) and the scenario period (2001-2050). Scenarios based on results of <i>ECHAM4</i> and <i>HADCM2</i>	90
Fig. 5.31	Climate change scenarios for Ceará, trends in precipitation, runoff and discharge for the period 2001-2050.	91
Fig. 5.32	Reservoir storage volume at the end of the rainy season (June) in Ceará simulated with <i>WASA</i> for the <i>ECHAM4</i> scenario, the <i>ECHAM4-B</i> and the <i>HADCM2</i> scenario	93
Fig. 5.33	Efficiency of new large reservoirs in Ceará for simulations with <i>WASA</i> based on two climate scenarios	94
Fig. 5.34	Reservoir storage volumes at the end of the rainy season (June) (a) and efficiency of additional dams (b) for <i>WASA</i> scenario simulations with additional small reservoirs based on the <i>ECHAM4</i> climate scenario	95
Fig. A.1	Landscape units in Ceará	123
Fig. A.2	Spatial pattern of natural vegetation in Ceará	125
Fig. A.3	Spatial pattern of mean annual precipitation, period 1960-1998, for the State of Ceará, according to different rainfall data sets used in this study.	127

Tables

Table 2.1	Major soil types and their percentage of the total study area of Ceará.	5
Table 2.2	Available spatial data covering the entire study area of Ceará.	6
Table 2.3	Attributes of three rainfall stations with time series of hourly resolution in the semi-arid north-east of Brazil.	7
Table 2.4	Mean annual climate characteristics in the representative basin of Tauá for the period 1978-1988 . . .	9
Table 4.1	Soil and terrain parameters in <i>WASA</i> at different spatial scale levels	51
Table 4.2	Vegetation parameters in <i>WASA</i>	52
Table 4.3	Parameters of the major land cover types of the study area	54
Table 5.1	Probabilities of the cascade generator for the three types of divisions for all position classes of rainfall boxes and volume classes	56
Table 5.2	Autocorrelation for observed and disaggregated 1-hour time series for station Picos in north-eastern Brazil.	56
Table 5.3	Comparison between validation variables for observed and disaggregated 1-hour data, example of station Tauá in north-eastern Brazil.	56
Table 5.4	Rainfall, measured and simulated annual runoff and simulated fraction of <i>HORTON</i> -type infiltration-excess surface runoff on total runoff, Caldeirão basin, period 10/80-09/88	59
Table 5.5	Distribution of reservoirs among reservoir classes in <i>WASA</i> for the Tauá basin.	61
Table 5.6	Rainfall, measured and simulated annual runoff, Tauá basin, period 10/78-09/88 for different simulations	62
Table 5.7	Characteristics of grid-based daily rainfall data used as input for <i>WASA</i> simulations	66
Table 5.8	Simulation results for different rainfall input and scaling factors. Mean annual results averaged over the 1460 grid cells of the study area, period 1960-98	66
Table 5.9	Observed and simulated mean annual discharge and their difference for various river basins in Ceará; simulations with different rainfall input time series	66
Table 5.10	Rainfall, observed and simulated mean annual discharge and their difference for various river basins in Ceará; simulations with different rainfall data sets.	70
Table 5.11	Effect of lateral redistribution on mean annual runoff and plant-available soil moisture (mean February-May) to a profile depth of 1 m (mm) for different simulations with <i>WASA</i> , averaged for all grid cells of the study area, period 1960-98	75
Table 5.12	Model sensitivity to changes in soil hydraulic conductivity on mean annual runoff, averaged for the study area, period 1960-98	78
Table 5.13	Sensitivity analysis for soil and terrain parameters on soil moisture available for plants to a soil depth of 1 m in the period February-May; median values for all sub-basins of the study relative to the reference model version, period 1960-98.	78
Table 5.14	Model sensitivity to changes in minimum stomatal resistance on mean annual	

	evapotranspiration and soil evaporation, averaged for the study area, period 1960-98.	80
Table 5.15	Difference in storage volume for various reservoirs classes between the end of the rainy season (June) and the dry season (December), average for Ceará and the period 1960-1998	82
Table 5.16	Qualitative interpretation of model performance criteria	84
Table 5.17	Validation results of <i>WASA</i> for various gauging stations in Ceará	85
Table 5.18	Validation results of <i>WASA</i> for various large reservoirs in Ceará	88
Table 5.19	Climate scenarios for Ceará and their effects on the water balance (calculated with <i>WASA</i>)	91
Table 5.20	Characteristics of daily precipitation time series of the historical and the scenario period	92
Table 5.21	Trends of water storage in reservoirs in Ceará, simulated with <i>WASA</i> for the period 2001-2050 at the end of the rainy season (June) and the dry season (December)	93
Table 5.22	Results of scenario runs with an increase of small reservoir storage capacity	94
Table A.1	Characteristics of gauging stations with available discharge data in Ceará	121
Table A.2	Parameters of large reservoirs in Ceará (storage capacity $>50 \cdot 10^6 \text{m}^3$) with explicit representation in <i>WASA</i>	122

Semi-arid areas are, due to their climatic setting, characterized by small water resources. An increasing water demand as a consequence of population growth and economic development as well as a decreasing water availability in the course of possible climate change may aggravate water scarcity in future, which often exists already for present-day conditions in these areas. Understanding the mechanisms and feedbacks of complex natural and human systems, together with the quantitative assessment of future changes in volume, timing and quality of water resources are a prerequisite for the development of sustainable measures of water management to enhance the adaptive capacity of these regions. For this task, dynamic integrated models, containing a hydrological model as one component, are indispensable tools.

The main objective of this study is to develop a hydrological model for the quantification of water availability in view of environmental change over a large geographic domain of semi-arid environments.

The study area is the Federal State of Ceará (150 000km²) in the semi-arid north-east of Brazil. Mean annual precipitation in this area is 850mm, falling in a rainy season with duration of about five months. Being mainly characterized by crystalline bedrock and shallow soils, surface water provides the largest part of the water supply. The area has recurrently been affected by droughts which caused serious economic losses and social impacts like migration from the rural regions.

The hydrological model WASA (Model of Water Availability in Semi-Arid Environments) developed in this study is a deterministic, spatially distributed model being composed of conceptual, process-based approaches. Water availability (river discharge, storage volumes in reservoirs, soil moisture) is determined with daily resolution. Sub-basins, grid cells or administrative units (municipalities) can be chosen as spatial target units. The administrative units enable the cou-

pling of WASA in the framework of an integrated model which contains modules that do not work on the basis of natural spatial units.

The target units mentioned above are disaggregated in WASA into smaller modelling units within a new multi-scale, hierarchical approach. The landscape units defined in this scheme capture in particular the effect of structured variability of terrain, soil and vegetation characteristics along toposequences on soil moisture and runoff generation. Lateral hydrological processes at the hillslope scale, as reinfiltration of surface runoff, being of particular importance in semi-arid environments, can thus be represented also within the large-scale model in a simplified form. Depending on the resolution of available data, small-scale variability is not represented explicitly with geographic reference in WASA, but by the distribution of sub-scale units and by statistical transition frequencies for lateral fluxes between these units.

Further model components of WASA which respect specific features of semi-arid hydrology are: (1) A two-layer model for evapotranspiration comprises energy transfer at the soil surface (including soil evaporation), which is of importance in view of the mainly sparse vegetation cover. Additionally, vegetation parameters are differentiated in space and time in dependence on the occurrence of the rainy season. (2) The infiltration module represents in particular infiltration-excess surface runoff as the dominant runoff component. (3) For the aggregate description of the water balance of reservoirs that cannot be represented explicitly in the model, a storage approach respecting different reservoir size classes and their interaction via the river network is applied. (4) A model for the quantification of water withdrawal by water use in different sectors is coupled to WASA. (5) A cascade model for the temporal disaggregation of precipitation time series, adapted to the specific characteristics of tropical convective rainfall, is applied for the generating rainfall time series of higher temporal resolution.

All model parameters of WASA can be derived from physiographic information of the study area. Thus, model calibration is primarily not required.

Model applications of WASA for historical time series generally results in a good model performance when comparing the simulation results of river discharge and reservoir storage volumes with observed data for river basins of various sizes. The mean water balance as well as the high interannual and intra-annual variability is reasonably represented by the model. Limitations of the modelling concept are most markedly seen for sub-basins with a runoff component from deep groundwater bodies of which the dynamics cannot be satisfactorily represented without calibration.

Further results of model applications are:

- (1) Lateral processes of redistribution of runoff and soil moisture at the hillslope scale, in particular re-infiltration of surface runoff, lead to markedly smaller discharge volumes at the basin scale than the simple sum of runoff of the individual sub-areas. Thus, these processes are to be captured also in large-scale models. The different relevance of these processes for different conditions is demonstrated by a larger percentage decrease of discharge volumes in dry as compared to wet years.
- (2) Precipitation characteristics have a major impact on the hydrological response of semi-arid environments. In particular, underestimated rainfall intensities in the rainfall input due to the rough temporal resolution of the model and due to interpolation effects and, consequently, underestimated runoff volumes have to be compensated in the model. A scaling factor in the infiltration module or the use of disaggregated hourly rainfall data show good results in this respect.

The simulation results of WASA are characterized by large uncertainties. These are, on the one hand, due to uncertainties of the model structure to adequately represent the relevant hydrological processes. On the other hand, they are due to uncertainties of input data and parameters particularly in view of the low data availability. Of major importance is:

- (1) The uncertainty of rainfall data with regard to their spatial and temporal pattern has, due to the strong non-linear hydrological response, a large impact on the simulation results.
- (2) The uncertainty of soil parameters is in general of larger importance on model uncertainty than uncertainty of vegetation or topographic parameters.
- (3) The effect of uncertainty of individual model components or parameters is usually different for years with rainfall volumes being above or below the average, because individual hydrological processes are of different relevance in both cases. Thus, the uncertainty of individual model components or parameters is of different importance for the uncertainty of scenario simulations with increasing or decreasing precipitation trends.
- (4) The most important factor of uncertainty for scenarios of water availability in the study area is the uncertainty in the results of global climate models on which the regional climate scenarios are based. Both a marked increase or a decrease in precipitation can be assumed for the given data.

Results of model simulations for climate scenarios until the year 2050 show that a possible future change in precipitation volumes causes a larger percentage change in runoff volumes by a factor of two to three. In the case of a decreasing precipitation trend, the efficiency of new reservoirs for securing water availability tends to decrease in the study area because of the interaction of the large number of reservoirs in retaining the overall decreasing runoff volumes.

Zusammenfassung

Semiaride Gebiete sind auf Grund der klimatischen Bedingungen durch geringe Wasserressourcen gekennzeichnet. Ein zukünftig steigender Wasserbedarf in Folge von Bevölkerungswachstum und ökonomischer Entwicklung sowie eine geringere Wasserverfügbarkeit durch mögliche Klimaänderungen können dort zu einer Verschärfung der vielfach schon heute auftretenden Wasserknappheit führen. Das Verständnis der Mechanismen und Wechselwirkungen des komplexen Systems von Mensch und Umwelt sowie die quantitative Bestimmung zukünftiger Veränderungen in der Menge, der zeitlichen Verteilung und der Qualität von Wasserressourcen sind eine grundlegende Voraussetzung für die Entwicklung von nachhaltigen Maßnahmen des Wassermanagements mit dem Ziel einer höheren Anpassungsfähigkeit dieser Regionen gegenüber künftigen Änderungen. Hierzu sind dynamische integrierte Modelle unerlässlich, die als eine Komponente ein hydrologisches Modell beinhalten.

Vorrangiges Ziel dieser Arbeit ist daher die Erstellung eines hydrologischen Modells zur großräumigen Bestimmung der Wasserverfügbarkeit unter sich ändernden Umweltbedingungen in semiariden Gebieten.

Als Untersuchungsraum dient der im semiariden tropischen Nordosten Brasiliens gelegene Bundesstaat Ceará (150 000 km²). Die mittleren Jahresniederschläge in diesem Gebiet liegen bei 850 mm innerhalb einer etwa fünfmonatigen Regenzeit. Mit vorwiegend kristallinem Grundgebirge und geringmächtigen Böden stellt Oberflächenwasser den größten Teil der Wasserversorgung bereit. Die Region war wiederholt von Dürren betroffen, die zu schweren ökonomischen Schäden und sozialen Folgen wie Migration aus den ländlichen Gebieten geführt haben.

Das hier entwickelte hydrologische Modell WASA (Model of Water Availability in Semi-Arid Environments) ist ein deterministisches, flächendifferenziertes Modell, das aus konzeptionellen, prozess-basierten Ansätzen aufgebaut ist. Die Wasserverfügbarkeit (Ab-

fluss im Gewässernetz, Speicherung in Stauseen, Bodenfeuchte) wird mit täglicher Auflösung bestimmt. Als räumliche Zieleinheiten können Teileinzugsgebiete, Rasterzellen oder administrative Einheiten (Gemeinden) gewählt werden. Letztere ermöglichen die Kopplung des Modells im Rahmen der integrierten Modellierung mit Modulen, die nicht auf der Basis natürlicher Raumeinheiten arbeiten.

Im Rahmen eines neuen skalenübergreifenden, hierarchischen Ansatzes werden in WASA die genannten Zieleinheiten in kleinere räumliche Modellierungseinheiten unterteilt. Die ausgewiesenen Landschaftseinheiten erfassen insbesondere die strukturierte Variabilität von Gelände-, Boden- und Vegetationseigenschaften entlang von Toposequenzen in ihrem Einfluss auf Bodenfeuchte und Abflussbildung. Laterale hydrologische Prozesse auf kleiner Skala, wie die für semiaride Bedingungen bedeutsame Wiederversickerung von Oberflächenabfluss, können somit auch in der erforderlichen großskaligen Modellanwendung vereinfacht wiedergegeben werden. In Abhängigkeit von der Auflösung der verfügbaren Daten wird in WASA die kleinskalige Variabilität nicht räumlich explizit sondern über die Verteilung von Flächenanteilen subskaliger Einheiten und über statistische Übergangshäufigkeiten für laterale Flüsse zwischen den Einheiten berücksichtigt.

Weitere Modellkomponenten von WASA, die spezifische Bedingungen semiarider Gebiete berücksichtigen, sind: (1) Ein Zwei-Schichten-Modell zur Bestimmung der Evapotranspiration berücksichtigt auch den Energieumsatz an der Bodenoberfläche (inklusive Bodenverdunstung), der in Anbetracht der meist lichten Vegetationsbedeckung von Bedeutung ist. Die Vegetationsparameter werden zudem flächen- und zeitdifferenziert in Abhängigkeit vom Auftreten der Regenzeit modifiziert. (2) Das Infiltrationsmodul bildet insbesondere Oberflächenabfluss durch Infiltrationsüberschuss als dominierender Abflusskomponente ab. (3) Zur aggregierten Beschreibung der

Wasserbilanz von im Modell nicht einzeln erfassbaren Stauseen wird ein Speichermodell unter Berücksichtigung verschiedener Größenklassen und ihrer Interaktion über das Gewässernetz eingesetzt. (4) Ein Modell zur Bestimmung der Entnahme durch Wassernutzung in verschiedenen Sektoren ist an WASA gekoppelt. (5) Ein Kaskadenmodell zur zeitlichen Disaggregation von Niederschlagszeitreihen, das in dieser Arbeit speziell für tropische konvektive Niederschlagseigenschaften angepasst wird, wird zur Erzeugung höher aufgelöster Niederschlagsdaten verwendet.

Alle Modellparameter von WASA können von physiographischen Gebietsinformationen abgeleitet werden, sodass eine Modellkalibrierung primär nicht erforderlich ist.

Die Modellanwendung von WASA für historische Zeitreihen ergibt im Allgemeinen eine gute Übereinstimmung der Simulationsergebnisse für Abfluss und Stauseespeichervolumen mit Beobachtungsdaten in unterschiedlich großen Einzugsgebieten. Die mittlere Wasserbilanz sowie die hohe monatliche und jährliche Variabilität wird vom Modell angemessen wiedergegeben. Die Grenzen der Anwendbarkeit des Modellkonzepts zeigen sich am deutlichsten in Teilgebieten mit Abflusskomponenten aus tieferen Grundwasserleitern, deren Dynamik ohne Kalibrierung nicht zufriedenstellend abgebildet werden kann.

Die Modellanwendungen zeigen weiterhin:

- (1) Laterale Prozesse der Umverteilung von Bodenfeuchte und Abfluss auf der Hangskala, vor allem die Wiederversickerung von Oberflächenabfluss, führen auf der Skala von Einzugsgebieten zu deutlich kleineren Abflussvolumen als die einfache Summe der Abflüsse der Teilflächen. Diese Prozesse sollten daher auch in großskaligen Modellen abgebildet werden. Die unterschiedliche Ausprägung dieser Prozesse für unterschiedliche Bedingungen zeigt sich an Hand einer prozentual größeren Verringerung der Abflussvolumen in trockenen im Vergleich zu feuchten Jahren.
- (2) Die Niederschlagseigenschaften haben einen sehr großen Einfluss auf die hydrologische Reaktion in semiariden Gebieten. Insbesondere die durch die grobe zeitliche Auflösung des Modells und durch Interpolationseffekte unterschätzten Niederschlagsintensitäten in den Eingangsdaten und die daraus folgende Unterschätzung von Abflussvolumen müssen im Modell kompensiert werden. Ein Skalierungsfaktor in der Infiltrationsroutine oder die

Verwendung disaggregierter stündlicher Niederschlagsdaten zeigen hier gute Ergebnisse.

Die Simulationsergebnisse mit WASA sind insgesamt durch große Unsicherheiten gekennzeichnet. Diese sind einerseits in Unsicherheiten der Modellstruktur zur adäquaten Beschreibung der relevanten hydrologischen Prozesse begründet, andererseits in Daten- und Parametersunsicherheiten in Anbetracht der geringen Datenverfügbarkeit. Von besonderer Bedeutung ist:

- (1) Die Unsicherheit der Niederschlagsdaten in ihrem räumlichen Muster und ihrer zeitlichen Struktur hat wegen der stark nicht-linearen hydrologischen Reaktion einen großen Einfluss auf die Simulationsergebnisse.
- (2) Die Unsicherheit von Bodenparametern hat im Vergleich zu Vegetationsparametern und topographischen Parametern im Allgemeinen einen größeren Einfluss auf die Modellunsicherheit.
- (3) Der Effekt der Unsicherheit einzelner Modellkomponenten und -parameter ist für Jahre mit unter- oder überdurchschnittlichen Niederschlagsvolumen zumeist unterschiedlich, da einzelne hydrologische Prozesse dann jeweils unterschiedlich relevant sind. Die Unsicherheit einzelner Modellkomponenten- und parameter hat somit eine unterschiedliche Bedeutung für die Unsicherheit von Szenarienrechnungen mit steigenden oder fallenden Niederschlagstrends.
- (4) Der bedeutendste Unsicherheitsfaktor für Szenarien der Wasserverfügbarkeit für die Untersuchungsregion ist die Unsicherheit der den regionalen Klimaszenarien zu Grunde liegenden Ergebnisse globaler Klimamodelle. Eine deutliche Zunahme oder Abnahme der Niederschläge bis 2050 kann gemäß den hier vorliegenden Daten für das Untersuchungsgebiet gleichermaßen angenommen werden.

Modellsimulationen für Klimaszenarien bis zum Jahr 2050 ergeben, dass eine mögliche zukünftige Veränderung der Niederschlagsmengen zu einer prozentual zwei- bis dreifach größeren Veränderung der Abflussvolumen führt. Im Falle eines Trends von abnehmenden Niederschlagsmengen besteht in der Untersuchungsregion die Tendenz, dass auf Grund der gegenseitigen Beeinflussung der großen Zahl von Stauseen beim Rückhalt der tendenziell abnehmenden Abflussvolumen die Effizienz von neugebauten Stauseen zur Sicherung der Wasserverfügbarkeit zunehmend geringer wird.

Introduction

1.1 Background and Motivation

About one-third of the world's population presently lives in countries of water stress (IPCC, 2001). Amongst these are semi-arid environments which are, by their natural setting, areas of small water resources. As limited water availability imposes strong restrictions on natural and human systems, the vulnerability of these areas to climate variability and possible future climate change is potentially high. The degree of vulnerability is, on the one hand, dependent on the impact of climate variability and change on the natural system, e.g., on the volume and timing of river discharge. On the other hand, the vulnerability depends on the adaptive capacity of the human system (economy, society), e.g., on the effectiveness of implementing water resources management structures to cope with the changed conditions. Societies in semi-arid areas of developing regions often are most vulnerable because already for present-day conditions the water demand approaches availability. Population growth and economic development may even increase the demand in future. Although the population's traditions and knowledge of the local conditions may help to mitigate the effect of water scarcity at the short term, this is not adequate to manage future changing boundary conditions and to reduce vulnerability per se. Similarly, the lack of an institutional framework for water resources management often enhances the vulnerability of these societies, as unmanaged systems are likely to be most vulnerable to climate change (IPCC, 2001).

According to the latest summary on possible future climate change for various global scenario assumptions (IPCC, 2001), global warming of 1.4-5.8°C can be expected for the period 1990-2100. While precipitation is expected to increase at the global scale, both increasing and decreasing trends are projected for low latitudes where most developing semi-arid areas are located. Concerning the El Niño-Southern Oscillation (ENSO), El Niño events are expected to increase in frequency and intensity and this is likely to apply also

for extremes which are usually related to El Niño, such as droughts in north-eastern Brazil.

In the above context, the challenge is to develop integrated solutions in the field of water resources which consider global change impact both on water availability and on water demand, including changing economic and social factors and their feedbacks, i.e., being a combination of supply management and demand management (e.g., KUNDZEWICZ ET AL., 2001). Environmental systems and in particular coupled managed systems, such as that of water resources, usually have a non-linear response to changes in climate forcing due to the existence of several thresholds where processes change (ARNELL, 2000). Understanding the mechanisms of such complex systems and assessing their response to possible changes is an essential prerequisite for the development of adaptation strategies. Mathematical models are an indispensable tool for this purpose. Integrated modelling approaches have been developed for climate change studies, linking component models of the climate, water, agricultural and the socioeconomic sector (for examples, see KROL ET AL., 2002). A hydrological module for quantifying water availability, which transforms the climate forcing into, e.g., river discharge or soil moisture, is of major concern within such an approach.

The joint Brazilian-German research project WAVES (Water Availability and Vulnerability of Ecosystems and Society in the North-East of Brazil) (GAISER ET AL., 2002a) studied the dynamic relationships between water availability, agriculture and quality of life in the rural semi-arid north-east of Brazil, taking into account changes in the driving forces of the system, such as climate or population growth. The region has been struck by recurrent drought periods, which caused fatalities, economic losses and migration (e.g., MAGALHAES ET AL., 1988). One objective within WAVES was to develop an integrated model (SIM, see KROL ET AL., 2001) which works at the scale of

Federal States, linking modules of water availability and use, crop yield, agro-economy and demography. The model allows to analyse possible climate change impacts and run scenario simulations in order to support the planning of regional development, particularly

in the field of water resources, in an integrative and sustainable sense as mentioned above. In this context, a hydrological model for the quantification of water availability is essentially required as one component of the integrated model and as a stand-alone version.

1.2 Objectives

The objective of this study is to develop a hydrological model for the quantification of water availability over a large geographic domain of a semi-arid environment. This general objective is specified according to the requirements within the framework of the WAVES project and the scientific interests in the field of hydrology as follows:

- (1) Water availability is to be assessed in terms of river discharge, reservoir storage and soil moisture. Quantification of groundwater resources, being of small importance in the study area, is not within the scope of this study.
- (2) Spatially distributed results on water availability are to be provided by the model for the Federal State of Ceará in Brazil with a total area of 150000 km². The spatial distribution primarily refers to sub-basins and administrative units (municipalities). Within these units, further distributed data on soil moisture are to be given for areas with differing soil characteristics. (To confine the size of this thesis, only the State with a better data availability (Ceará) is considered here, although WAVES covered two States (Ceará and Piauí)).
- (3) The modelling concept should be applicable to the semi-arid environment of the study area in view of its specific hydro-climatological and physiographic conditions. The relevance of these features for the assessment of water availability is to be assessed.
- (4) The model should be able to capture the influence of a changing environment on water availability. This primarily refers to the effects of a changing regional climate in the course of global climate change. Other changes include those of land cover and water infrastructure.
- (5) Beside of being a stand-alone hydrological model, one model version has to serve as a module of the integrated model SIM (see Chapter 1.1). Thus, adequate interfaces to adjacent modules are to be provided in terms of input/output variables and their spatial and temporal scale. In this respect, one important component is to quantify soil moisture as input of a crop production model.
- (6) Uncertainties in the results of model application are to be identified and assessed in the interpretation of the results.

1.3 Structure of this Study

As a basis for working on the above objectives, the study area is characterized with respect to its main features relevant for hydrology and water resources in Chapter 2, including a summary of available data. Defining the state of the art of knowledge in the hydrology of semi-arid environments is another prerequisite for this study, given in Chapter 3. The literature review describes the most important hydrological processes, while specifying what is known about them in the study area. Additionally, the scientific basis is set in Chapter 3 on how this knowledge is transferred into hydrological models, both for individual processes as well as for more complex watershed modelling.

Taking into consideration the objectives of this study (Chapter 1), the characteristics of the study area (Chapter 2) and the scientific basis (Chapter 3), the re-

search needs and the modelling concept for this study are defined in Chapter 3.5. The term modelling concept refers not only to the requirements on a hydrological model itself, but comprises adequate ways of model parameterization, validation and the assessment of reliability of model results.

The features of the hydrological model WASA, of which the development is the main topic of this study, are described in Chapter 4. In Chapter 5, results of model applications are presented and analysed. This includes sensitivity analysis, model validation and scenario calculations at different spatial scales. Chapter 6 brings together the results into a final discussion on the potentials and limitations of the modelling concept and concludes with further research needs.

Study Area

2.1 Federal State of Ceará, Brazil

2.1.1 Location and overview

The study area of the Federal State of Ceará is located in the north-east of Brazil between 2° to 8° South and 37° to 42° West (Fig. 2.1). In the north, Ceará borders on the Atlantic Ocean. The study area is 146350 km² in size. Elevation reaches 700-950 m in the mountainous areas at the western and southern border and in some coastal mountain ridges. The population of Ceará is 7.4 Mio of which about 2.7 Mio live in the metropolitan area of Fortaleza, the capital of the State (CEARÁ, 2002).



Fig. 2.1 Location of the study area (Federal State of Ceará, Brazil).

According to ARAÚJO (1990), more than 90% of the area of Ceará are located in the so-called ‘drought polygon’. This is a zone of in total about 1·10⁶ km² which spreads out on several States of north-eastern Brazil, being characterized by a semi-arid climate of high variability (see Chapter 2.1.2 for more details) and by recurrent drought periods due to one or more consecutive years of low and/or poorly distributed precipita-

tion. The population has directly been affected by these droughts by lack of drinking water, food and work. Economic losses have been considerable, particularly in the agricultural sector. Migration to the coastal centres and to the Amazonian region has been a common response of the rural population (see, e.g., MAGALHAES ET AL., 1988).

2.1.2 Climate

The large-scale circulation pattern which controls the

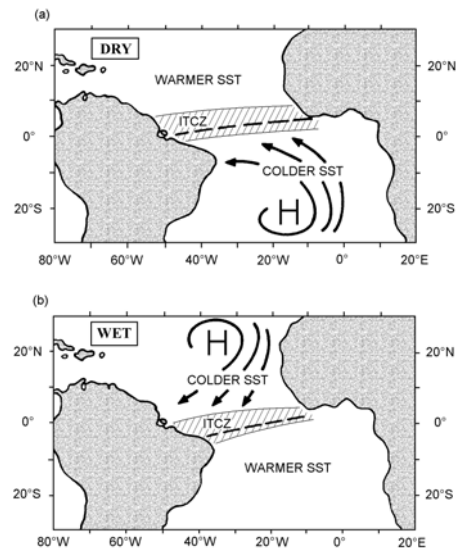


Fig. 2.2 Scheme of the large-scale circulation patterns over the tropical Atlantic Ocean, causing (a) dry and (b) wet conditions in north-eastern Brazil (from WERNER & GERSTENGARBE, 2002).

annual and seasonal cycle of climate in north-eastern Brazil is illustrated in Fig. 2.2. The two seasons of this area, i.e., a rainy and a dry period, are determined by the position of the Intertropical Convergence Zone

(ITCZ) which moves south- and northward during the year, reaching its southernmost position about in March. Rainfall in Ceará mainly occurs if the ITCZ is located in the study area. Its position is determined by atmospheric high pressure areas over the Atlantic Ocean, which, in turn, depend on the sea surface temperature (SST). If the ITCZ does not shift south enough to reach the continent due to anomalies in the oceanic patterns, this may considerably decrease the rainfall amounts in the rainy period of Ceará and possibly cause a drought event as mentioned in Chapter 2.1.1 (e.g., HASTENRATH & GREISCHAR, 1993; WERNER & GERSTENGARBE, 2002). This situation, i.e., droughts in north-eastern Brazil, are often related to the low

phase of the Southern Oscillation (ENSO), i.e., El Niño events (summarized in IPCC, 2001).

In the study area of north-eastern Brazil the principal mechanisms which generate rainfall are: (1) The ITCZ (the dominant mechanism, see above), (2) cold fronts and their remnants from high latitudes of the southern hemisphere, (3) tropical meso-scale mechanisms, like upper tropospheric cyclonic vortices, land-sea circulations and topography-driven meso-scale circulations and (4) local convection due to surface heating (RAMOS, 1975; KOUSKY, 1979; KOUSKY, 1980; KOUSKY & GAN, 1981; NOBRE & MOLION, 1988). All mechanisms produce favourable conditions for ascending motion of moist air and the generation of con-

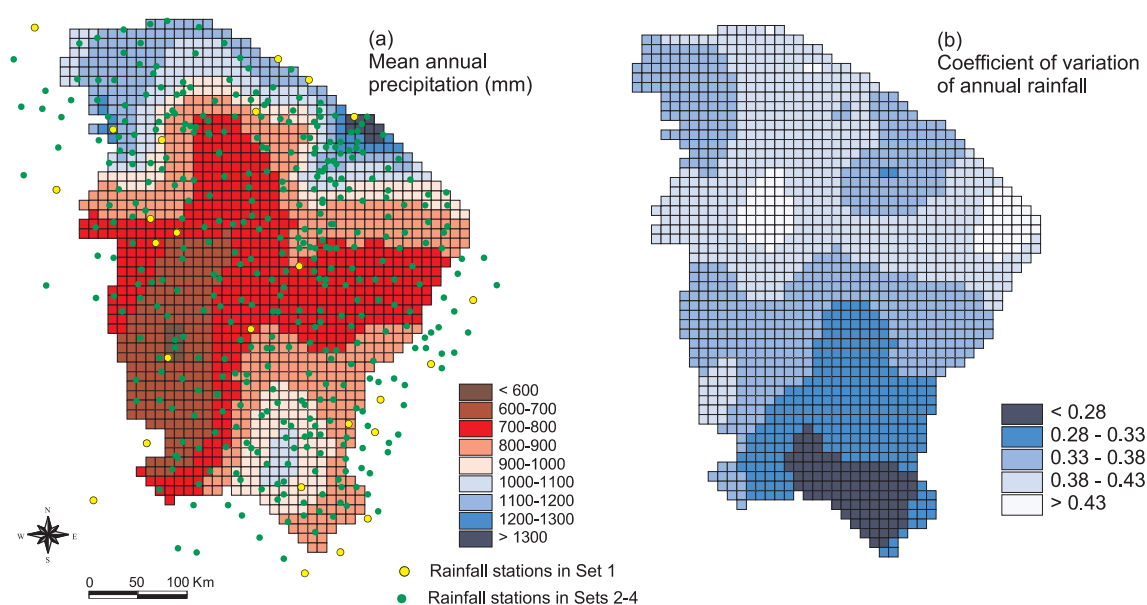


Fig. 2.3 Spatial distribution of (a) mean annual precipitation and of (b) the coefficient of variation of annual precipitation in Ceará, period 1960-1998, data Set 2 (see Chapter 2.1.6.2).

vective precipitation (NOBRE & MOLION, 1988).

The rainfall regime is characterized by a rainy season with duration of about 5 months between January and June and a maximum in March or April (Fig. 2.4). Mean annual rainfall in Ceará varies between 550 mm in the interior to more than 1500 mm in mountainous areas in the north-west and in the coastal zone (see the spatial pattern for the data available in this study in Fig. 2.3, and also, e.g., UVO & BERNDTSSON, 1996; GERSTENGARBE & WERNER, 2002). The seasonal and interannual variability is very high. The coefficient of variation of annual precipitation is 0.35 in the example of Fig. 2.4, 0.36 in average for the study area and may reach more than 0.40 in some parts (Fig. 2.3), as reported also by KOUSKY (1979) for north-eastern Bra-

zil. This is in the range of Mediterranean drylands, where a typical value is 0.35 (THORNES, 1996).

The temporal and spatial variability of other climate elements in the study area is comparatively low. For an annual mean temperature of about 25°C, the seasonal variation is in the range of 3°C, with its maximum around December and its minimum in June. Relative humidity of the air is about 60% in average and direct insolation reaches 2800 hours yearly (ARAÚJO, 1990; WERNER & GERSTENGARBE, 2002, see also Table 2.4).

According to the classification of UNESCO (1979), the degree of aridity of climate regimes is based on the ratio of mean annual precipitation to mean annual potential evaporation estimated by the PENMAN ap-

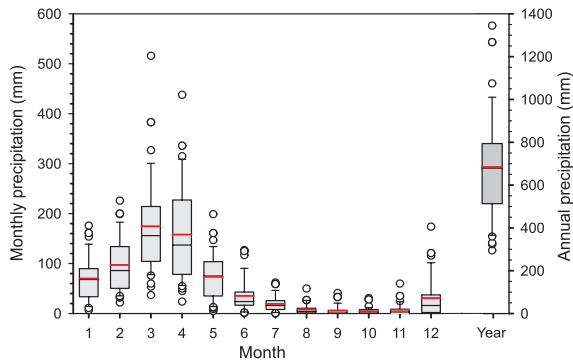


Fig. 2.4 Annual rainfall and monthly distribution in the interior of Ceará, example for the watershed of reservoir Várzea do Boi (1400 km²), period 1960-98 (Data Set 2, Chapter 2.1.6.2). Boxes are limited by the 25th and 75th percentiles, black line within box = median, red line = mean, whiskers mark 10th and 90th percentiles.

proach. Areas for which this ratio drops below 0.2 are classified as arid, areas up to a value of 0.5 are semi-arid. With mean annual precipitation of about 860mm and potential evaporation of about 2100mm (estimated from the available climate data, Chapter 2.1.6.2), Ceará is within the semi-arid range.

2.1.3 Vegetation

The natural vegetation in large parts of the study area is called *caatinga*. It is a woodland with a mixture of trees and shrubs with mainly small and few leaves which are deciduous in the dry season, and an annual herbaceous understorey. Thorn-bearing species and xerophytes are frequent in the drier parts of the area. The morphology of the *caatinga* vegetation is, unlike to some other semi-arid areas, e.g., as shown for the Rambla Honda site in Spain (DOMINGO ET AL., 1998) or for tiger-bush in the Sahel region (LLOYD ET AL., 1992), usually not characterised by a sharply contrasting pattern of individual shrubs or perennial grasses with open areas of bare soil, except of some heavily degraded areas. Instead, the *caatinga* vegetation builds a comparatively continuous vegetation layer of more or less density. Canopy density, height and the proportion of non-deciduous species generally increases with the amount of mean annual rainfall. The most elevated, humid parts of the study area (less than 1% of total area) are covered by evergreen forests or their remnants. The main agricultural use is by extensive cattle farming and cultivation of crops for subsistence use (mainly beans and maize). Other plantations, which partly include crops for export, have a less im-

portant spatial extension relative to the total study area (e.g., cashew, rice, banana, cotton, vegetables) (see e.g., ANDRADE-LIMA (1981), MDME (1981a,b), MAGALHAES ET AL. (1988) and SAMPAIO (1995) for an overview on land cover characteristics.)

2.1.4 Geology and soils

The main geological unit in about 80% of the study area of Ceará is the Precambrian and Proterozoic crystalline basement. Elevated parts at the western (Serra do Ibipapa), southern (Chapada do Araripe) and eastern (Chapada do Apodí) fringe of the study area are built of younger (mainly Mesozoic) sedimentary layers. In the coastal zone, the basement is covered by tertiary sediments, and in valleys of the crystalline alluvial deposits of the Holocene occur (see DNPM, 1983).

Table 2.1 Major soil types and their percentage of the total study area of Ceará.

Soil type	Fraction of area (%)
Litólicos	24.2
Podzólicos	24.1
Bruno Não Calcico	12.5
Planosolos	10.0
Latosolos	6.8
Solonetz	6.4
Areias quartzosas	5.9
Alluvial soils	2.9
Rock outcrops	1.7
Vertisolos	1.0
Others	4.5

Soils (JACOMINE ET AL., 1973) on the crystalline basement tend to be shallow and clayey and often contain a significant amount of rock fragments. They can roughly be classified as shallow, poorly developed or eroded Regosols or Leptosols ('Litólicos' according to the Brazilian classification), stronger developed non-calcareous eutrophic cambisols ('Bruno Não Calcico') or, mainly in areas with more rainfall, deeper luvisols with indication of displacement of clay particles ('Podzólicos'). On eutrophic bedrock heavy clay soils with shrinking characteristics may develop ('Vertisolos'). Larger rock outcrops are frequent. In lower topographic positions, alluvial soils and soils with hydromorphic characteristics, including a sandy top soil and a very dense, clayey subsoil ('Planosolos') and, in some parts, salinization characteristics ('Planosolos solódicos' or 'Solonetz') occur. Soils on the sed-

imentary rocks tend to be deep and more sandy, being mainly classified as Ferralsols ('Latosolos') or Arenosol (quartz sand soils) ('Areias quartzosas'). The distribution of these main soil types in the total study area is summarized in Table 2.1 based on JACOMINE ET AL. (1973) and GAISER ET AL. (2002b) and corresponds to the distribution among the modelling units later used in the hydrological model (Chapter 4.3.1 and Chapter 4.3.2).

2.1.5 Hydrology and water resources

For natural conditions, rivers in the study area flow periodically during the rainy season only. Runoff ceases often shortly after the end of a rain period, in smaller headwater catchments even within minutes or hours after a rainfall event (see also Chapter 2.2). In the crystalline area with shallow soils on a basement of very low permeability, runoff ratios (i.e., the ratio between runoff and precipitation) are in general higher than in the sedimentary area with permeable soils (e.g., CADIER, 1996), but this pattern is modified by the annual precipitation amount. In the dry crystalline interior of the study area runoff ratios are about 10%, reaching values of more than 20% in the more humid areas in the north-west and close to the coast (see also Fig. 5.22). Beside of the clear distinction in a rainy and a dry season, the intermittency of river runoff is also due to the lack of important groundwater reservoirs which could provide baseflow, i.e., groundwater runoff lasting into the dry period after the end of rains. The only exception are the sedimentary areas in the South and West of the study area (Serra do Ibibapa, Chapada do Araripe) where groundwater is closer to the land surface or perennial springs from deep groundwater bodies emerge at steep slopes at the edges of sedimentary plateaus.

The interannual variability of streamflow is high, exceeding that of rainfall. The coefficient of variation of annual discharge is, similar to other semi-arid areas, above 1.0 for many catchments (see also Chapter 5.4.1).

The natural regimes of river discharge in the study area is considerably altered by human impact due to the construction of dams for water storage to supply water during the dry season. 91% of the total water demand in Ceará is supplied by surface water from the reservoirs (ARAÚJO ET AL., 2002). (The other 9% are taken from groundwater resources.) There exists a wide range of dam types, from small farm dams with a storage capacity of less than $0.1 \cdot 10^6 \text{ m}^3$ to large reservoirs, some of them with a storage capacity of more than $1 \cdot 10^9 \text{ m}^3$. More than 7000 dams exist in the state

of Ceará according to the available data (Chapter 4.2.7), with a total storage capacity of about $15 \cdot 10^9 \text{ m}^3$, of which nearly 40% is attributed to smaller reservoirs with storage capacity less than $50 \cdot 10^6 \text{ m}^3$ each. In some regions, the water surfaces of reservoirs amount to 5% of total basin area in the rainy season (CADIER, 1996). In dependence on their size, the reservoirs provide interannual or intra-annual storage, with the latter type drying out during the dry season. Smaller dams usually provide water for human and animal use and for small-scale irrigation in the surroundings and immediately downstream of the dam. Water from larger dams is additionally used for larger irrigation perimeters and for industrial use, as well as for long-distance supply of areas of high water demand. River flow in the downstream sections of these reservoirs is perennialized. For water supply of the metropolitan area of Fortaleza, a system of channels and reservoirs has been constructed which transfers water from the lower Jaguaribe river to that area.

2.1.6 Available data

2.1.6.1 Spatial physiographic data

Table 2.2 gives an overview on available maps with the main physiographic features of the study area. These spatial data were digitized (except for the DEM) and used for delineation and parameterization of modelling units (see Chapter 4.1.2, Chapter 4.3).

Table 2.2 Available spatial data covering the entire study area of Ceará.

Theme	Scale	Source
Topography Digital Elevation Model (DEM)	Grid spacing: 30 arcsec. (~900meter)	USGS (1999)
Vegetation	1:1 Mio	MDME (1981A,B)
Soil associations, landscape units	1:1 Mio	JACOMINE ET AL. (1973)
Geomorphology, topography	1:1 Mio	MDME (1981A,B)

2.1.6.2 Climate data

Overview

For the climate elements precipitation, air temperature, relative humidity, wind velocity and short-wave radiation, station data were collected from different sources in the framework of the WAVES project. On this basis, time series with daily resolution for the period 1921-98 were provided by GERSTENGARBE &

WERNER (2002), interpolated to the scale of municipalities, i.e., to the centre point of each municipality. The interpolation method used for all climate elements is described in SHEPARD (1968) and is similar to the CRESMAN-scheme of SCHRODIN (1995). For the determination of the value at the point of interest, the method considers data from surrounding points with weights as a function of their distance and direction to the point of interest. Concerning climate data for the scenario period, see Chapter 5.5.1.

Precipitation

Resulting from the above procedure, the basic data set with daily rainfall time series used here (*Set 1*) is based on about 25 stations in and around the study area (see Fig. 2.3, Fig. A.3). This small number of stations is due to the low data availability in general, and additionally due to the fact that for this data set only those stations were selected by GERSTENGARBE & WERNER (2002) which have a long measurement period of high quality which is required for the construction of the climate scenarios (see Chapter 5.5.1).

In order to have for the historical study period rainfall data which rely on the maximum of available information, the complete set of altogether 403 stations in and around the study area for the time period 1960-1998 was used (Fig. 2.3). The individual time series of these stations, however, do mainly not cover the entire period. Thus, the number of simultaneously available station data throughout the study area is variable. The maximum data coverage occurs in the late 1960s and steadily declines towards the end of the study period (Fig. 2.5). The mean station density is in average one station per 700km².

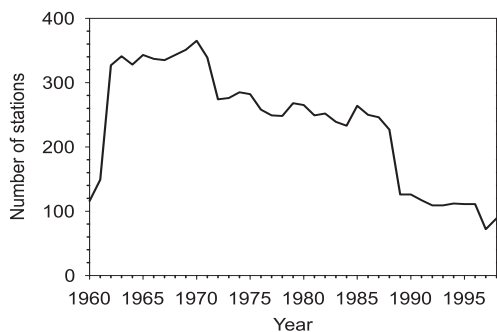


Fig. 2.5 Number of stations in Ceará with complete annual time series of daily rainfall data for the years in the period 1960-1998.

On the basis of this denser station network, additional data sets of daily resolution were generated by interpolation to a grid. Considering the density of available

rainfall stations and the scale of spatial correlation of rainfall on a daily basis in the order of some ten kilometres (Fig. 3.1), a grid resolution of 10x10km² is considered to be an appropriate resolution for interpolation. Different data sets were generated (BÁRDOSSY, 2001, see Fig. A.3 for the spatial patterns):

- *Set 2*: Interpolation by ordinary kriging. The examination of the empirical variograms on a daily basis resulted in a relationship between the parameters of the adjusted theoretical spherical variogram and the skewness of the distribution of the rainfall volumes of the day. With the help of this relationship, day-specific variograms are used for interpolation.
- *Set 3*: Interpolation by ordinary kriging as in Set 2, superimposed by a stochastic component to enhance the spatial and temporal variability of rainfall after the loss of variance by interpolation.
- *Set 4*: Interpolation by external drift kriging, with a linear function of position (x, y) and elevation (from Digital Elevation Model, Table 2.2) as external drift, derived by multiple regression at the daily scale.

Rainfall time series with high temporal resolution

Rainfall time series of hourly resolution for three stations in north-eastern Brazil were available for a approximately three year period (data measured at climate stations installed during the WAVES project by the Potsdam Institute for Climate Impact Research). These stations are located on a 450 km northeast-southwest transect in the interior of the semi-arid area. Mean annual precipitation increases from about 550 mm at station Tauá within the area of this study to 950 mm at station Projeto Piloto, approaching the humid Amazonian region (Table 2.3).

Table 2.3 Attributes of three rainfall stations with time series of hourly resolution in the semi-arid north-east of Brazil. (CV: coefficient of variation of 1-hour rainfall volumes).

Name of station	Projeto Piloto	Picos	Tauá
Region	Southern Piauí	Central Piauí	Ceará
Latitude	8°26'S	7°01'S	6°00'S
Longitude	43°52'W	41°37'W	40°25'W
Altitude (m a.s.l.)	250	220	400
Time period	07/95 -03/99	05/95 -03/99	05/95 -11/99
Mean annual rainfall (mm)	950	650	550
Percentage of 0-values	96.1	96.5	97.2
CV	1.90	1.88	1.71

2.1.6.3 Discharge and reservoir storage time series

Discharge data of several gauging stations in the study area and data on actual storage volumes of some larger reservoirs are available in this study (runoff data provided by the Global Runoff Data Centre (GRDC), Koblenz, Germany, and by various organisations in

Brazil (SUDENE, FUNCEME, COGERH) collected during the WAVES project. Reservoir data were also summarized by ARAÚJO (2000a)). Most time series are of monthly resolution, for some stations daily discharge data are available. The length and time period of available data varies considerably between the stations. Fig. 2.6, Table A.1 and Table A.2 (see Appendix) summarize their location and characteristics.

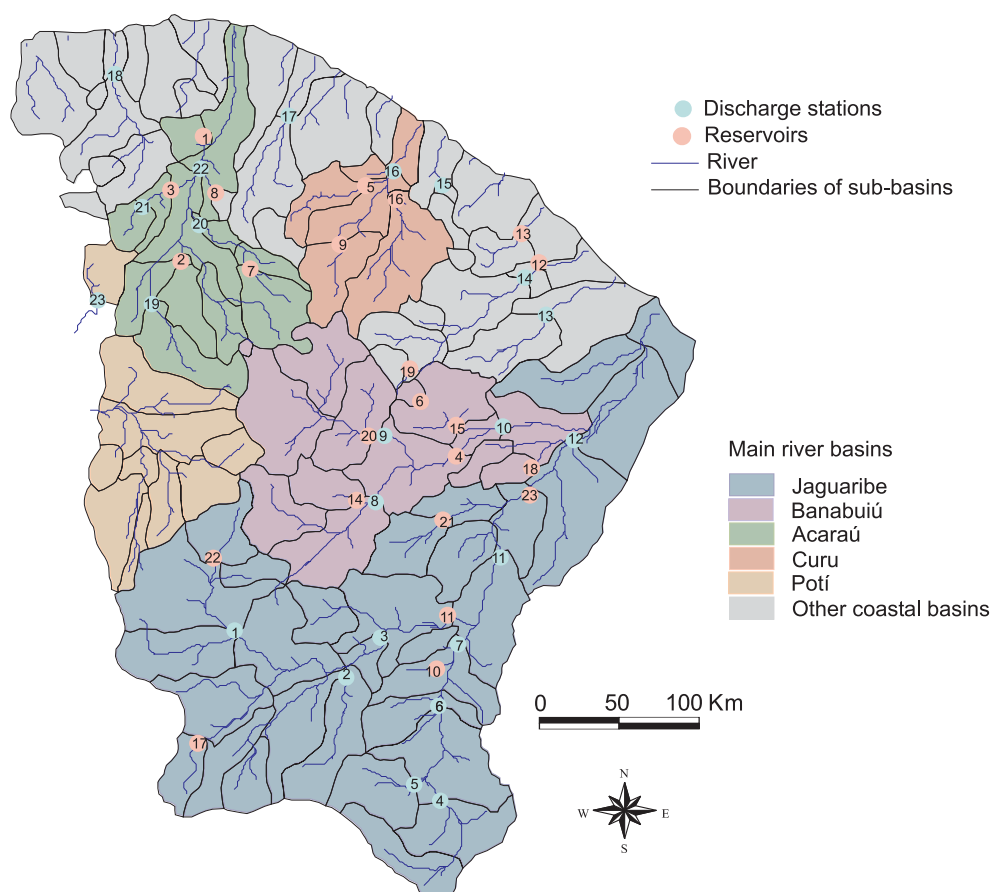


Fig. 2.6 Major river basins of the study area (State of Ceará, Brazil); discharge gauging stations and large reservoirs with time series used for model validation (Station and reservoir numbers correspond to those in Table A1 and A2). River network and sub-basins derived from Digital Terrain Model (Chapter 2.1.6.1), sub-basin boundaries partly corrected on the basis of topographic maps.

The quality of the available discharge data for calibration and validation purposes is limited because the time series often cover only a short time period, which may not include a sufficient range of wet and dry conditions to allow a reliable calibration and evaluation of model performance for highly variable conditions. Additionally, as the available data periods do partly not correspond between stations, a strict simultaneous calibration or validation at several points, e.g., of nested catchments, is restricted. Finally, the quality of available data is limited by the accuracy of discharge meas-

urements. Particularly for arid and semi-arid areas with intermittent runoff conditions, as for most rivers in the study area, and for remote locations measurements errors can be expected to be high. This is due to non-unique rating curves (stage-discharge-relationships), to a rapidly changing geometry of the river bed (particularly in the case of intermittent flow with flash flood characteristics), to undefined rating curves for large floods and, in general, to failures of the measurement devices (see, e.g., PILGRIM ET AL., 1988 and for stations in the study area, CEARÁ, 1992). The qual-

ity of data on storage volumes of reservoirs can be assumed to be higher in general, as they are based on lake level measurements which can accurately be made. The main source of error may be the level-volume relationship which, however, can usually be

2.2 Small-scale Basin Tauá

The Tauá basin corresponds to the watershed of Riacho Cipó in the municipality of Tauá, being located in the uppermost Jaguaribe basin in Ceará (Fig. 2.7). The basin was intensively studied between 1977 and 1988 as a 'Representative Hydrological Basin' within a series of similar studies in the semi-arid of Northeastern Brazil by SUDENE and ORSTOM. The results are summarized in CAVALCANTE ET AL. (1989). The basin is considered to be representative for large parts of the study area on crystalline, quasi-impermeable bedrock, relatively gentle topography, caatinga-type vegetation in different states of degradation and generally high variability of seasonal and interannual rainfall (CAVALCANTE ET AL., 1989). The total basin (194 km² at the river gauging station Pirangi) is subdivided into several, partly nested sub-basins. The smallest sub-basin which is equipped with a runoff gauging station (Caldeirão, 0.77 km²) is a headwater catchment in the sloping part of the Tauá basin, located above the valley bottoms of Riacho Cipó (Fig. 2.7). Elevation in the Tauá basin varies between 625 m in its uppermost parts and 430 m at the outlet. The difference in elevation between the 5% and 95% points of its hypsometric curve is 60 m. The range of elevation in the Caldeirão sub-basin is about 25 m. Table 2.4 summarizes principal climate characteristics as given by CAVALCANTE ET AL. (1989). Minimum and maximum annual rainfall were 216 mm in 1983 and 1169 mm in 1985, respectively. The seasonal distribution is similar to that presented in Fig. 2.4.

The distribution of soil types in the Tauá basin is estimated as follows (CADIER, 1993):

- Bruno Não Calcico (60%)
- Planosolos and Solonetz (15%)
- Vertisol (15%)
- Litólicos (5%)
- Rock outcrops (5%)

Thus, all important soil types relevant on crystalline bedrock for the study area in Ceará, except for the deeper Podzólicos, are present (compare Table 2.1). Available information on the soil characteristics in CAVALCANTE ET AL. (1989) is confined to qualitative descriptions of their hydrological behaviour and some

determined with small errors. An additional source of data uncertainty is the possible loss of storage volume by sedimentation (e.g., ARAÚJO ET AL., 2000b) which is usually not taken into account in the available data.

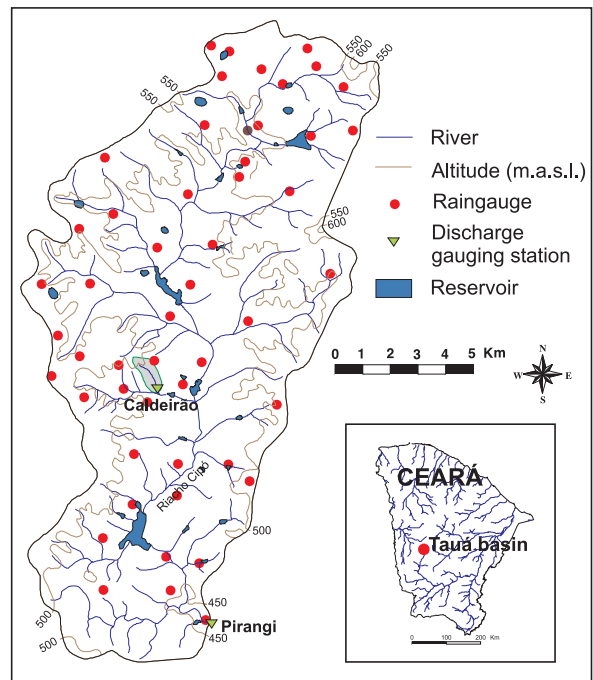


Fig. 2.7 Location of the Tauá basin (194 km² at station Pirangi) and Caldeirão research basin (0.77 km²).

values on infiltration capacities derived from ring infiltrometer experiments. No data on soil texture, soil-water retention characteristic, etc., are given.

Table 2.4 Mean annual climate characteristics in the representative basin of Tauá for the period 1978-1988 (CAVALCANTE ET AL., 1989).

Climate element		
Precipitation	mm	572
Daily mean air temperature	°C	25.8
Daily maximum air temperature	°C	31.1
Daily minimum air temperature	°C	20.5
Relative humidity of air (9:00 h)	%	69
Relative humidity of air (15:00 h)	%	51
Wind velocity	m s ⁻¹	1.9
Direct insolation (daily mean)	hours	7.7
Evaporation (Class-A-Pan)	mm	3102

In CAVALCANTE ET AL. (1989), 22 reservoirs are listed for the Tauá basin. The individual storage capacity varies in the range of $0.02 \cdot 10^6$ - $1 \cdot 10^6$ m³. For half of them, however, no detailed information on storage volume nor on geometry is available. The total storage capacity of the reservoirs in the Tauá basin is estimated to $4.5 \cdot 10^6$ m³, including those reservoirs without quantitative data, for which the storage capacity was roughly estimated based on their location and the maximum water surface area as given in a map of the basin (see Fig. 2.7). The small Caldeirão basin does not include any reservoir, which gives the opportunity to study runoff generation directly without any influence by retention in reservoirs.

Available time series of precipitation and discharge from CAVALCANTE ET AL. (1989) are for an 8-year period (10/1980 - 09/1988) in Caldeirão and for a 10-year period (10/1978 - 09/1988) for the entire Tauá basin. Rainfall data have daily resolution, representing area average values derived by interpolation with the THIESSEN-polygon method from a dense network, including 3-8 rainfall gauges in the case of Caldeirão, and around 50 rainfall gauges in the case of the entire Tauá catchment. Runoff time series are also of daily

resolution. It has to be noted that these data imply considerable uncertainty due to the inherent difficulties of runoff measurements (see Chapter 2.1.6.3). Gaps in the available runoff time series have been filled by modelling with a simple, semi-graphical hydrological model calibrated and successfully validated for each of the above basins (CAVALCANTE ET AL., 1989).

The headwater basin Caldeirão and the larger Tauá basin differ considerably in their runoff behaviour when compared in terms of the summary statistic runoff ratio (i.e., the ratio between runoff and precipitation in percent). For the common measurement period 1980-1988, the runoff ratio is 15.4% in Caldeirão and 7.7% in Tauá (see Chapter 5.2.1 and Chapter 5.2.2 for details). Main reasons for this considerably lower value in the larger Tauá basin, in accordance with the discussion in CAVALCANTE ET AL. (1989), are retention and evaporation in reservoirs (absent in Caldeirão), a smoother topography with a larger fraction of alluvial zones, including more permeable soils with higher storage capacity, and a larger fraction of less degraded vegetation on the total basin area in the case of Tauá.

Processes and Models of Semi-Arid Hydrology

The goal of this chapter is to give, first, a summary of the scientific knowledge about the behaviour of hydrological systems in semi-arid environments and their representation in hydrological models. The most important hydrological processes and their governing factors are described, stressing similarities and differences to processes in humid temperate zones. Modelling approaches are presented for individual processes as well as for entire watersheds, again highlighting specific concepts and parameterizations for applica-

tions in semi-arid areas. An additional focus of the review is related to the objectives of this study, i.e., modelling for large areas and scaling issues, and modelling in the framework of impact assessment.

Finally, based on the above scientific background, conclusions are drawn on the modelling concept in this study. Taking into account the objectives and data availability in this study, the choice of an appropriate model structure, of process formulations and of the general modelling strategy is expounded.

3.1 Precipitation

3.1.1 Process overview

Precipitation is one major driving variable of hydrological systems. Precipitation in semi-arid tropical areas is mainly of convective type (for rainfall generation mechanisms, see Chapter 2.1.2). Convective type rainfall events are, in general, characterized by short duration, high intensities and large spatial heterogeneity. Giving quantitative measures of their characteristics is often prevented by a low density of rain gauges, e.g., in the Africa or South America. Radar or satellite data may, however, provide additional information. Studies at the spatial scale of smaller than one kilometre show very high spatial variability at the event scale (e.g., TAUPIN, 1997; GOODRICH ET AL., 1995) but also at the seasonal scale, e.g., with a difference of rainfall volumes up to 15% between rain gauges within an area of 1 km² in the Sahel region (TAUPIN, 1997). For distances between rain gauges in the order of 5 km in the Walnut Gulch basin (Arizona), RENARD ET AL. (1993) report differences in seasonal rainfall of up to 35%. Nevertheless, the analysis of rainfall fields at larger spatial scales in the Sahel region resulted in a range of spatial correlation in the order of 10-50 km

(TAUPIN ET AL., 1996, cited in TAUPIN, 1997). For the study area of Ceará, UVO & BERNDTSSON (1996) found spatial correlation structures of daily rainfall for interstation distances smaller than about 100 km. These patterns varied among sub-regions of Ceará according to topography and the major processes of rainfall generation. Here, patterns of rainfall intensities were derived for the study area from passive microwave remote sensing data of the SSM/I satellite using a scattering approach (GRODY, 1991; FERRARO ET AL., 1994; FERRARO & MARKS, 1995). The analysis revealed a mean range of spatial correlation of about 60 km, based on a 10x10 km grid of 'snapshot' rainfall intensities at the time of satellite overpass (Fig. 3.1).

Maximum rainfall intensities for a couple of events in the semi-arid climate of south-eastern Spain are up to 135 mm h⁻¹ for 10-min intervals, with a mean of 34 mm h⁻¹ (DOMINGO ET AL., 1998). Typical intensities for convective storms in the Walnut Gulch basin (Arizona) are up to 300 mm h⁻¹ for 1-min intervals (RENARD ET AL., 1993). The median rain rate in the Sahel region is 35 mm h⁻¹ with 35% of the rain falling with an intensity of greater than 50 mm h⁻¹ (LEBEL ET

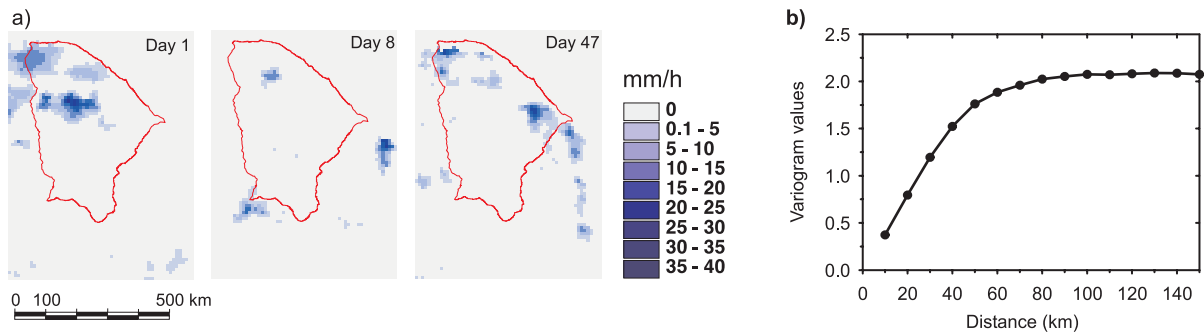


Fig. 3.1 (a) Rainfall patterns in the study area of Ceará (red line), three examples from Jan/Feb 1994 derived from SSM/I satellite data, grid resolution 10x10 km, (b) Mean variogram of rainfall intensities derived from 17 SSM/I satellite images covering the entire study area in the period Jan/Feb 1994.

AL., 1997). Maximum intensities for hourly intervals found for rainfall stations available in this study (Chapter 2.1.6.2) of north-eastern Brazil are about 60 mm h^{-1} .

The short duration and the strong temporal variability of convective type rainfall events is illustrated in Fig. 3.2, compared to an example of temperate climate with predominance of frontal precipitation. The majority of rainfall events in the study area has a duration of one hour or less, five or more consecutive hours with rainfall are very rare. Similarly, the auto-correlation of the hourly time series is generally low, dropping to insignificant values for time lags of more than two hours.

Rainfall in semi-arid tropics is often characterized by a typical diurnal temporal distribution. UVO & BERNDTSSON (1996) suppose that a maximum of morning rainfall due to orographic effects found by RAMOS (1975) for a location slightly south of Ceará may also apply to larger valley systems within the study area. The analysis of available hourly data of the sites in Tauá and Picos (Chapter 2.1.6.2) shows such a morning maximum in terms of frequency and volume of rainfall events.

Several studies showed the significance of spatial variability of rainfall on the hydrological response of catchments and on modelled hydrograph properties (for an overview, e.g., SHAH ET AL., 1996). For a 4.4 ha sub-basin of the semi-arid Walnut Gulch catchment in Arizona, FAURÈS ET AL. (1995) demonstrated that disregarding the spatial variability of rainfall leads to large uncertainties in runoff estimation. CHAUBEY ET AL. (1999) showed that at the event-scale a large uncertainty in calibrated parameters is due to spatial variability of rainfall. For areas where infiltration-excess runoff is significant, MILLY & EAGLESON (1988) concluded that spatially variable rainfall produces more surface runoff than spatially

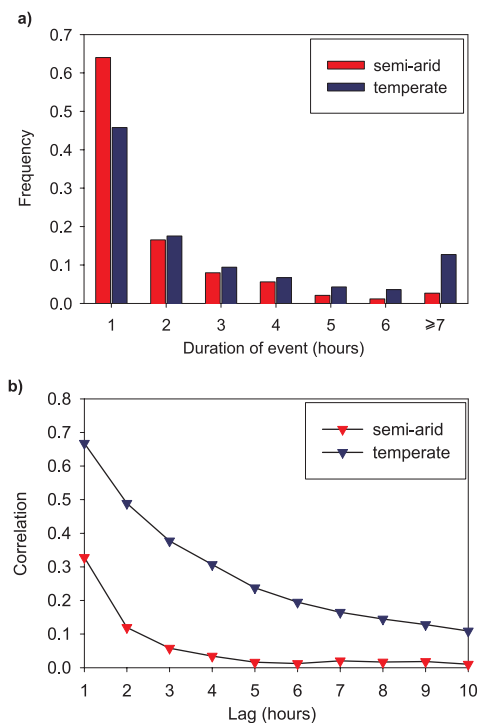


Fig. 3.2 (a) Frequency of rainfall events of certain duration as fraction of all events, (b) Auto-correlation of hourly precipitation time series. 3-year time series for stations in a semi-arid climate (Tauá, north-eastern Brazil) and a humid temperate climate (Tweed, southern Scotland).

uniform rainfall of the same volume. For modelling units being larger than characteristic storm sizes, some description of the spatial variability of rainfall events should be included. In GIESEN ET AL. (2000), spatial and temporal variability of rainfall helps to explain the observation of decreasing runoff coefficients within

increasing slope length. Similarly, PUIGDEFABREGAS ET AL. (1999) stressed the importance of the duration of rainfall bursts and pauses on maximum flow distances of surface runoff. Various modelling studies show that using a high time resolution (at least one hour) is required if an adequate representation of infiltration-excess surface runoff is to be achieved. Otherwise, due to underestimated rainfall intensities, surface runoff is underestimated (e.g., BRONSTERT & KATZENMAIER, 2001). Rainfall variability at a larger temporal (seasons) and spatial scale (regions) induces variability in the phenology of vegetation, which in turn influences, e.g., the leaf area index and thus evapotranspiration (TAYLOR, 2000). For the adequate representation of the pattern of evapotranspiration a description of the variability in time and space of vegetation characteristics as function of rainfall input may be required.

3.1.2 Rainfall models

As input for hydrological models, rainfall data are required which cover the entire area of model application. In many cases, these data sets are derived by interpolation of station data. Common methods include simple geometric (e.g. THIESSEN-polygons), geostatistical (KRIGING) or polynomial approaches (e.g. Spline-interpolation). For an overview on advanced techniques, see DUBOIS (1998). An example for using additional information if only a sparse raingauge network is available is given by GRIMES ET AL. (1999) for the semi-arid by merging raingauge and satellite data. Simulation methods (e.g. Monte-Carlo, Turning-Band) are used to generate rainfall distributions which reflect the spatial variability of rainfall also between observation points (see, e.g., BÁRDOSSY, 1993). Referring to the temporal scale, rainfall data often are not available at the resolution required for the purpose of hydrological model being applied. Various types of stochastic models are used to generate rainfall time series with the resolution of interest. Some were adapted to use them for disaggregation of low resolution time series, from daily to hourly data, for instance. These include methods based on fitting theoretical probability distribution functions to variables such as number of events per day, starting times, event volume and duration (e.g., HERSHENHORN & WOOLHISER, 1987; ECONOPOULY ET AL., 1990; CONNOLLY ET AL., 1999). Another group started out from rectangular pulses stochastic rainfall models (RODRIGUEZ-ITURBE ET AL., 1987, 1988) and devised ways to use these for disaggregation (e.g., BO ET AL., 1994; GLASBEY ET AL., 1995; COWPERTWAIT ET AL., 1996). Using directly observed properties of

precipitation, BÁRDOSSY (1998) presented a method for generation of precipitation time series with simulated annealing. Another type of approach is based on random cascade processes (SCHERTZER & LOVEJOY, 1987), which were proposed to reproduce the empirically observed scaling behaviour of rainfall, i.e., a log-log linear relationship between statistical moments of various orders and a scale parameter. This concept was incorporated into temporal and spatial rainfall disaggregation methods (HUBERT ET AL., 1993; OLSSON ET AL., 1993; TESSIER ET AL., 1993, 1996; DE LIMA & GRASMAN, 1999; MENABDE ET AL., 1997, 1999; DEIDDA ET AL., 1999). OLSSON (1998) developed a comparatively simplistic cascade-based model for disaggregation of continuous rainfall time series (see Chapter 3.1.3 for details). As precipitation is a process both in time and space, both aspects should, at the best, be jointly treated. However, also due to the complexity of the issue, there is a comparatively small number of models for the coupled spatio-temporal simulation of rainfall (see BÁRDOSSY, 1993). A space-time disaggregation model for the semi-arid tropical Sahel region was presented by LEBEL ET AL. (1998).

Studies on the effect of the performance of rainfall models in generating space-time precipitation series on hydrological applications are generally rare. For a large scale application, HABERLANDT & KITE (1998) demonstrated that advanced geostatistical methods for interpolation may improve the results of hydrological simulations.

3.1.3 Cascade-based model for temporal rainfall disaggregation

The cascade-based model for temporal disaggregation of continuous rainfall time series developed by OLSSON (1998) is introduced here with more detail because it is further developed and adapted to the characteristics of rainfall in the semi-arid within this study (Chapter 5.1). In the sense used here, a cascade process repeatedly divides the available space of any dimension (here rainfall time series) into smaller regions, while in each step redistributing the quantity of interest to the smaller regions according to rules specified by the so-called cascade generator. In the approach by OLSSON (1998), it is assumed that a dependency exists between the cascade generator and two properties of the time series values to be disaggregated, namely their rainfall volume and their position in the rainfall sequence. The model employed is a multiplicative random cascade of branching number 2 with exact conservation of mass (Fig. 3.3). The multiplicative weights W_1 and W_2 associated with one

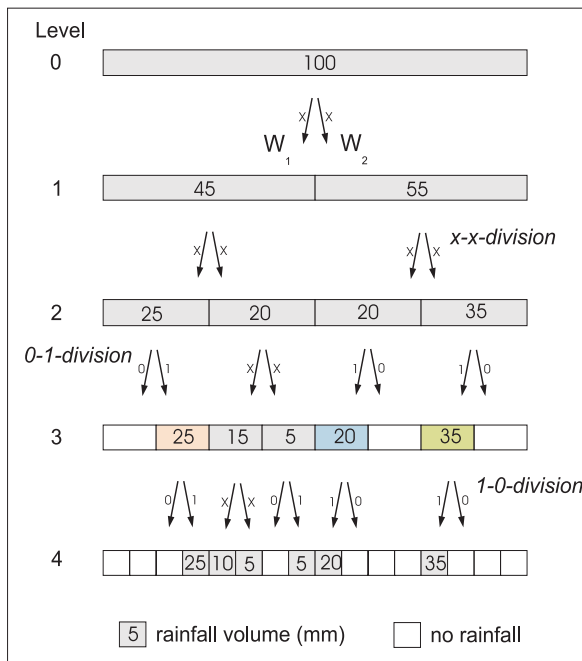


Fig. 3.3 Exemplary scheme of the cascade process used in the temporal disaggregation model, with each level representing a rainfall time series with specific resolution (e.g., at level 0: 24 hours, at level 4: 1.5 hours). Example at level 3: starting box (red), enclosed box (grey), ending box (blue), isolated box (green), (after OLSSON, 1998, modified).

branching are specified by the following cascade generator (Eq. 3.1):

$$W_1, W_2 = \begin{cases} 0 \text{ and } 1 & \text{with prob. } P(0/1) \\ 1 \text{ and } 0 & \text{with prob. } P(1/0) \\ W_{x/x} \text{ and } 1 - W_{x/x} & \text{with prob. } P(x/x) \end{cases} \quad (3.1)$$

where $0 < W_{x/x} < 1$ and $P(0/1) + P(1/0) + P(x/x) = 1$

The probabilities P and the probability distribution of $W_{x/x}$ are assumed to be approximately constant over a range of time scales (or, equivalently, temporal resolu-

tions), i.e., to be scale invariant. In practice, the above formulation means that the model repeatedly divides the series into non-overlapping time intervals (boxes). If the total rainfall volume in a box is V , $V_1 = W_1 \times V$ is assigned to the first half and $V_2 = W_2 \times V$ to the last. The type of the division (0-1, 1-0 or x-x-division) is selected for each box to be divided with respect to the probabilities P by drawing a random number in the range 0 to 1. Each disaggregated box is then similarly branched to a doubled resolution, and so on. To make the cascade generator dependent on the position within the rainfall sequence, a division into position classes is employed, i.e.: (1) box preceded by a dry box ($V=0$) and succeeded by a wet box ($V>0$) (*starting box*), (2) box preceded and succeeded by wet boxes (*enclosed box*), (3) box preceded by a wet box and succeeded by a dry box (*ending box*), and (4) box preceded and succeeded by dry boxes (*isolated box*). Additionally, to accommodate the volume dependence, each position class is divided into two volume classes. For each position and volume class, a specific parameterization of the cascade generator in terms of the probabilities P and the probability distribution of $W_{x/x}$ is used. When applying and testing the model for an observed time series, starting from the resolution of the data, consecutive box volumes are added two by two. The weights W_1 and W_2 can then be directly estimated as the ratio of each volume to their accumulated volume. By repeating this procedure to successively lower resolutions, all weights can be extracted, the probabilities P and the distribution of $W_{x/x}$ at each resolution estimated, their degree of scale-invariance assessed and aggregated to a set of parameters applicable at all scales of the disaggregation procedure.

It has to be emphasized that the above cascade approach does not cover the simulation of regularities in the timing of rainfall events at scales smaller than the one from which the disaggregation started. Thus, diurnal patterns as those found for data of the study area (Chapter 3.1.1) cannot be reproduced.

3.2 Evapotranspiration

3.2.1 Process overview

Evapotranspiration is composed of the following three components: (1) evaporation of water intercepted by the vegetation canopy, (2) evaporation of the soil, and (3) transpiration of the plants through leaf stomata. Main governing factors are the climatic conditions

above and within the canopy (e.g., radiation, water vapour pressure deficit, wind speed), general canopy characteristics (e.g., height, fractional ground cover, leaf area index), physiological characteristics of the plants (e.g., stomata regulation in dependence of soil water availability and temperature), and soil characteristics at the surface and within the soil (e.g., texture at

the soil surface, actual soil moisture). All three components of evapotranspiration are closely related to each other. For instance, thin layers of intercepted water on leaves influence stomata transpiration, or evaporation from the soil surface may change microclimatological conditions and, thus, transpiration within the canopy (see, e.g., MENZEL, 1997).

For semi-arid environments, evapotranspiration is a key component of the hydrological cycle, consuming more than 80% of rainfall at the long term, in arid catchments more than 95% (PILGRIM ET AL., 1988). A characteristic feature of these areas, affecting evapotranspiration, is their generally sparse vegetation cover. Two typical aspects of land cover may be distinguished: (1) Vegetation is uniformly distributed, i.e., characterized by a continuous but sparse canopy, with in contrary to humid areas a small amount of green biomass (leaves), thus a small leaf area index. (2) Vegetation is heterogeneously distributed without a continuous canopy but with distinct vegetated patches, interspersed by patches of bare soil ('clumping' of vegetation). These characteristics influence the evapotranspiration process in a different way than for a closed canopy for dense vegetation in a humid area. For the energy balance, i.e., the splitting up of available energy into latent and sensible heat fluxes, the exchange at the soil surface is of much greater importance. If wet, there is a considerable amount of evaporation directly from the surface (e.g., KABAT ET AL., 1997; WALLACE & HOLWILL, 1997; BRISSON ET AL., 1998; TAYLOR, 2000). For dry conditions, a larger amount of sensible heat flux produced at the soil surface (BLYTH ET AL., 1999) has its feedbacks on plant transpiration, e.g., by enhancing the water vapour deficit within the canopy (BRENNER & INCOLN, 1997; KABAT ET AL., 1997). Additionally, the architecture of a sparse or heterogeneous canopy may influence aerodynamic turbulence and, thus, advection of moist air, in a different way than a dense closed canopy (e.g., LLOYD ET AL., 1992; HUNTINGFORD ET AL., 2000). Many plants in semi-arid environments are deciduous during the dry period (drought-deciduous). The resulting seasonal variation of vegetation characteristics (in albedo and leaf area index, for instance) may have an important effect on the radiation balance of the land surface and evapotranspiration (e.g., ALLEN ET AL., 1994). Availability of soil moisture may, however, be an even more influencing factor on stomata regulation and, thus, actual evapotranspiration (DOMINGO ET AL., 1999; TAYLOR, 2000).

Soil evaporation amounts to about 28% of annual rainfall for an area of patterned woodland in the Sahel, the percentage being even higher in dry years (WAL-

LACE & HOLWILL, 1997). Rock fragments on the soil surface, frequent on semi-arid soils, usually reduce the evaporation rate of the soil (POESEN & BUNTE, 1996). E.g., a stone cover of 30% and 60% of the total soil surface reduced evaporation in a semi-arid environment in the Ebro Valley, Spain, by about 10% and 20%, respectively, as compared to bare soil (AUSTIN ET AL., 1998).

Studies of interception for dryland plant communities are rare compared to humid forest studies (DUNKERLEY & BOOTH, 1999). The fraction of total annual rainfall attributed to interception loss (i.e., evaporation from the wet canopy) for semi-arid vegetation varies in a large range. DUNKERLEY (2000), in an overview of existing studies, cites values between 3% and 30%. Results of studies differ due to differences in canopy coverage of the soil, differences in canopy structure, in rainfall properties, and in the methodology applied, in terms of its scale and measurement techniques. For open savanna with shrubs in semi-arid South Africa, DE VILLIERS (1982) found losses due to interception evaporation to be in the range of 15-20% of gross rainfall at the event scale. Evaporation rate and rainfall rate were the primary influencing variables, whereas different canopy characteristics of the plots under study did not significantly influence interception differences. Interception studies of DOMINGO ET AL. (1998) at the plant scale at Rambla Honda site in the semi-arid Southeast of Spain, gave values of 21-40% interception loss on gross rainfall for grasses and shrubs, depending on rainfall volumes and varying with the type of the canopy. The values of interception evaporation found for the semi-arid are in the range of those of crops and forests in the humid temperate zone (5-50% of annual rainfall according to the summary in BAUMGARTNER & LIEBSCHER, 1990). In the semi-arid case, evaporation rates, but also rainfall intensities, are higher than in the temperate climate, which tends to result, very roughly, in similar net interception evaporation relative to total rainfall.

3.2.2 Interception models

The model representation of interception is based on a storage approach, where the interception storage provided by the plant surfaces is seen to be filled by rainfall and emptied by evaporation and, partly, drainage. One of the most comprehensive interception models is the RUTTER model (RUTTER ET AL., 1971, 1975; RUTTER & MORTON, 1977). It represents various individual processes such as throughfall and drainage from the interception storage of the plants, usually working with high temporal resolution. Evaporation depends

on the actual content of the interception storage relative to its maximum capacity. The large number of five parameters, which are difficult to determine, limits its applicability. DOMINGO ET AL. (1998) estimated these parameters for three plant species in the semi-arid Spain from measurements and obtained good agreement of observed and simulated interception. Although being a simplification of the RUTTER model, the problem of parameter estimation applies also for the GASH interception model (GASH, 1979), which is an analytical model, working usually on a daily time-step. It was successfully applied for savanna vegetation in semi-arid South Africa (DE VILLIERS, 1982). The model has later been reformulated with special reference to modelling of sparse forests (GASH ET AL., 1995). Even more complex models of interception distinguish between different layers within the vegetation stand or include evaporation on the basis of individual water drops (see, e.g., MENZEL, 1997).

The most simple and widely applied approach is a bucket model, where no drainage occurs as long as the interception storage does not meet its maximum capacity, and drainage of all incoming rainfall occurs if the interception capacity is exceeded. Maximum interception evaporation is usually set to equal the potential evaporation for the given climatic conditions. It should be pointed out that due to the dynamic interaction between transpiration and interception storage and evaporation, both processes should in principle be modelled simultaneously. MENZEL (1997) gives a pragmatic equation to combine both processes for the calculation of total evapotranspiration as a function of the actual content in the interception storage. The approach, however, requires a higher than daily temporal resolution.

3.2.3 Soil evaporation models

A common example for simulation of soil evaporation by simple empirical models is the approach of RICH-TIE (1972), which subdivides the evaporation process into a phase of evaporation at potential rate immediately after the wetting of the soil surface, and a second phase where soil evaporation declines as a function of time after the last rainfall event. Some studies which define the only parameter of this model for semi-arid conditions are summarized in WALLACE & HOLWILL (1997). Another group of models uses the concept of resistances (see also Chapter 3.2.4), where actual soil evaporation is a function near-surface soil water content θ , parameterized by a soil surface resistance r_s . Relationships for estimation of this parameter were compared by CAMILLO & GURNEY (1986), MA-

HOUF & NOILHAN (1991), WALLACE (1995) and DAAMEN & SIMMONDS (1997), varying widely due to differing soil conditions and differences in the integration depth to determine soil water content. However, a relationship of the form $r_s = a\theta^b$ was found for most of them, with a considerable increase of r_s only for low soil moisture (<10-15 Vol%). A similar relationship was found by DOMINGO ET AL. (1999) for semi-arid conditions. The advantage of this resistance approach is that it can be included directly into evapotranspiration models which simulate soil evaporation and transpiration in an integrative way, including possible interactions (Chapter 3.2.4).

3.2.4 Evapotranspiration models

Approaches for modelling evapotranspiration in hydrological applications cover a wide range in the detail of process representation, parameterization and data demand (see, e.g., DVWK (1996) for an overview). The most simple models rely on temperature as meteorological driving variable only, other models additionally take into account radiation, humidity, wind speed and/or land cover dependent parameters. Particularly simpler models with empirical components and a small number of influencing factors are usually restricted to the specific climate conditions for which they were developed. The simple equations provide potential evapotranspiration, i.e., a maximum value for the given climatic conditions. This value has to be reduced to actual evapotranspiration depending on plant characteristics, which is mainly done by plant specific factors and as function of soil moisture (e.g., FEDDES ET AL., 1978). For semi-arid areas, OWE & VAN DE GRIEND (1990) adapted the PRIESTLEY-TAYLOR model (PRIESTLEY & TAYLOR, 1972). Performance was strongly dependent on adequate values for its empirical constant, differentiated between vegetation-covered and bare soil areas. For estimation of reference evapotranspiration in the study area of north-eastern Brazil, the PENMAN-MONTEITH approach (see below) outperforms the simpler HARGREAVES equation (HARGREAVES, 1974; HARGREAVES & SAMANI, 1985), which was being frequently used for planning purposes (OLIVEIRA ET AL., 1998).

A comprehensive concept for modelling evapotranspiration is the PENMAN-MONTEITH approach (PENMAN, 1948; MONTEITH, 1965). Although being burdened with high data requirements, the approach is widely applied in hydrological modelling. It respects two major factors influencing the evapotranspiration process: (1) Plant physiological processes regulating transpiration as a function of environmental conditions

and (2) physical effects of canopy characteristics on the movement of air and, thus, advection of moist air. In analogy to OHM's law, a relationship between the environmental potential for evaporation and the actual fluxes is used, where two parameters (stomata/canopy resistance and aerodynamic resistance) represent the above factors. The key assumption of this concept is that all the mass and energy exchange of the canopy occurs only in one layer at the canopy top ('big-leaf' approach, Fig. 3.4a). This is approximately valid only for closed and dense canopies, where energy exchange (and thus evaporation) at the soil surface is negligible. Consequently, the concept may lead to unsatisfactorily results for agricultural applications (e.g., crops in

rows) or generally for most arid and semi-arid regions with sparse vegetation (SHUTTLEWORTH & WALLACE, 1985; STANNARD, 1993; LHOMME, 1997).

Recognizing the above limitation of the PENMAN-MONTEITH approach, a variety of alternative concepts have been developed. Most of them are similar to the original PENMAN-MONTEITH approach, in the sense that they also incorporate the concept of resistances for the parameterization of flux calculations. Generally, they are more complex, with the end of regarding the system under study as a continuum which is, thus, being represented within an integrated model (Soil Vegetation Atmosphere Transfer (SVAT) Schemes).

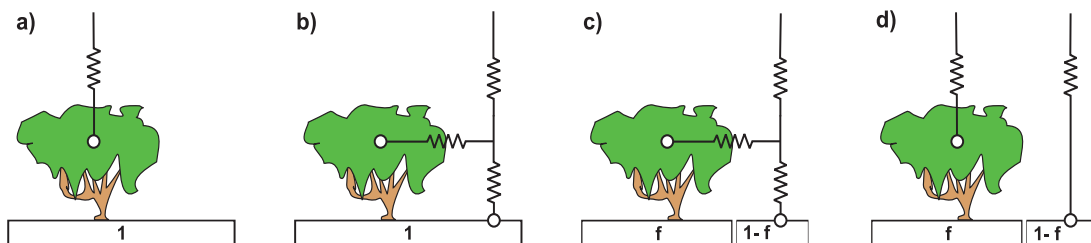


Fig. 3.4 Schematic description of Soil-Vegetation-Atmosphere-Transfer models. (a) One-source model (PENMAN-MONTEITH), (b) One-compartment, two-layer model (SHUTTLEWORTH & WALLACE), (c) Two-compartment model with interaction, (d) Two-compartment model without interaction (mosaic approach). f denotes the fraction of the vegetation-covered surface area on total terrain surface area.

Classifying these SVAT models, a basic distinction can be made with respect to their way of subdividing the landscape surface, i.e., defining sources of heat and water fluxes. The group of one-compartment models keeps the idea of a continuous canopy cover, but they differentiate into two interrelated source layers of energy and momentum exchange, one above the other, i.e., the soil surface and a canopy layer (two-layer models, Fig. 3.4b)(SHUTTLEWORTH & WALLACE, 1985). Another group of models describes the sparseness of vegetation by assuming two adjacent sources, bare soil and vegetation, respectively (two-compartment models, Fig. 3.4c)(DOLMAN, 1993; BLYTH & HARDING, 1995; NORMAN ET AL., 1995; BRENNER & INCOLN, 1997, BLYTH ET AL., 1999). An additional parameter defines the fraction of vegetation cover on total surface area. Different degrees of interaction between the fluxes to and from the two sources are assumed, with the extreme of no interaction in the case of two adjacent one-compartment models ('mosaic' approach, Fig. 3.4d)(see an example in HUNTINGFORD ET AL., 1995). One main consideration in defining this degree of interaction concerns how radiation fluxes should be organized in the model. For instance, to which extent does the vegetation canopy

reduce incoming solar radiation before reaching the soil surface? Another key consideration concerns interaction of aerodynamic fluxes. For instance, two which extent do the plants influence aerodynamic turbulence above bare soil? Accordingly, each model has a different configuration of canopy and aerodynamic resistances.

HUNTINGFORD ET AL. (1995) showed for transpiration modelling from Sahelian savannah that for dry conditions a PENMAN-MONTEITH type single-source model performs similar to a two-layer model, with the two layers representing bushes and a herbaceous understorey, respectively. However, the need to include the soil surface as another source was highlighted, as shown also in BLYTH ET AL. (1999) where a two-layer model performed better for sparse vegetation in the Sahel than a one-layer model.

BRENNER & INCOLN (1997) and BOULET ET AL. (1999) demonstrated that for a sparsely vegetated site with heterogeneous vegetation distribution, a two-compartment approach gave better results compared to the one-compartment approach. The latter underestimated soil surface temperature and sensible heat flux. Contrarily, on a site with sparse but homogeneously distributed vegetation, the one-compartment, two-layer

er approach performed better than the two-compartment approach, both for sensible and latent heat flux as compared to measurements. Similar results were obtained by BLYTH & HARDING (1995). Main reasons are, for instance, a considerable flux of heat from bare soil areas to the vegetated patches for heterogeneous vegetation and its feedback on transpiration, which is not taken into account by a mosaic approach. On the other hand, if the distances between vegetation and bare soil patches are small, turbulence above both sources is similar and the use of two different roughness lengths as in the two-compartment models is not justified. In summary, splitting the surface cover into two separate compartments for modelling of latent and sensible heat fluxes is only appropriate at a certain degree of heterogeneity between vegetation and soil patches. RAUPACH (1992) and BLYTH & HARDING (1995) proposed a vegetation sparseness index to quantify this threshold, i.e., related to the ratio of vegetation height to cluster distances.

The SVAT schemes presented above allow to include the effect of environmental conditions on bulk stomata behaviour of a canopy, and thus on transpiration, via the canopy resistance parameter. The most common concepts are the empirical JARVIS-type models (JARVIS, 1976; STEWART, 1988), which combine a minimum stomatal resistance with a series of stress functions in a multiplicative way. Each function represents one independent influencing factor, i.e., mainly solar radiation and leaf water potential (often expressed by soil water content), but also air temperature and humidity or atmospheric CO₂. The parameters of this functions were derived from measurements (for an overview see LHOMME ET AL., 1998). Recent studies on the behaviour of stomata resistances for vegetation under semi-arid conditions include e.g. VALENTINI ET AL. (1991), AMUNDSON ET AL. (1995), KUSTAS ET AL. (1996), PUIGDEFABREGAS ET AL. (1996), BRENNER & INCOLLN (1997), HANAN & PRINCE (1997), KABAT ET AL. (1997), RANA ET AL. (1997), ROCKSTRÖM ET AL. (1998) and BLYTH ET AL. (1999). Generalisations of the findings are restricted by the variety of specific environmental conditions, species and temporal as well as spatial scales of the studies. A valuable summary of data related to canopy and stomatal conductances for a broad range of global vegetation types is given in KÖRNER (1994) and KELLIHER ET AL. (1995). KÖRNER (1994) concludes that differences of maximum stomatal conductance (the re-

ciprocal value of minimal resistance mentioned above) between the major biomes of the globe is small. The global mean of woody vegetation types is $218 \pm 24 \text{ mmol m}^{-2} \text{ s}^{-1}$ (corresponds to a minimum resistance of $\sim 190 \text{ s m}^{-1}$), for semi-arid shrubs a mean value of $198 \text{ mmol m}^{-2} \text{ s}^{-1}$ ($\sim 207 \text{ s m}^{-1}$) was found. HOLBROOK ET AL. (1995) confirmed that dry forests do not differ from moist forests in terms of stomatal conductance. Thus, canopy conductance is mainly determined by LAI and the seasonal, daily and diurnal variations of stomatal conductance.

Diurnal variations of meteorological parameters are most pronounced between day and night for the radiation balance and for temperature. Concerning plant physiological characteristics, canopy resistance is increased during night-time by stomata closure. Due to the strong non-linearities of the evapotranspiration process, these variations may have an important effect on simulation results if taken into account explicitly as compared to simulations using daily mean parameters. SCHULLA (1997) demonstrated for an application of the PENMAN-MONTEITH approach that this variability can be efficiently represented on the basis of daily meteorological data by sub-dividing into a daytime and a night-time simulation period. Results approach those obtained with an hourly timestep, and are, at an annual basis, about 20% larger than those resulting from a daily model with daily means of climate data and parameters. OWE & VAN DE GRIEND (1990) stressed problems of an overestimated evapotranspiration in semi-arid conditions if soil heat fluxes are disregarded in daily model applications, even if they balance to zero when integrating over 24 hours.

For an extensive comparison of simple empirical and complex physically-based evapotranspiration models at the continental scale, VÖRÖSMARTY ET AL. (1998) concluded that both types may be of use for large-scale applications. However, differences between methods were most pronounced in hot and dry areas. The empirical, temperature-based HAMON model (HAMON, 1963) as well as the complex model by SHUTTLEWORTH & WALLACE (1985) performed best for present climate conditions. However, for studies involving climate or land cover change, the more complex methods are better suited because they should respond better to meteorological and physiological changes (FEDERER ET AL., 1996; VÖRÖSMARTY ET AL., 1998).

3.3 Runoff Generation

3.3.1 Process overview

The term 'runoff generation' is used here in a wide sense, implying all processes that transfer precipitation from the soil surface to the outlet of a catchment and thereby determine the final runoff volume at the outlet. By this definition, both vertical and lateral flow processes are included. Lateral flow processes comprise also transport in the channel network, which, contrary to humid areas, may change runoff volume considerably by transmission losses (see Chapter 3.3.1.3).

3.3.1.1 Infiltration and infiltration-excess runoff

Runoff generation in semi-arid environments is generally dominated by fast surface runoff components during and immediately after a rainfall (e.g., YAIR & LAVEE, 1985; PILGRIM ET AL., 1988; EL-HAMES & RICHARDS, 1994). A major reason is that rainfall is mainly of high intensity (see chapter Chapter 3.1.1) which may exceed the infiltration capacity of the soil. Thus, infiltration-excess runoff (HORTON-type runoff) (HORTON, 1933) is generated. The infiltration capacity of the soil is, in turn, related to a variety of event-dependent (e.g., soil moisture) and independent factors (e.g., soil texture). In semi-arid environments, the infiltration capacity is often low because the soil surface is compacted and covered by a crust. One main reason is the sparse vegetation cover, typical for these environments, which may only partially protect the soil surface from compaction by the kinetic energy of raindrops.

An extensive classification of surface crusts according to their generation processes, morphological and physical properties was made by VALENTIN & BRESSON (1992). Their thickness often is only a few millimetres, with infiltration capacities of generally lower than 20 mm h^{-1} , for some crust types even lower than 2 mm h^{-1} . The type and degree of surface crusting has been found to be a major factor in explaining the variance of infiltration capacities in the semi-arid west of Africa (CASENAVE & VALENTIN, 1992; D'HERBES & VALENTIN, 1997). Other important factors were vegetation cover, which is inversely related to crusting by preventing crust formation under dense canopies, and fauna activity (termites) which increases infiltration capacity by generating macropores. Similar results on the importance of crusts and its relation to vegetation and land use for semi-arid areas were shown, e.g., in

PERROLF & SANDSTRÖM (1995), PEUGEOT ET AL., (1997), ZHU ET AL. (1997), BAJRACHARYA & LAL (1999), PUIGDEFABREGAS ET AL. (1999), ZHU ET AL. (1999). For the semi-arid north-eastern Brazil, CADIER (1996) states that crust formation at the soil surface is of much less importance than in the Sahel region of Africa because the caatinga vegetation has, if not heavily degraded, a continuous canopy cover which protects the soil surface from raindrop impact. However, if the vegetation cover is removed and the upper soil horizon gets compacted, an increase of annual runoff by a factor of more than 10 was observed in small catchments (CADIER, 1996).

As mentioned above (CASENAVE & VALENTIN, 1992), another important factor governing soil surface characteristics and thus infiltration are macropores. Although macropores may constitute only a small portion of soil porosity, they can transport large amounts of water due to their high conductivity (e.g., BEVEN & GERMANN, 1982). Particularly for intense rainfall where the infiltration capacity of the soil matrix is exceeded, flow into macropores may become prevalent (e.g., GERMANN, 1986). Macropores may be formed by plant roots, soil fauna, or shrinkage of fine soils in the state of low soil moisture. Their existence is, thus, often linked to the presence of a vegetation cover and is lost after deforestation or soil erosion (e.g. BURCH ET AL., 1987). Similar differences are also found between bare soil patches and soils beneath plants in clumped vegetation forms which are typical for semi-arid environments. In consequence, together with related differences in the occurrence of crusts, infiltration rates are generally lower bare soil surfaces than for surfaces under vegetation (SCOGGING & THORNES, 1979; PUIGDEFABREGAS ET AL., 1999).

Rock fragments in the soil have a variety of effects on hydrological processes. According to POESEN & BUNTE (1996), a general distinction should be made between rock fragments at the soil surface and rock fragments below the surface. By interception of rainfall, rock fragments at the surface prevent direct infiltration into the soil. On the other hand, infiltration may be enhanced, as rock fragments protect the soil surface from sealing due to raindrop impact. Whether rock fragments at the surface finally increase or decrease infiltration volumes depends on various factors, such as their position, size, total coverage of the surface and characteristics of the surrounding fine earth (e.g., VALENTIN & CASENAVE, 1992). In this context, vegetation interacts due to its importance for the development of crusts. ABRAHAMS & PARSON (1991) re-

port on the different effects of stone cover for infiltration on shrub and inter-shrub areas. The net effect on infiltration may also change with time, e.g., in the course of land use changes (POESEN & BUNTE, 1996). The usually high spatial variation may assemble areas with surface stoniness favourable for the generation of overland flow with nearby areas of enhanced infiltration capacity due to rock fragments, reducing overall runoff generation again. Summarizing the effects of surface stoniness on overall runoff production, POESEN & BUNTE (1996) state that during a rainfall event many contrasting effects take place over short distances leading to important compensating effects. Rock fragments below the soil surface are found to reduce the saturated hydraulic conductivity of soils with textural porosity and, thus, reduce percolation to deeper soil layers (e.g. BRAKENSIEK ET AL., 1986).

3.3.1.2 Saturation-excess runoff

Saturation-excess runoff, generated on saturated soils independent of their infiltration characteristics and of rainfall intensity, is generally considered to be of less importance in semi-arid landscapes than infiltration-excess runoff. The groundwater surface is often at larger depths, disconnected with surface hydrology (PILGRIM ET AL., 1988). However, soil saturation may occur during the rainy period in alluvial zones in the valley bottoms (e.g., CEBALLOS & SCHNABEL, 1998; GIESEN ET AL., 2000), on soils of relatively high infiltration capacities (MARTINEZ-META ET AL., 1998) or on soils of low storage capacity, i.e., shallow soils above a low permeable bedrock. Saturation-excess runoff by this latter mechanism was found to be the most important runoff component to produce channel flow in a semi-arid basin in Spain. Once these saturated conditions have been met, additional rainfall may lead to widespread surface flow whereas infiltration-excess overland flow is limited in space and time due to rapid re-infiltration (PUIGDEFABREGAS ET AL., 1998). Similarly, CADIER (1993) describes the occurrence of shallow soils in north-eastern Brazil which become runoff source areas if saturated.

3.3.1.3 Lateral redistribution

Lateral subsurface flow is commonly not considered to be an important process contributing to runoff in semi-arid landscapes. PUIGDEFABREGAS ET AL. (1998) showed, that for a semi-arid area in Spain with 300 mm of annual precipitation the favourable conditions for lateral subsurface flow are rarely met. Hillslopes show poor hydrologic connectivity over longer

distances and time periods. There are some studies in which, however, lateral subsurface flow was found to be an important mechanism of runoff generation. WILCOX ET AL. (1997) found that lateral subsurface flow occurred on a hillslope in New Mexico especially in years of above-average precipitation in winter, also building a snowpack. In these periods, a perched water table may develop above a shallow restrictive horizon where water moves mainly through a network of macropores. The effect of lateral subsurface flow for generation of saturated areas in valley bottoms has also been reported by GIESEN ET AL. (2000), for an sub-humid area in West Africa with an average rainfall of 1200 mm. In general, it may be concluded that, beside of topographic, geological and soil conditions, the importance of lateral subsurface flow increases with an increasing soil moisture status of the catchment which provides connectivity of subsurface flow over larger distances (see also BECKER ET AL., 1999). Accordingly, the importance of lateral subsurface flow increases from the dry to wet season within a catchment and with mean annual precipitation between catchments.

The complexity of lateral redistribution of water with regard to surface flow and the importance of re-infiltration along a toposequence was shown for the study area in north-eastern Brazil (CADIER ET AL., 1996). Fig. 3.5 shows two strips with low infiltration capacities (rock outcrops and solodic soils), just upslope of soils of high infiltration capacity which absorb runoff generated upslope as long as they are not saturated. Runoff at the base of such hillslopes is thus considerably less than what can be expected by simply summing up the contributions of each soil component.

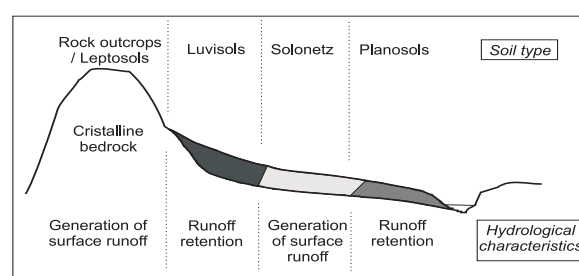


Fig. 3.5 Characteristic toposequence in the Juatama basin, Ceará, north-eastern Brazil, and its effect on runoff generation characteristics (after CADIER ET AL., 1996, modified).

Similarly, for hillslope transects, characteristic sequences of different surface types (vegetation cover and crusts) and thus different infiltration characteris-

tics were shown for semi-arid Southern Africa (PERROLF & SANDSTRÖM, 1995) and for the Sahel region (D'HERBES & VALENTIN, 1997). Observations of decreasing runoff coefficients with increasing slope length were also made, for instance, by WILLIAMS & BONELL (1988) and PUIGDEFABREGAS ET AL. (1998). In the latter study, for a semi-arid area in Spain, runoff coefficients by infiltration-excess at the event scale may be locally very high for patches of the scale of 10 m (40%), but were found to decrease considerably at the hillslope scale of 40-50 m (<5%) because the variability of local soil characteristics favours reinfiltration after short flow distances. The intensity of reinfiltration is, beside of soil moisture and soil infiltration characteristics, governed by the degree of surface roughness induced by texture and plant elements like stems and litter (ABRAHAMS ET AL., 1994).

A characteristic change of surface material properties is often found between the sloping areas and the valley bottom. YAIR & LAVÉE (1985) demonstrated the importance of a colluvium at the foot of slopes to absorb runoff of the high responsive slope areas, thus inhibiting completely channel flow in many occasions. Also PUIGDEFABREGAS ET AL. (1998) stresses the significance of the slope areas and alluvial plains as runoff source and sink areas, respectively. The runoff losses in lower parts of a toposequence are, on the one hand, due to reinfiltration of surface runoff in the form of sheet-flow in soils of higher infiltration capacity if runoff has not yet concentrated into channels. On the other hand, if already converged into rill or channel flow, runoff may travel along a dry channel bed leading to losses into the alluvium (transmission losses). The amount of these losses is primarily dependent on pre-event moisture conditions of the alluvium, i.e., on time spans between runoff events, but also on flow rates, channel geometry, texture and layering of alluvial sediments (LANE, 1983; WALTERS, 1990; HUGHES & SAMI, 1992; RENARD ET AL., 1993, EL-HAMES & RICHARDS, 1994; LANGE, 1999; PARSONS ET AL., 1999). Transmission losses in rills were found to be larger than diffusive losses in inter-rill areas (PARSONS ET AL., 1999).

Decreasing runoff coefficients with the basin area increasing from the field to the small basin scale due to losses into alluvial deposits were also reported by DE BOER (1992) for a temperate semi-arid area in Canada. It was stressed that differences in runoff coefficients between both scales were more pronounced for events with a dry as compared to a wet antecedent moisture status of the basin. Similarly, CEBALLOS & SCHNABEL (1998) argued that the distinct hydrological behaviour of the hillslope zone and sediment fills in

valley bottoms accounts for a decline of runoff coefficients from 11.5% for hillslopes to 1.1% for the complete 0.4 km² catchment in semi-arid Spain. PEUGEOT ET AL. (1997) found discontinuities of water transmission along catenas and small catchments for the Sahel zone which significantly affect the runoff amount reaching larger river stretches. Also for small basins of north-eastern Brazil, CADIER ET AL. (1996) and CADIER (1996) found that with increasing basin area, runoff coefficients generally decrease, particularly in dry years, and that the variability of annual runoff increases. Main reasons are the larger relative importance of alluvial areas in valley bottoms as well as the increasing number of small dams. However, they also state that this effect is in general less pronounced in north-eastern Brazil than in the semi-arid Sahel of Africa because of a stronger undulated relief in Brazil with no endoreic zones (as described for the Sahel in DESCONNETS ET AL., 1997) and the relevance of plain valley bottoms being comparatively small. The above spatial sequence of runoff source zones in upper parts of the landscape and sink zones in lower parts may also be in reverse for specific geological settings, as in Walnut Gulch (ABRAHAMS, 1988). Generalizing the observations from several watersheds in Walnut Gulch (semi-arid Arizona), GOODRICH ET AL. (1997) found an increasing non-linearity in basin response (mean runoff and peak response) with increasing basin scale for a threshold basin area of about 0.5 km². They attribute this observation to (1) an increasing role of channel transmission losses as compared to hillslope processes and (2) a decline of the fractional coverage of storm rainfall with increasing basin area.

Beside of the soil and vegetation properties of each location on the one hand, the above observations on lateral redistribution of surface and subsurface runoff contribute, on the other hand, to the characteristic spatial pattern of soil moisture in a catchment, which in turn controls runoff generation mechanisms. GRAYSON ET AL. (1997) denotes these two influencing aspects as 'local' and 'non-local' control on soil moisture patterns. The above studies in semi-arid environments suggest that structuring the landscape according to toposequences, i.e., different topographical zones, particularly slope areas on the one hand and valley bottoms on the other hand, is adequate to explain some important aspects of its variability in soil moisture and hydrological behaviour. This concept of catenas or toposequences goes back to MILNE (1935a,b) (cited in BIRKELAND, 1999). There, it was used to capture the variability of soils along a hillslope, where each soil shows a distinct relationship to the soils upslope and downslope for a variety of geo-

morphologic, pedological and hydrological reasons. In this respect, at longer time scales than those of most hydrological studies, soil catenas are the result of, e.g., hydrological processes at the hillslope. However, the point of view can be reversed, using catenas as a concept for structuring the landscape as basis for assessing its present hydrological behaviour, while assuming that characteristics of the catena do not change within the study period. Nevertheless, using such a concept does not necessarily mean that topographic control on hydrological processes and the distribution of soil moisture is dominant. As shown in PUIGDEFABREGAS ET AL. (1998), local soil factors are more important to explain spatial patterns of soil moisture, especially in the dry season. However, lateral redistribution processes and, thus, the degree of non-local control may change with the season, being more significant for wet conditions, i.e. the rainy season or a wet year, as also illustrated for more humid areas (GRAYSON ET AL., 1997; WESTERN ET AL., 1999).

FLERCHINGER ET AL. (1998) compared simulations with uniform and distributed parameters for a small semi-arid watershed in Idaho, USA. The largest differences in total basin response between the two approaches occurred for evapotranspiration. Differences were larger in dry years where water was a stronger limiting factor. The uniform version could not represent some areas having more soil water available for transpiration, being however important for the basin response. This suggests that a uniform approach for evapotranspiration modelling, not taking into account spatial variability of soil moisture or leaf area index, can be applied more easily when water is not limiting, which, however, does usually not apply for semi-arid environments.

In summary of runoff generation in the semi-arid north-east of Brazil, CADIER (1993) and CADIER ET AL. (1995) concluded that the soil type (mainly defined by infiltration capacity and storage capacity, i.e., depth to bedrock) and the vegetation form (mainly defined by its sparseness or degree of degradation) are the dominant physiographic influencing factors. Additional factors for runoff at larger spatial scale are the extent of re-infiltration zones for runoff and the density of small reservoirs.

3.3.2 Modelling approaches

3.3.2.1 Models for infiltration and vertical soil water movement

In a porous medium, as it is the soil matrix, water moves in the direction of a decreasing hydraulic po-

tential. The main components building up the hydraulic potential are gravitational and capillary forces. The flow rate is, in principle, expressed by the DARCY equation as a function of this gradient and the ability of the soil to transmit water, i.e., its hydraulic conductivity. The conductivity and the matrix potential are, in turn, dependent on the actual soil moisture status of the matrix in the form of non-linear functions. Including these relationships leads to a generalisation of the DARCY equation for unsaturated flow in the soil matrix in the form of a partial differential equation (RICHARDS equation) (RICHARDS, 1931).

Observations in natural soils, however, have frequently shown (see the examples above) that the concept of a homogeneous soil matrix is not valid due to the existence of macropores in which water movement is mainly influenced by gravitational forces (BEVEN & GERMANN, 1982). Water movement in natural soils for modelling purposes is, thus, often considered as a dual-domain process. Separate model components for flow within the macropores have been developed and coupled to the above RICHARDS equation to allow for interaction between both domains (for an overview, see BRONSTERT, 1999).

A large number of physically-based models use the above concept based on the RICHARDS equation for modelling vertical soil water movement (see examples in Chapter 3.3.2.2), partly also including a coupled macropore module. The soil column is sub-divided into several layers between which downward (percolation) or upward (capillary rise) fluxes are simulated, usually with high temporal and spatial resolution. These models may equally be used for modelling infiltration, setting rainfall volumes as an upper boundary condition. Large uncertainties remain for this type of models with respect to an adequate formulation of some processes, particularly related to macropore flow, and they are demanding in parameters and computational resources (e.g., BRONSTERT, 1999).

In simpler modelling approaches, soil layers are treated as storage volumes which transfer water to the next deeper layer or to a groundwater storage according to a conceptual approach. Commonly, percolation occurs in this type of approach if the actual soil moisture of the layer exceeds field capacity (e.g., in PRMS, LEAVESLEY ET AL., 1983). The volume of percolation may depend on the actual storage volume in the form of a linear storage approach, parameterized by a storage coefficient which can be completely empirical and, thus, is calibrated or related to changing unsaturated conductivity with actual soil moisture (SWRRB, ARNOLD ET AL., 1990, in ARNOLD & WILLIAMS, 1995). UHLENBROOK (1999) uses the soil moisture ac-

counting routine of the HBV model (BERGSTRÖM, 1992) to compute percolation to a runoff generation storage. In this concept, percolation may already occur if field capacity is not yet reached, which is considered to implicitly incorporate the effect of fast transfer of water to deeper soil layers by macropores. A simplified routine for water flow in macropores is also incorporated in some other conceptual soil water modules (e.g., in a modified version of WASIM-ETH (NIEHOFF, 2002) and for cracks in soils of high clay content in SWRRB (ARNOLD ET AL., 1990)). Likewise, both components are included by simple means in a soil water and plant dynamics model for semi-arid ecosystems (WALKER & LANGRIDGE, 1996). However, these extensions involve additional parameters which are difficult to determine or have to be calibrated.

Particular in the conceptual soil water models, infiltration is simulated by a separate routine which then delivers the amount of infiltrating water as input to the soil water module. Beside of the physically-based approach mentioned above, a variety of empirical or conceptual models exist in the literature. Empirical models generally relate the infiltration rate or volume to the time after the onset of a rainfall event, adapted by some soil specific parameters, and do not explicitly respect the actual soil moisture content (e.g., HORTON, 1940; HOLTAN, 1961). Although not being strictly an infiltration model, the widely used SCS curve number model (SCS, 1972) should be mentioned here in the context of empirical models. The method estimates surface runoff on an average event basis by accounting for interception, surface detention and infiltration losses, which are all parameterized by an empirical factor (curve number) in dependence of soil and vegetation characteristics as well as of antecedent runoff conditions. However, its applicability is largely limited in the case of dynamic modelling with historic rainfall data or for conditions not covered by the curve number parametrization.

The most widely applied conceptual model, which represents the infiltration process in the simplified form of the governing physical equations is the model of GREEN & AMPT (1911). Water is assumed to infiltrate in the form of piston flow with a clearly defined wetting front that gradually moves from the soil surface deeper into the soil. This wetting front separates a saturated zone above from a zone of initial water content below. The main assumption of the approach which may not be valid for many natural soils is that of a homogeneous soil matrix which does not contain macropores. Several extensions have been made to the original approach in order to remove some of its limitations, e.g., for infiltration in layered soils (PESCHKE,

1977), for crusted soils (AHUJA, 1983) or for time-variable rainfall intensities (PESCHKE, 1987). A broad study on the parametrization of the model for rangelands with sparse vegetation cover is presented in KIDWELL ET AL. (1997).

3.3.2.2 Models for lateral flow processes

For the description of lateral flow at the hillslope scale, one approach is to use physically based distributed models (see also Chapter 3.3.2.1), for instance, SHE (ABBOTT ET AL., 1986a,b), IHDM (BEVEN ET AL., 1987), HILLFLOW (BRONSTERT, 1994), SAKI (MERZ, 1996), MEDALUS (KIRKBY ET AL., 1996), CATFLOW (MAURER, 1997), KINEROS (WOOLHISER ET AL., 1990). These models use different forms of hillslope discretization (e.g., grids, flow strips, slope segments, rectangular planes) and represent one or more lateral flow processes (overland flow, unsaturated subsurface flow, saturated subsurface flow). Subsurface flow is simulated by a 2- or 3-dimensional version of the RICHARDS equation (see Chapter 3.3.2.1). Overland flow is represented by the ST. VENANT equations or its derivations, using data on slope gradients and surface roughness. However, using these high resolution, parameter demanding models is not feasible in large scale applications. TOPOG / THALES (VERTESSY ET AL., 1993; GRAYSON ET AL. 1992) use a more simple approach, where saturated subsurface flow along hillslope streamlines is approximated by a kinematic approach (BEVEN, 1982). Similarly, the SWRRB model uses a formulation based on a kinematic storage model (SLOAN ET AL., 1983, cited in ARNOLD & WILLIAMS, 1995), where lateral flow at the base of the hillslope is a function of the water volume stored in the saturated zone, hillslope width and gradient, and soil conductivity. An approach based on terrain analysis of grid elevation models to consider the interaction of lateral flow along hillslopes (reinfiltration, return flow) was presented by SCHUMANN & FUNKE (1996) and SCHUMANN ET AL. (2000), where by statistical means transition frequencies between grid cells with different soil-vegetation combinations are defined. In TOPMODEL (BEVEN & KIRKBY, 1979), a topographic index is used to represent the effect of lateral subsurface flow on soil moisture at downslope positions. The application of this concept is, though, limited to wet areas with shallow groundwater tables (BEVEN, 1995), which mostly excludes semi-arid regions where lateral flow of infiltration-excess runoff is thought to be dominant. Another procedure was shown in the models WATBAL (KNUDSEN ET AL., 1986) and PRMS (FLÜGEL, 1995), where the discretization of the study

area into hydrological response units respected their topographical position. This allowed to include by conceptual storages the lateral subsurface drainage from upland areas to slopes and to the groundwater in valley floors, while respecting its effect on soil water in the downslope topographic units. In the case of WATBAL, the concept includes also the redistribution of surface runoff between units of different topographic position. Otherwise, in most conceptual models, particularly in those for large-scale applications, lateral redistribution at the hillslope scale is not explicitly taken into account. Water which percolates vertically through the soil profile is added to one or more lumped linear or non-linear storages (for rapid and slow subsurface runoff components) of which the outflow dynamics to river runoff (without interaction in zones of lower topography) are controlled by a storage coefficient, a conceptual parameter to be calibrated (e.g., in SLURP (KITE, 1978), HBV (BERGSTRÖM, 1992)). Generated surface runoff of each modelling

unit is assumed to reach directly the river network without interaction with other units. Modelling of lateral flow is then constrained to runoff routing in the river network.

Particularly in modelling of arid catchments, specific modules assess transmission losses in dry river beds. They combine procedures of channel routing, i.e., the translation of a flood wave, with infiltration models into the channel sediments. Various empirical (e.g., LANE, 1983; WALTERS, 1990; SHARMA & MURTHY, 1994; LANGE, 1999) or numerical approaches (e.g., FAULKNER, 1992; SHARMA ET AL., 1994) have been developed. Neglecting transmission losses in a modelling system designed to simulate runoff from semi-arid or arid catchments could result in serious errors, according to HUGHES & SAMI (1992). However, for large scale applications, it may be more feasible to use some approximate concept based on the antecedent moisture status of the catchment instead of an explicit description of the loss processes.

3.4 Watershed Models

3.4.1 Scale and variability

Hydrological processes, the observation of these processes and hydrological models are each linked to certain spatial and temporal scales, i.e., the process scale, the observation scale and the modelling scale (BLÖSCHL & SIVAPALAN, 1995). In other words, when moving from one scale to another, the observable processes change, as do the modelling concepts which have to be related to the scale of the process to be represented. This scale dependency is due to the heterogeneity of the physiographic landscape characteristics, the variability of hydrological state variables and processes (in space and time) and the importance of individual processes relative to others which changes with scale. The distinction between the above three categories of scale gets relevant for hydrological modelling if these categories do not coincide in scale for a specific application. This is the case for most model applications. Then, scaling techniques are required which enable the transfer of data, model formulations and/or parameters between scales and scale categories.

If the hydrological model is to be applied for a large geographic domain as in this study, a discrepancy commonly exists between the modelling scale and the process scale. The modelling scale of interest (e.g. a river basin) is usually larger than the typical scale of the relevant processes, which involves considerable

variability at the modelling scale (sub-grid variability). This variability may be of deterministic/structured or of stochastic nature (see SEYFRIED & WILCOX (1995) for an overview on the terminology). In the case of structured variability, some sort of organisation can be observed in the spatial distribution of terrain characteristics or processes, i.e., there is a relationship between these characteristics and their location. In contrary, in the case of stochastic variability, terrain characteristics and processes are considered to be independent of the location. The need to incorporate these types of variability for accurate results at the modelling scale has been illustrated for several examples in Chapter 3.1-Chapter 3.3. The following approaches can be taken into consideration in order to cope with the scale problem:

- (1) Explicit representation of sub-grid variability by using modelling units small enough to capture processes and their variability at the scale where the variability occurs, followed by the aggregation of the individual results to the scale of interest. In most cases, this approach is practically not feasible due to limited data availability and computational constraints.
- (2) Use of effective parameters in process scale equations being applied at the modelling scale. The effective parameters are assumed to incorporate sub-grid variability, thus resulting in an accurate de-

scription of the model response at the modelling scale. This approach is used, implicitly or explicitly, in most hydrological models. One limitation is that such an effective parameter may not exist, particularly when processes are non-linear (BLÖSCHL & SIVAPALAN, 1995). Additionally, effective parameters lack of physical meaning and often have to be derived by calibration.

- (3) Use of distribution functions which do not represent the exact pattern of sub-grid variability, but its fractional distribution at the modelling scale. Examples in hydrological models are distribution functions of soil moisture deficit (BEVEN & KIRKBY, 1979), storage compartments (MOORE & CLARKE, 1981) and infiltration capacities (ZHAO, 1992; WOOD ET AL., 1992; TODINI, 1996). Examples of more complex approaches for land surface parameterization in General Circulation Models (GCMs) are the statistical-dynamical concepts of ENTHEKHABI & EAGLESON (1989), AVISSAR (1992) and FAMIGLIETTI & WOOD (1994). These methods can serve as an effective way to represent effects of sub-grid variability, however, they rely on information about probability distributions and their parameters which may be difficult to provide. Additionally, structured variability cannot be represented by a distribution function.
- (4) Use of lumped equations at the modelling scale which describe in an integrative way smaller scale processes and their variability. An example (given in BLÖSCHL & SIVAPALAN, 1995) is DARCY's equation, where instead of modelling flow through each pore of the porous medium a lumped equation with one integrative parameter (hydraulic conductivity) is used. Other examples are on overland flow in rills (MOORE & BURCH, 1986) and the 'big-leaf' approach for canopy evapotranspiration in the PENMAN-MONTEITH equation (MONTEITH, 1965) instead of individual leaf modelling. This approach is restricted by the fact that for a lot of processes relevant to large scale model applications lumped equations do not exist (e.g., infiltration at the hillslope or catchment scale) (O'CONNELL & TODINI, 1996).
- (5) Definition of terrain patches with similar response in terms of the hydrological quantity of interest. Only those processes and heterogeneities are taken into account for the delineation of the modelling units (patches), which are relevant for the objective of model application. On this principle, the spatial concept of several distributed hydrological models is based, with the patches also being called hydrological response units (LEAVESLEY ET AL.,

1983) or hydrotopes (BECKER & PFÜTZNER, 1987). A critical problem is the adequate definition and delineation of the terrain patches with regard to the above objectives. The representative elementary area concept of WOOD ET AL. (1988) was one attempt to find such an preferred element size where the variability of the hydrological behaviour is at a minimum. In many applications, patches are derived by intersecting maps of different types of physiographic data (topography, soils, vegetation, etc.) in Geographical Information Systems (GIS). The selection of which data are relevant is based on expert knowledge, the perception of the study area, and on comparative studies evaluating the performance of models for different ways of delineation of patches (e.g., FLÜGEL, 1995; BECKER & BRAUN, 1999). In most of these concepts, the criteria for delineation of patches is their similarity with regard to vertical hydrological processes (i.e., infiltration, percolation, evapotranspiration). In order to give the response at the modelling scale including lateral processes, the individual responses of the patches are aggregated without allowing for interaction between them. BECKER & NEMEC (1987) and BECKER (1995) propose to use two different spatial discretization schemes for vertical and lateral processes, respectively. However, it remains unclear in which way patches, once defined with respect to similar behaviour of vertical processes, should be interrelated to give another type of patches with similarity in lateral function.

3.4.2 Watershed models for semi-arid areas

The features of semi-arid zone hydrology summarized in Chapter 3.1-Chapter 3.3 underline the need for a modelling concept at the watershed scale which may include different approaches than for humid zones, as also stressed by, e.g., PILGRIM ET AL. (1988). At least, models developed for temperate climates should be thoroughly tested before being transferred to the semi-arid (GIESEN ET AL., 2000).

A great variety of types of hydrological models exist, differing in their degree of determination (deterministic – stochastic models), in their type of process representation (process-based – conceptual – empirical models), in the extent and resolution of temporal and spatial scales they cover (e.g., lumped – distributed models, event-based – continuous models). Accordingly, hydrological models at the watershed scale are composed of several modules for the different processes which are to be represented, with some exam-

ples of these individual modules given in Chapter 3.2 and Chapter 3.3.

Often, hydrological models for semi-arid areas are simple empirical formulae which relate some catchment characteristics to a flow characteristic of interest at the catchment outlet. These models do not directly consider the governing physical relationships of the processes involved in runoff generation. However, they may contain a valuable set of expert knowledge on how observable catchment properties act on the hydrological response. An example for semi-arid West Africa is a scheme based on the classification of the landscape according to soil and vegetation characteristics, which determines runoff for each class by an experimentally determined function respecting rainfall and soil moisture (CASENAVE & VALENTIN, 1992). For semi-arid north-eastern Brazil, MOLLE & CADIER (1992) and CADIER (1993, 1996) presented an empirical, static model for regionalization of mean annual runoff among small watersheds up to 100 km². Beside of mean annual precipitation, the soil type, the degree of degradation of vegetation, the density of small reservoirs, and the extent of infiltration zones for runoff, each represented by an empirical parameter, were respected as influencing factors. For larger basins in north-eastern Brazil (~10000 km²), REIMERS (1990) used multiple regression models to determine mean runoff from various catchment characteristics. However, such types of empirical models is not suitable for dynamic models and/or hardly transferable to sites other than those for which their relationships were derived.

A large number of conceptual rainfall-runoff models have been developed for hydrological applications. These models represent hydrological processes by simplified formulations and analogues of the underlying physical laws, usually by mutually interrelated conceptual storages, and include some amount of empiricism. The models contain parameters which lack of direct physical meaning and have to be derived from calibration. Some conceptual models have been developed specifically for semi-arid catchments. A main difference to models developed for humid areas is that semi-arid models often include some approach of modelling infiltration-excess runoff and transmission losses, which is not necessarily included in models for humid areas. For small semi-arid watersheds, LANE (1982) presented a distributed model with empirical components for the event scale, using the SCS method for runoff volume estimation and including transmission losses. A simple distributed model with two calibration parameters was successfully applied for a basin within Walnut Gulch by WHEATER ET AL.

(1997). On a monthly basis, a widely applied model in semi-arid southern Africa is the conceptual storage model of PITMAN (1973). A conceptual model with a very large number of approaches which are a specific attribute to semi-arid hydrology is the semi-distributed model of HUGHES & SAMI (1994). They include, e.g., a variable time resolution for infiltration modelling in dependence of rainfall intensities, distribution functions to account for sub-area variability, re-infiltration of surface runoff at the hillslope scale as function of saturated catchment portions, transmission losses, small dam storage). Thus, the model includes many aspects of perceptual knowledge on semi-arid catchment behaviour, but finally results in a large number of parameters. They can mainly be derived from small-scale physical catchment characteristics, with a broad field / expert knowledge of the basin response requested. Some parameters, however, remain to be calibrated. A comprehensive and flexible conceptual model, starting out from an agrohydrological perspective, but being extended to a wide range of application in the field of water resources, including large-scale applications for semi-arid areas in Africa, is the ACRU modelling system (SCHULZE, 1995). A model developed for the north-east of Brazil is MODHAC (LANNA & SCHWARZBACH, 1989), a lumped conceptual model with eight principal calibration parameters, which lead to good model performance as compared to observed runoff. The model is frequently applied for water resources planning purposes in north-eastern Brazil (FORMIGA ET AL., 1999; COGERH, 2000). Other conceptual models applied in the semi-arid study area are SMAP (LOPES ET AL., 1981), in daily lumped version with seven calibration parameters (applications in e.g., ASFORA & CAMPELLO (2000); BARBOSA ET AL., 2000; COSTA ET AL., 2000) or in an hourly version (ARAÚJO FILHO ET AL., 2000), and the distributed grid model SIMMQE / AÇUMOD (DNAEE, 1983; PAIVA ET AL., 1999; SILVA JUNIOR ET AL., 2000; PASSERAT DE SILANS ET AL., 2000).

Comparing three conceptual models of different complexity (number of parameters) for semi-arid watersheds, YE ET AL. (1997) concluded that for monthly flow volumes a simple model (with 6 parameters) is able to satisfactorily represent the nonlinearities of low-yielding catchments in terms of monthly runoff. For daily flow and for catchments with runoff coefficients <10%, however, a more complex model might be required. In HUGHES (1995), a daily model did not show better results than a monthly model for large African catchments, mainly due to the lack of adequate rainfall data. MICHAUD & SOROOSHIAN (1994) found a physically-based model not to perform better at the

event scale than a distributed conceptual model after calibration for a 150 km² semi-arid basin (see also below). REFSGAARD & KNUDSEN (1996), for continuous simulations, came to similar results for semi-arid basins in Zimbabwe. Both studies showed that distributed, more physically-based models performed better if no calibration was done. For large-scale applications covering several climate zones, CHIEW ET AL. (1995) found that after calibration, the performance of a conceptual rainfall-runoff model (MODHYDROLOG) to reproduce monthly flows may be lower for semi-arid and arid catchments. Similar results for large-scale models were obtained by RUSSELL & MILLER (1990) and ABDULLA & LETTENMAIER (1997).

Generally, most studies with conceptual models highlight the importance of adequate rainfall data to obtain satisfactory simulation results. Deficiencies in this respect may more than compensate favourable effects of a more appropriate model conceptualization. Some approach for transmission losses and of rainfall-dependent vegetation dynamics should be included even in simple models for semi-arid environments (HUGHES, 1995). Calibrating conceptual models in semi-arid regions may require long calibration periods to obtain reliable simulation results, due to the high variability of runoff behaviour (e.g., GÖRGENS, 1983) and missing watershed information encountered during no-flow periods of ephemeral streams (YE ET AL., 1997).

Physically-based models were applied to some small semi-arid catchments with an extensive data base. For example, the event-based, complex distributed KINEROS model (WOOLHISER ET AL., 1990), which was specifically developed for semi-arid regions, gave good simulation results for small catchments up to about 10 km², within the Walnut Gulch, Arizona, USA (SMITH ET AL., 1995; GOODRICH ET AL., 1997), but reached beyond the conditions of its applicability to give reasonable runoff simulations for the entire catchment (150 km²) (MICHAUD & SOROOSHIAN, 1994). The application of TOPOG (GRAYSON ET AL. 1992) to a tributary of the Walnut Gulch basin was shown to be highly dependent on parameter values, with reasonable simulation results only after calibration. Similar results with TOPOG for a semi-arid agricultural catchment were obtained by ZHU ET AL. (1999), with the performance being better for larger storm events. In both applications, large uncertainties remain in model structure, data and parameters due to the lack of adequate field data in the resolution required by this type of model. The costs associated with the detailed basin characterization as basis for applications of these detailed, physically-based models

are not feasible for large watersheds (MICHAUD & SOROOSHIAN, 1994).

3.4.3 Watershed models for the assessment of climate change impacts

In general, a widely used method for evaluating the impact of climate change on water resources includes four elements (summarized, e.g., in BOORMAN & SEFTON, 1997): (1) a study area for which the effect of changed climate is to be evaluated, (2) a method for providing historical climate data and plausible scenarios of changed climate in the future, (3) a hydrological model transforming the climate input into a response of the hydrological system, being validated (and possibly calibrated) on historical data and re-run with the changed climate input, and (4) one or more target variables out of the field of water resources for which the effect of climate change is to be evaluated by any statistics.

A large variety of hydrological models of the different types mentioned in Chapter 3.4.2 have been applied in the above context of impact analysis. Several critical aspects are implied in the application of this methodology, as summarized, e.g., in LEAVESLEY (1994), BOORMAN & SEFTON (1997), SCHULZE (1997), BONELL (1998), XU (1998). Two major aspects are (1) the scale problem, mainly the mismatch between, on the one hand, coarse-resolution data of climate change scenarios derived from output of global General Circulation Models (GCMs) and, on the other hand, data needed in the hydrological application for regional or small-scale impact studies, and (2) the non-stationarity of the system leading to the question of the applicability of a hydrological model for future situations which differ from those of the historical time period used for model development and calibration.

Referring to the first point above, the fundamental difficulty is that the ability of GCMs to provide reliable climate data decreases with increasing temporal and spatial resolution, whereas for hydrological applications in contrary, the importance of accurate climate data increases in that direction. This may apply particularly for precipitation data, where not only the mean and its direction and magnitude of change is of importance for hydrology, but especially the rainfall variability, the persistency of, e.g., wet and dry time intervals, or characteristics of extreme events. Different types of downscaling techniques have been developed to bridge the gap between data resolution of climate and hydrological models (for an overview, see, e.g., WILBY & WIGLEY, 1997), for instance, sim-

ple interpolation methods, statistical or dynamical downscaling techniques, where the latter may also include the use of nested regional climate models within a GCMs. However, the quality of downscaled data depends critically on the simulations of the driving GCM and costs and benefits of different downscaling techniques have not been comprehensively evaluated yet (IPCC, 2001). Climate simulations of various GCMs, in turn, may be considerably different from each other in space and time, particularly when comparing the results at the regional scale (IPCC, 2001). These differences may have huge implications for the direction and magnitude of simulated changes in the hydrological response (e.g., ARNELL, 1999).

The second critical aspect of the methodology for impact assessment mentioned above refers to the applicability of a hydrological model for the changed conditions of the scenario period. As pointed out by KLEMES (1985), one main criteria for the suitability of a model in this respect is its sound physical foundation. A model structure is required which enables to reproduce non-linear responses associated with, e.g., changes in rainfall characteristics on runoff generation, and/or changes in temperature on evaporation rates, and/or changes in CO₂ concentrations on transpiration rates. Hence deterministic, process-based and distributed-parameter models will in principle be most appropriate in this context (LEAVESLEY, 1994). Models which require a calibration of its parameters face the serious limitation that the historical conditions for which the model is calibrated do not correspond to the conditions of the scenario period. Thus, while good results for the calibration period may be obtained, no conclusion can be drawn if the calibrated parameter set applies also to give an adequate response for changed conditions, and if and how possible adaptations of the parameters to the changed conditions should be made. This implies also the risk of giving in the calibration period the right response of a hydrological variable for the wrong reason with respect to processes due to intercorrelation of parameters. SCHULZE (1997) summarizes that 'models requiring any form of external calibration, particularly of location-specific exponents and physically non-meaningful parameters are inherently not usable for climate-change driven hydrological impact studies'. As a consequence, the need to develop and apply process-based, non-calibrated models for climate change impact assessment was put forward (e.g., GLEICK (1986), NASH & GLEICK, 1991; LEAVESLEY, 1994; MCCABE & HAY, 1995; IPCC, 2001).

As mentioned at various places during the previous sections, the application of hydrological models and

hence the results of climate change impact simulations comprise a large range of uncertainties, which can be grouped into three main source categories (e.g. THORSEN ET AL., 2001): (1) uncertainty in input data, i.e. driving variables such as climate data and model parameters such as soil physical characteristics, (2) uncertainty in model structure, i.e., due to insufficient process knowledge, due to simplification in process representations, including, e.g., their temporal and spatial resolution, and (3) numerical uncertainty. The call for assessing the reliability in model predictions has constantly accompanied the discussion in the literature on applications of hydrological models (e.g., BEVEN, 1989; BEVEN & BINLEY, 1992; EWEN & PARKIN, 1996), but there is still a considerable deficit in today's model applications as this has usually not yet become 'a matter of routine' (BEVEN, 2001).

A fundamental step towards the assessment of the reliability of model results consists in the application of a rigorous validation scheme which compares model results with observations and, thus, allows to give an estimate of the accuracy of the results. KLEMES (1986) was one of the first to suggest a systematic approach of testing for stationary and non-stationary conditions and with regard to the geographic transferability of models. The need for extended methods of model validation has frequently been pointed out, including multi-criterial and multi-scale approaches, as for the validation of internal stages and of spatial patterns in the case of distributed models (ROSSO, 1994; GRAYSON ET AL., 1995; REFSGAARD & STORM, 1996; BEVEN, 1997; MROCKOWSKI ET AL., 1997; PINOL ET AL., 1997; REEFSGARD, 1997; GÜNTNER ET AL., 1999). However, such a comprehensive validation is rare, mainly due to the lack of suitable data (see GÜNTNER ET AL. (1999) for an overview).

The broader approaches for the assessment of model uncertainty use joint stochastic-deterministic methods. They consider input data as realisations of stochastic variables with given statistical properties which are then applied to the hydrological model by, e.g., Monte-Carlo simulations. A more comprehensive methodology, which allows also to include uncertainty related to model structure, is the generalised likelihood uncertainty estimation by BEVEN & BINLEY (1992). In general, model validation and the analysis and discussion of model uncertainty should be directed towards the objectives of model application and the type of simulation results of interest, as pointed out in THORSEN ET AL. (2001), for instance.

Finally, recent overviews on the possible impact of climate change on water resources in semi-arid areas are given, e.g., in IPCC (2001) and DAM (1999). They

summarize that studies are generally low in number for semi-arid zones, compared to other climate regions. The general finding is that semi-arid regions are very sensitive to changes in rainfall, as a given percentage change in rainfall can produce a considerably larger percentage change in runoff (see also ARNELL, 2000). Similarly for soil moisture, CHIEW ET AL. (1995) found for Australian basins that the amplification factor, which relates changes in precipitation to changes in a hydrological variable of interest, is higher in drier catchments. A similar effect has been found for groundwater recharge in semi-arid Tanzania by SANDSTRÖM (1995). Concerning evapotranspiration, the actual rate of evapotranspiration can be expected to increase by a smaller percentage than the possible increase of the atmospheric demand for evaporation,

as particularly in dry areas the actual rate is water limited by available soil moisture (ARNELL, 1996, cited in IPCC, 2001). Increasing atmospheric CO₂ reduces the stomatal conductance of plants and thus transpiration, on the one hand, and may be associated with an increased plant growth and thus more water use by the plants, on the other hand. The net effect on plant transpiration and consequently one catchment-scale evapotranspiration is matter of debate and there is a large degree of uncertainty (IPCC, 2001). IPCC (2001) summarizes that, although large uncertainties are comprised within the application of hydrological models, the greatest uncertainties in the effects of climate on streamflow arise from uncertainties in climate change scenarios.

3.5 Conclusions on a Modelling Concept in this Study

3.5.1 General aspects

The term modelling concept in the context used here refers not only to a hydrological model itself, i.e., a specific model code which represents the occurring hydrological processes at a certain temporal and spatial scale, but it also includes approaches for model parametrization, validation and for the assessment of reliability of model results. Meaningful model results can only be obtained if an adequate modelling concept has been chosen. The most important criteria which have to be taken into account in this context are:

- Which are the objectives of model application ?
- Which are the hydrological processes being of relevance for the study ?
- Which is the spatial scale (extension and resolution) of interest and required for process representation ?
- Which is the temporal scale (extension and resolution) of interest required for process representation ?
- What is feasible with regard to data availability ?
- What is feasible in terms of time needed for model implementation, computation time of model runs, etc. ?

Due to the distinct features of hydrology in semi-arid zones (Chapter 3.1-Chapter 3.3), an adequate modelling concept may have to include approaches which are different from those for humid zones. Additionally, in view of the objectives of model application (Chapter 1.2) for large areas, within the context of (climate change) impact analysis, and within an inte-

grated model with specific requirements on interfaces between modules, there was no model found in the literature which could fulfil the requirements related to this set of objectives (Chapter 3.4). Thus, a new hydrological model is developed in this study, called WASA ('Model of Water Availability in Semi-Arid Environments').

3.5.2 Model type, calibration, validation and uncertainty

The dynamic description of the historical and future water balance and of water availability requires a deterministic, continuous model. In addition, according to the conceptual limitations in the use of a calibrated model for impact studies presented in Chapter 3.4.3, WASA should be process-based and should include no or at least a minimum of parameters to be calibrated. There are some additional aspects specific for this study which would aggravate the plausibility of model calibration:

- The low availability of streamflow data with longer time series and, in parts, the lack of overlapping periods for different gauging stations, together with an often poor data quality (Chapter 2.1.6.3, Chapter A.1) restrict the potential for model calibration (and for the required validation on a different period in the form of a split-sample test). Furthermore, periods without streamflow in the dry season, which usually make up about half of the measurement periods, offer no information on the moisture status of the catchment.

- The general high uncertainty of input data and parameters for the study area enhances the risk that calibration leads to good results for the wrong reason. This also refers to the large number of reservoirs in the study area (Chapter 2.1.5), which can be expected to heavily influence streamflow, while the knowledge of their characteristics (number, location, operation rules) is very limited. Hence calibration of parameters of the runoff generation routines might reflect to a large extent storage effects instead of aspects of runoff generation itself. Additional criteria other than streamflow such as soil moisture, which could confine the equifinality of different parameter sets, are not available (reservoir storage is not strictly another variable).
- As the model is to be applied over a large geographic domain, calibration for a large number of sub-basins would have to be carried out, which is impractical to be done manually. An automatic calibration procedure, on the other hand, implies a larger risk of resulting in parameter sets which represent an unrealistic process behaviour. In addition, a large number of ungauged sub-basins remains, to which the calibrated parameters had to be transferred by some regionalization procedure. However, a clear relationship between basin characteristics and calibration parameters may be hard to find in the view of the low resolution and high uncertainty of available information.

As a consequence, the basic concept for model development in this study is to set up a model which basically does not need calibration of its parameters, but for which all parameter values can be derived from available climate and physiographic data of the study area and from information of similar environments given in the literature. Within such a process-based approach, and in view of the objectives of impact assessment at large spatial scales, it is essential to appropriately tackle scaling issues (Chapter 3.4.1) in order to relate changes which might occur at the process scale of a hillslope, for instance, with the impacts at the final scale of interest of a sub-basin, for instance. This requires an appropriate way of process representation (Chapter 3.5.3) and, closely related to that, of spatial model structure (Chapter 3.5.4). Clues on its definition and parametrization for large-scale models may provide the study of smaller basins with detailed approaches which finally may lead to simpler formulations appropriate for the large-scale model, as outlined in set of papers by EWEN (1997), EWEN ET AL. (1999) and KILSBY ET AL. (1999). In this context, the model in this study is examined for small experimental basins which are considered to have characteristics

typical for wide parts of the entire study area (Chapter 5.2).

Model validation should in general be closely related to the objectives of model application (e.g., KLEMES, 1986). Having in mind to apply the model for simulations of the effects of climate or other environmental change, it is on the one hand essential to get an idea of how the model performs in terms of the representation of the dominant hydrological processes, particularly of runoff generation. Using only low resolution data at larger temporal and spatial scales, which implies temporal averaging and superimposition of a variety of processes, prevents to a large extent such a more process-related validation of the model. This is done, however, for the closer defined boundary conditions at the small-basin scale mentioned above (Chapter 5.2).

On the other hand, the model is to be validated directly at the scale of interest of model results. The evaluation of model performance for historical or present-day conditions is the basis for the interpretation of model simulations for future changed conditions. Here, as the main interest is on evaluating water availability for time periods of several decades for large spatial units, the focus during model validation is on the performance at the monthly and annual scale, including the variability at these scales, i.e., seasonal and interannual variability (see Chapter 5.4.3.1 for validation criteria). Due to the limited data availability in the study area (Chapter 2.1.6), model validation, as in most hydrological studies, is restricted to comparison with data related to runoff (river discharge, storage volumes in reservoirs) (Chapter 5.4.3). A more powerful validation approach (see Chapter 3.4.3) using additional criteria, e.g., soil moisture, cannot be performed here.

The deviations between observed and simulated data give an estimate on the reliability of model results for the points of validation and, if taking into consideration the entire set of validation results, the uncertainty of model predictions for ungauged basins of the study area. A main goal is to assess the effect of uncertainty from different sources (i.e., input data, model structure, see Chapter 3.4.3) in its sensitivity on model results. With regard to impact studies, this includes the sensitivity for small-scale properties at the scale of interest and the degree of sensitivity of, e.g., specific parameters for different boundary conditions. In this respect, as the main changing factor for scenario calculations in this study is rainfall, this means a separate evaluation of sensitivity for particularly dry or wet conditions (Chapter 5.3). In general for the modelling concept in this study following, e.g., BRON-

STERT (1999), it is rather the intention to give by simple means some bounds of model uncertainty in view of the available data instead of optimizing the fit of the model results with regard to measurements.

3.5.3 Process representation

Within the overall goal of a process-based model (Chapter 3.5.2), it is the intention to focus on the representation of those processes which are dominant for the conditions of the study area. Surface processes (infiltration-excess runoff including lateral interaction and evapotranspiration) were shown to prevail in semi-arid environments, whereas lateral subsurface processes (groundwater flow) are generally less important (Chapter 3.3.1.1). It is primarily the intention to select existing process formulations from the literature which fulfil the requirement of no need for calibration and which can be parameterized with the available information. These approaches are integrated into the newly developed spatial and temporal structure of WASA with more or less modifications (described in detail in Chapter 4). The main components which are based on existing approaches are:

- **The evapotranspiration model.** The literature review (Chapter 3.2) highlights the need to include evaporation from the soil surface and its interaction with transpiration for sparsely vegetated land surfaces. As the structure of vegetation in the study area is predominantly characterized by a uniform layer of more or less density instead of by a patchy spatial distribution (Chapter 2.1.3), a one-compartment, two-layer model based on SHUTTLEWORTH & WALLACE is selected (Chapter 4.2.2). The additional advantage as compared to a two-compartment model is that no additional parameter which defines the areal fraction of unvegetated surface is required (see Fig. 3.4), which would be hard to be define.
- **The infiltration model.** The infiltration process formulation in WASA is based on the widely used GREEN-AMPT approach (Chapter 3.3.2.1, Chapter 4.2.3), which can be considered to be a reasonable, parsimonious approximation to a fully physically-based approach, which is due to its complexity not feasible for a type of model as in this study (see Chapter 3.3.1.1). A limitation of the GREEN-AMPT-based approach may be its assumption of homogeneous soil conditions. However, there is no quantitative information on macroporosity and surface crust development in the study area which could be used for an extended formulation. The interaction between both opposing factors and also of surface stoniness at very small spatial scales

(e.g. shrub / inter-shrub scale) may have a compensating net effect (Chapter 3.3.1.1). Hence the assumption made here is that this type of variability can be efficiently represented by setting homogeneous conditions, whereas the variability in infiltration and interaction at the next larger scale between soil types and vegetation units is of more importance for the scale of interest and thus represented in the model (see Chapter 3.5.4).

Major process formulations for which a development specifically for WASA is required as no adequate existing approaches are found in the literature are:

- **The soil water model,** including lateral transfer of water. The literature review revealed the large importance of the spatial variability of soil moisture and of lateral re-infiltration of surface runoff particularly for dry environments (Chapter 3.3.1.3). Large-scale models, however, do mainly not include modelling concepts with which these effects could be represented (Chapter 3.3.2.2). This leads to the development of a novel approach in WASA for the determination of the soil water balance, which respects beside of vertical water fluxes within the soil also lateral fluxes between the soil profiles of adjacent modelling units (Chapter 4.2.4 - Chapter 4.2.5). It is not that much the fundamentals of this flux calculation which is new, as it is gravity-driven and based on the well-known DARCY-equation, but rather the type of interaction and redistribution within a specifically developed spatial model structure (Chapter 3.5.4).
- **The reservoir model.** Artificial surface reservoirs have a major impact on runoff concentration and water availability in the study area (Chapter 2.1.5). However, particularly for small and medium-sized reservoirs, no detailed information on their characteristics (e.g. geometry) nor on their exact location are known. Additionally, it would not be feasible to represent such a large number of individual elements explicitly in a large-scale model. This can be done only for a small number of the largest reservoirs with more detailed information (Chapter 4.2.7.2). Otherwise, a scheme is developed which allows to represent in an aggregate manner the effect of reservoirs on streamflow and water storage, while pertaining some aspects of their interaction and size-dependent behaviour (Chapter 4.2.7.1).

Finally, the large importance of rainfall, particularly of its high variability in space and time, for the hydrology of semi-arid areas has been pointed out at several places in the literature review (Chapter 3.1.1,

Chapter 3.2.1, Chapter 3.4.2). Thus, the modelling concept applied here has to take into consideration in an extended form the effects of rainfall on process representation and parametrization. One main aspect refers to the temporal resolution required for a process-based infiltration modelling. Relevant real-world rainfall intensities are usually to be given at an hourly or higher temporal resolution for the convective rainfall events of the study area (Chapter 3.1). On the other hand, however, broadly available rainfall data have a daily resolution in maximum (Chapter 2.1.6.2). Additionally, a higher than daily resolution might not be feasible in terms of computation time for a distributed model applied over several decades. Thus, the concept in this study is to use the available hourly rainfall time series (Chapter 2.1.6.2) for the derivation of a scheme to disaggregate the common daily time series to a higher resolution (Chapter 5.1). These disaggregated time series are then used at the small-basin scale where more detailed process-related modelling studies can be made (see above in Chapter 3.5.2) to derive a simple scaling relationship to be applied in the coarser large-scale model (Chapter 5.2.1). Another important aspect to be studied with regard to the representation of rainfall in the large-scale model refers to the effect of interpolation from station data to the scale of modelling units (Chapter 5.3.1).

3.5.4 Spatial model structure

The following conclusions on the definition of an appropriate way for structuring the study area into spatial modelling units in WASA are drawn:

- The target units of model application (sub-basins or administrative units with an area in the order of magnitude of 10^3 km^2) are to be represented explicitly to provide results at the scale of interest. As also data on soil moisture on different soil types within these areas are required (Chapter 1.2), some form of further spatial sub-division is required. This is also needed for a process-based representation of runoff generation (see below).
- Considering the scaling issues in Chapter 3.4.1, the definition of terrain patches with similar response in terms of the hydrological quantity of interest (which is primarily runoff at the scale of the target units in this study) is an attractive approach to capture spatial variability at scales smaller than the above target units.
- The process review in Chapter 3.2 and Chapter 3.3 indicates that soil and vegetation characteristics are

the dominant factors influencing soil moisture and runoff generation at the plot scale and might be used as criteria for the definition of the above terrain patches. The runoff response at the hillslope and basin scale in semi-arid environments is, however, not simply the aggregate of individual responses at the plot scale, but it may be considerably influenced by their interaction in terms of redistribution of lateral flow components and re-infiltration (Chapter 3.3.1.3). Thus, modelling units with a similar runoff response at the scale of interest in this study are defined to show similarity in terms of lateral flow processes within them. These units are called *landscape units* in WASA (Chapter 4.1.2, Fig. 4.1).

- The definition of landscape units implies, in turn, that the units are also similar with regard to their sub-scale variability of those factors which govern the vertical processes, as they generate water fluxes which may be subsequently transformed in the domain of lateral processes. It may not only be the percentage of various sub-scale units on the total landscape unit area which is of importance for capturing the variability and its effect on total response, but also their position relative to each other. Chapter 3.3.1.3 shows in this respect that toposequences with characteristic differences in, e.g., soil properties between areas of different topographic position may explain an important part of the variability. This type of structured sub-scale variability is captured in WASA by the so-called *terrain components* (Chapter 4.1.2, Fig. 4.1). Additional sub-scale variability induced by soil and vegetation characteristics for which no relation to the geographic location can be defined has to be respected as a type of stochastic variability (*soil-vegetation components*, see Chapter 4.1.2, Fig. 4.1).
- The generally poor and low-resolution availability of spatially distributed terrain characteristics in the study area (Chapter 2.1.6) does not allow a bottom-up approach for defining modelling units within the study area, as it is not sufficient to delineate units with quasi-homogeneous characteristics with geographically explicit locations. Instead, a top-down approach is called for, which enables to disaggregate the study area into smaller modelling areas or fractional sub-areas without geographic reference to a degree which is supported by resolution and type of available data (and which is desired with regard to the detail of process representation in the model).

Model Description

4.1 Model Structure

4.1.1 General features

The hydrological model which has been developed in this study is called WASA, which stands for 'Model of water Availability in Semi-Arid environments'. WASA is a deterministic rainfall-runoff model for continuous simulation. The temporal resolution of the model, i.e., the duration of one model timestep, usually is one day. For smaller-scale studies also an hourly resolution can be applied in the soil moisture routine. Referring to the spatial resolution, WASA is a distributed model in the sense that the study area can be sub-divided into smaller areas of geographically referenced location in order to account for the variability of the hydrological behaviour within the study area (e.g., landscape units within watersheds). However, at some spatial scale in WASA the variability at even smaller scales is not represented by modelling units of geographically referenced location, but only by their distribution within larger areas (e.g., soil-vegetation components within terrain components). In this sense, WASA has the aspect of a semi-distributed model. Additionally, WASA also works in the form of a spatially lumped model when at some spatial scale the variability at even smaller scales is not represented at all (e.g., variability of soil hydraulic conductivity within a soil-vegetation component). Concerning the degree of its physical foundation, WASA is a process-based model in the sense that all water fluxes represented in the model are assigned to a certain real-world hydrological process. As these processes are represented in the model by approximate, simplifying analogues of the underlying physical laws, WASA fulfils criteria common definition for a conceptual model. However, using another widely disseminated definition in hydrology, WASA is a physically-based model in the sense that its parameters can be derived from measurable physical characteristics of the study area.

4.1.2 Structure of spatial modelling units

The theoretical background for the way of structuring the study area into spatially distributed modelling units in WASA has been presented in Chapter 3.5.4. A hierarchical top-down disaggregation scheme is applied in order to capture the influence of spatially variable land-surface properties on soil moisture patterns and runoff generation. This hierarchy comprises five spatial scale levels (Fig. 4.1). The largest scale (level 1) is made up of *sub-basins* which are defined according to the location of gauging stations of river discharge, of large reservoirs with a storage capacity of more than $50 \cdot 10^6 \text{ m}^3$, and of the confluence of major rivers. Their size is in the order of 10^3 km^2 (Fig. 2.6). Alternatively, administrative units (*municipalities*) or *grid cells* can be used as the largest spatial units. If more than one grid cell compose a sub-basin (which is usually the case for grid cells in this study with an area of 100 km^2), their individual runoff responses are added up to give the total basin response. At this first level of the hierarchy, runoff routing in the river network (Chapter 4.2.8), including the retention and water balance of reservoirs (Chapter 4.2.7) and water use (Chapter 4.2.9) is simulated.

The subsequent structure at smaller scales of the hierarchy (levels 2-5 in Fig. 4.1) is based on the SOTER concept (Soil and TERRain digital database) (FAO, 1993), which establishes a way to structure the landscape according to geological, topographic and soil characteristics. The terrain and soil information of the study area by JACOMINE ET AL. (1973) has been transformed into the structure of SOTER (GAISER ET AL., 2002b) and modified and extended for hydrological purposes in this study. The units of level 1 are disaggregated into *landscape units* at level 2 (Fig. 4.1), which represent modelling units with similar charac-

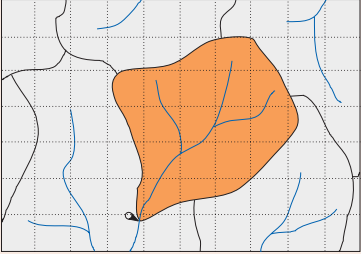
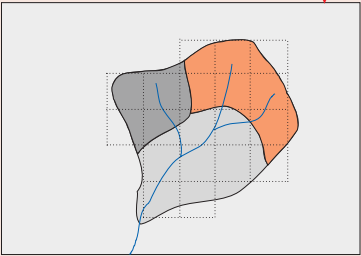
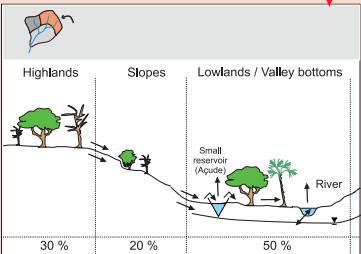
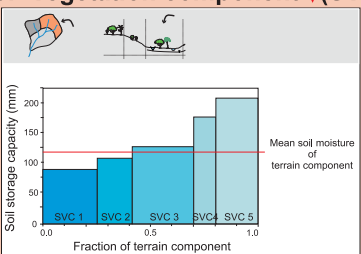
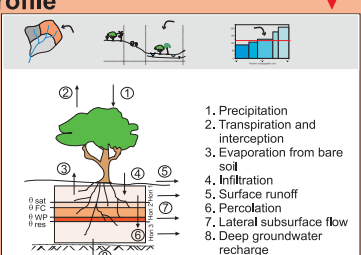
Level	Type and criteria of delimitation	Function
1 Sub-basin / Municipality / Grid cell 	<ul style="list-style-type: none"> - Polygons with geographically referenced location - Data source of basins: Terrain analysis of 30"-USGS-DEM and digitized topographic maps - Municipalities: administrative boundaries (municipios) 	<ul style="list-style-type: none"> ➤ Runoff routing, including retention in reservoirs and withdrawal by water use ➤ If grid cells smaller than sub-basin / municipalities are used: Runoff responses of all grid cells pertaining to a sub-basin are added up to give the basin response. Further sub-division (levels 2-5) starts from the grid cell level.
2 Landscape unit (LU) 	<ul style="list-style-type: none"> - Polygons with geographically referenced location - Similarity of <ul style="list-style-type: none"> - major landform - general lithology - soil associations - toposequences 	<ul style="list-style-type: none"> ➤ Modelling unit with similar characteristics referring to lateral processes and similarity of sub-scale variability in vertical processes ➤ Composed of 1 - 3 terrain components ➤ Runoff responses of all landscape units are added up to give total response of sub-basin / municipality / grid cell
3 Terrain component (TC) 	<ul style="list-style-type: none"> - Fraction of area of landscape unit (no geographic reference) - Similarity of <ul style="list-style-type: none"> - slope gradients - position within toposequence - soil associations 	<ul style="list-style-type: none"> ➤ Lateral transfer of surface and subsurface runoff between terrain components of different topographic position by upland-lowland relationships ➤ Reinfiltration and exfiltration (return flow) in component with lower topographic position
4 Soil-Vegetation component (SVC) 	<ul style="list-style-type: none"> - Fraction of area of terrain component - Characterized by specific combination of <ul style="list-style-type: none"> - Soil (sub-)type - Vegetation / land cover class 	<ul style="list-style-type: none"> ➤ Variability of soil moisture within terrain component ➤ Lateral redistribution of surface and subsurface runoff among soil-vegetation components ➤ Variability of soil moisture storage capacity within soil-vegetation component (partial area approach for saturation-excess surface runoff)
5 Profile 	<ul style="list-style-type: none"> - Representative profile of soil-vegetation component - Several soil horizons of variable depth - Lower limit by depth of root zone or bedrock 	<ul style="list-style-type: none"> ➤ Calculation of water balance in the profile for each soil-vegetation component ➤ Determination of vertical and lateral water fluxes for individual horizons

Fig. 4.1 Hierarchical multi-scale disaggregation scheme for structuring river basins into modelling units in WASA

teristics in terms of lateral processes and of the variability in vertical processes (Chapter 3.5.4). This is assumed to be the case if landscape units are similar in the underlying lithology and characterized by a typical toposequence, i.e., by a certain form of the general landscape surface and hillslope topography which may be associated in its different topographic parts with a specific soil association (i.e., a group of different soil types). The topographic part of this approach, i.e., similarity with regard to the major landform, is illustrated in Fig. 4.2, where different landscape units

are characterized by a typical slope length between the divide of singular valleys and the creek and by a typical mean slope gradient. These attributes of the spatial units of MDME (1981a,b) were combined with the mapping units of (JACOMINE ET AL., 1973) to derive for WASA the landscape units with geographically referenced location covering the entire study area of Ceará (Fig. A.1). The runoff volumes generated in each landscape unit of a sub-basin are added up to give the total response of the sub-basin.

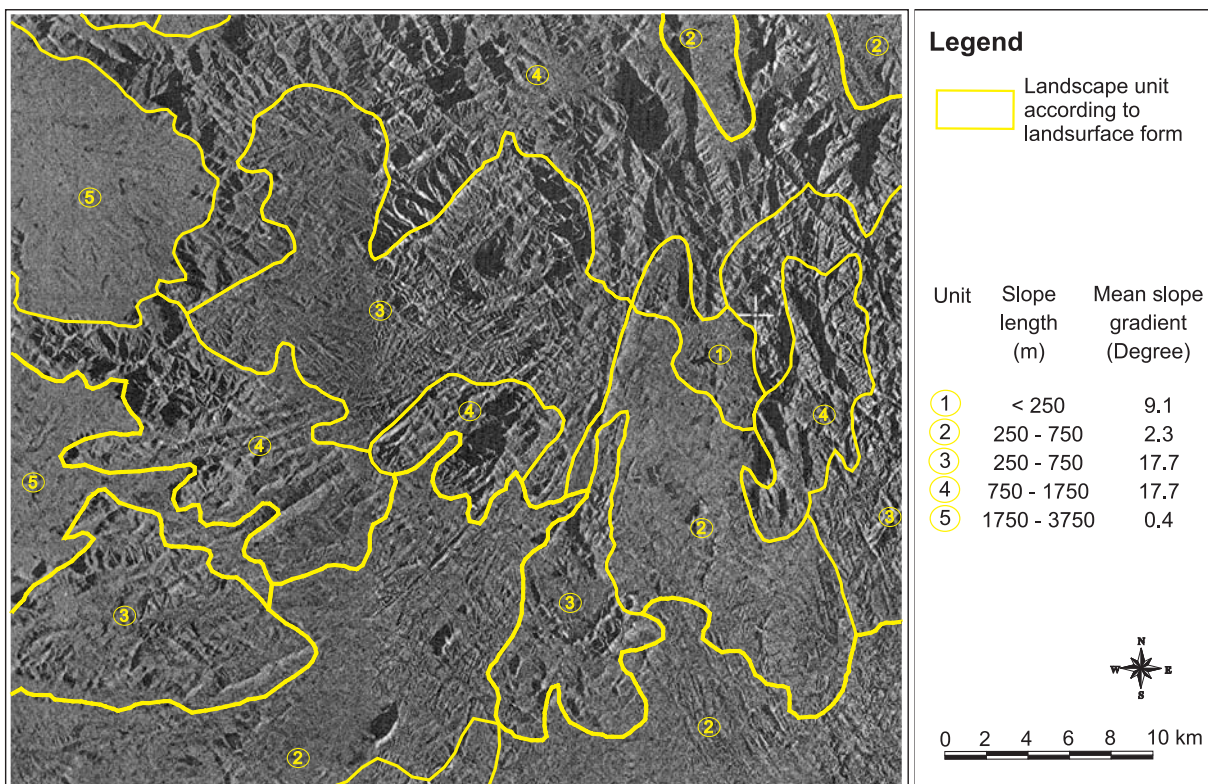


Fig. 4.2 Air-borne radar image of the Itatira region, Ceará, north-eastern Brazil, with delimitation and parametrization of landscape units with similar topography, based on MDME (1981A,B).

For the description of structured variability within the landscape units (Chapter 3.5.4), they are sub-divided into *terrain components* at level 3 of the hierarchy (Fig. 4.1). Each landscape unit is composed of three terrain components at most, representing highlands, slopes and valley bottoms, respectively. It is assumed that by using these three zones, the most important differences among topographic zones along the hillslope can be captured. Each terrain component is then characterized by a specific mean slope gradient, its position relative to other terrain components within the toposequence and by the occurrence of a specific soil type or soil association. If in a landscape

unit no significantly different topographic zones exist, the number of terrain components is reduced to two or one. In the study area, there is often no distinct highland zone, such that the number of terrain components for many landscape units is two. Terrain components are not represented by their exact geographic location in WASA, but only by their fraction of area within the landscape units. The definition of different terrain components allows to explicitly represent the interaction of surface and subsurface lateral flow components from upslope topographic zones with those at downslope position, including infiltration and return flow (see Chapter 4.2.5 and Chapter 4.1.3).

In order to describe the heterogeneity of soil moisture within terrain components, they are further subdivided into *soil-vegetation components* at the next smaller spatial scale (level 4 in Fig. 4.1). These are modelling units being each characterized by a specific combination of soil type and land cover (see Chapter 4.3.1). They are represented by their fraction of area within the terrain component without geographic reference. A partial contributing area approach (following CAPPUS, 1960; DUNNE & BLACK, 1970) is applied for the generation of saturation-excess surface flow in each soil-vegetation component. The water storage capacity of the soil as given by the representative soil profile (see below) is set to be variable within the soil-vegetation component in the form of a sectional linear distribution function (Fig. 4.3). Thus, for a given mean soil moisture of the soil-vegetation component, a certain fraction of its area can be saturated and generate surface runoff. The base points for the definition of the distribution are roughly estimated from data of soil types for which more than one exemplary soil profile is available. Assuming stochastic variability (Chapter 3.5.4) in the spatial distribution of soil-vegetation components within terrain components and their location relative to each other, lateral redistribution of surface and subsurface flow between them is taken into account (see Chapter 4.2.5 and Chapter 4.1.3).

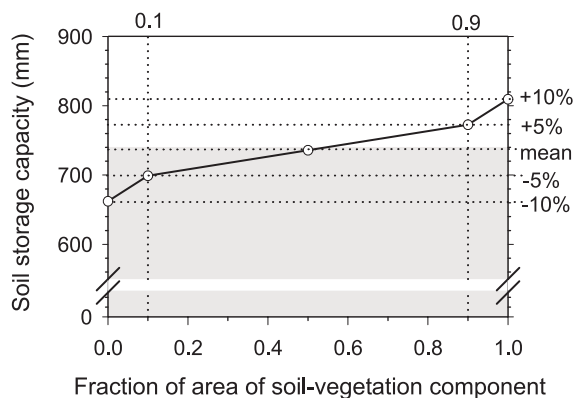


Fig. 4.3 Example for the distribution function of soil water storage capacity in a soil-vegetation component

Finally, at the smallest scale of the hierarchy (level 5 in Fig. 4.1), each soil-vegetation component is described by a representative *soil profile*, as given by JACOMINE ET AL. (1973) and GAISER ET AL. (2002b), combined with the vegetation information (Chapter 4.3.3). The number of soil horizons can be freely chosen and varies between different soil-vegeta-

tion components in WASA. In this study, it is set to the number of characteristic horizons for each soil type as given in the description of the representative profiles. The lower boundary of the profile is mainly set to the depth of bedrock or, if this is assumed to be too deep below the surface to influence surface processes, to the depth of the root zone (see also Chapter 4.3.2). The water balance of the profile is calculated including vertical processes as well as lateral flow components (Chapter 4.2). The latter are quantified for each horizon, which allows to capture, e.g., the saturated flow which may develop above less permeable layers or above bedrock (see also Chapter 4.2.4). Extending the profile to the depth of bedrock allows to represent near-surface groundwater bodies which may develop during the rainy season and reach into the root zone or to the soil surface.

4.1.3 Temporal sequence of process modelling

The temporal sequence of process modelling related to soil moisture dynamics and runoff generation within each timestep in WASA is as follows:

- 1.) Start with the terrain component of the highest topographic position within the landscape unit and do the following steps 2-10 for all soil-vegetation components (SVCs) in this terrain component.
- 2.) Update soil moisture of all horizons due to lateral subsurface inflow (produced in the previous timestep) from upslope terrain components and from SVCs of the same terrain component (Chapter 4.2.4, Chapter 4.2.5). If, due to this inflow, the soil water content of a profile exceeds its maximum possible water content at saturation, the surplus lateral inflow becomes surface runoff (return flow).
- 3.) Determine retention of precipitation in the interception storage and calculate interception evaporation (Chapter 4.2.1).
- 4.) Determine saturation-excess surface runoff by precipitation or lateral surface inflow (produced in the same timestep) from upslope terrain components onto a saturated fraction of the soil-vegetation component, as determined in the previous timestep (see point 9 below).
- 5.) Calculate infiltration with input from rainfall and lateral surface flow (produced in the same timestep) from upslope terrain component and from other SVCs of the same terrain component (Chapter 4.2.3). In parallel, the infiltration routine determines surface runoff due to infiltration-ex-

cess and saturation-excess (if the soil profile becomes completely saturated by the infiltrating water during the timestep).

- 6.) Update soil moisture of the uppermost and possibly deeper horizons by the infiltrated amount of water.
- 7.) Calculate plant transpiration and evaporation from the soil surface (both also as function of actual soil moisture) (Chapter 4.2.2) and update accordingly the soil moisture of all horizons.
- 8.) Calculate for each soil horizon the vertical water flux to the next deeper horizon or to deep groundwater and determine the lateral subsurface flow volumes to adjacent SVCs and to the

next downslope terrain component or to the river. Update the soil moisture of all horizons according to these outflows (Chapter 4.2.4).

- 9.) Determine the saturated fraction of the SVC as function of the actual soil moisture content of its representative soil profile (Fig. 4.3).
- 10.) Add up lateral outflow of all SVCs of the current terrain component (surface and subsurface flow, respectively) and distribute among river runoff and inflow to downslope terrain component (Chapter 4.2.5).
- 11.) Repeat steps 2-10 for all SVCs of the next downslope terrain component.

4.2 Process Representation

4.2.1 Interception model

For modelling of interception, a simple bucket approach is used in WASA. Rainfall above the canopy is added to the interception storage. If its maximum capacity is reached, surplus rainfall is attributed to the infiltration routine at the soil surface (Eq. 4.1).

$$I_t = I_{t-1} + P_I - E_I \quad (4.1)$$

with

$$P_I = \min(P, (I_c - I_{t-1})) \quad (4.2)$$

$$E_I = \min(E_{pot}, I_t) \quad (4.3)$$

I_t	Water in interception storage at timestep t	[mm]
I_c	Capacity of canopy interception storage	[mm]
P	Precipitation	[mm]
P_I	Intercepted precipitation	[mm]
E_I	Evaporation from interception storage	[mm]
E_{pot}	Potential evaporation	[mm]

I_c is dependent on the type of vegetation and its actual state of growth. A common approach is to describe this relationship based on the leaf area index Λ [m^2m^{-2}] of the canopy (DICKINSON, 1984):

$$I_c = h_I \cdot \Lambda \quad (4.4)$$

h_I Interception coefficient [mm per unit Λ]

Thus, the only parameter of the interception model is h_I , which can be related to the thickness of a water film on the leaves, with maximal values of 0.15-0.20 mm (MENZEL, 1997). However, using a daily

timestep, the parameter loses some of this physical meaning as it implicitly includes the temporal dynamics within a day, i.e., repeated partial filling and emptying of the interception storage. Thus, in daily models, a larger value of h_I is usually set. Here, in accordance with ZHU ET AL. (1999) for semi-arid conditions, $h_I = 0.3$ mm is used. E_{pot} is based on evaporation E_{PM} of the Penman-Monteith approach, setting $r_s = 0$ (Eq. 4.7).

If $E_I > 0$, it is assumed that in this timestep soil evaporation E_S and transpiration of the plants E_T are restricted by a reduced vapour pressure deficit within the canopy and, in addition for transpiration, by the water film on leaves. The reduction of E_T and E_S is assumed to be higher for a larger E_I or for a lower evaporation demand of the atmosphere. Thus, E_T and E_S are reduced, in total, by the amount of $1 - E_I/E_{pot}$. This amount is split up to give the individual amounts of reduction for E_T and E_S , respectively, depending on their ratio as calculated in Eq. 4.9 and Eq. 4.10.

Using WASA with an hourly timestep, a modification of the above interception model can be used in order to represent more dynamics of the interception process: (1) The interception storage may be refilled only partially during a timestep in the case of low rainfall intensities (Eq. 4.5, according to MENZEL, 1997) and (2) potential evaporation decreases as function of the actual content of the interception storage (Eq. 4.6, according to LIANG ET AL., 1994).

$$P_I = \min(I_c \cdot [1 - \exp(-0.75P)], I_c - I_{t-1}) \quad (4.5)$$

$$E_{pot} = E_{PM} \cdot \left(\frac{I_t}{I_c}\right)^{2/3} \quad (4.6)$$

4.2.2 Evapotranspiration model

The classical PENMAN-MONTEITH approach (PENMAN, 1948; MONTEITH, 1965), being used in WASA in a simplified form for evaporation calculation from the interception storage (Chapter 4.2.1) and from open water bodies (Chapter 4.2.7), reads:

$$E_{PM} = \frac{t}{\lambda} \left[\frac{\Delta A + \rho c_p D / r_a^a}{\Delta + \gamma(1 + r_s^c / r_a^a)} \right] \quad (4.7)$$

E_{PM}	Evapotranspiration	[mm per timestep]
t	Number of seconds in timestep	[-]
λ	Latent heat of vaporization of water	[J kg ⁻¹]
Δ	Gradient of the saturated vapour pressure curve	[hPa K ⁻¹]
A	Available energy	[J m ⁻² s ⁻¹] (= [W m ⁻²])
ρ	Density of air	[kg m ³]
c_p	Specific heat of moist air	[J kg ⁻¹ K ⁻¹]
D	Vapour pressure deficit at reference level	[hPa]
r_a^a	Aerodynamic resistance	[s m ⁻¹]
r_s^c	Canopy resistance	[s m ⁻¹]
γ	Psychrometric constant	[hPa K ⁻¹]

In WASA, the two-layer approach of SHUTTLEWORTH & WALLACE (1985) (S&W-model) (see Chapter 3.2.4) is used. Total evapotranspiration E of the land surface is composed of plant transpiration E_T and soil evaporation E_S (Eq. 4.8).

$$E = E_T + E_S \quad (\text{all in [mm]}) \quad (4.8)$$

Both components can be determined separately according to Eq. 4.9 and Eq. 4.10, but including their interrelation via the vapour pressure deficit of the air (according to Eq. 4.11). Three additional resistance parameters (all in [s m⁻¹]) are introduced (Fig. 4.4):

- r_a^c : bulk boundary layer resistance which controls the transfer between the leaf surfaces and a hypothetical mean canopy airstream at height z_m
- r_a^s : aerodynamic resistance which controls the transfer between the soil surface and z_m
- r_s^s : soil surface resistance of the substrate

$$E_T = \frac{t}{\lambda} \left[\frac{\Delta(A - A_s) + \rho c_p D_m / r_a^c}{\Delta + \gamma(1 + r_s^c / r_a^c)} \right] \quad (4.9)$$

$$E_S = \frac{t}{\lambda} \left[\frac{\Delta A_s + \rho c_p D_m / r_a^s}{\Delta + \gamma(1 + r_s^s / r_a^s)} \right] \quad (4.10)$$

A_s	Available energy at the soil surface	[J m ⁻² s ⁻¹]
D_m	Vapour pressure deficit inside the canopy	[hPa]

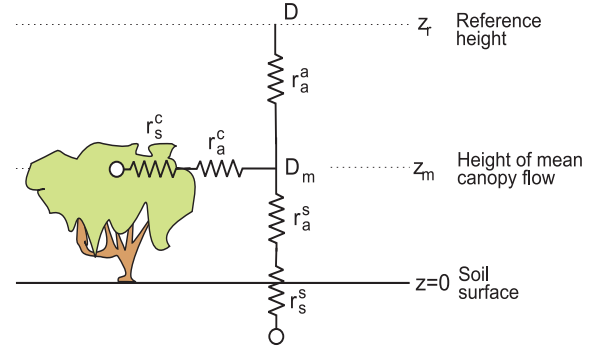


Fig. 4.4 Scheme of surface and aerodynamic resistances in the S&W-model

The vapour pressure deficit within the canopy D_m is related to D at the reference level above the canopy z_m by:

$$D_m = D + \frac{[\Delta A - (\Delta + \gamma)E] \cdot r_a^a}{\rho c_p} \quad (4.11)$$

Inserting Eq. 4.11 into Eq. 4.9 and Eq. 4.10, and combining both in Eq. 4.8 allows, after some transformations and elimination of D_m (see SHUTTLEWORTH & WALLACE (1985) for details), to solve for E . Inserting E into Eq. 4.11 gives D_m , and, finally, both evapotranspiration components can be calculated separately using D_m in Eq. 4.9 and Eq. 4.10. Determination of the remaining parameters (resistances and available energy) is described below.

In order to capture the important day-night nonlinearities of the evapotranspiration process (see Chapter 3.2.1), a concept of SCHULLA (1997) is used in WASA which allows to calculate daily evapotranspiration data with daily meteorological input by sub-dividing into a daytime (E_{Day}) and a night-time (E_{Night}) period internally in the model. Due to the location of the study area close to the equator, a good approximation is a duration of 12 hours for both periods throughout the year.

$$E = E_{Day} + E_{Night} \quad (\text{all in [mm]}) \quad (4.12)$$

Available energy for evapotranspiration modelling in Eq. 4.9 and Eq. 4.10 is determined from net radiation R_n (see also Eq. 4.20) and from soil heat flux G :

$$A = R_n - G \quad (4.13)$$

$$A_s = R_n^s - G \quad (4.14)$$

Net radiation during the day is made up of the short-wave radiation balance R_{sw} (Eq. 4.16) and long-wave radiation balance R_{lw} (Eq. 4.17, according to BRUNT, 1932; DYCK & PESCHKE, 1995). During the night, only R_{lw} applies as $R_G = 0$. Net radiation is negative.

$$R_n = R_{sw} + R_{lw} \quad (4.15)$$

$$R_{sw} = (1 - \alpha) \cdot R_G \quad (4.16)$$

$$R_{lw} = -f\sigma(0.52 + 0.065 \cdot \sqrt{e})(T + 273.2)^4 \quad (4.17)$$

α	(Short-wave) albedo of land surface	[-]
R_G	Total incoming short-wave radiation	[J m ⁻² s ⁻¹]
σ	STEFAN-BOLTZMANN constant	[J m ⁻² K ⁻⁴ s ⁻¹]
e	Vapor pressure	[hPa]
T	Air temperature	[°C]

α is dependent on the land cover type and the actual phenological state of vegetation (see Table 4.3). With regard to T , different values are used for day and night calculations. According to data of the study area given in CAVALCANTE ET AL. (1989), mean temperature during day and night are assumed to be 2.5°C higher and lower, respectively, than 24h-daily-mean temperature. f in Eq. 4.17 is a correction factor to represent cloudiness on incoming long-wave radiation (Eq. 4.18-Table 4.19) (summarized in SHUTTLEWORTH, 1992).

$$f = a_1 + a_2 \frac{n}{N} \quad (4.18)$$

$$\frac{n}{N} = \frac{R_G/R_{ex} - 0.18}{0.55} \quad (4.19)$$

n	Actual bright sunshine hours per day	[h]
N	Possible bright sunshine hours per day	[h]
R_{ex}	Radiation at top of atmosphere	[J m ⁻² s ⁻¹]
a_1, a_2	Empirical constants, $a_1 = 0.1, a_2 = 0.9$ for arid areas according to SHUTTLEWORTH (1992)	

In general, net radiation at the soil surface R_n^s is less than net radiation above the canopy R_n (all in [J m⁻² s⁻¹] = [W m²]) due to absorption within the canopy. This can be written using BEER's law:

$$R_n^s = R_n \cdot e^{-\kappa \Lambda} \quad (4.20)$$

κ Canopy extinction coefficient for net radiation [-]

κ was arbitrarily set to 0.7 in SHUTTLEWORTH & WALLACE (1985) and this value was used in several studies (e.g., BLYTH ET AL., 1999; WANG & TAKAHASHI, 1999). However, values given in other studies,

particularly those including semi-arid vegetation, are in the range of 0.3-0.7, with lower values for sparse field crops, intermediate for shrub canopies and larger values for denser broad-leaved forest canopies (KELLHER ET AL., 1995; NORMAN ET AL., 1995; SELLERS ET AL., 1996; WALKER & LANGRIDGE, 1996; BRISSON ET AL., 1998; ROCKSTRÖM ET AL., 1998; DOMINGO ET AL., 1999). DOMINGO ET AL. (1999) showed for semi-arid shrubs, that varying κ in the range 0.35-0.5 resulted in changes of simulated evapotranspiration of only 2%. In WASA, $\kappa = 0.5$ is used.

The soil heat flux G in Eq. 4.13 and Eq. 4.14 is set as a fraction of R_n^s . Maximum values of this fraction during midday may reach 0.35 for bare soil conditions (NORMAN ET AL., 1995). As an average fraction for the daytime period a value of 0.20 is used in WASA, in accordance with data given in OWE & VAN DER GRIEND (1990), STANNARD (1993), WALLACE & HOLLWILL (1997) and KABAT ET AL. (1997). As soil heat flux during the night accounts for a large part of net radiation, for the night-time period in WASA $G = 0.7 \cdot R_n$ is used.

The aerodynamic resistances in Eq. 4.9-Eq. 4.11 are all dependent on vegetation characteristics. r_a^c is influenced by the present surface area of leaves within the canopy (SHUTTLEWORTH & WALLACE, 1985):

$$r_a^c = r_a^l / (2\Lambda) \quad (4.21)$$

r_a^l Average boundary layer conductance of leaves (set to 25 s m⁻¹) [s m⁻¹]

r_a^a and r_a^s are influenced by canopy height h [m] and leaf area index (Eq. 4.22-Eq. 4.27, according to SHUTTLEWORTH & GURNEY, 1990). A logarithmic wind profile above the vegetation is assumed and the eddy diffusion coefficient, describing the turbulence within the canopy, is assumed to decrease exponentially within the canopy. The height of mean canopy flow z_m is set to 0.76 h . r_a^a is composed of an aerodynamic resistance above the canopy and a resistance between the top of the canopy and z_m (Eq. 4.23).

$$r_a^s = \frac{h \cdot \exp(c)}{c \cdot K_h} \cdot [\exp(-cz_o^s/h) - \exp(-cd/h)] \quad (4.22)$$

$$r_a^a = \frac{1}{ku} \cdot \ln\left(\frac{z_r - d}{h - d}\right) + \frac{h}{cK_h} \cdot \{\exp[c(1 - z_m/h)] - 1\} \quad (4.23)$$

with

$$d_p = 1.1h \cdot \ln(1 + 0.07\Lambda^{0.25}) \quad (4.24)$$

$$z_o = \begin{cases} z_o^s + 0.3h(0.07\Lambda)^{0.5} & 0 < 0.07\Lambda < 0.2 \\ 0.3h(1 - d_p/h) & \text{otherwise} \end{cases} \quad (4.25)$$

$$u = k \cdot w / \ln[(z_r - d_p)/z_o] \quad (4.26)$$

$$K_h = ku(h - d_p) \quad (4.27)$$

c	Eddy diffusivity decay constant in the canopy (=2.5)	[-]
K_h	Eddy diffusion coefficient at top of canopy	[m ² s ⁻¹]
k	KARMAN's constant	[-]
z_o^s	Roughness length of bare soil surface (=0.01)	[m]
z_o	Roughness length of canopy	[m]
d_p	Displacement height of canopy	[m]
w	Wind speed at reference height z_m	[m s ⁻¹]

The soil surface resistance is parameterized as function of soil water content in the uppermost soil horizon θ [m³ m⁻³], according to a relationship of DOMINGO ET AL. (1999) and averaging their parameters for bare soil and bare soil under plant canopies (see also Chapter 3.2.3):

$$r_s^s = a(\theta/\delta)^{-b} \quad (4.28)$$

δ	Bulk density of soil horizon	[kg m ⁻³]
a, b	Empirical constants $a = 26$, $b = -1$	[-]

Soil moisture in Eq. 4.28 refers, strictly in the sense of DOMINGO ET AL. (1999), to the first few centimetres of the soil column only. However, for simplicity, in WASA the complete first horizon is used, independent of its depth. As the soil dries out from the top in periods of no rainfall, soil moisture may, on the one hand, be assumed to be overestimated by this simplification. On the other hand, the effect of upward capillary flow, which provides additional moisture at the soil surface, is not considered otherwise in WASA. Both effects may be compensated to some degree by using the soil moisture of entire first horizon for parameterization of surface evaporation.

For estimation of canopy surface resistance, soil moisture, solar radiation and humidity of the air are taken into consideration as environmental stress factors which may increase minimum resistances by stomata closure (see also Chapter 4.2.2). Water stress in terms of low soil water availability is respected by a linear function of actual soil water potential Ψ [hPa] (see HANAN & PRINCE (1997) for a similar approach):

$$f_\Psi = \begin{cases} 1.0 & \Psi > \Psi_{cr} \\ 1 - \frac{\Psi - \Psi_{cr}}{\Psi_{wp} - \Psi_{cr}} & \Psi_{cr} > \Psi > \Psi_{wp} \\ 0.01 & \Psi < \Psi_{wp} \end{cases} \quad (4.29)$$

f_Ψ	Soil water stress factor	[-]
Ψ_{wp}	Soil water potential at wilting point	[hPa]
Ψ_{cr}	Critical soil water potential below which transpiration is reduced by stomata closure	[hPa]

First, f_Ψ is calculated for each horizon of the rooted soil zone. Then, a mean value of f_Ψ for the root zone is derived by averaging the individual values, weighted by the depth of the respective horizon. For estimation of Ψ see Chapter 4.3.2, for derivation of the parameters in Eq. 4.29 see Chapter 4.3.3.

The effect of a high vapour pressure deficit D [hPa] of the air is expressed according to STEWART (1988) (Eq. 4.30), with parameter $p = 0.03$ [hPa⁻¹] being an average of individual parameters for different semi-arid plant species given by HANAN & PRINCE (1997).

$$f_D = 1/(1 + pD) \quad (4.30)$$

f_D	Air humidity stress factor	[-]
-------	----------------------------	-----

According to JARVIS (1976) and STEWART (1988) the effect of the environmental stress factors can be combined multiplicatively:

$$\frac{1}{r_s^l} = g_s^l = g_{s,max}^l \cdot f_\Psi \cdot f_D \quad (4.31)$$

r_s^l	Stomatal resistance of leaf	[s m ⁻¹]
g_s^l	Stomatal conductance of leaf	[s m ⁻¹]
$g_{s,max}^l$	Maximum stomatal conductance of leaf	[s m ⁻¹]

$g_{s,max}^l$ is the reciprocal value of the minimum stomatal resistance $r_{s,min}^l$. Going from the leaf scale to the entire canopy, Eq. 4.31 is usually multiplied by the leaf area index Λ . However, a lower radiation input to leaves within the canopy as compared to the top of the canopy may lead to a lower stomatal conductance in lower parts of the canopy. This light dependence is included in the integration from leaf to canopy resistances by BALDOCCHI ET AL. (1991) and SAUGIER & KATERJI (1991) (Eq. 4.32).

$$\frac{1}{r_s^c} = g_s^c = \left(\frac{g_s^l}{\kappa}\right) \cdot \ln\left(\frac{b_R + \kappa R_G}{b_R + \kappa R_G \exp(-\pi\Lambda)}\right) \quad (4.32)$$

g_s^c	Canopy conductance	[s m ⁻¹]
b_R	Empirical plant-specific constant (=100)[J m ⁻² s ⁻¹]	

4.2.3 Infiltration model

Infiltration is simulated in WASA on the basis of the GREEN-AMPT approach in an adaptation of PESCHKE (1977, 1987) (see Chapter 3.3.2.1) and SCHULLA (1997) (see for details on the derivation of the approach in SCHULLA, 1997). Modifications were made here in terms of infiltration into layered soils, a two-iteration approach to capture lateral surface inflow, and a scaling factor for the hydraulic conductivity (see below).

The input to the infiltration routine R_F (Eq. 4.33, all in $[\text{mm } \Delta t^{-1}]$) is the precipitation P of the actual timestep, reduced by the amount being retained in the interception storage P_I , and increased by lateral surface inflow from a terrain component of a higher topographic position $R_{s,TC}$ and from other soil-vegetation components (SVCs) within the same terrain component $R_{s,SVC}$ (see Chapter 4.2.5). In order to account in an approximate manner for $R_{s,SVC}$, which may be produced on other SVCs of this terrain component during the same timestep, the below infiltration routine is applied with two iterations. In a first iteration, $R_{s,SVC}$ is set to be 0, and for each SVCs the infiltration-excess runoff of the timestep as caused by precipitation input and lateral flow from an upper terrain component is computed as a first estimation. Distributing these estimations among all SVCs (Chapter 4.2.5.1), this additional input for infiltration in terms of $R_{s,SVC}$ is taken into account in the second iteration of the infiltration routing for the same timestep, which produces the final values of infiltration and surface runoff for each SVC.

$$R_F = P - P_I + R_{s,TC} + R_{s,SVC} \quad (4.33)$$

The infiltration procedure checks first, starting with the uppermost horizon ($i = 1$), if and when during a time step saturation of its surface occurs. Saturation may only occur, if the saturated hydraulic conductivity $k_{s,i}$ of the soil horizon i , modified by the scaling factor s_F (see below), is lower than the available input rate R_F . If this is the case, then the moment in time $t_{s,i}$, when saturation of the surface of the horizon occurs is calculated by Eq. 4.34-Eq. 4.37.

$$t_{s,i} = F_{s,i} / R_F \quad (4.34)$$

with

$$F_{s,i} = d_{s,i} \cdot n_{a,i} \quad (4.35)$$

$$d_{s,i} = \frac{\Psi_{f,i}}{R_F / (k_{s,i} / s_F) - 1} \quad (4.36)$$

$$n_{a,i} = n_{t,i} - \theta_i \quad (4.37)$$

$F_{s,i}$	Infiltration volume until time $t_{s,i}$	[mm]
$d_{s,i}$	Depth of wetting front below top of horizon i at time $t_{s,i}$	[mm]
$n_{a,i}$	Refillable porosity of horizon i	[-]
$n_{t,i}$	Total porosity of horizon i	[-]
θ_i	Initial water content of horizon i	[Vol%/100] [-]
$\Psi_{f,i}$	Suction at wetting front of horizon i	[mm]
$k_{s,i}$	Saturated hydraulic conductivity	[mm $\Delta t^{-1}]$
s_F	Scaling factor	[-]

If $t_{s,i}$ is calculated to be larger than the duration of the timestep, no surface saturation occurs in this timestep and all precipitation infiltrates into this horizon. Otherwise, precipitation infiltrates at full rate into the soil horizon until $t_{s,i}$. After that, the infiltration rate decreases from $t_{s,i}$ until the end of the timestep at t approaching its limiting value $k_{s,i}$, with the cumulative infiltration amount F_i of the entire timestep being calculated according to Eq. 4.38.

$$F_i = F_{s,i}(t - t_{s,i}) + c \cdot \ln \frac{F_i + c}{F_{s,i} + c} + F_{s,i} \quad (4.38)$$

with

$$c = n_{a,i} \cdot \Psi_{f,i} \quad (4.39)$$

Eq. 4.38 is solved iteratively. If $i = 1$, the surplus of R_F (available input at the soil surface) which exceeds F_i is infiltration-excess surface runoff.

In the case of a layered soil, there are two possibilities that deeper horizons than the actual horizon i are also tested for infiltration excess:

- (1) If $d_{s,i}$ in Eq. 4.36 is larger than the total depth of the horizon i , $d_{h,i}$.
- (2) If R_F , reduced by the volume which was already retained to saturate possible upper horizons, exceeds the total refillable volume of this horizon ($n_{a,i} \cdot d_{h,i}$) due to limited horizon depth. This may happen if $t_{s,i}$ in Eq. 4.34 is larger than t or even if $k_{s,i}$ is larger than the precipitation rate.

In both cases, the horizon becomes completely saturated within the time $t_{s,i}$, using Eq. 4.40 instead of Eq. 4.34, without producing infiltration excess and setting $d_{s,i} = d_{h,i}$ in Eq. 4.35.

$$t_{s,i} = (d_{h,i} \cdot n_{a,i}) / R_F \quad (4.40)$$

In these cases, the above procedure is repeated for the next horizon j below, assuming the same input intensity as that of rainfall at the soil surface. Saturation at the soil surface occurs, if $t_{s,j}$ of this deeper horizon, increased by the duration needed for saturating the

above horizons, $t_{s,i}$, is smaller than time t at the end of the timestep. The total infiltration amount into the soil profile is then the sum of $F_{s,i}$ of the above horizons and F_j of the actual horizon being tested. The difference to R_F is surface runoff. The procedure is repeated for all successively deeper soil horizons until one with infiltration excess occurs or until the total infiltrated volume in all checked horizons equals the amount of available input R_F .

The scaling factor s_F in Eq. 4.36 is introduced primarily in order to counteract the underestimation of rainfall intensities when the temporal resolution of the model is lower than that of rainfall events and their internal variability. Accordingly, a rough estimate of the value of s_F is the ratio of average rainfall intensities of high resolution data (which are close to real rainfall intensities) to average rainfall intensities of data with the time resolution of the model. Additionally, the scaling factor may also be seen to adjust the infiltration routine to soil surface conditions which are not explicitly represented, i.e., surface crusts, macropores or small-scale variability. In this context, s_F is a calibration parameter. (See Chapter 5.2.1, Chapter 5.3.1.1, Chapter 5.3.3.1 and Chapter 6.1.3 for its derivation, sensitivity studies and discussion.)

4.2.4 Soil water model

The task of the soil water module is to determine, at the scale of a soil profile (Chapter 4.1.2), the soil moisture θ at each timestep t by balancing water fluxes going into the soil with those leaving the soil. Additionally, as the soil profile in WASA is sub-divided into various horizons, the vertical fluxes between these horizons are quantified. Only fluxes from top to down (percolation) are represented, reverse fluxes (capillary rise) are disregarded. For each horizon i , the soil water balance in a general form reads:

$$\theta_{i,t} = \theta_{i,t-1} + R_i - Q_i \quad (4.41)$$

The incoming fluxes R in Eq. 4.41 are:

- Infiltration, being added to soil moisture in the uppermost horizon only or in some cases also to lower horizons if they are tested for infiltration-excess (Chapter 4.2.3).
- Lateral subsurface flow (from terrain components of upslope position and from adjacent soil-vegetation components of the same terrain component, Chapter 4.2.5).
- Percolation from above horizon (see below).

The outgoing fluxes Q in Eq. 4.41 are:

- Evaporation at the soil surface (Chapter 4.2.2), being subtracted from soil moisture in the uppermost horizon only.
- Transpiration by vegetation. The total transpiration of the canopy determined in Chapter 4.2.2 is distributed among all horizons in the root zone to be subtracted from soil moisture by using a weighting factor for each horizon. The weighting factor is determined as the fraction of available field capacity in the horizon relative to total available field capacity in the root zone. The sum of weighting factors for all horizons equals 1.
- Percolation to the next horizon below, or to deep groundwater for the lowest horizon (see below).
- Lateral subsurface flow (to terrain components of downslope position or to the river and to adjacent soil-vegetation components of the same terrain component, Chapter 4.2.5)

The temporal order of modelling the above components within a timestep is given in Chapter 4.1.3.

Percolation $Q_{v,i}$ [mm] from one horizon i next horizon below (Eq. 4.42) is assumed to occur if the actual soil moisture exceeds soil moisture at field capacity. Following ARNOLD ET AL. (1990) (in ARNOLD & WILLIAMS, 1995) a temporal delay in percolation is assumed to depend on the travel time through the layer, which in turn is related to its actual (unsaturated) hydraulic conductivity (Eq. 4.43).

$$Q_{v,i} = \begin{cases} 0 & \text{if } \theta_i \leq \theta_{FC,i} \\ (\theta_i - \theta_{FC,i}) \cdot (1 - \exp(-1/t_{d,i})) & \text{if } \theta_i > \theta_{FC,i} \end{cases} \quad (4.42)$$

$$t_{d,i} = (\theta_i - \theta_{FC,i}) / k_{u,i} \quad (4.43)$$

θ_i	Actual soil moisture of horizon i	[mm]
$\theta_{FC,i}$	Soil moisture at field capacity in horizon i	[mm]
$t_{d,i}$	Travel time in horizon i	[hours or days]
$k_{u,i}$	Unsaturated hydraulic conductivity	[mm Δt^{-1}]

The volume of percolation from horizon i may be limited by the refillable porosity of the lower horizon, if the latter is smaller than $Q_{v,i}$ according to Eq. 4.43, or by its saturated conductivity. If the lowest horizon of the profile is situated above bedrock, percolation to deep groundwater may be limited by its hydraulic conductivity ($k_{s,LU}$).

For the quantification of lateral flow leaving the horizon $Q_{l,i}$, a simple relationship for saturated flow based on the DARCY-equation is applied (Eq. 4.44). The hydraulic gradient is given by the slope gradient of the terrain component s_{TC} [-] in which the actual

soil-vegetation component, represented by the soil profile, is located. Within in the structure of spatial units in WASA (Chapter 4.1.2), see Fig. 4.5 for illustration of the remaining geometric attributes to quantify the cross section A_Q [m²] of lateral flow.

$$Q_{l,i} = A_Q \cdot k_{s,i} \cdot s_{TC} \quad (4.44)$$

with

$$\begin{aligned} A_Q &= 2 \cdot l_{SVC} \cdot d_{s,i} = 2 \cdot \frac{\frac{1}{2} \cdot A_{SVC}}{a_{TC} \cdot l_{LU}} \cdot d_{s,i} = \\ &= \frac{a_{TC} \cdot a_{SVC} \cdot A_{LU}}{a_{TC} \cdot l_{LU}} \cdot d_{s,i} = \frac{a_{SVC} \cdot A_{LU}}{l_{LU}} \cdot d_{s,i} \quad (4.45) \end{aligned}$$

$$d_{s,i} = d_i \cdot \frac{\theta_i - \theta_{FC,i}}{\theta_{sat,i} - \theta_{FC,i}} \quad (4.46)$$

$Q_{l,i}$	lateral outflow from horizon i	[m ³ Δt ⁻¹]
$k_{s,i}$	Saturated hydraulic conductivity	[m Δt ⁻¹]
l_{SVC}	Contour length of soil-vegetation component being parallel to downslope TC or to river	[m]
$d_{s,i}$	Saturated depth of horizon i	[m]
d_i	Total depth of horizon i	[m]
A_{LU}	Area of landscape unit	[m ²]
A_{SVC}	Area of soil-vegetation component	[m ²]
l_{LU}	Slope length of landscape unit	[m]
a_{TC}	Fraction of area of TC in landscape unit	[-]
a_{SVC}	Fraction of area of SVC in terrain component	[-]
$\theta_{sat,i}$	Soil moisture at saturation in horizon i	[mm]

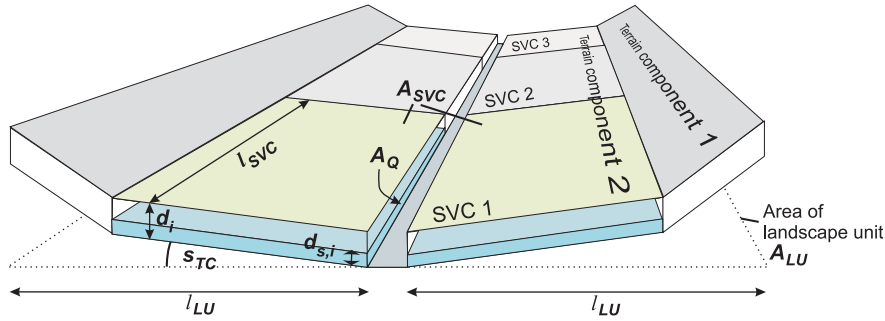


Fig. 4.5 Scheme of the structure terrain components (TCs) and soil-vegetation components (SVCs) within a landscape unit, with geometric attributes to calculate lateral subsurface flow, here for SVC 1 as an example. For simplicity, the soil profile of SVC 1 is composed of one horizon ($i=1$) only.

The factor 2 in the first term of Eq. 4.45 is introduced because the terrain components, and thus soil vegetation-components with their cross section for lateral flow are assumed to occur symmetrically on hillslopes on both sides of the river. The factor finally equals out in Eq. 4.45. The saturated zone of the horizon which contributes to lateral flow is assumed to build up on the lower boundary of the horizon, with its depth depending on the actual moisture content relative to saturation (Eq. 4.46).

The total amount of water which is available in each horizon for both percolation and lateral outflow is determined by the soil moisture which exceeds the field capacity of the horizon. Both flow components are reduced if their sum is exceeding the available soil moisture according to Eq. 4.47-Eq. 4.48:

$$Q_i = Q_{v,i} + Q_{l,i} \quad (4.47)$$

$$\text{if } Q_i > (\theta_i - \theta_{FC,i}) \left\{ \begin{aligned} Q_{v,i,red} &= Q_{v,i} \cdot \frac{Q_{v,i}}{Q_i} \\ Q_{l,i,red} &= Q_{l,i} \cdot \frac{Q_{l,i}}{Q_i} \end{aligned} \right. \quad (4.48)$$

The total lateral outflow of a profile $Q_{l,SVC}$ is the sum of the individual flows from each horizon.

4.2.5 Lateral redistribution among spatial units

Lateral redistribution of surface and subsurface runoff components and their interaction between different spatial units is taken into account in WASA at two different scale levels (see also Chapter 4.1.2):

1. Redistribution between soil-vegetation components (SVCs) within one terrain component (TC)
2. Redistribution between terrain components of different topographic position

As the above spatial units are known only by their percentage fraction of area within the next larger unit, redistribution between them is done on a statistical basis by deriving transition frequencies between them as a function of the above percentages.

4.2.5.1 Redistribution between soil-vegetation components

For each SVC within a terrain component, the generated runoff Q_{SVC} is separated into flow to a lower TC or to the river (Q_{TC}) and into flow to SVCs of the same TC (R_{SVC}), according to Eq. 4.49 and Eq. 4.50 (see also Fig. 4.6). Contrary to representation in the simplified scheme in Fig. 4.6, it is assumed that each SVC occurs distributed into several smaller patches within a terrain component, forming a randomly distributed mosaic of SVCs. Thus, lateral redistribution

may occur among all SVCs and Eq. 4.50 is calculated for all SVCs in the terrain component ($y=1$ to n).

$$Q_{TC} = \sum_{x=1}^n (Q_{SVC,x} \cdot a_{SVC,x}) \quad (4.49)$$

$$R_{SVC,y} = \sum_{x=1, x \neq y}^n (Q_{SVC,x} \cdot a_{SVC,y}) \quad (4.50)$$

- x Index of spatial unit (SVC) which is runoff source area for flow to be redistributed ($x=1$ in Fig. 4.6)
- y Index of spatial unit (SVC) which is runoff sink area of redistributed flow ($y=2$ and $y=3$ in Fig. 4.6)
- a_{SVC} Fraction of area of SVC in terrain component
- n Number of SVCs within a terrain component

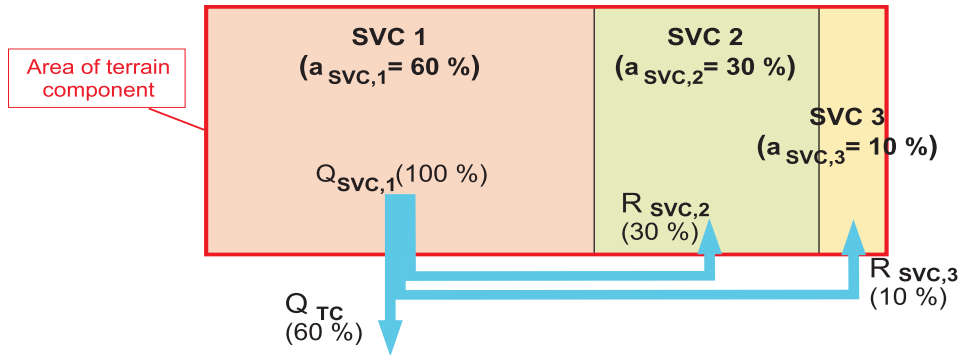


Fig. 4.6 Simplified scheme of lateral redistribution of water fluxes among soil-vegetation components (SVCs) within a terrain component (Tc). Example for a Tc composed of three SVCs and for SVC1 as source area of lateral flow. See Eq. 4.50 for explanation of flow percentages among SVCs.

Eq. 4.49 and Eq. 4.50 apply for surface and for subsurface runoff. In the case of surface flow, in receiving units, $R_{SVC,y}$ is added as input to the infiltration routine (Chapter 4.2.3). An equal spatial distribution within the receiving SVC is assumed, neglecting that runoff may be partly concentrated in rills. In the case of subsurface flow, lateral inflow into receiving SVCs is attributed to soil horizons with a similar depth below the terrain surface as the depth of the horizon in the source SVC (or to a horizon closer to the surface if the receiving soil profile is too shallow). If a soil profile is too wet or too shallow to absorb all incoming lateral subsurface flow, the remaining flow volume becomes surface runoff (return flow).

4.2.5.2 Redistribution between terrain components

Runoff generated in a terrain component $Q_{TC,x}$ is separated into flow to downslope TCs ($R_{TC,y}$) and to the river (R_{river}) (Eq. 4.51 and Eq. 4.52, Fig. 4.7). Eq. 4.52 is calculated for all terrain components of lower topographic position, i.e., for the slope area ($y=2$ in Fig. 4.7) which receives inflow from the highlands ($x=1$ in Fig. 4.7), and for the lowland area ($y=3$ in Fig. 4.7) which receives inflow both from the highlands and the slope area. Eq. 4.52 is calculated for the highlands which is the TC of the highest topographic position and cannot receive lateral inflow from above. The percentages of how much runoff from a higher TC is attributed as inflow to a TC of lower position or to the river is again a function of their respective fractions of area within the landscape unit. It is assumed

in this concept that a terrain component which makes up a larger fraction of the landscape unit may also retain a larger fraction of runoff originating from upslope areas.

$$R_{river} = \sum_{x=1}^m \left(Q_{TC,x} \cdot \frac{a_{TC,x}}{\sum_x a_{TC,x}} \right) \quad (4.51)$$

$$R_{TC,y} = \sum_{x=1}^{y-1} \left(Q_{TC,x} \cdot \frac{a_{TC,y}}{\sum_x a_{TC,x}} \right) \quad (4.52)$$

a_{TC} Fraction of area of TC in landscape unit [-]
 x Index of spatial unit (TC) which is runoff source area for flow to be redistributed
 y Index of spatial unit (TC) which is runoff sink area of redistributed flow
 m Number of TCs within a landscape unit

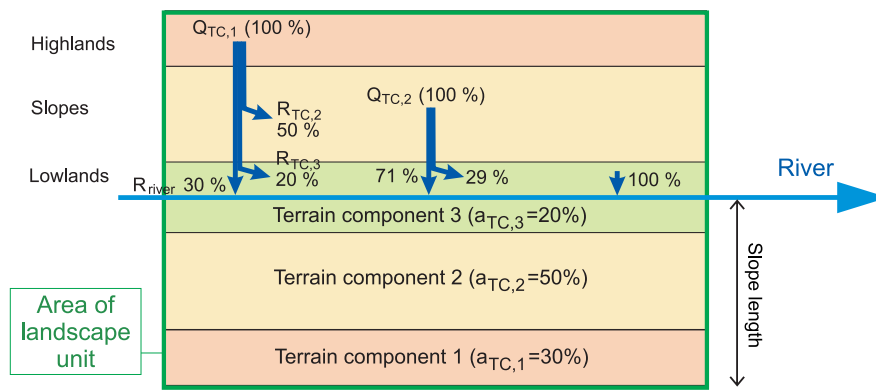


Fig. 4.7 Simplified scheme of lateral redistribution of surface water fluxes between terrain components. See Eq. 4.51 and Eq. 4.52 for explanation of the flow percentages among terrain components and the river.

Eq. 4.51 and Eq. 4.52 apply only for redistribution of surface runoff between terrain components. One part of surface runoff goes into the river network without interaction with downslope TCs, which can be attributed to channel flow which is not influenced by transmission losses. In the case of subsurface flow, $Q_{TC,x}$ is completely attributed to the next downslope TC, or to the river if the lowest TC has been reached. In this case of the lowest TC within a landscape unit, lateral subsurface flow may contribute to river runoff only if the saturated part of the runoff generating profile is located above the river bed. Parameter d_{rb} defines the depth of the river bed below the terrain surface of the lowest TC (in the simple example of Fig. 4.5 applies $d_{rb} = d_i$). For both surface and subsurface flow, lateral inflow from upslope TCs ($R_{TC,y}$) is distributed among all SVCs of the receiving TC according to the fraction of area of each SVC within the TC. Within the profiles of each SVCs, lateral inflow from a higher TC is distributed among horizons weighted by horizon depth.

4.2.6 Deep groundwater

Due to the dominance of near-surface processes for hydrology in semi-arid environments and in particular in the study area of Ceará, no extended approach for modelling of deep groundwater is included in WASA (see also Chapter 3.5.3). Near-surface saturated soil zones which may develop above the bedrock are included in the soil water module and the concept of lateral redistribution as shown in the previous chapters. Soil water which percolates below the soil zone being captured in the model or into the bedrock can be handled in different forms in WASA, being defined at the scale of the landscape units:

- In areas where no groundwater body of relevance for surface hydrology below the soil zone being captured by the model or within the underlying bedrock exists, the percolated water is assumed to be lost to deep groundwater and does not contribute anymore to the hydrological cycle within the model. This is the assumption made for areas of crystalline bedrock in the study area, where percolation

into the partly fractured bedrock is very low and its contribution to streamflow is assumed to be negligible within this study.

- In areas where a groundwater body with a significant contribution to streamflow is assumed, of which the groundwater level is however below the soil zone captured in the model or within the bedrock, the percolated water which leaves the lower boundary of the modeled soil zone is attributed to a conceptual groundwater storage with two outflow components: (1) a loss to deep groundwater which does not contribute to the hydrological cycle of interest or is lost by evaporation from the groundwater storage, defined as a constant fraction f_{GW} of input to the groundwater storage, and (2) outflow to the river network in the form of a simple linear storage approach (Eq. 4.53).

$$Q_{GW} = V_{GW}/k_{GW} \quad (4.53)$$

Q_{GW}	Outflow from deep groundwater storage	$[\text{m}^3 \text{d}^{-1}]$
V_{GW}	Actual stored volume in groundwater storage	$[\text{m}^3]$
k_{GW}	Storage constant	$[\text{d}]$

This approach is applied to the landscape units on sedimentary bedrock with deep soils or higher bedrock conductivity in the study area. k_{GW} can be derived from recession analysis or by calibration. For simplicity in the uncalibrated model version, k_{GW} is set to 1 (no time delay of groundwater outflow) and f_{GW} is set to 0.1, indicating a small loss of recharge to deeper groundwater.

4.2.7 Reservoir storage

4.2.7.1 Small and medium-sized reservoirs

The several thousands of small and medium-sized reservoirs (storage capacity smaller than $50 \cdot 10^6 \text{ m}^3$) (Chapter 2.1.5) are represented in WASA in an aggregated manner (see also Chapter 3.5.3). A cascade routing scheme is applied, where, for each sub-basin or municipality, the reservoirs are grouped into five size classes according to their storage capacity (Fig. 4.8). The number of reservoirs n_r in each class r is known for the year 1992 from CEARÁ (1992) and ARAÚJO (2000a). In order to account for the construction of new reservoirs during the simulation period, the actual number of reservoirs in each class is updated in every year of the simulation period. According to data given in BAZIN (1993) for the municipality of Tauá, the number of reservoirs increases exponentially between the year 1900 and 1992. This relationship is applied here to all reservoir classes in all municipalities or

sub-basins of the study area to give their number for the simulation year, resulting in the final, most recent data mentioned above for the year 1992. No general information is available for the temporal development in later, so the number of reservoirs is kept constant in the model after 1992.

For each class, the water balance is calculated for one hypothetical representative reservoir rm of mean characteristics, i.e., with a storage capacity $V_{max,rm}$ equal to the mean value of the respective class. The water balance of this mean reservoir is calculated on a daily basis according to Eq. 4.54.

$$V_{t,rm} = V_{t-1,rm} + (Q_{in,r} - U_r) / n_r - Q_{out,rm} + (P - E_{pot}) \cdot A_{rm} - R_{b,rm} \quad (4.54)$$

$V_{t,rm}$	Storage volume of mean reservoir rm in class r at timestep t	$[\text{m}^3]$
$Q_{in,r}$	Inflow to reservoir class r	$[\text{m}^3 \text{d}^{-1}]$
U_r	Withdrawal water use from class r	$[\text{m}^3 \text{d}^{-1}]$
$Q_{out,rm}$	Outflow from reservoir rm	$[\text{m}^3 \text{d}^{-1}]$
P	Sub-basin precipitation	$[\text{m}]$
E_{pot}	Potential evaporation (Eq. 4.7)	$[\text{m}]$
A_{rm}	Water body surface area of reservoir rm	$[\text{m}^2]$
$R_{b,rm}$	Infiltration losses to bedrock	$[\text{m}^3 \text{d}^{-1}]$

The total actual storage volume $V_{t,r}$ of reservoir class r is then obtained by:

$$V_{t,r} = V_{t,rm} \cdot n_r \quad (4.55)$$

For quantification of the inflow $Q_{in,r}$ to each reservoir class (Eq. 4.56), the following assumptions are made, which can be approximately justified when examining the spatial distribution of reservoirs within in river basins on topographical maps of the study area:

- The small and medium-sized reservoirs are located at tributaries to the main river of the sub-basin. Thus, inflow is provided only by runoff which is generated within the sub-basin itself where the reservoirs are located. (There is no runoff contribution from upstream sub-basins, which is attributed only to the large reservoirs of the main river, see Chapter 4.2.7.2).
- As no information on the exact location of the reservoirs is available, the total sub-basin area is equally distributed as runoff contributing area among the reservoir classes. To each of the five reservoir classes, one-sixth of the total sub-basin runoff Q_{gen} (added up from all landscape units, Chapter 4.1.2) in the actual timestep is attributed as direct inflow (without previous interaction with other reservoir classes). Another sixth part of the generated sub-basin runoff is directly attributed to

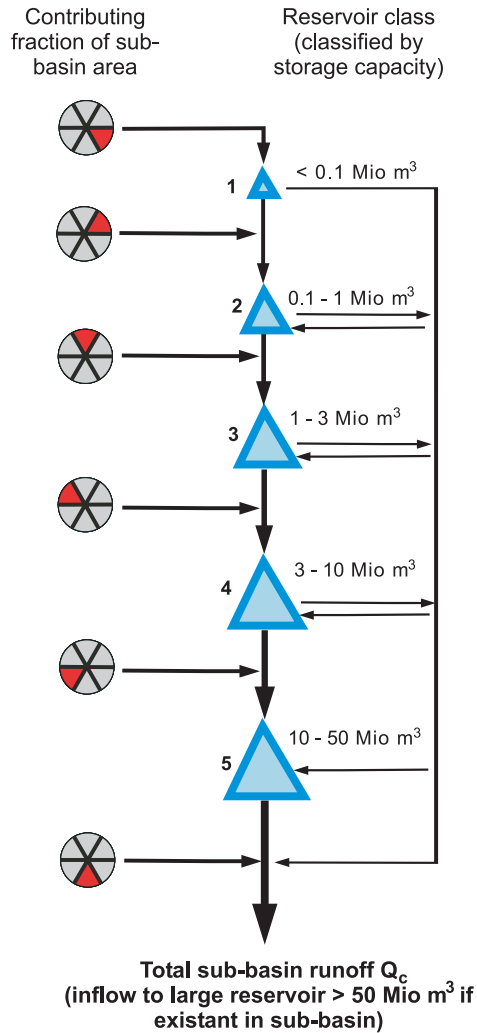


Fig. 4.8 Cascade scheme for runoff retention and routing between small and medium-sized reservoirs in each sub-basin or municipality in WASA.

the final sub-basin discharge without retention in any reservoir class (Fig. 4.8).

- Smaller reservoirs are located upstream of larger-sized reservoirs. Thus, additional inflow to a reservoir class r may be provided from outflow of reservoir classes x of smaller storage capacity (Eq. 4.56 and Fig. 4.8).

$$Q_{in,r} = Q_{gen}/6 + \sum_{x=1}^{r-1} ((Q_{out,xm} \cdot n_x)/(6-x)) \quad (4.56)$$

Outflow from the reservoirs $Q_{out,rm}$ of the five volume classes is assumed to occur only if the actual storage volume exceeds their storage capacity $V_{max,rm}$. This is valid particularly for small reservoirs, which are mainly simple earth dams without devices for regulated outflow. The latter may be available for some of them medium-sized dams, however, as information on operation and outflow volumes are rare, the above simplifying assumption is also applied to them.

In each timestep, the water balance of the reservoir classes is calculated, starting with the class 1, and proceeding to classes with successively larger storage capacity. Thus, outflow from one reservoir class is accounted for when determining inflow of larger reservoir classes in the same timestep, without time delay. The total runoff Q_c of a sub-basin or a municipality after the passage of the reservoir cascade of Fig. 4.8 is finally given by Fig. 4.57.

$$Q_c = Q_{gen}/6 + \sum_{r=1}^5 ((Q_{out,rm} \cdot n_r)/(6-r)) \quad (4.57)$$

The reservoir water surface area A_{rm} in Eq. 4.54 is estimated as a function of actual storage volume according to a relationship for small reservoirs derived from MOLLE (1989) (Fig. 4.58):

$$A_{rm} = c \cdot d \cdot \left(\frac{V_{t,rm}}{d} \right)^{((c-1)/c)} \quad (4.58)$$

c, d Empirical constants describing reservoir geometry (average values of Molle (1989):
 $c=2.7$ and $d=1000$)

Due to percolation into the underlying material, losses of the storage volume of small reservoirs (storage capacity $< 2 \cdot 10^6 \text{ m}^3$) were found to be in average 34% of evaporation losses (MOLLE, 1989). This relationship was used to estimate $R_{b,rm}$ in Eq. 4.54 for the three smallest reservoir classes (with storage capacity $< 3 \cdot 10^6 \text{ m}^3$). For the two larger classes, no information on percolation losses were available. A decreasing relative importance of percolation losses with increasing size of the reservoir can be assumed, because lateral outflow in the alluvial material below the dam, which is a major reason for the losses estimated by MOLLE (1989) for small reservoirs, will be less significant for the water balance of larger reservoirs. For reservoir classes 4 and 5 (storage capacity $3 \cdot 50 \cdot 10^6 \text{ m}^3$) $R_{b,rm}$ was set to 0.

4.2.7.2 Large reservoirs

For each of the about 45 large reservoirs with a storage capacity of more than $50 \cdot 10^6 \text{ m}^3$, the water balance is calculated explicitly in WASA. These reservoirs are located at larger rivers, at the most downstream location of a sub-basin (Chapter 4.1.2) and may obtain inflow Q_c from this sub-basin after the passage of the cascade of small and medium-sized reservoirs (Chapter 4.2.7.1) and inflow from upstream sub-basins via the river network (Q_{in}). The water balance of a large reservoir LR is calculated on a daily basis according to Eq. (see also Eq. 4.54).

$$V_t = V_{t-1} + Q_c + Q_{in} - Q_{out} - U_{LR} + (P - E_{pot}) \cdot A_{LR} \quad (4.59)$$

V_t	Storage volume at timestep t	$[\text{m}^3]$
Q_{out}	Outflow from reservoir	$[\text{m}^3 \text{ d}^{-1}]$
U_{LR}	Withdrawal water use from reservoir	$[\text{m}^3 \text{ d}^{-1}]$
A_{LR}	Water surface area of reservoir	$[\text{m}^2]$

Losses by percolation into the bedrock of the reservoirs are not accounted for as no information is available. Outflow Q_{out} is composed of

- 1) Uncontrolled outflow over the spillway (Q_{exc}) in the case that the storage capacity of the reservoir V_{max} is exceeded by the actual storage volume
- 2) Controlled outflow by reservoir management (Q_{contr})

Exact operation rules for reservoir outflow as function of actual storage volume and water demand are not available. Instead, simple rules according to ARAÚJO (2000) are applied for estimation of Q_{contr} , summarizing common practice of reservoir management in the study area:

- The outflow is a fraction f_Q of Q_{90} , i.e., the annual runoff from a reservoir which is provided with a probability of 90% (in 90% of all years). Q_{90} is given for the large reservoirs based on simple hydrological modelling, e.g., in CEARÁ (1992), COGERH (2000), and summarized also in ARAÚJO (2000a). The fraction f_Q of Q_{90} is equally distributed to daily runoff among all days of the year, seasonal variations are not taken into account due to the lack of detailed information.
- f_Q is set to 0.8 for so-called strategic reservoirs (i.e., reservoirs with a storage capacity greater than than 300 Mio. m^3 , and reservoirs important for water supply of the metropolitan area of Fortaleza), and f_Q is set to 0.9 for the other large dams.

- If the actual storage volume of the reservoir falls below a reservoir-specific alert volume V_{al} , the above outflow is reduced by a factor f_{al} , defined here as:

$$f_{al} = (V_t - V_{min}) / (V_{al} - V_{min}) \quad (4.60)$$

V_{min} Dead volume of reservoir below which outflow equals 0 $[\text{m}^3]$

For reservoirs for which the above information was not available, V_{al} and/or V_{min} are set to 0.

The surface area A_{LR} of the reservoir is calculated by an volume-area function (Eq. 4.61), of which the parameters c_{LR} and d_{LR} were derived by fitting the function to geometric data of the individual reservoirs as summarized by ARAÚJO (2000a).

$$A_{LR} = c_{LR} \cdot (V_t)^{d_{LR}} \quad (4.61)$$

For reservoirs without available geometric data, mean values of c_{LR} and d_{LR} , derived from all other reservoirs with available information, are used. An additional parameter required for each large reservoir is its year of inauguration, from which on the reservoir is considered in the model.

The above reservoir parameters are based on different sources, in particular on a summary by ARAÚJO (2000), and additionally on information given in ARAÚJO (2000a), CEARÁ (1992), FUNCEME (1998a) and COGERH (2000). All parameters values are listed in Table A.2.

4.2.8 River network routing

Sub-basins or municipalities are connected to each other within a dendritic river network. In the case of municipalities, an approximate network is established by attributing to each municipality a stretch of the next major river. The routing process of river runoff through each of these units is approximated by a daily linear response function (Eq. 4.62. and Fig. 4.9)

$$Q_{out,j} = \sum_{i=1}^j Q_{in,i} \cdot h_{j-i+1} \quad (4.62)$$

$Q_{out,j}$	Outflow from sub-basin at timestep j	$[\text{m}^3 \text{ d}^{-1}]$
$Q_{in,i}$	Inflow into sub-basin at timestep i	$[\text{m}^3 \text{ d}^{-1}]$
h_i	Value of the response function, with $h_i > 0$ and $\sum h_i = 1$	$[-]$

The response function is characterized by the parameter t_l which specifies the lag time between a runoff

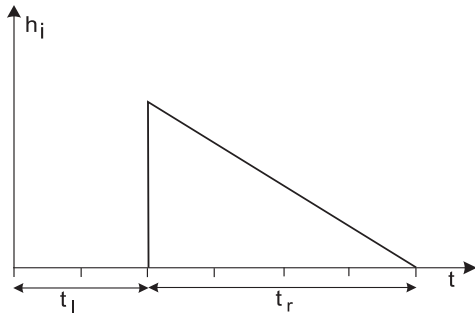


Fig. 4.9 Scheme of the linear response function for runoff routing in the river network.

input to the sub-basin and the first runoff response at its outlet, and by parameter t_r which specifies the maximum retention time in the sub-basin, i.e., the time period over which the runoff response to a given input is distributed by the routing process. t_r is used to describe the triangular distribution as shown in Fig. 4.9. Both parameters are estimated by dividing the channel length in the sub-basin (derived from GIS terrain analysis) by a mean, minimum and maximum flow velocity in the river of a sub-basin, based on the MANNING-STRICKLER equation for different flow depths (BRONSTERT ET AL., 1999).

In each sub-basin, transmission losses are subtracted from the inflow $Q_{in,i}$. In this context, WASA accounts for direct withdrawal from the river due to water use (Fig. 4.2.9) and for evaporation losses from the river surface. Infiltration losses are not accounted for in this model version as no reliable information on their magnitude for different boundary conditions are available. Evaporation losses are computed by multiplying the potential evaporation rate (Eq. 4.7) with the evaporating water surface, which is, in turn, being derived from the channel length in the sub-basin (see above) and the channel width w_{ch} [m], estimated as function of discharge Q [$m^3 s^{-1}$] by a global relationship derived from LEOPOLD (1994):

$$\log(w_{ch}) = \log(Q) \cdot 0.494 + 1.031 \quad (4.63)$$

4.2.9 Water use

The quantification of water use in WASA is based on the water use model NOWUM (Nordeste Water Use Model) (HAUSCHILD & DÖLL, 2000), being coupled with WASA according to the implementation of both components (WASA and NOWUM) into the integrated model of the WAVES project, SIM (KROL ET AL., 2001) (Chapter 1.1).

NOWUM computes water use for each municipality of the study area. Five water use sectors are distinguished (HAUSCHILD & DÖLL, 2000):

- *Irrigation water use* is calculated following the method of CROPWAT (FAO, 1992). It is a function of irrigated agricultural area per crop class (9 crop classes are differentiated here), climate (potential evaporation, precipitation), and a crop coefficient varying with the phenological state of the crop.
- *Livestock water use* is determined by multiplying the number of livestock and a livestock-specific water use value.
- *Domestic water use* is calculated as a function of population number and withdrawal water use per person. It is differentiated between self-supplying population and population connected to the public water supply system.
- *Industrial water use* is computed as the product of the required water volumes per production output and the industrial gross domestic product for different industry branches.
- *Touristic water use* is determined as a function of overnight stays and withdrawal water use per tourist.

The temporal resolution of water use values varies among the five sectors as a function of the available data (e.g., daily for irrigation water use, annual for livestock water use). In the case that water use data have of a lower than the regular daily resolution of WASA, they are equally distributed among all days of the given period. Water use is, first, computed as withdrawal water use, i.e., the quantity of water taken from its source location (e.g., from a river or reservoir). This value depends, beside of the maximum demand as explained above, on the actual water availability, i.e., withdrawal water use is reduced if available water resources area small in dry years or in the dry season. Subsequently, applying specific coefficients of the water use efficiency for each sector, the amount of consumptive water use for each municipality is calculated, i.e., the quantity lost in the system during the water use activity, e.g., by evaporation. The difference between withdrawal and consumptive use is returned into the river and reservoir network, being available for further use at downstream positions. The distribution of water withdrawal among different sources is controlled by global values for Ceará, given in the model SIM (about 70% from reservoirs, 20% from rivers and 10% from groundwater). Further details on the methodology for water use calculation and its parametrization are given in HAUSCHILD & DÖLL (2000). The given basic data, e.g., irrigation areas,

livestock numbers, population numbers, industrial production and tourism are mainly derived from surveys of the study area in the late 1990s. The interannual variability and long-term trends of the resulting water use data are introduced only by climatic variability, but not by regional development as the expansion of irrigation zones, industrialization and population in-

crease. Thus, water use in earlier decades may be overestimated with the given data in the model. If WASA is run at the scale of sub-basins, water use is nevertheless determined for municipalities as explained above, and then attributed to the sub-basins by weighting with the fraction of area of the municipalities pertaining to a sub-basin.

4.3 Derivation of Modelling Units and Parameters

4.3.1 Derivation of soil-vegetation components

The definition of landscape units and terrain components within the multi-scale spatial concept has already been illustrated in Chapter 4.1.2 (see also Chapter 4.3.2). Due to the complexity, the derivation of soil-vegetation components which represent the combined spatial distribution of soil and land cover in the landscape as sub-scale units of landscape units and terrain components, is here explained separately. A scheme was developed to merge land cover data (natural vegetation and agricultural use) and soil data from different sources with, consequently, differing data type and resolution. Land cover data of agricultural land use as well as data on the spatial distribution of soil types were available only as percentages of area within larger units of which the exact location is known (i.e., municipalities and landscape units, respectively). The data preparation methodology thus includes, on the one hand, the intersection of different data layers with geographic reference in a Geographical Information System (GIS) (steps 2-3 in Fig. 4.10). On the other hand, the combination of vegetation and soil units is done also at the sub-grid scale of these geographically referenced units (steps 4-7). Here, instead of a simple uniform merging of all land cover units with all soil components (SCs), i.e., soil types, the approach respects preferred combinations of land cover and soils by using suitability indices of soil components for agricultural use (step 5) (GAISER ET AL., 2002b). The agricultural area of different crops in each municipality per suitability index class (step 6) is known from an agricultural census (IBGE, 1996). The suitability indices allow to allocate crop areas to the different SCs in each municipality (step 6), while the area of natural vegetation attributed to these SCs in the previous steps 2-4 is reduced accordingly. Similarly, fallow areas and degraded areas (including long-term fallow areas and forest pasture) are attributed to the SCs, assuming that they also primarily occur on SCs

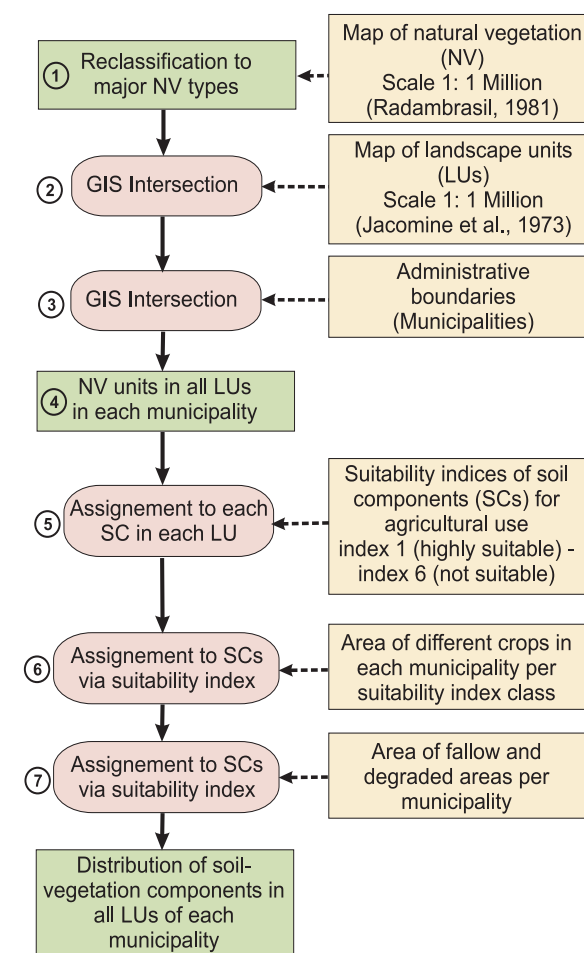


Fig. 4.10 Scheme for derivation of soil-vegetation components (see also text for explanations).

better suitable for agricultural production (step 7). Similarly to the scheme in Fig. 4.10, the distribution of soil-vegetation components can be derived for river basins by using basin boundaries in step 3 and assigning agricultural and degraded areas to basins by merging the data of the municipalities of each basin. In order to maintain a manageable number of units in the

model, soil-vegetation components of small spatial extent (< 1% fraction of area within terrain component) were skipped. The number of SVCs in the terrain components of the study area is in average about 10, with a maximum number of 25. For the final distribution of the major soil and land cover types in the study area, see Table 2.1 and Table 4.3, respectively

4.3.2 Soil and terrain parameters

Table 4.1 gives an overview on the required soil and terrain parameters at the different scale levels. If not otherwise explained in the following, the above parameters were derived from a soil and terrain data base of the study area, which has been set up by GAISER ET AL. (2002b) on the basis of the soil survey of JACOMINE ET AL. (1973) (see also Chapter 4.1.2). The mapping units of JACOMINE ET AL. (1973) correspond to the landscape units within the structure of WASA (see also FIG. A.1). Accordingly, about 150 landscape units are differentiated in the study area, however, some of them with very small areas or small differences in their characteristics. No attempt was made to aggregate them to a lower number as this would have included subjective reasoning in skipping some of the detailed information. l_{LU} was derived from interpreted radar remote sensing data of MDME (1981a,b) (see Fig. 4.2). A weighted mean value of l_{LU} was built if more than one slope length class of MDME (1981a,b) were located within the landscape units. Derived slope lengths in the study area vary between about 0.2-2.5 km. The hydraulic conductivity of the bedrock is required only in those landscape units where the soil depth being modelled in WASA reaches down to the bedrock, i.e., with mainly shallow soils. This is the case for the crystalline area where $k_{s,LU}$ is set to a low value of 0.1 mm d^{-1} , which implies nearly impermeable conditions as assumed in hydrological surveys of the area (e.g., CADIER, 1996). If not given by the profile description (see below), the maximum profile depth to bedrock d_{max} was set to 1.8 m in the crystalline area, according to information given in JACOMINE ET AL. (1973). For alluvial soils in valley bottoms, a mean value of $d_{max} = 4.5 \text{ m}$ was estimated from data on the depth of alluvial wells throughout the study area (data base of CPRM, 1999) and from rough mean data of CPRM (1996) and MANOEL FILHO (2000). For landscape units on sedimentary bedrock, values of $k_{s,LU}$ were estimated on the base of data from hydrogeological studies (CEARÁ, 1992; MARWELL FILHO, 1995; DNPM, 1996) and d_{max} was usually set to 2.5 m. For the deep soils on plateaus of the Serra Grande and the Exu formation, the soil profile was not

at all confined by bedrock in the model. For parameter d_{rb} no data are available in the literature. According to field observations and hydrological reasoning, it was set to 1.8 m. This implies that all common, shallow soils on crystalline bedrock can drain completely into the river, except for especially deep soils like alluvial soils. These latter may be saturated in the lower parts without contributing to runoff, as frequently observed in the study area, particularly in the dry season.

Table 4.1 Soil and terrain parameters in WASA at different spatial scale levels.

Landscape unit		
A_{LU}	Area	[km ²]
l_{LU}	Mean slope length	[m]
$k_{s,LU}$	Hydraulic conductivity of bedrock	[mm d ⁻¹]
d_{max}	Maximum profile depth to bedrock	[m]
d_{rb}	Depth of river bed below terrain surface	[m]
Terrain component		
a_{TC}	Fraction of area in landscape unit	[-]
s_{TC}	Slope gradient	[-]
Soil-vegetation component		
a_{SVC}	Fraction of area in terrain component	[-]
Soil profile (parameters for each horizon)		
n_t	Porosity (Vol%/100)	[-]
k_s	Saturated hydraulic conductivity	[mm d ⁻¹]
ψ_f	Suction at wetting front	[mm]
s_F	Scaling factor for hydraulic conductivity	[-]
ϕ_c	Content of coarse fragment (Vol%/100)	[-]
θ_{res}	Residual water content (Vol%/100)	[-]
λ_s	Pore-size index	[-]
h_b	Bubbling capillary pressure	[mm]

The extensive explanatory information on terrain characteristics and distribution of soil types in the landscape given in JACOMINE ET AL. (1973) was used to estimate the terrain component parameters a_{TC} and s_{TC} for all landscape units. Additional information on the spatial distribution of alluvial soils in valley bottoms was included based on the soil map of SARA (1987). The resulting distribution of soil (sub-)types within terrain components was combined with information on land cover according to Chapter 4.3.1 to give a_{SVC} .

It has to be noted that the terrain parameters, including the spatial distribution of different sub-units, are based on rough estimates of low spatial resolution and partly on qualitative data. They are, thus, burdened with high uncertainty.

For parameterization of soil profiles, for each of the about 50 different soil types or sub-types differentiated in the study area, one or more exemplary profiles are available from the above mentioned data base. In the case that several exemplary profiles were available for one soil type, a mean profile was derived while retaining the characteristic horizons of the soil type. Relevant given soil physical properties used here were soil texture (sand, silt and clay content), bulk density ρ_b [g cm^{-3}] and the content of coarse fragments ($>2\text{mm}$) ϕ_c . Soil porosity n_t was derived by Eq. 4.64.

$$n_t = 1 - \rho_b / \rho_p \quad (4.64)$$

ρ_p Soil particle density (=2.65) [g cm^{-3}]

For estimating water retention characteristics, i.e., the relationship between matrix potential and soil water content ($\Psi(\theta)$ or $\theta(\Psi)$, which includes the specific values at field capacity and wilting point, θ_{FC} (Eq. 4.42) and Ψ_{wp} (Eq. 4.29)), the model of VAN GENUCHTEN (1980) is applied in WASA. Its parameters θ_{res} , λ_s and h_b , required as input data (Table 4.1), were derived from soil texture based on regression equations by RAWLS & BRAKENSIEK (1985) as cited in RAWLS ET AL. (1992). The wetting front suction ψ_f required for the infiltration model (Eq. 4.36) was also derived from these parameters using a relationship of RAWLS & BRAKENSIEK (1983) as cited in RAWLS ET AL. (1992).

Saturated hydraulic conductivity k_s is estimated based on a KOZENY-CARMAN-type equation which was adapted to Brazilian tropical soils, including some of the study area, by TOMASELLA & HODNETT (1997). Assuming that n_t equals approximately the effective porosity of the soil the relationship reads (Eq. 4.65):

$$k_s = 24 \cdot 56540 \cdot n_t^{4.5359} \quad (4.65)$$

Unsaturated conductivity as a function of water content ($k_u(\theta)$, Eq. 4.43) is again estimated by the relationship of VAN GENUCHTEN (1980).

In order to account for the content of coarse fragments in the soil, which is assumed to reduce water storage capacity as well as conductivity, water content characteristics (as θ_{WP} , θ_{FC} , n_t) as well as conductivities are multiplied by ϕ_c after the application of the above pedo-transfer-functions.

4.3.3 Vegetation parameters

Table 4.2 summarizes vegetation-specific parameters required for evapotranspiration and soil moisture modelling in WASA.

Table 4.2 *Vegetation parameters in WASA; (var) indicates that these parameters may vary between the rainy and dry season.*

h	Canopy height (var)	[m]
d_r	Root depth (var)	[m]
Λ	Leaf area index (var)	[-]
α	Albedo (var)	[-]
$r_{s,min}^l$	Minimum stomatal resistance	[s m^{-1}]
Ψ_{wp}	Soil matrix potential at wilting point	[hPa]
Ψ_{cr}	Critical soil matrix potential below which stomata closure occurs	[hPa]
h_I	Interception coefficient	[mm]

Quantitative data of vegetation characteristics for the vegetation types of the study area are rare. Some data on vegetation height and biomass are given in MDME (1981a,b), PFISTER & MALACHEK (1986), HAYASHI (1995), SAMPAIO (1995), FUNCEME (1998b), SAMPAIO ET AL. (1998), TIESSEN ET AL. (1998). HALM (2000) is the only study giving α and Λ for caatinga, cerrado and some crops, including their annual course. Information on root depth is included in JACOMINE ET AL. (1973).

Due to the limited availability of vegetation data from the study area itself, results from other semi-arid areas, mainly at small scales, were taken into consideration, particularly for estimation of ranges of α and Λ (ALLEN ET AL., 1994; BLYTH & HARDING, 1995; HUNTINGFORD ET AL., 1995; BRENNER & INCOLLN, 1997; HANAN & PRINCE, 1997; KABAT ET AL., 1997; ROCKSTRÖM ET AL., 1998; BLYTH ET AL., 1999; BOULET ET AL., 1999; DOMINGO ET AL., 1999; WANG & TAKAHASHI, 1999; HUNTINGFORD ET AL., 2000; TAYLOR, 2000). Additional information on α and Λ and their annual course is provided by parameterizations at the global scale, i.e., for major biomes of the world including semi-arid environments (DORMAN & SELLERS, 1989; DOLMAN, 1993; SCHULZE ET AL., 1994; KELLIHER ET AL., 1995; FENNESSY & XUE, 1997; MARTIN, 1998). Data on plant characteristics of agricultural crops are provided by crop files of the agricultural production models EPIC (WILLIAMS ET AL., 1984) and CROPWAT (FAO, 1992), which were partly adapted to the conditions of the study area (HILGER ET AL., 2000).

Additionally, an estimate of maximum Λ for caatinga vegetation during the rainy period was based on leaf biomass data. Summarizing data from various vegetation types in wet and dry environments for which leaf biomass as well as corresponding leaf area index values were given (WALTER & BRECKLE, 1991; MENAUT ET AL., 1995; DIAMANTOPOULOS ET AL., 1996; PUIG-DEFABREGAS ET AL., 1996) resulted in a reasonably defined linear relationship (Fig. 4.11).

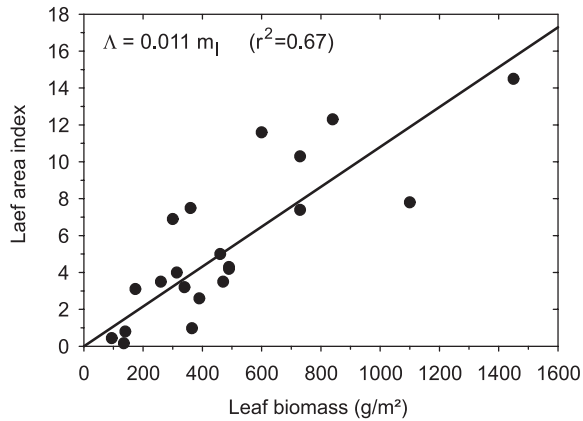


Fig. 4.11 Relationship between leaf biomass m_l and leaf area index Λ derived from various vegetation types.

For leaf biomass data of a natural stand of caatinga (HAYASHI, 1995), a maximum value of $\Lambda = 5.1$ is obtained according to Fig. 4.11. This value corresponds to data given by HALM (2000). Lower values of $3.2 < \Lambda < 4.3$ result for biomass data of Tiessen et al. (1998) and PFISTER & MALACHEK (1986) ($\Lambda = 1.3$). The latter two studies were made in caatinga stands used for cattle grazing. The range of above Λ values for typical vegetation of the study area demonstrates the large variety of caatinga forms in dependence of local climatic and pedological conditions and human activity.

Concerning minimum stomatal resistance ($r_{s,min}^l$, Eq. 4.31), KÖRNER (1994), in a broad review, gives as maximum stomatal conductance for semi-arid shrubs a mean value of $198 \text{ mmol m}^{-2} \text{ s}^{-1}$, which corresponds to $r_{s,min}^l \approx 200 \text{ s m}^{-1}$, with similar values also for other global vegetation types (Chapter 3.2.1). This value is set here for woody vegetation. Lower values were reported in KÖRNER (1994) for grasslands and agricultural crops, being applied also in this study. In the case of a steppe vegetation, being a mixture of woody and grassy species, intermediate values were accordingly used (Table 4.3).

Ψ_{cr} and Ψ_{wp} (Eq. 4.29) were estimated from data of LARCHER (1984), HOLBROOK ET AL. (1995) and LHOMME ET AL. (1998). Note that Ψ_{wp} of plants which are adapted to dryland conditions is, due to their higher root suction, lower than the conventional value applied in agricultural and soil scientific studies for temperate climate conditions and vegetation type.

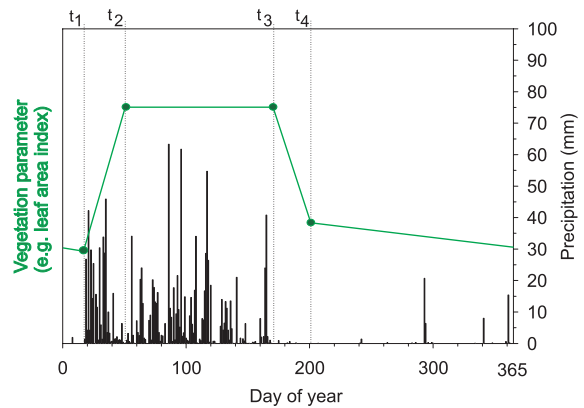


Fig. 4.12 Scheme of the seasonal distribution of vegetation parameters in WASA; with example of temporal distribution of daily rainfall.

Some of the vegetation parameters may change between the dry and the rainy season in the course of the phenological development of the plants as function of water availability. To describe this temporal distribution, a simple approach is applied, in its form similar to that of SCHULLA (1997). For base points in time, specifying certain days during the year, vegetation-specific parameters are required, with the values varying linearly between these points (Fig. 4.12). The base points are:

- t_1 Start of vegetation period, minimum foliage development (begin of rainy season)
- t_2 Maximum foliage development (natural vegetation), or characteristic phenological state (crops)
- t_3 Begin of degradation of foliage (end of rainy season or harvest of crops)
- t_4 End of main phase of foliage degradation, remaining foliage may be further reduced during the following dry season

Points t_1 and t_3 are related to the onset and the end of the rainy season. Singular rainfall events occurring before or after that may, however, not significantly affect vegetation development. The key points t_1 and t_3 are consequently derived by the application of an objective method which determines the start and end of the rainy period by defining the points in time when a statistically significant change in the trend of the

precipitation time series occurs (GERSTENGARBE & WERNER, 1999). Thus, smaller events before or after the rainy period may be discarded. The method is applied on the basis of the daily precipitation input data of WASA, explicitly for each year of simulation and each municipality or sub-basin. Thus, important inter-annual and spatial variability of vegetation characteristics as function of the rainfall distribution is captured

in the model. Key points t_2 and t_4 are estimated to be 30 days later than t_1 and t_3 , respectively.

In summary, Table 4.3 gives the vegetation parameters derived from the various sources mentioned above for the land cover classes in WASA. An additional land cover class which is not listed in Table 4.3 are bare rocky surfaces without vegetation. Due to the limited data availability, the parameters are mainly rough estimates including high uncertainty.

Table 4.3 Parameters of the major land cover types of the study area (A is the percentage of the land cover type on the total study area (Ceará, 150000 km²); t_1 - t_4 are the base points during a year for the seasonal parameter distribution).

Vegetation type	A %	$r_{s,min}^l$ m s ⁻¹	Ψ_{cr} kPa	Ψ_{wp} kPa	h [m]				d_r [m]				Λ [-]				α [-]			
					t_1	t_2	t_3	t_4	t_1	t_2	t_3	t_4	t_1	t_2	t_3	t_4	t_1	t_2	t_3	t_4
Dense tree caatinga	9.5	200	-10	-40	3.5	3.5	3.5	3.5	1.5	1.5	1.5	1.5	0.2	5.0	5.0	1.3	0.28	0.18	0.18	0.25
Open tree caatinga	44.2	200	-10	-40	2.5	2.5	2.5	2.5	1.0	1.0	1.0	1.0	0.1	4.0	4.0	0.4	0.28	0.22	0.22	0.25
Shrub caatinga	0.9	200	-10	-40	2.0	2.0	2.0	2.0	1.0	1.0	1.0	1.0	0.1	4.0	4.0	0.8	0.28	0.21	0.2	0.25
Transition caatinga-forest	3.2	200	-10	-35	7.8	7.8	7.8	7.8	1.5	1.5	1.5	1.5	0.8	6.5	6.5	1.7	0.25	0.16	0.16	0.23
Semi-deciduous forest	1.0	200	-10	-25	15.0	15.0	15.0	15.0	2.0	2.0	2.0	2.0	4.5	9.0	9.0	6.0	0.18	0.13	0.13	0.16
Moist forest	0.9	160	-10	-20	20.0	20.0	20.0	20.0	2.5	2.5	2.5	2.5	10.0	10.0	10.0	10.0	0.12	0.12	0.12	0.12
Grassland with trees	1.0	150	-10	-30	1.5	1.5	1.5	1.5	1.0	1.0	1.0	1.0	0.4	3.5	3.5	0.8	0.27	0.20	0.20	0.25
Dense tree caatinga*	3.6	200	-10	-40	1.8	1.8	1.8	1.8	0.8	0.8	0.8	0.8	0.1	2.5	2.5	0.7	0.28	0.23	0.23	0.27
Open tree caatinga*	18.0	200	-10	-40	1.3	1.3	1.3	1.3	0.5	0.5	0.5	0.5	0.1	2.0	2.0	0.2	0.28	0.25	0.25	0.27
Shrub caatinga*	0.2	200	-10	-40	1.0	1.0	1.0	1.0	0.5	0.5	0.5	0.5	0.1	2.0	2.0	0.4	0.28	0.25	0.24	0.27
Transition caatinga-forest*	1.1	200	-10	-35	3.9	3.9	3.9	3.9	0.8	0.8	0.8	0.8	0.4	3.3	3.3	0.8	0.27	0.22	0.22	0.25
Semi-deciduous forest*	0.3	200	-10	-25	7.5	7.5	7.5	7.5	1.0	1.0	1.0	1.0	2.3	4.5	4.5	3.0	0.23	0.21	0.21	0.22
Moist forest*	0.2	160	-10	-20	10.0	10.0	10.0	10.0	1.3	1.3	1.3	1.3	5.0	5.0	5.0	5.0	0.20	0.20	0.20	0.20
Grassland with trees*	0.3	150	-10	-30	0.8	0.8	0.8	0.8	0.5	0.5	0.5	0.5	0.2	1.8	1.8	0.4	0.28	0.24	0.24	0.27
Pasture (1)	1.1	100	-10	-20	0.1	0.2	0.5	0.1	0.5	0.5	0.5	0.5	0.1	3.0	3.0	0.1	0.28	0.25	0.25	0.28
Beans (2)	2.8	80	-10	-20	0.1	0.5	0.5	0.1	0.1	0.3	1.0	0.1	0.1	1.0	2.0	0.1	0.28	0.25	0.25	0.28
Maize	3.2	80	-10	-20	0.1	0.6	1.2	0.1	0.1	0.3	1.3	0.1	0.1	1.5	3.0	0.1	0.28	0.24	0.22	0.28
Cashew (4)	2.0	80	-10	-20	3.0	3.0	3.0	3.0	1.4	1.4	1.4	1.4	2.0	5.0	5.0	2.0	0.25	0.23	0.23	0.25
Banana	0.2	80	-10	-20	2.0	2.0	2.0	2.0	0.8	0.8	0.8	0.8	3.0	4.0	4.0	3.0	0.22	0.22	0.22	0.22
Rice	0.2	80	-10	-20	0.1	0.2	0.3	0.1	0.1	0.3	0.6	0.1	0.1	2.0	4.0	0.1	0.28	0.20	0.18	0.28
Fallow	5.1	200	-10	-30	0.8	0.8	0.8	0.8	0.5	0.5	0.5	0.5	0.1	2.0	2.0	0.2	0.28	0.25	0.25	0.27

* : degraded areas, including forest pasture, long-term fallow; (1): class includes capim (forage grass); (2): class includes other bushy vegetables or fruits (melon, tomato, cassava); (3): class includes other large fruits and crops (mango, palms, sugar cane).

Model Applications

5.1 Rainfall Disaggregation

The cascade model for disaggregation of continuous rainfall time series described in Chapter 3.1.3 was tested for three rainfall stations in the semi-arid north-east of Brazil, for which data with hourly resolution were available (see Chapter 2.1.6.2). It was modified and extended here compared to the original version of OLSSON (1998), and parameterized and validated for disaggregation of daily to hourly time series. For validation, 100 realizations of disaggregated hourly time series were performed and their mean statistics compared to the observed data. The main results are presented below, more details are given in GÜNTNER ET AL. (2001).

The following model modifications were realized:

- Since the cascade model comprises temporal resolutions expressed as the highest resolution multiplied by a power of two (e.g., in the range 1 (2^0) to 32 (2^5) hours), this limits its real-world applicability. On the one hand, for model parametrization as in this application, available data with the highest temporal resolution are hourly data (which can be successively aggregated into 32-hour data for parameter estimation). On the other hand, for model application, usually daily data are given which result in 1.5-hour or 45-min values after disaggregation. This in turn means that they are mainly not usable in subsequently applied hydrological models, which use timesteps of whole hours. Thus, the model was extended and evaluated here to use a parameterization based on the given 1-hour data and their aggregation steps up to the scale of 32 hours, while performing the disaggregation starting from the 24-hour level down to the 45-min scale with a subsequent aggregation step to the 1-hour level for practical use.
- For derivation of the probabilities P (Eq. 3.1) from observed high resolution rainfall data by averaging over a range of resolutions, a weighting was intro-

duced. To each value of P derived at a specific scale transition a weight was assigned according to the number of boxes used in its calculation at this scale. Generally, the higher the resolution, the larger is the number of contributing boxes and, consequently, the higher is the accuracy of the estimated P value and, thus, its relative contribution to the average scale-invariant value.

- For deriving the distribution of $W_{x/x}$ (Eq. 3.1), OLSSON (1998) included both weights W_1 and W_2 , leading to symmetrical distributions of $W_{x/x}$ (since $W_1=1-W_2$). In the present study in contrary, only the values of W_1 were used (and W_2 was calculated as $1-W_1$). The former approach, while facilitating the fitting of a theoretical distribution, implies that any asymmetry in the empirical distribution of W_1 and W_2 is neglected. The approach used here allows to reproduce the internal event asymmetries in the observed data to some extent, e.g., the observation that in the case of isolated boxes most of the total event volume occurs during the first half of the event. In the present context, this means that $W_1>W_2$ or, in probabilistic terms, $P(W_1>0.5)>P(W_1<0.5)$. Due to marked variations in the shape of the empirical distributions between position classes and, to some extent, between volume classes, the actual empirical distributions were used in the disaggregation model in the present study instead of fitted theoretical distributions.

The application of the modified cascade model to rainfall time series of the study area gives the following results:

- In the range of time scales studied (1-24 hours), the assumptions of scale-invariance of model parameters, which implies the applicability of the same cascade generator at each scale level of the disaggregation process, is fulfilled.

- The mean volume of rainfall intervals within each position class is an appropriate limit for separation of the lower and upper volume classes within each position class. This is, e.g., justified by the ob-

served form of the increase of $P(x/x)$ with increasing rainfall volume of the box to be branched, which roughly approaches a plateau above the mean volume.

Table 5.1 Probabilities of the cascade generator for the three types of divisions for all position classes of rainfall boxes (see also Fig. 3.3) and volume classes (below and above mean box rainfall volume), derived from time series of station Tauá (resolution 1-32 hours).

Position	starting		enclosed		ending		isolated	
	below	above	below	above	below	above	below	above
$P(0/1)$	0.51	0.45	0.27	0.13	0.24	0.06	0.41	0.27
$P(1/0)$	0.22	0.12	0.23	0.13	0.48	0.42	0.43	0.32
$P(x/x)$	0.27	0.43	0.50	0.74	0.28	0.53	0.16	0.40

- The parameters of the cascade generator show a clear dependence on the volume and the position in the rainfall frequency of the time interval with rainfall to be disaggregated, e.g., $P(x/x)$ is larger for the above than for the below mean volume class, $P(x/x)$ is higher for boxes inside a rainfall sequence than boxes at the edge of it. Also, $P(1/0)$ was substantially lower for a box at the beginning of a rainfall sequence than one at the end, and vice versa for $P(0/1)$ (Table 5.1).
- By disaggregation from daily data, the model reproduces a range of hourly rainfall characteristics (e.g., hourly rainfall volumes, event volumes, event duration, extreme value characteristics) with high accuracy for all stations in the semi-arid. A slightly lower performance was found for the number of wet intervals, which was overestimated in the disaggregated time series as compared to the observations, and for the autocorrelation of hourly rainfall values which was underestimated by the model, albeit being low also in the observed data (Fig. 5.1, Table 5.2, Table 5.3).

Table 5.2 Autocorrelation for observed (obs) and disaggregated (dis) 1-hour time series for station Picos in north-eastern Brazil.

time lag [hours]	1	2	3	4	5	6
obs	0.33	0.12	0.06	0.03	0.02	0.01
dis	0.25	0.08	0.06	0.04	0.04	0.03

- Transferability of parameters in time is associated with a comparatively higher uncertainty for the semi-arid rainfall characteristics (as compared to humid temperate climate rainfall) due to its higher interannual variability and lower percentage of rainy intervals within the limited period of available data for model parametrization.

- For parameter transferability in space, no restrictions is found between the three tested Brazilian stations, for which similar parameter sets were derived (contrary to British stations in humid temperate climate, where regional differences were more pronounced).

Table 5.3 Comparison between validation variables for observed (obs) and disaggregated (dis) 1-hour data, example of station Tauá in north-eastern Brazil (No: number; Mn: mean; Sd: standard deviation; Max: maximum; iv: non-zero 1-hour rainfall volume [mm]; ev: event volume [mm]; ed: event duration [hours]; dp: length of dry period [hours]; subscripts 1 or 4: minimum number of dry hours to separate two independent rainfall events (rainfall intervals separated by a lower number of dry intervals are considered to pertain to the same rainfall event); NE: number of exceedances; nMn: volume threshold of n times Mn(iv); L1: the 20 largest rainfall volumes at the 1-hour level).

	obs	dis		obs	dis
No(iv)	634	708	No(ev ₄)	261	263
Mn(iv)	2.1	1.9	Mn(ev ₄)	5.2	5.1
Sd(iv)	3.7	4.0	Sd(ev ₄)	10.6	10.2
Mn(dp ₁)	64.0	59.8	Mn(ed ₄)	2.9	3.3
Sd(dp ₁)	155.9	152.1	Sd(ed ₄)	3.1	3.5
Max(iv)	48.4	65.3	NE(5Mn)	59	50
Mn(L1)	28.4	35.5	NE(10Mn)	7	13

- Additionally, the comparison between the model application for rainfall time series of the semi-arid and the a humid temperate climate (British stations) shows that (1) model parameters distinctly differ between both climates, reflecting the dominance of convective processes in the semi-arid rainfall and of advective processes associated with frontal passages in the British rainfall, (2) the overall model performance is better for the semi-arid tropical rainfall, particularly because of the inability of the

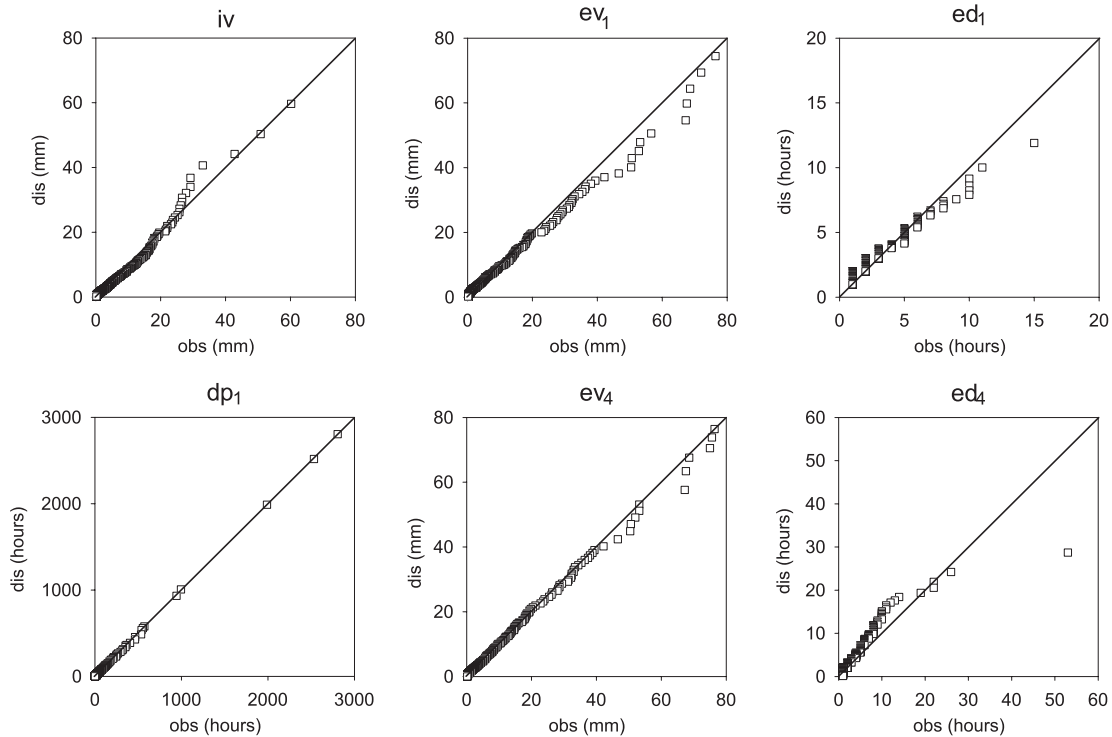


Fig. 5.1 Comparison of the distributions of validation variables for observed (*obs*) and disaggregated (*dis*) 1-hour data, example for station Picos in north-eastern Brazil, period 05/95-03/99 (*iv*: non-zero 1-hour rainfall volume [mm]; *ev*: event volume [mm]; *ed*: event duration [hours]; *dp*: length of dry period [hours]; subscripts 1 or 4: minimum number of dry hours to separate two independent rainfall events (rainfall intervals separated by a lower number of dry intervals are considered to pertain to the same rainfall event)).

model to reproduce a sharp decrease of extremes of rainfall volumes with increasing temporal resolution for the frontal-dominated temperate regions.

In summary, the overall high accuracy of disaggregated rainfall data supports the potential usefulness of the cascade model for the semi-arid study area. Tests using the disaggregated data in hydrological model applications, however, are additionally required to evaluate their practical value (Chapter 5.2.1). An advantage of the approach compared to other models (see Chapter 3.1.2) is its simplicity and applied nature. The few parameters are directly linked to rainfall time series characteristics and reflect by this way rainfall generation mechanism. This improves the process-related transferability of the model in time and space.

Furthermore, the model can also be calibrated using the daily time series only, without the need for higher resolution data. This possibility is a notable advantage as compared to other approaches. The underlying assumption of scale invariance of the parameters beyond the daily to hourly scale examined here is to be closer assessed in future work. On the other hand, the cascade model used here model does not allow to reproduce diurnal rainfall patterns. If these are of relevance for hydrological applications, the model has to be extended by an additional parameter, e.g., corresponding to the parameter storm starting time used in some previous approaches (e.g., HERSHENHORN & WOOLHISER, 1987).

5.2 Small-Catchment-Scale Application

5.2.1 Caldeirão basin

WASA was applied to the Caldeirão basin (0.77 km²), the smallest sub-catchment with runoff data within the Tauá basin (see Chapter 2.2). Being a headwater catchment which does not comprise valley bottoms and where, in addition, no systematic differences can be found in slope, soil or vegetation characteristics between upper and lower topographic parts, Caldeirão is represented within the spatial concept of WASA by one terrain component. This terrain component is subdivided into five soil-vegetation components (SVCs). For all of them (except for bare rock surfaces), degraded tree caatinga is taken as the land cover type (CAVALCANTE ET AL., 1989, Table 4.3). The SVCs thus differ in soil type only, with the following percentages of the terrain component area (CADIER, 1993):

- Bruno Não Calcico (70%)
- Solonetz (10%)
- Vertisol (10%)
- Litólicos (5%)
- Rock outcrops (5%)

For each soil type, the soil parameters of the representative soil profiles being equally used in the regional-scale application of WASA (Chapter 4.3.2) were applied in Caldeirão. This applies also for the vegetation parameters (Chapter 4.3.3). Several simulations differing in temporal resolution and parameter values were run. For daily simulations, area average rainfall data were used (Chapter 2.2). For simulations with hourly resolution, the daily time series was disaggregated by applying the random cascade model which has been adapted to the rainfall characteristics of the study area (Chapter 5.1). 50 realisations of the hourly time series were generated. For each realization, WASA was applied and the results compared to the observations, giving finally a mean performance at the hourly scale by averaging over all realizations.

Uncalibrated daily simulation (D1)

The simulation in the daily mode results in a slightly overestimated mean annual runoff (by 6%, Table 5.4). Although roughly reproducing the sequence of wet and dry years, the model overestimates the interannual variability, i.e., runoff volumes are simulated too large in wet years (1981, 1985) and too low in dry years (1982-1984, 1987). The distribution of daily runoff shows that, contrary to observations, no runoff occurs in the simulations for some rainfall events in the dry

years or before or after the main rainy period in wet years, whereas during the rainy season of wet years, daily runoff is often overestimated (Fig. 5.2c).

Uncalibrated hourly simulation (H1)

Using the same parameters as in simulation D1, the hourly simulation results in a higher overestimation of mean annual runoff (by 10%, Table 5.4). While runoff volumes in wet years are nearly the same as for D1, some runoff is simulated in dry years for H1 as compared to zero runoff for D1. In dry years, these results are closer to the observations than in the case of D1, although runoff is still underestimated. The reason are larger rainfall intensities for precipitation with hourly resolution, which tend to produce more HORTON-type infiltration-excess runoff than the underestimated rainfall intensities when using a daily time step. In the dry years (1982-1984), nearly all runoff is produced by this mechanism according to the simulation results (Table 5.4). This is reasonable as rainfall volumes for these conditions may not be sufficient to produce saturated soil profiles and thus saturation-excess runoff. In wet years, the larger amount of infiltration-excess runoff for H1 leads to a later saturation of the soil profile than for D1, thus less saturation-excess runoff, and, in summary, similar runoff volumes for both simulations. Looking at the daily distribution of runoff (Fig. 5.2d), H1 performs better because some of the runoff events in dry years and outside of the major rainy period are represented by the model.

Adjusted hourly simulation (H2)

It can be argued, that using an hourly time-step is still too coarse to capture rainfall intensities relevant for infiltration-excess runoff generation for the usually short-term convective events of the study area (see Chapter 3.1.1). This may be a reason for the underestimation of runoff by the model for dry pre-event conditions revealed by simulation H1. As no rainfall data with higher resolution are available, alternatively the scaling factor s_F in the infiltration routine (Chapter 4.2.3) can be increased to compensate for underestimated rainfall intensities. Assuming a factor of 2.5 for this underestimation, i.e., setting s_F to 2.5 in H2 (instead of $s_F=1$ in H1), thus reducing the hydraulic conductivity of the soil horizons for infiltrating water by this factor relative to its given value, results in runoff volumes in dry years which correspond to the observations (Table 5.4). On the other hand, mean annual runoff is now simulated considerably too large, which is predominantly the effect of overestimated

runoff volumes in wet years, where saturation-excess runoff occurs beside of infiltration-excess (HF is in the range of 50-60% in Table 5.4, the remaining runoff can be mainly attributed to saturation-excess runoff because lateral subsurface flow is of minor

importance with a fraction on total runoff of less than 2%). Thus, in wet years, saturation of the soil profiles occurs too frequently, which might be due to an underestimated soil storage capacity in the model.

Table 5.4 Rainfall (mm), measured and simulated annual runoff Q (mm) and simulated fraction of HORTON-type infiltration-excess surface runoff on total runoff (HF (%)), Caldeirão basin, period 10/80-09/88.

Year	1981		1982		1983		1984		1985		1986		1987		1988		mean	
Rainfall	651		304		202		453		1125		771		377		625		564	
	Q	HF	Q	HF	Q	HF	Q	HF	Q	HF	Q	HF	Q	HF	Q	HF	Q	HF
Measured	170	-	13	-	5	-	23	-	250	-	126	-	21	-	90	-	87	-
D1	251	15	0	0	0	0	1	0	275	10	134	13	1	0	76	16	92	13
H1	251	30	5	93	3	96	6	86	280	28	134	41	7	89	77	58	95	36
H2	254	51	15	98	8	98	22	95	295	48	141	74	20	95	90	87	106	61
H3	220	66	14	98	8	98	20	95	263	56	113	87	18	96	74	94	91	71
D2	231	90	16	98	7	94	8	83	275	69	118	93	14	91	82	94	93	83

Adjusted hourly simulation (H3)

As a consequence of the low performance of simulation H2 in wet years, an additional modification of model parameters was done in H3: the influence of an increased soil storage capacity by extending the profile depths was tested. The depth of each soil profile to the bedrock was increased by 30% by extending the depth of the lowest horizon. For the dominant soil type in the Caldeirão basin (Bruno Não Calcico, see above), for instance, this means an increase of the total soil depth from 65 cm to 85 cm, corresponding to an increase in storage capacity (total pore volume) from 295 mm to 385 mm. By this means, runoff volumes in wet years are closer to the observations due to less saturation-excess runoff which is indicated by an increase in HF as compared to simulation H2 (Table 5.4). Runoff in dry years, however, is nearly not changed relative to H2 because infiltration-excess runoff generation is influenced to a less extent by the total storage capacity of the soil. The pattern of daily runoff resulting from H3 is very close to the observations for both dry and wet pre-event conditions (Fig. 5.2e).

Adjusted daily simulation (D2)

The adjustments of parameters derived in H2 and H3 were transferred to the application of WASA with a daily timestep in simulation D2. Soil profile depth is increased by 30% as in H3. Concerning the scaling factor s_F , it has to be adjusted for daily calculations to compensate for underestimated rainfall intensities when going (1) from the daily to the hourly scale, and (2) from the hourly to the sub-hourly (event) scale. The second point has been addressed in H2, showing

that $s_F=2.5$ is an appropriate value. With reference to the first point, a simple approach may be to derive the scaling factor by the comparison of observed rainfall intensities at both daily and hourly time scales. For time series of the station Tauá (see Table 2.3), the mean intensity of hourly rainfall is 2.14 mm h^{-1} , for aggregated daily data it is 0.36 mm h^{-1} . This gives a ratio of intensities between both scales of about 6. Thus, an appropriate scaling factor for daily model applications taking into account sub-daily rainfall intensities is estimated here as multiplicative combination of factors from the two steps above, resulting in $s_F=15$.

The results show that, while giving a similar mean annual runoff as compared to the uncalibrated simulation D1, the annual distribution between dry and wet years is considerably closer to the observations in D2. In particular, the model reproduces the runoff in dry years. The slight overestimation of the annual mean can mainly be attributed to the first simulation year which is difficult to reproduce (also in the other simulations above), which may also be due to exceptional rainfall characteristics or data errors. The results of D2 are also similar to the best-estimate version on an hourly basis (H3). The fraction of overland flow is even larger in D2 than in H3. This can be directly attributed to the time resolution, where a runoff event on the daily basis is produced by one infiltration-excess event, whereas in the hourly version, the same daily runoff may be composed of infiltration-excess runoff at the beginning of the event and saturation-excess during later hours with rainfall. The daily runoff pattern of D2 is similarly well represented compared to the observations and considerably better than D1

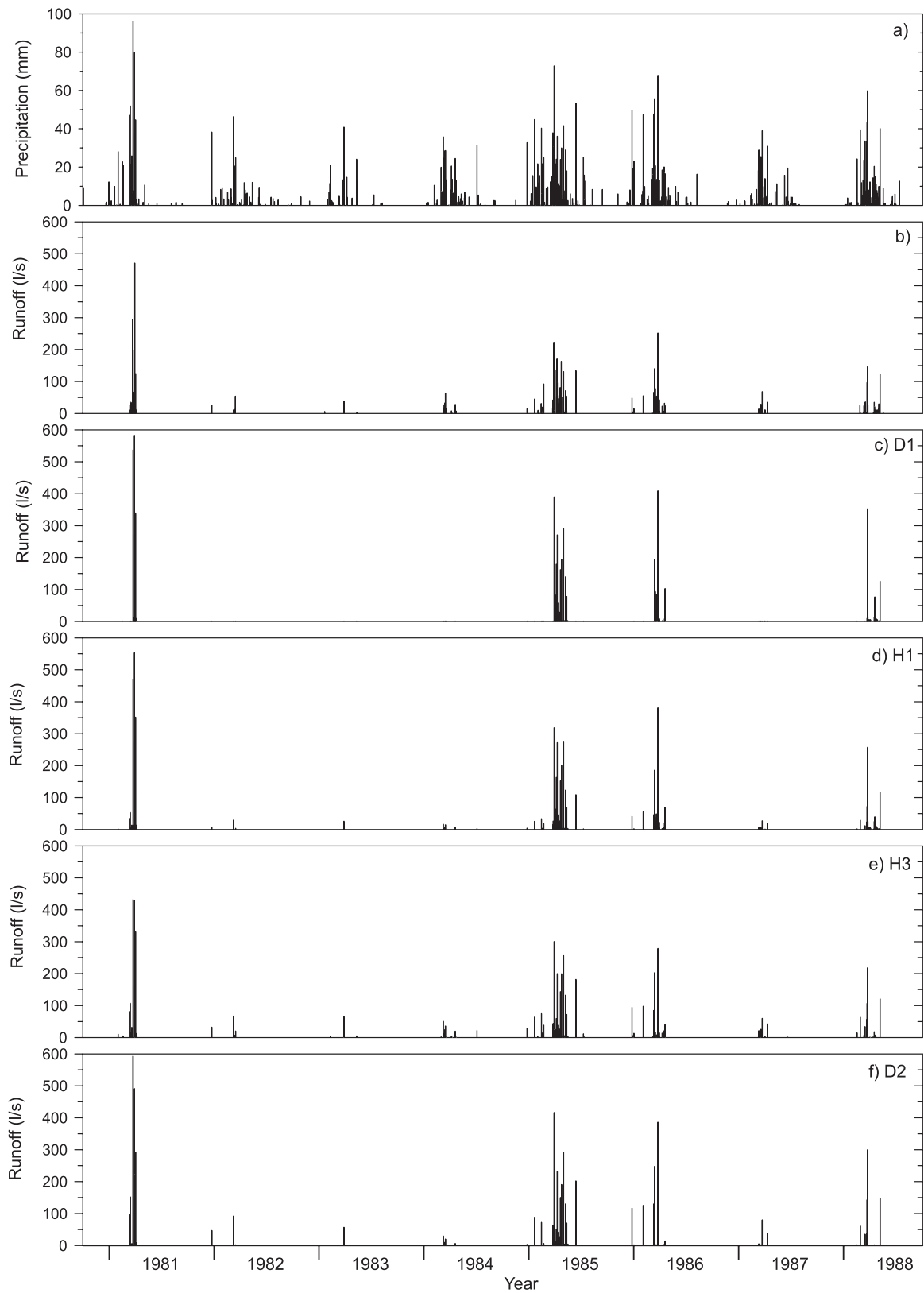


Fig. 5.2 Caldeirão basin (0.77 km²), period 10/80-09/88, daily time series of (a) precipitation, (b) measured discharge, and (c)-(f) simulated discharge, for different daily and hourly versions of WASA (see text).

(Fig. 5.2f), particularly what concerns the occurrence of runoff events for drier pre-event conditions. The number of simulated days with runoff and the general distribution of daily runoff is in the range of the observations (Fig. 5.3). However, a slight underestimation in the number of mid-range events (50-100 l/s), compensated by too many larger events, is found. One reason can be the linearity of the simple scaling approach. The scaling factor is applied equally to all days although the underlying ratio of rainfall intensities at the hourly and daily scale may be smaller for days with large rainfall volumes. This may lead to an overestimation of surface runoff and the mentioned bias in the distribution of daily runoff volumes.

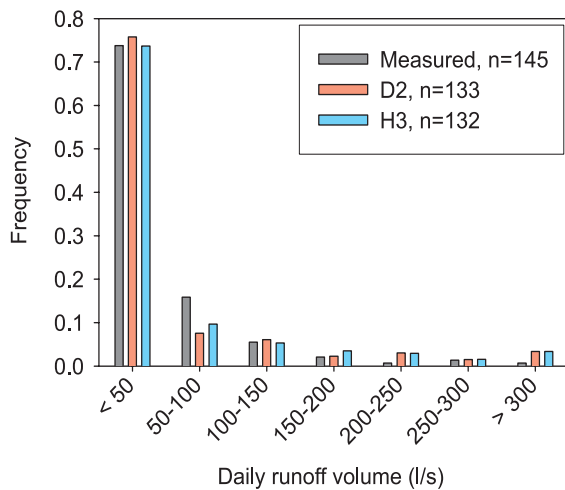


Fig. 5.3 Distribution of daily runoff volumes, basin Caldeirão, period 10/80-09/88, observations and simulations D2 and H3; n : number of days with runoff > 0.

In summary, the small-scale application demonstrates that WASA can well represent the highly variable hydrological response for the given semi-arid conditions, if rainfall time series of high temporal resolution are available. For practical model applications in this study, based on daily data, the introduction of a scaling factor to compensate for underestimated rainfall intensities proves to be a reasonable approximation.

5.2.2 Tauá basin

At a larger spatial scale, WASA was applied to the Tauá basin (194km², see Chapter 2.2 for a description). The reference simulation (T1) used a daily time-step with locally measured basin-averaged rainfall time series (Chapter 2.2). Concerning terrain, soil and land cover information, the definition of modelling units and their parametrization was taken from the

data available for the regional-scale applications of WASA (Chapter 4.1.2, Chapter 4.3). There, the Tauá basin is completely located within one landscape unit which is composed of two terrain components. One of them (fraction on total area 65%) represents the steeper sloping area with a higher topographic position, whereas the other terrain component (35% of the landscape unit) represents flatter areas of a lower topographic position, including the valley bottoms. The soil types in the higher terrain component are Bruno Não Calcico (50% of the total area of the landscape unit) and Litólicos (15%), in the lower terrain component occur Planossolos (18%), Solonetz (13%) and alluvial soils (4%). This distribution of soil types is close to that described in CADIER (1993) for the Tauá basin (Chapter 2.2). Concerning land cover, the combination of soil types and land cover classes into soil-vegetation-components as derived for the total municipality of Tauá (3940 km², Chapter 4.3.1) for the regional-scale application was applied to the Tauá basin, which is located within this municipality. According to the results of Chapter 5.2.1, the scaling factor s_F for soil hydraulic conductivity in the infiltration routine was set to 15 in order to compensate for underestimated rainfall intensities when running the model with a daily time-step. Reservoirs (see also Chapter 2.2) were grouped into five classes according to their storage capacity (Table 5.5, for the concept see Chapter 4.2.7.1). Extraction of stored water for human use or agriculture was disregarded, as no information is available for the Tauá basin.

Table 5.5 Distribution of reservoirs among reservoir classes in WASA for the Tauá basin; n : number of reservoirs in each class; n_{obs} : number of reservoirs with observed time series of storage volume.

Reservoir class	1	2	3	4	5
Storage capacity (10 ⁶ m ³)	<0.03	0.03-0.1	0.1-0.5	0.5-1	1-3
n	9	5	4	2	1
n_{obs}	2	2	0	2	0

The simulation results (Table 5.6, Fig. 5.4) generally correspond well to the observations in terms of discharge. Mean annual runoff as well as its interannual variability is reasonably captured by the model. A tendency of overestimating runoff in wet years and underestimating it in dry years might be seen in the results, although a generalization of this discrepancy is limited by the small number of simulation years. Differences between observations and simulations can be

attributed to the rough resolution of physiographic data, as mainly regional-scale information on terrain, soils and land cover is being applied to this small basin (see Chapter 5.3.3 on the order of magnitude of model sensitivity to uncertainty in parameters). Addi-

tionally, it has to be noted that the spatial variability of rainfall is not taken into account. Nevertheless, the results show that taking large-scale physiographic data and local precipitation data may result in reasonable runoff simulations at the local scale.

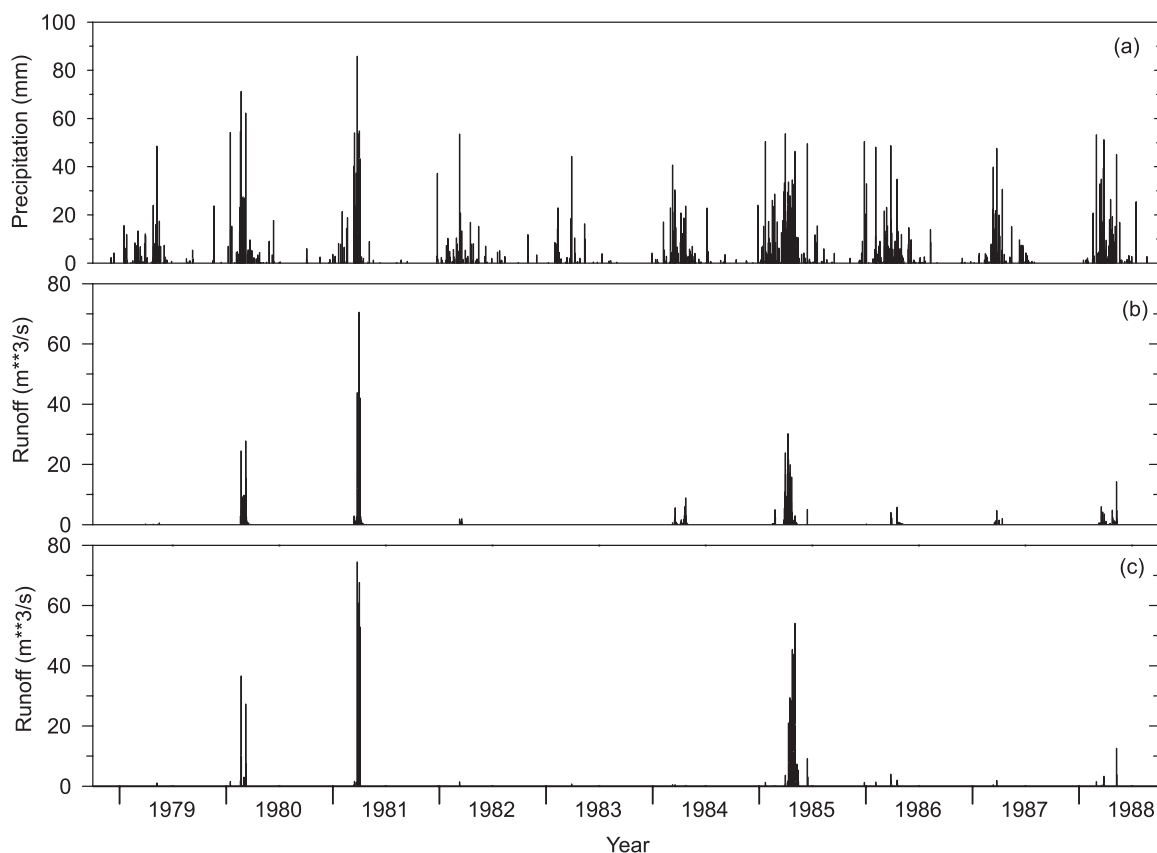


Fig. 5.4 Tauá basin (194 km^2), period 10/78-09/88, daily time series of (a) precipitation, (b) measured discharge, and (c) simulated discharge with WASA, reference simulation T1.

Table 5.6 Rainfall, measured Q_{obs} and simulated Q_{sim} annual runoff, Tauá basin, period 10/78-09/88 (all in mm), for different simulations (see text).

Year	1979	1980	1981	1982	1983	1984	1985	1986	1987	1988	mean
Rainfall	331	544	662	318	216	516	1168	707	385	620	547
Q_{obs}	1	52	139	3	0	22	143	9	5	28	40
Q_{sim} , Simulation T1	1	44	169	1	0	1	178	7	1	13	42
Q_{sim} , Simulation T2	4	65	183	5	2	5	202	17	8	29	52
Q_{sim} , Simulation T3	1	66	193	2	1	2	197	28	5	39	54
Rainfall, Simulation T4	421	514	537	374	271	770	1169	999	467	658	619
Q_{sim} , Simulation T4	0	0	31	0	0	28	119	73	0	0	25

Fig. 5.5 illustrates the different storage behaviour of reservoirs in the case of simulation T1. Smaller reservoirs, i.e., those of lower storage capacity, show a stronger variability in their storage volumes, falling to very low levels or drying out completely during each dry season. Larger reservoirs generally exhibit a smoother behaviour, with a stronger interannual variability as compared to the intra-annual variability. The frequency of overflowing, but also that of drying out completely is smaller than for the small reservoirs. This different behaviour is mainly a consequence of the non-linearity of the volume-surface area-relationship (Chapter 4.2.7), leading to, in relative terms, a weaker susceptibility to evaporation losses for larger reservoirs. The validation of these simulation results by comparison with available observed reservoir storage data of the Tauá basin (CAVALCANTE ET AL., 1989) is limited by the low number of monitored reservoirs (Table 5.5). Thus, discrepancies in Fig. 5.5 between observations and simulation may be attributed to the particularities of the observed reservoirs in their geometry or catchment characteristics which differ from the average characteristics represented by WASA in the respective reservoir class. The overestimation of inflow to classes 1 and 2 in dry years may be due to the simplified model assumption of attributing one-sixth of the total basin area of Tauá to each reservoir class (see concept in Chapter 4.2.7.1). This is a too large area when compared to the catchment area of the reservoirs for which measurements are available. In class 4, storage volume during the dry period in the observations tend to decrease more rapidly than in the simulations, which may be an effect of discrepancies in the assumed reservoir geometry or due to additional water use from the reservoirs which is not taken into account in the model. Nevertheless, the above described more balanced storage behaviour of larger as compared to smaller reservoirs is reasonably captured by the model. Also the variability between years, with a tendency of reservoirs volumes to reach the storage capacity in the years 1981, 85, 86 and 88 is in general represented in the simulations.

The comparison of the reference simulation T1 with a model run which does not take into account any retention in reservoirs (Simulation T2) shows that losses in reservoirs cause a reduction of mean annual basin discharge of about 20% (Table 5.6). In relative terms, the reservoir effect on discharge is stronger in dry years.

In another simulation (Simulation T3), no lateral redistribution of runoff or soil moisture among terrain components or soil-vegetation-components was taken into account. It results that the mean annual discharge

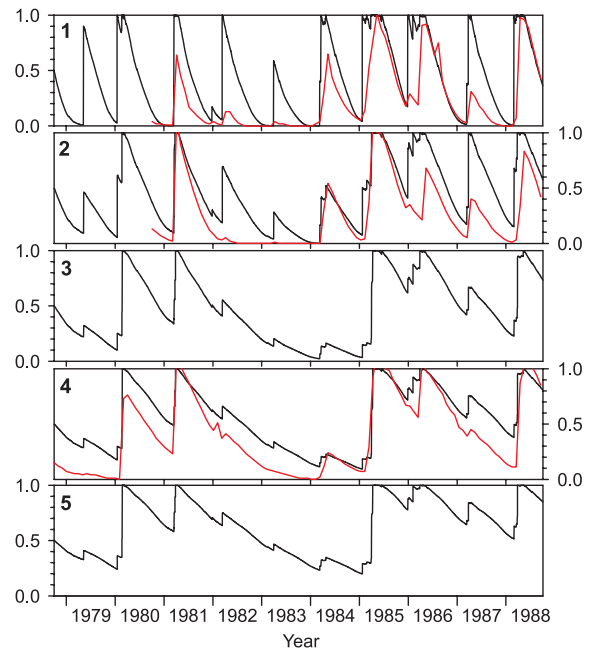


Fig. 5.5 Storage volume relative to storage capacity for the 5 reservoir classes in Pirangi; black line: simulation with WASA, period 10/78-09/88; red line: observations (see also Table 5.5).

of the Tauá basin is about 22% lower in the reference simulation T1 as compared to T3 without lateral redistribution, mainly as an effect of reinfiltration of surface runoff (Table 5.5). The effect of lateral redistribution in terms of soil moisture is illustrated in Fig. 5.6 by comparing simulations T1 and T3. First, the plant-available soil moisture is larger in absolute values in the terrain component of a lower topographic position (Fig. 5.6b) compared to the terrain component of the higher topographic position (Fig. 5.6a). This reflects the different soil characteristics, with in average shallower soils of a higher content of coarse fragments in the higher terrain component. Here, the difference between T1 and T3 is small as this unit does not receive inflow from another (higher) terrain component in T1. The slightly higher soil moisture during wet periods in T1 demonstrates the effect of lateral redistribution among the soil-vegetation-components (SVCs) within this terrain component, i.e., surface runoff may be generated on one SVC and partly reinfiltrate in an adjacent SVC with initially lower soil moisture. The small differences between T1 and T3 show that this effect is small, which points to small differences among the SVCs with regard to their hydrological behaviour. For the lower terrain component differences between T1 and T3 are considerably more obvious. Here, the inflow from the higher terrain com-

ponent enhances soil moisture during the rainy season. This effect occurs particularly a certain period after the onset of the rainy season, where soil moisture in the higher terrain component is already large enough to generate large volumes of surface runoff during rainfall events and, simultaneously, soil moisture in the deeper, more porous soils of the lower terrain component is still low enough to absorb a substantial amount of this incoming flow from the sloping region

(e.g., see the peak in the difference between T1 and T3 in early 1985, Fig. 5.6b). This increased soil moisture during the rainy period by lateral inflow causes a larger amount of soil moisture to be available for a longer time during the subsequent dry season in the lower terrain component, at least after a rainy season with a high precipitation sum (see differences between T1 and T3 in the ‘recession’ of soil moisture during the dry season in Fig. 5.6).

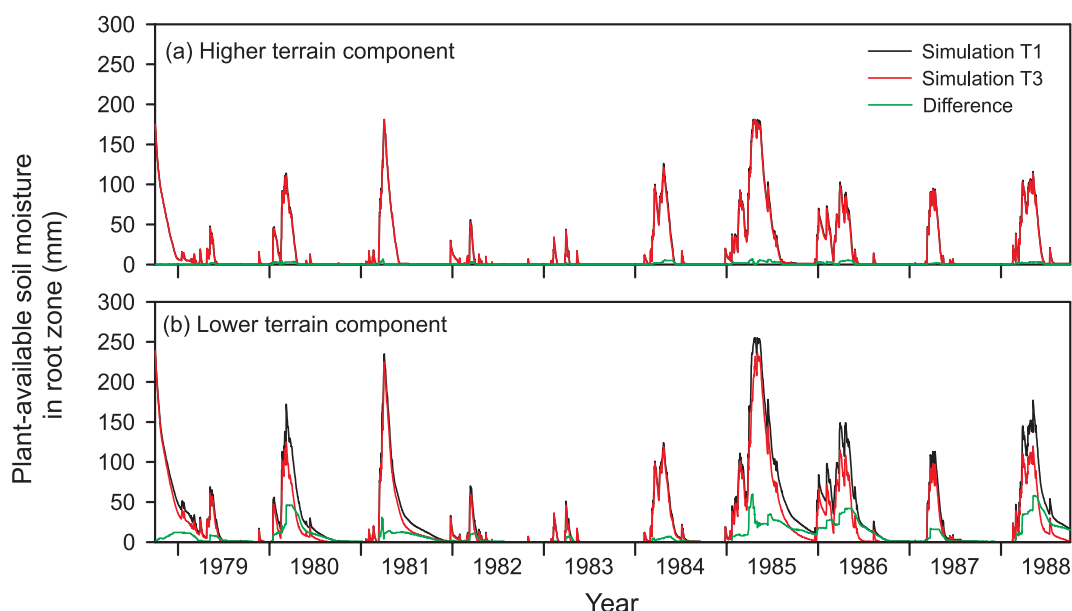


Fig. 5.6 Plant-available soil moisture in the root zone for both terrain components in the Tauá basin (mean of all soil-vegetation-components in each terrain component). Simulations with WASA with (T1) and without (T3) lateral redistribution.

A further simulation with WASA was performed in order to test the effect of using the rainfall data which are available for the regional scale simulations, based on a small number of stations, on the accuracy of model results at the local scale. In simulation T4, WASA was run for the Tauá basin using the rainfall time series interpolated to a $10 \times 10 \text{ km}^2$ grid by ordinary kriging (Set 2 in Chapter 2.1.6.2), while all other model settings were equal to the reference simulation T1 with local rainfall data. For the 10-year simulation period, the difference in mean annual rainfall of T4 to T1 is +13%, with deviations in individual years of up to 50% (Table 5.6). Differences between T4 and T1 in simulated basin discharge are, on the other hand, in average -38%. Thus, in spite of larger rainfall volumes, T4 results in considerably lower discharge. The main reason is the modification of rainfall time series characteristics by interpolation in the case of T4, which lead to a loss in variance and lower intensities at the daily scale. For instance, the mean rainfall volume at wet days in T1 is 6.1 mm d^{-1} as opposed to

4.0 mm d^{-1} in T4 (see Chapter 5.3.1.1 for details of temporal rainfall characteristics on runoff simulations).

In summary, the simulations at the small-basin scale show that reasonable results for discharge and reservoir storage volumes can be obtained even if the coarse regional-scale physiographic information is used. The accuracy of simulation results at the small-basin scale in this example is more dependent on rainfall input, of which, in turn, deviations of short-term time series characteristics rather than of mean annual values are more sensitive. Furthermore, the simulations show that to the considerable decrease in the runoff ratio when going from the headwater or hillslope scale (15.4% in the Caldeirão basin, Chapter 5.2.1) to the small-basin scale (7.7% in Tauá) contribute, by roughly equal importance, discharge losses in reservoirs, on the one hand, and infiltration of runoff due to a different topographic and pedological setting at the larger scale, on the other hand.

5.3 Sensitivity Analysis at the Regional Scale

In the following, a variety of model applications of WASA at the regional scale for the entire study area of the State of Ceará are presented. With these simulations it is intended to evaluate model sensitivity to data, parameters and model structure and to assess related uncertainty in combination with the quantification of model performance for the historical time period in Chapter 5.4.

A *reference version of WASA* is used in several of the following chapters for comparison with other runs of changed input data, parameters, etc. This reference version is considered to be the conceptually best model version for the study area because it uses the maximum of available data for derivation of model input and parameters. The reference version

- is uncalibrated, i.e., setting for each parameter the value as derived from physiographic data or literature information as described in Chapter 4,
- runs at the scale of grid cells ($10 \times 10 \text{ km}^2$) at level 1 of the spatial model structure of WASA (Fig. 4.1), which are aggregated to give the response of sub-basins,
- uses data Set 2 as daily rainfall input (with all available stations and ordinary kriging for interpolation to the grid cells) (see Chapter 2.1.6.2),
- uses the adaptation of the scaling factor for infiltration modelling as derived in Chapter 5.3.1.1.

5.3.1 Model sensitivity to precipitation input

Various simulations which differ in their precipitation input with regard to the underlying station data base, the interpolation methods and their temporal and spatial variability were performed in order to test the effects on the simulation results. All simulations used daily rainfall time series (see Chapter 2.1.6.2 for more information on the data sets).

5.3.1.1 Temporal rainfall characteristics

The following simulations differing in the temporal characteristics of their rainfall input are compared:

- *Simulation P1*: Grid-based simulation, rainfall interpolation by ordinary kriging (Set 2 in Chapter 2.1.6.2). According to the result from the small-scale application (Chapter 5.2.1), the scaling factor s_F in the infiltration routine is set to $s_F=15$ in order to adjust the soil hydraulic conductivity to underestimated sub-daily rainfall intensities when

running WASA with daily resolution. This setting of s_F applies also for P2-P4 described below.

- *Simulation P2*: Grid-based simulation with rainfall data Set 3, i.e., ordinary kriging superimposed by a stochastic component.
- *Simulation P3*: Grid-based simulation, assigning to each cell the precipitation time series of the municipality in which this cell is located. These data are based on the interpolation to the municipality scale with a smaller number of stations than in P1 and P2 (Set 1 in Chapter 2.1.6.2). For each cell, the daily time series is then multiplied, separately for each year, by the fraction of the total annual rainfall as derived in Set 2 to the total annual rainfall resulting from Set 1. In this way, the resulting daily time series of each cell has the same annual total and inter-annual variability as the data from Set 2 with more stations, but a temporal sequence at the daily scale which is identical to the underlying interpolation to the municipality scale in Set 1.
- *Simulation P4*: Grid-based simulation, assigning to each cell the precipitation time series of the station which is located closest to the center of the cell (similar to the interpolation method by THIESSEN polygons). Similarly to P3, the rainfall volumes of the time series of each cell are then conditioned to give annual rainfall volumes as derived from Set 2 while pertaining the temporal sequence at the daily scale inherent to the station data.

Rainfall time series characteristics vary apparently between the different simulations. Compared to P4, rainfall time series in P1-P3 show a considerably larger number of days with precipitation, and mean daily rainfall volumes are lower by a factor of about 2-3 as compared to the time series in P4 (Table 5.7). Similarly, the distribution of daily rainfall volumes shows the dominance of small values for P1-P3, whereas in the case of P4 the frequency of volumes $>10\text{mm}$ is much higher (Fig. 5.7a). This is directly due to the loss of variance at the daily scale introduced by interpolation from the station to the grid scale in the cases of P1-P3, whereas P4 maintains the station-scale characteristics. As another consequence, much longer periods of consecutive days with precipitation occur in the case of P1-P3 (Table 5.8, Fig. 5.7b). The additional stochastic component in P2 increases the variance which has at the beforehand been lost during interpolation as in P1, however, the overall effect on the time series properties examined here is small when compared to P4. Time series in P3 are characterized by a stronger

variability at the daily scale than P1 and P2 which can be related to differences in the interpolation methodology (see Chapter 2.1.6.2).

Table 5.7 Characteristics of grid-based daily rainfall data used as input for WASA simulations (maximum resolution 0.1mm). Events are defined as consecutive days with rainfall >0. Mean values averaged for the 1460 grid cells of the study area and the period 1960-98.

Simulation	P1	P2	P3	P4
Number of rain days per year	172	154	125	57
Daily rainfall volume of wet days (mm)	5.0	5.5	7.1	15.5
Variance of daily volumes	132	158	112	282
Event duration (days)	4.8	4.0	2.8	1.8

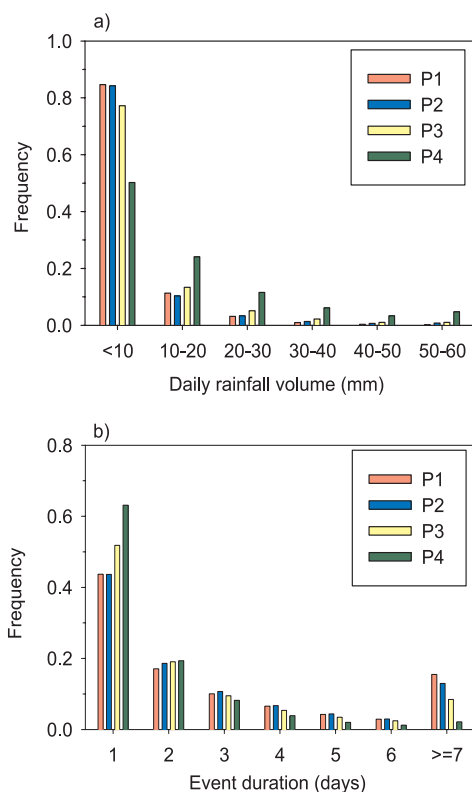


Fig. 5.7 Distributions of (a) daily rainfall volumes and (b) event duration of different grid-based daily rainfall time series P1-P4, averaged for the 1460 grid cells of the study area and the period 1960-98. Events are defined as consecutive days with rainfall >0.

Simulations P1-P4 are thus all characterized by the same annual precipitation volumes and by the same model parametrization, differing only in the variability

within the rainfall time series at the daily scale. Mean simulated runoff at the scale of the grid cells increases in the order $P1 < P2 < P3 < P4$, being about 40% larger in P4 as compared to P1, while evapotranspiration declines in the same order. In particular, evaporation from the interception storage for P4 is less than half the amount of that in simulation P1 (Table 5.8). The

Table 5.8 Simulation results for different rainfall input and scaling factors. Mean annual results (in mm) averaged over the 1460 grid cells of the study area, period 1960-98.

Simulation	P1	P2	P3	P4	P5
Rainfall	861	861	861	861	861
Total evapotranspiration	714	712	709	662	694
Interception evaporation	110	100	82	49	53
Total runoff	128	130	133	178	147
Infiltration-excess runoff	44	52	53	79	64

comparison with discharge observations for larger river basins of the study area shows the general tendency of an underestimation of runoff in the case of the simulations with interpolated time series (Table 5.9). For simulation P4, on the other hand, runoff volumes are simulated too large.

Table 5.9 Observed (Q_{obs}) and simulated (Q_{sim}) mean annual discharge and their difference Δ for various river basins in Ceará; simulations with different rainfall input time series; validation periods vary between stations within 1960-98 (see Fig. 2.6 and Fig. A.1 for more information on the gauging stations).

Station	Basin area km ²	Q_{obs} m ³ s ⁻¹	P1		P4	
			Q_{sim} m ³ s ⁻¹	Δ %	Q_{sim} m ³ s ⁻¹	Δ %
3	19250	32.5	28.0	-13.8	56.4	+73.3
7	11890	28.7	27.4	-4.4	47.2	+64.7
10	18270	39.8	20.8	-47.7	34.1	-14.3
12	47300	120.9	85.8	-29.0	159.5	+32.0
16	7339	21.2	16.3	-23.0	25.4	+20.1
22	11210	76.2	69.6	-8.7	88.6	+16.3

These results can be closely related to the above characteristics of the rainfall time series used in each simulation. The higher rainfall intensities in P3 and particularly in P4 amplify the generation of infiltration-excess runoff and, thus, total runoff. This in turn decreases the infiltration amount and soil moisture available for evapotranspiration. Additionally, the

larger number of days with rainfall in P1-P3 gives rise to a more frequent refilling and emptying of the interception storage and thereby an overall higher amount of interception evaporation. This is enhanced by the usually large evaporation rates for the given climate conditions which in general exhaust completely the actual storage volume of the interception storage on a rain day, thus providing again the maximum storage capacity for the next simulation day.

As for all practical applications of WASA interpolated rainfall time series are used as input, such as those of the type of P3 for the scenario calculations (Chapter 5.5), an approximate method is required to compensate for the above interpolation effects. The following approach is tested (*Simulation P5*, reference version of WASA):

- Underestimated rainfall intensities at the daily scale due to loss of variance by interpolation is compensated by decreasing the hydraulic conductivity of the soil for infiltration modelling. This is done by increasing the scaling factor s_F , similarly to the adjustment for underestimated sub-daily rainfall intensities (Chapter 5.2.1). The ratio r_{prec} of mean daily rainfall volumes of the station-based rainfall time series (P4) to mean volumes of the interpolated time series is used as an approximate value for s_F . Its spatial distribution shows a slight tendency of higher values in the dryer parts of the study area (Fig. 5.8, compare with Fig. 2.3). r_{prec} is multiplicatively combined with the value $s_F=15$, derived for the adjustment to sub-daily rainfall intensities (Chapter 5.2.1), to give the final scaling factor for each grid cell.
- The overestimation of interception due to an overestimated number of rain days after interpolation of the rainfall time series is compensated by a reduction of the capacity of the canopy interception storage, i.e., the interception coefficient h_I (Eq. 4.4). At the scale of the grid cells, a strong relation between the ratio r_{EI} (ratio of interception evaporation simulated in P1 to interception evaporation of P4) and r_{prec} is found (Fig. 5.9). This indicates that the overestimation of interception evaporation in P1 relative to P4 increases with the increasing loss of variance and increasing number of rain days induced by rainfall interpolation. Eq. 5.1, derived from Fig. 5.9, is used to define an adjusted interception coefficient h_{Ic} for each grid cell.

$$h_{Ic} = h_I / (0.35 + 0.65 \cdot r_{prec}) \quad (5.1)$$

Results for simulation P5 with the above two adjustments of the scaling factor and of the interception coefficient are given in Table 5.8. The long-term mean

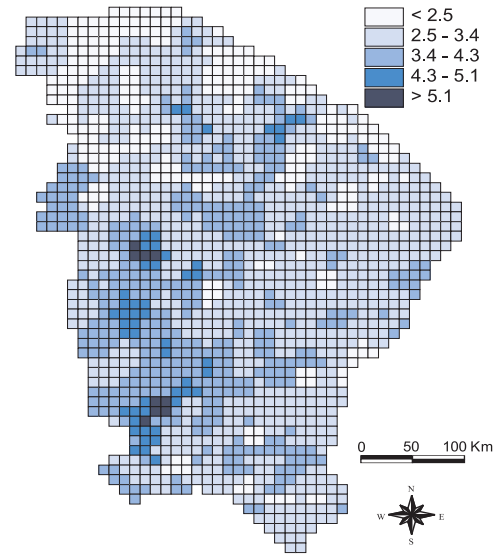


Fig. 5.8 Ratio r_{prec} of daily rainfall volumes of station-based time series (P4) to daily volumes of interpolated time series with ordinary kriging (P1). Mean of period 1960-98.

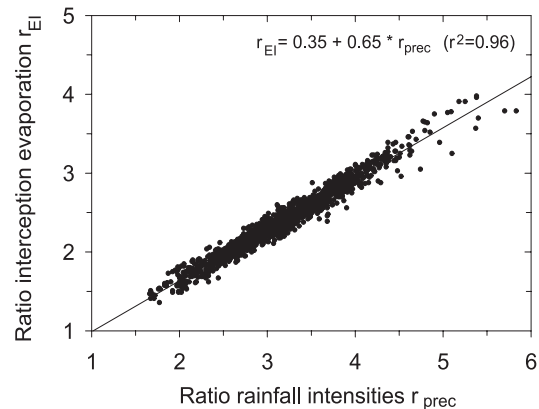


Fig. 5.9 Relationship between ratios of mean daily rainfall intensities and mean annual interception evaporation for simulation with rainfall time series P1 (interpolated) and P4 (station-based); each dot represents one of the 1460 grid cells of the study area. Simulation period 1960-98.

interception evaporation is now close to simulation P4 with station-based rainfall time series. Although at the cost of accuracy at the scale of individual days (where interception evaporation is now supposed to be underestimated due to the above reduction of the interception coefficient), the model adjustment for interception is reasonable with regard to the primary objectives of model applications for long-term water balance stud-

ies. Here, the bias of interception evaporation introduced by the effect of interpolation on the temporal sequence of rainfall time series is efficiently reduced. It is justified to use station-based rainfall data as a reference for this model adjustment, as also for model applications at large spatial scales the temporal structure of rainfall at the point (station) scale governs the interception process.

With regard to runoff, results of simulation P5 are intermediate to those of P1 and P4 (Table 5.8). The generation of infiltration-excess runoff is less than for P4 with station-scale data, which indicates that the scaling factor s_F does not completely compensate for underestimated rainfall intensities relative to P4 with regard to runoff generation. However, for runoff generation, a toposequence within the landscape units is the relevant spatial scale in WASA. Thus, at this scale, due to the spatial variability of rainfall, relevant rainfall intensities for runoff generation can be expected to be lower than those measured at the point scale. The point scale will then not be the fully adequate reference scale for model adjustment. In this context, the model adjustment by the scaling factor applied here, leading to intermediate runoff volumes, can be considered to be a reasonable approximation. However, it has to be noted that the temporal structure of the rainfall time series used in P5, i.e., the sequence of wet and dry days, is equal to that of P1, implying an overestimation of rain days, also if the focus is set to the scale of toposequences. Thus, the above approach is limited as it does not explicitly take into account other effects of this biased temporal sequence, e.g., on percolation of soil water and on evapotranspiration by plants and from the soil surface (see also Chapter 6.1.3 for a discussion of the approach).

5.3.1.2 Spatial rainfall variability

Simulation experiments were performed in order to examine the effect of the spatial variability of rainfall input on simulation results at the scale of sub-basins. Three model runs differing in the rainfall input at the grid scale, but being equal with regard to annual rainfall at the sub-basin scale, were examined:

- *Simulation P5* (the reference version of WASA, see beginning of Chapter 5.3), corresponding to that of Chapter 5.3.1.1, with daily rainfall distributed among cells according to the interpolation by ordinary kriging.
- *Simulation P6*, where to each cell within a sub-basin the same rainfall time series is attributed. This time series is taken from P5 from one grid cell in the sub-basin while conditioning its daily volumes

to give the same total annual rainfall of the sub-basin as in P5 after averaging over all grid cells.

- *Simulation P7*, is similar to P2 in Chapter 5.3.1.1 in the sense that a stochastic component was added at the cell scale to the interpolation by ordinary kriging (Set 3 in Chapter 2.1.6.2), but contrary to P2, here it is run with the scaling factor as derived in Chapter 5.3.1.1.

No significant differences in annual mean runoff at the scale of sub-basins is found between simulation P5 and P6 or P7, respectively (Fig. 5.10). This means that variability between grid cells is averaged out at the catchment scale when regarding its long-term water balance. Additionally, the model does not take into account possible interactions between grid cells within a catchment, i.e., transmission losses of runoff in downstream cells. Thus, a reduction of basin runoff volumes due to rainfall variability, which may occur particularly for drier catchment conditions, cannot be captured. The slight tendency of low-yielding catchments (<150mm mean annual runoff) to give higher runoff volumes in the case of P7 than for P5 (Fig. 5.10b) can be mainly attributed to the enhanced temporal variability of the time series in P7 (see Chapter 5.3.1.1) rather than to an effect of spatial variability.

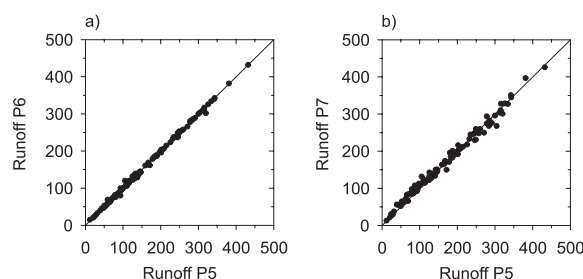


Fig. 5.10 Mean annual runoff (mm) of the 118 sub-basin of the study area for simulations P5-P7 with different spatial variability of rainfall, period 1960-98.

The importance of spatial variability of rainfall on catchment variables is expected to increase when going to smaller temporal scales, as rainfall variability itself increases in this direction. Looking at soil moisture, a higher spatial variability within a catchment at the monthly scale is found for simulation P7 with the highest variability of rainfall input of the three simulations (Fig. 5.11a). Differences between P5 and P6 are small, which demonstrates that the spatial rainfall variability at the grid-scale in P5 is very low after interpolation and already close to no variability as in P6. The difference between P7, on the hand, and

P5 or P6, on the other hand, is considerably more pronounced in the wet season as compared to the dry season. The annual course of soil moisture variability shows its maximum in the dry period where the variability is dominated by varying soil properties throughout the catchment to retain soil moisture for longer periods without recharge. Here the effect of rainfall variability is small, as rainfall volumes are very low and most of the signal of rainfall variability originating from the wet period is lost after drying of the soils. In the wet season, infiltration of rainfall dampens the soil moisture variability induced by the soil properties, i.e., the dynamic rainfall characteristics gain influence on soil moisture variability relative to the static soil factors. Thus, also the effect of spatial rainfall variability is more pronounced, as seen in the simulation results. In line with the above reasoning, variability of soil moisture is generally higher in dry years (Fig. 5.11b) than in wet years (Fig. 5.11c). However, no significant difference between dry and wet years concerning the relative effect of simulations with higher or lower spatially variable rainfall input is found.

In summary, the simulation experiments with rainfall input of different spatial variability indicate that its effect on simulated long-term average runoff at the sub-basin scale is small. However, for characterizing the variability within sub-basins, e.g. with respect to soil moisture availability, simulations with interpolated or basin-mean rainfall input underestimate markedly the variability, in particular during the rainy period. This is to be taken into account for subsequent applications of the model results at the scale of sub-basins for which the sub-scale variability might be of importance, i.e., for crop production modelling. For the scale of municipalities similar results as those for sub-basins studied here can be assumed because of their same mean size.

5.3.1.3 Mean rainfall volume

Due to low data availability, the rainfall input to model applications is highly uncertain not only in terms of its temporal and spatial variability at smaller scales, but also with regard to the pattern of long term mean rainfall volumes for the study area. WASA was applied to quantify the effect of different mean rainfall volumes on simulation results. The following model runs were examined:

- *Simulation P5* (reference version of WASA), corresponding to that of Chapter 5.3.1.1 and Chapter 5.3.1.2, with daily rainfall distributed

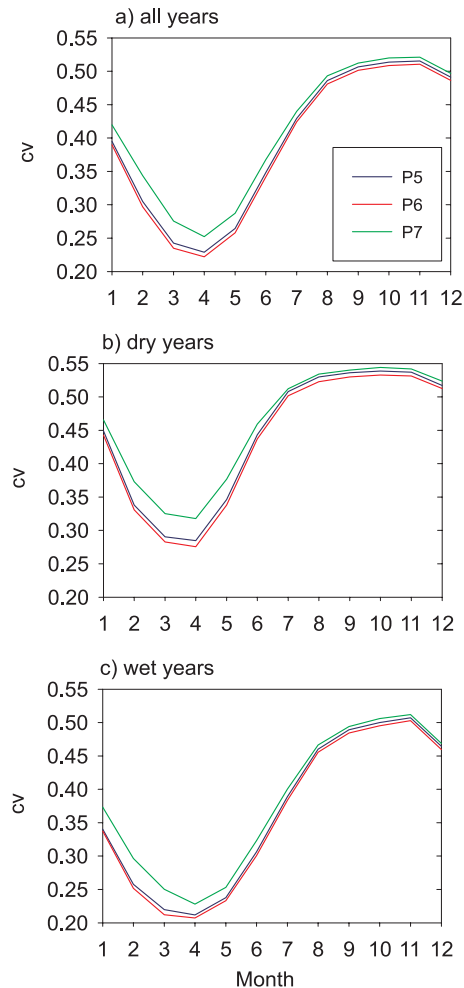


Fig. 5.11 Monthly coefficients of variation (*cv*) of soil moisture to a depth of 1 m within sub-basins of the study area with an area of more than 500 km², calculated from cell-based soil moisture values within each sub-basin, and averaged for all sub-basins. (a) all years of period 1960–98, (b) 10 driest years, (c) 10 wettest years. For simulations P5–P7 with different rainfall variability among grid cells.

among cells by interpolation with ordinary kriging (Set 2 in Chapter 2.1.6.2).

- *Simulation P8*, with daily rainfall interpolated by external drift kriging (Set 4 in Chapter 2.1.6.2).
- *Simulation P9*, at the scale of municipalities, with one rainfall time series attributed to each municipality. This time series is taken from Set 2 from one grid cell in the municipality while conditioning its daily volumes to give the same total annual rainfall of the municipality as in P5 after averaging over all grid cells of this municipality.

- *Simulation P10*, at the scale of municipalities, with one rainfall time series attributed to each municipality as given by the rainfall Set 1 (interpolation with a smaller number of stations, see Chapter 2.1.6.2).

Comparing P5 and P8 at the scale of grid cells, differences in mean annual rainfall due to the interpolation methods are in the range of -11% to +55%. For most cells, the differences in simulated mean annual runoff are considerably larger than the changes in rainfall, in average by a factor of about 2.5 (Fig. 5.12a). In aver-

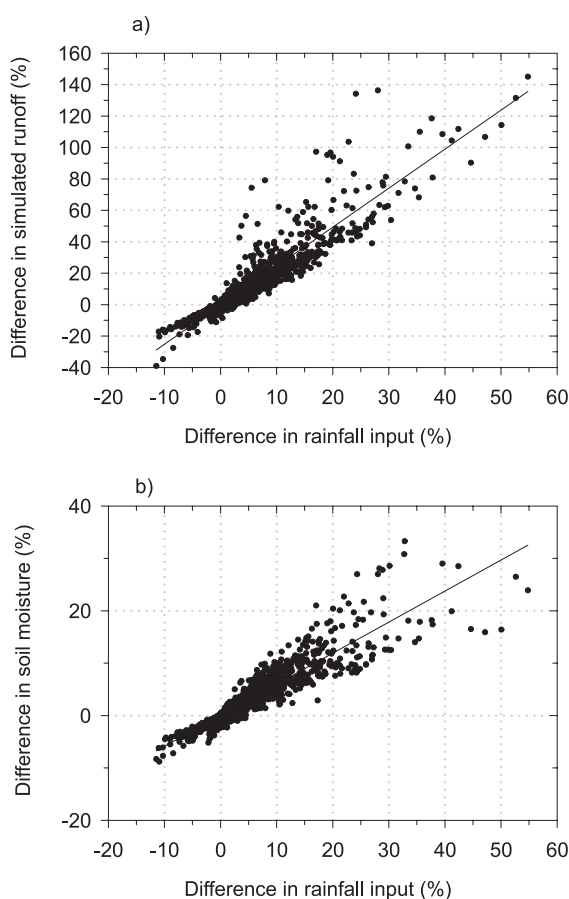


Fig. 5.12 Effect of variation in rainfall input between simulations P8 and P5 on (a) simulated runoff and (b) simulated plant-available soil moisture to a soil depth of 1m, mean for the months Feb-May; for the 1460 grid cells of the study area Ceará, period 1960-98.

age for the total study area, precipitation is about 5% higher in the case of P8 with external drift kriging (903mm as compared to 861mm for P5), which results in runoff being simulated larger by about 11% (163mm and 147mm for P8 and P5, respectively).

Changes in soil moisture available for plants (above wilting point suction) during the main vegetation period (February to May) also shows a close relationship to changes in rainfall input (Fig. 5.12b). However, the percentage change is smaller than that of rainfall, with a factor of 0.6 in average.

Regarding the spatial rainfall pattern (Fig. A.3), P8 represents the higher annual precipitation in elevated regions, particularly at the southern and western border of the study area, better than P5 in terms of what is expected from qualitative knowledge of the study area. However, some areas in the dry interior of the study area receive, contrary to the expectations, more rainfall than in P5 and the increase with elevation can be considered to be too large. The function of precipitation increase with elevation used as external drift may be largely influenced by the a stronger dependency found in the border areas and coastal mountains regions, which may, however, be exaggerated for the regions in the interior of the study area. E.g., BÖHM (1999) found even a weak decrease of rainfall with elevation when examining the entire semi-arid region of north-eastern Brazil. A quantitative measure of the performance of different interpolation methods results from statistical procedures such as cross-validation, which however were not done for the interpolations used here. An additional method may be to compare

Table 5.10 Rainfall (P), observed (Q_{obs}) and simulated (Q_{sim}) mean annual discharge and their difference Δ for various river basins in Ceará; simulations with different rainfall data sets; validation periods vary between stations within 1960-98 (see Fig. 2.6 and Table A.1 for more information on gauging stations).

Station	Basin area km ²	Q_{obs} m ³ s ⁻¹	P5			P8		
			P	Q_{sim} m ³ s ⁻¹	Δ %	P	Q_{sim} m ³ s ⁻¹	Δ %
1	6040	6.6	584	5.0	-14.3	638	7.8	+18.8
3	19250	32.5	742	37.4	+15.0	790	42.0	+28.9
7	11890	28.7	942	33.7	+17.3	980	37.2	+29.7
10	18270	39.8	732	26.9	-32.4	765	29.9	-24.9
12	47300	120.9	817	109.8	-9.1	846	118.8	-1.7
16	7339	21.2	776	19.6	-7.3	818	21.4	+1.1
22	11210	76.2	857	76.0	-0.3	889	82.9	+8.8

the simulated discharge on the basis of the different rainfall interpolation schemes with observed discharge. Generally, the effect of different rainfall input on runoff simulations and model performance is more pronounced for smaller basins. However, no clear ten-

gency can be drawn from this evaluation which rainfall data set gives results being closer to the observations, as positive as well as negative deviations from the observations occur for both simulations P5 and P8 due to the uncertainty of many other factors (Table 5.10).

For further model applications and sensitivity analysis in this study, the interpolation by ordinary kriging as used in P5 is taken as the reference rainfall input. It can be considered to be a best estimate in the sense that it uses all available rainfall information and a robust interpolation method. It is preferred to the interpolation in P8 because it does not rely on additional information which again is subject to uncertainty (as elevation in P8) and which may vary in its relevance for the spatial rainfall pattern across the study area. This would require a closer analysis first before such a more sophisticated approach could be justified to be more suitable than the simpler approach relying on the basic information only.

At the scale of the municipalities, mean rainfall attributed to each municipality differs considerably between simulations P9 and P10. Deviations are in the range of -40% to +40% for the annual mean (Fig. 5.13). Rainfall in P10 is underestimated particu-

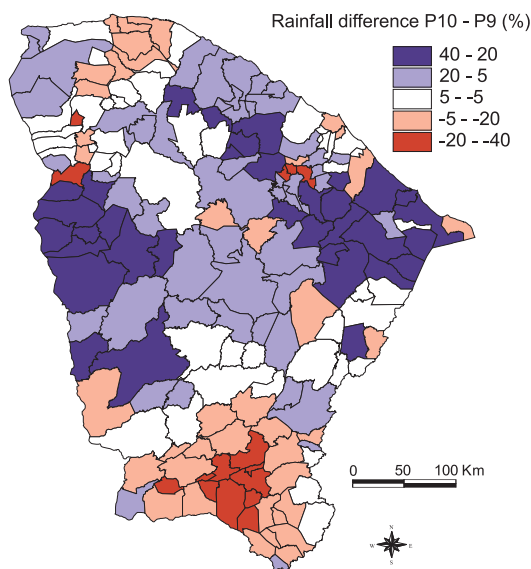


Fig. 5.13 Difference in mean annual rainfall at the scale of municipalities between the rainfall data sets of simulations P10 and P9, period 1960-98; compare Fig. A.3.

larly in the southern part of the study area, whereas rainfall in the central part is in general overestimated. These differences can mainly be attributed to the

markedly lower number of stations used for interpolation in P10 (Chapter 2.1.6.2), but may in parts also be caused by the different interpolation schemes. The effect of these differences in rainfall input on simulated runoff confirms the results found at the scale of grid cells, with a stronger percentage change in generated runoff, here by a factor of 2.3 in average, as compared to the underlying change in rainfall (Fig. 5.14). The spatial pattern of changes to runoff is close to that of variation in rainfall as shown in Fig. 5.13. Concerning exceptions from the above rule on changes in runoff relative to changes in rainfall as those seen in Fig. 5.14, it has to be taken into account that rainfall input to P9 and P10 does not only differ in its annual sums, but also in its temporal variability at shorter time scales which may counteract the effect of rainfall volumes, e.g., resulting in lower runoff volumes because of lower intensities at the short time scale albeit long-term total rainfall is larger (see Chapter 5.3.1.1).

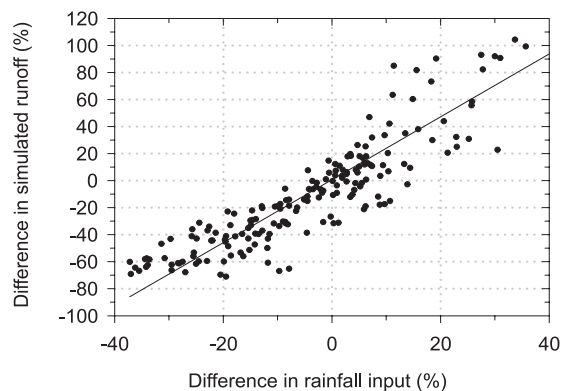


Fig. 5.14 Effect of variation in rainfall input between simulations P10 and P9 on simulated runoff for the 184 municipalities of the study area, period 1960-98.

In summary, large differences exist in the spatial distribution of long-term mean rainfall in the study area between the best-estimate data sets of P5 and P9 (which is derived from P5), on the one hand, and P10 being based on less data, on the other hand. The historical time series resulting in the spatial pattern of P10 were, however, used as basis for the construction of the climate scenarios (Chapter 5.5.1). Thus, the historical reconstruction of water availability with WASA in P10 at the scale of municipalities as basis for the evaluation of scenarios, as well as the scenario results themselves, are restricted in their reliability by the above deviations of their underlying rainfall input, among other factors. Fig. 5.13 and Fig. 5.14 give an estimate on the spatial patterns in direction and mag-

nitude of these deviations which have to be considered in scenario evaluation. Additionally, the large effect of changes in rainfall volume on runoff shown in this chapter demonstrates that model performance, when evaluated against measured runoff data, can heavily vary in dependence of the underlying rainfall input. This applies also for simulations P5 or P9, although based on a comparatively denser rainfall data base. Nevertheless, data availability is still low and, thus, uncertainty of rainfall input, and to an even larger extent, related uncertainty of runoff, is large.

5.3.2 Sensitivity to model structure

5.3.2.1 Spatial structure of modelling units

Different simulations with WASA were performed in order to evaluate the effect of structure and resolution of modelling units on results and model performance.

- *Simulation S1*: The reference version of WASA (see beginning of Chapter 5.3), based on grid cells ($10 \times 10 \text{ km}^2$), where in each grid cell two landscape units are distinguished, i.e., those two which have the largest spatial coverage of the grid cell after the GIS-based intersection of cells and landscape units. Rainfall input is given at the grid scale by interpolation with ordinary kriging (see simulation P5 in Chapter 5.3.1.1). All grid cells pertaining to each of the sub-basins in simulation S3 are aggregated to give the model response at the sub-basins scale.
- *Simulation S2*: Similar to S1, but reduced in the sense that only one landscape unit is taken for each cell, i.e., that with the largest spatial coverage of the grid cell after the GIS-based intersection of cells and landscape units.
- *Simulation S3*: Simulation on the basis of sub-basins without grid cells, where for each sub-basin all landscape units with a spatial coverage of more than 8% of the total basin area are considered in the model. The average size of sub-basins is 1350 km^2 . One rainfall time series is attributed to each sub-basin, taken from S1 from one grid cell in the sub-basin while conditioning its daily volumes to give the same total annual rainfall of the sub-basin as in S1 after averaging over all grid cells of this sub-basin (rainfall input corresponds to that of simulation P6 in Chapter 5.3.1.2).
- *Simulation S4*: Similar to S3, but instead of using sub-basins as the basic spatial unit, municipalities are used. All landscape units with more than 8% of the total area of the municipality are considered. The average size of municipalities is 810 km^2 , thus in the same order of magnitude as for sub-basins in

S3. Rainfall time series are attributed to each municipality from grid data in a similar way as in S3 for sub-basins.

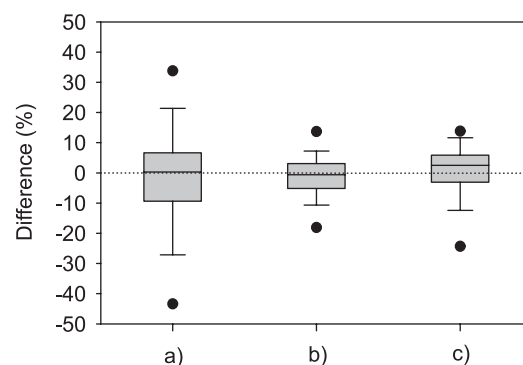


Fig. 5.15 Percentage difference in mean annual runoff (period 1960-98) for (a) 1460 grid cells in Ceará, difference simulations S2-S1, (b) 137 sub-basins in Ceará, difference S2-S1, (c) sub-basins, difference S3-S1. Boxes are limited by the 25th and 75th percentiles, black line within box = median, whiskers mark 10th and 90th percentiles, dots 5th and 95th percentiles.

At the scale of grid cells, differences in simulated mean runoff between simulations of lower and higher resolution of landscape data (S2 and S1) are within $\pm 30\%$ for most grid cells (Fig. 5.15a). At the scale of sub-basins, differences between both simulations are smaller (about $\pm 10\%$, Fig. 5.15b). Here, the larger sensitivity which exists at the cell scale is reduced after summarizing the response of individual cells. Enough information on the variability of soil and landscape characteristics is however pertained for most sub-basins to result in a similar runoff response at the sub-basin scale as in the case of the more detailed simulation. This is also expressed by the median of the differences of all sub-basins being close to 0 which indicates no systematic deviation. Similarly, also for simulation S3 with an even coarser soil and landscape data resolution the remaining captured variability of landscape units is generally sufficient to give similar results at the sub-basin scale than those with detailed data (Fig. 5.15c). The additional (small) effect of a reduced spatial variability of rainfall in S3 has been tested in Chapter 5.3.1.2.

For simulation S4 using administrative instead of physiographic units at the largest spatial scale, major differences in discharge simulations as compared to S1 or S3 occur due to deviations in size of the contributing areas for the gauging stations under study (Fig. 5.16, Table A.1). These differences in size, and correspondingly in discharge, may be more than 20%

for basins with an area of less than 15000km². They decrease with increasing basin area as the importance of diverging natural and administrative boundaries decreases relatively with total size. For smaller sub-basins, however, an adequate set of municipalities which drain to the sub-basin outlet may not be found at all. Beside of the size and location of the contributing area, other less important factors for different simulation results in S4 and S1 is the assignment of data on reservoirs and water use aspects (Chapter 4.2.9) as well as on agricultural land use (Chapter 4.3.1), which are available only at the scale of municipalities, to the sub-basin scale. This results in slightly different flow cascading in the river network and different combinations of soil-vegetation components within municipalities and sub-basins, respectively. These differences are reflected in the simulation results.

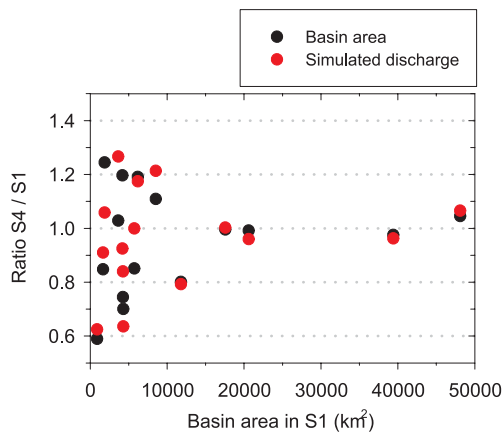


Fig. 5.16 Ratio of contributing basin area and of simulated mean annual discharge between simulation S4 (based on municipalities) and simulation S1 (based on cells and sub-basins).

In summary, being of practical relevance for scenario applications for which scenario data and other modules are available only at the municipality scale, the above results indicate that for the scale of interest of sub-basins or municipalities (in the order of 1000km² in size) and for the given resolution of landscape and soil data, a comparatively rough sub-division of these largest spatial units into landscape units (when compared to the cell-based sub-division) does not imply a loss of information which may significantly influence the accuracy of simulation results. This applies also for municipalities with regard to the assessment of surface water availability which is generated within these municipalities. For municipalities for which inflow from other municipalities with an upstream position is relevant for the assessment of water

availability, uncertainty can be expected to be larger for municipalities with a small contributing upstream area as for those with a larger one, because deviations between catchment and administrative boundaries tend to decrease with increasing area in their relative influence on flow assessment. It has to be noted that this discussion on the influence of spatial resolution applies to soil and landscape data only. Concerning the spatial structure with regard to rainfall data, a higher resolution might be required to capture the essentials of spatial variability (see Chapter 5.3.1.2).

5.3.2.2 Lateral redistribution of runoff

Fig. 5.17 compares *simulation L1* (with lateral redistribution of runoff at the scale of toposequences according to Chapter 4.2.5, i.e., the standard version of WASA) with *simulation L2* where no lateral redistribution is allowed, i.e., there is neither the possibility of reinfiltration of generated runoff or redistribution of subsurface runoff in adjacent soil-vegetation components (Chapter 4.2.5.1) nor in a terrain component of lower topographic position within the toposequence (Chapter 4.2.5.2). L2 results in markedly larger runoff volumes in most parts of the study area at the cell or sub-basin scale. In the case of L1, in general, surface runoff reinfiltrates in other modelling units with larger infiltration capacity and is available for evapotranspiration there instead of contributing to the total runoff of the grid cell. The spatial pattern in Fig. 5.17a shows that runoff is reduced by reinfiltration particularly in areas of crystalline bedrock where surface runoff is the most important runoff component. Variations between cells in the effect of lateral redistribution within the crystalline area depend on the variability of soil characteristics within the landscape units. The effect is more pronounced if soils of strongly differing water retention characteristics exist close to each other within or between terrain components. For instance, the effect increases with the fraction in area of soils with high infiltration and storage capacity, as alluvial soils. This applies, e.g., for areas in the Rio Potí basin in the central West of Ceará, and for parts of the middle and lower Jaguaribe basin. Comparatively larger differences between L1 and L2 are also found for grid cells which are composed of landscape units with rough topography, i.e., steep slope gradients. Here, the generation of lateral subsurface runoff is of more importance in the sloping region, i.e., in higher terrain components in WASA. This runoff component contributes directly to total runoff in L2, whereas in L1 it is routed to soil units with lower soil moisture or to the valley bottoms, i.e., the lowest terrain component, where it

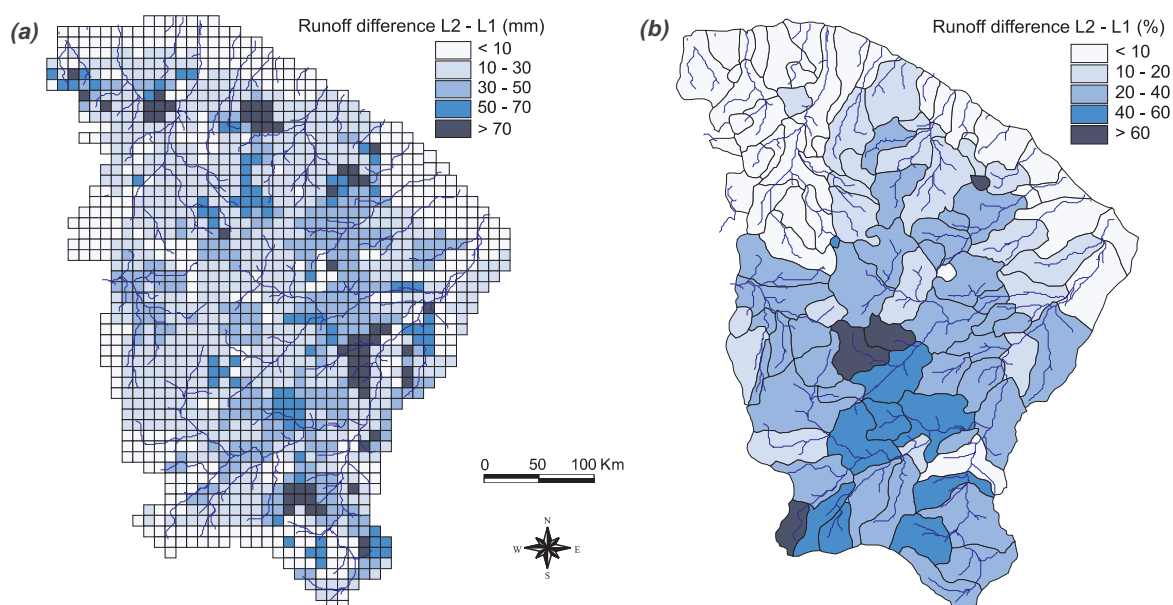


Fig. 5.17 Differences in simulated mean annual runoff between simulations L2 and L1 without and with lateral redistribution, period 1960-98, (a) at the scale of grid scales in mm, (b) at the scale of sub-basin as percentage difference of total runoff.

primarily fills up the alluvial storage and evaporates later. Thus, its contribution to total runoff is low or only in an indirect way by enhancing the susceptibility of these downslope areas to generate saturation-excess runoff. This effect of taking into account lateral redistribution within the model is shown in Fig. 5.17a by larger differences between L1 and L2 in the mountainous regions along the coast and in upper tributary areas of the Jaguaribe river.

For the scale of sub-basins, differences between L2 and L1 may be considerably large if expressed as percentage of total mean annual runoff (Fig. 5.17b). Particularly in the dry interior of Ceará, where absolute runoff volumes are low, using no lateral redistribution in L2 yields simulated runoff to be 20% to more than 60% higher than with lateral redistribution in L1.

Averaged for the entire study area, runoff is simulated 13% lower with lateral redistribution (L1) as compared to L2 without lateral redistribution (Table 5.11). Soil moisture available for plants, in contrary, is larger in L1, which is directly the effect of reinfiltration of surface runoff into otherwise drier units.

In an additional simulation (*Simulation L3*), lateral redistribution and reinfiltration was allowed only between soil-vegetation components within the terrain components (according to Chapter 4.2.5.1), but not between terrain components (according to Chapter 4.2.5.2). The results (Table 5.11) show that,

in average for the entire study area, runoff is reduced by about 10% compared to L2 without any redistribution. Thus, about three quarters of the total runoff reduction effect of lateral redistribution is attributed to stochastic variability of soil and vegetation characteristics between soil-vegetation components within the terrain components (see also Chapter 3.5.4), and the remaining effect to structured variability between terrain components. This comparatively large effect of stochastic variability at small scales (i.e., at scales smaller than a complete toposequence within the model concept used here) for the study area is, on the one hand, in principle reasonable in the view of similar observations in many other semi-arid environments (Chapter 3.3.1). On the other hand, one may argue that it is partly overestimated if considering how the available soil information is attributed to the modelling units with regard to stochastic or structured variability. Here, all information on different soil types available (only) at the scale of landscape units which cannot be related to structured variability between terrain components, is taken as stochastic variability by defining different soil-vegetation components within a terrain component (see also Chapter 4.3). This approach may, however, overestimate stochastic variability, as there possibly exist other factors (geology, slope gradients, etc.) within this landscape unit which are not resolved in the given data, but which will explain the given variability of soils in a more structured way. For ex-

ample, if more detailed information was available, one might come to the conclusion of delineating two different toposequences within the landscape unit under study, as one soil type occurs only in a certain part of the area with some specific conditions. This reformu-

Table 5.11 Effect of lateral redistribution on mean annual runoff Q (mm) and plant-available soil moisture θ (mean February-May) to a profile depth of 1m (mm) for different simulations with WASA, averaged for all grid cells of the study area, period 1960-98, subscript *dry* summarizes the 10 driest years only, subscript *wet* only the 10 wettest years within this period.

	Q	Q_{wet}	Q_{dry}	θ	θ_{wet}	θ_{dry}
Simulation L2	169	322	59	93	127	61
Simulation L1	147	298	41	106	142	72
Difference L2-L1 (%)	13.0	7.5	30.5	-14.0	-11.8	-18.0
Simulation L3	152	303	45	102	138	69
Difference L2-L3 (%)	10.0	5.9	23.7	-9.6	-8.7	-13.1

lation would increase the structured variability but, at the same time, decrease stochastic variability within each terrain component of the newly defined toposequences. The relative effect of both types of variability on runoff with regard to lateral redistribution of water fluxes would change accordingly. The net effect of both types on total runoff at the grid or basin-scale may finally be similar to the first formulation, however. In a similar sense, the comparatively large effect of stochastic variability found in Table 5.11 is also partly due to fact that no information on structured variability could be extracted from the available data for several landscape units, i.e., for these landscape units only one terrain component was defined in the model, which implies the occurrence of exclusively stochastic variability in the sense used here.

The effect of lateral redistribution on runoff and soil moisture is much more apparent in dry years as compared to wet years (Table 5.11). A larger fraction of generated runoff in soil-vegetation-components and terrain components is retained before reaching the outlet of a landscape unit in dry than in wet years. This is reasonable, as in dry years the refillable soil moisture storage in units adjacent to those generating runoff is expected to be larger in average and so infiltration is more pronounced. The coefficient of variation of annual runoff, averaged for all grid cells, is 0.96 in simulation L2 as compared to 1.20 in simulation L1. Thus, respecting lateral redistribution processes in the model increases the interannual variability of the results with regard to runoff generation at the grid or sub-basin scale.

5.3.2.3 Temporal scale in evapotranspiration modelling

Two simulations are compared to test the effect of temporal resolution on modelling of actual evapotranspiration (interception evaporation, soil evaporation and plant transpiration). In a first model run, evaporation is calculated on a daily basis with mean daily climate data as input. In the second run, the reference version of WASA (see beginning of Chapter 5.3) is applied with evapotranspiration modelling separated in a day and a night component. The climate variables radiation and air temperature are distributed among day and night according to the description in Chapter 4.2.2.

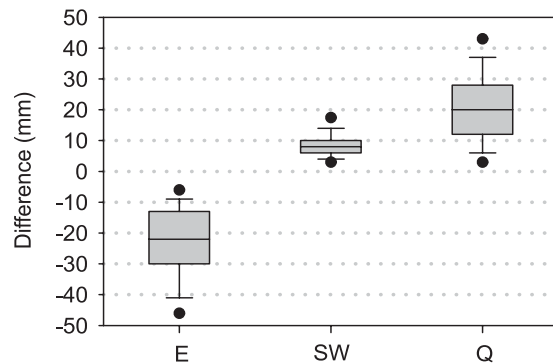


Fig. 5.18 Difference in actual evapotranspiration (E), plant-available soil moisture (SW) to a profile depth of 1m during the rainy period, months Feb-May, and runoff (Q) between simulations with mean daily evapotranspiration modelling and with separate day-night calculations; annual mean of period 1960-98 for for all 1460 grid cells of the study area; the box-whisker plots describe the variability among grid cells with: Boxes limits at the 25th and 75th percentiles, black line within box = median, whiskers mark 10th and 90th percentiles, dots mark 5th and 95th percentiles.

The mean daily simulation results in actual evapotranspiration volumes which are in average about 20 mm lower in the annual mean than those for the day-night calculation, which corresponds to a percentage difference of total annual evapotranspiration of -3.3%. This difference corresponds in direction, although being smaller in magnitude, to that found by SCHULLA (1997) for a humid temperate environment. It is caused by the strong difference in available energy between the day and the night situation, particularly with respect to short-wave radiation input. The underestimated evapotranspiration in the daily mean version results, consequently, in an overestimation of soil

moisture and runoff. Due to the small absolute runoff volumes in most parts of the study area, the difference of about 20 mm causes a percentage overestimation of runoff relative to the reference model by in average 14.3% for all grid cells. The 5th and 95th percentiles of the effect on all cells correspond to a relative change of runoff of 6% and 29%, respectively. Due to its non-linear effect on the evapotranspiration process, these results demonstrate that using daily mean input of the climate elements radiation and air temperature is not appropriate for this type of environment and may lead to a considerable bias in the quantification of runoff generation.

5.3.3 Sensitivity to model parameters

Sensitivity analysis were realized to test the effect of changes in parameters values on model results. The focus is on those parameters which were derived from terrain, soil and vegetation data of the study area and which are characterized by uncertainty of different degree depending on the quality and resolution of the available information. In comparison to the reference version of WASA, for each analysed parameter two simulations with decreased and two simulation with increased parameters values were run. The first step of negative or positive changes to the parameter values is based on an estimate of what can be expected to be a likely range of uncertainty of this parameter in the given data. The second, more severe step of negative or positive changes being examined represents the estimate of a maximum range of uncertainty of the respective parameters. Thus, by this simple approach, an assessment of the uncertainty of variables of interest for the quantification of water availability, i.e., runoff and soil moisture, due to parameter uncertainty is made in Chapter 5.3.3.1 and Chapter 5.3.3.2. The focus is on mean annual values as well as on particularly dry and wet conditions, which might be of most relevance for climate change impact assessment.

5.3.3.1 Soil and terrain parameters

The sensitivity of soil and terrain parameters (see parameter overview in Table 4.1) on runoff simulations varies considerably between the parameters. The first row of Fig. 5.19 presents the results for terrain parameters which are model input at the scale of landscape units or terrain components. Slope length and gradient are relevant only for those sub-basins where lateral subsurface flow in the soil zone is of importance. Comparatively small median changes in total runoff for changed parameters (Fig. 5.19a, b) indicate the

generally low importance of this runoff component for the entire study area, which is line with the expectations for semi-arid environments (see Chapter 3.3.1.3). However, the large variability among sub-basins in Fig. 5.19b and particularly in Fig. 5.19a stresses that this process may in parts be of importance, e.g., for areas with high relief intensity (see also Chapter 5.3.2.2).

Bedrock characteristics influence runoff generation only in the crystalline area with shallow soils. A decrease in the hydraulic conductivity $k_{s,LU}$ (Fig. 5.19c) has only a minor effect on runoff, as it is already set to a very low value for the crystalline (nearly impermeable bedrock) in the reference version of WASA. An increase of $k_{s,LU}$, on the other hand, may decrease runoff volumes considerably, as a larger fraction of soil moisture is lost in the form of groundwater recharge to the bedrock aquifer. In areas of tectonic activity with a more intensely fractured bedrock the low value of $k_{s,LU}$ set in the reference version may lead to an overestimation of runoff volumes. However, such geological information is not available in this study. Note that the model sensitivity to $k_{s,LU}$ is more pronounced in wet than in dry years, because only under wet conditions rainfall is in general sufficiently high for percolation to penetrate the total soil profile and thus to be influenced by bedrock characteristics. This applies also for the soil depth to bedrock, a parameter of large uncertainty as it is given for the exemplary soil profiles only, but may vary considerably throughout the study area. The main reason for model sensitivity to this parameter is the related change of total soil storage capacity, and, thus, the tendency of a soil component to be source area of saturation-excess runoff. Changing its value for about 50% results in changes in mean annual runoff of up to 15% at the sub-basin scale (Fig. 5.19d). This comparatively small effect points to the fact that soil saturation is usually confined in space to smaller areas for this type of environments and a stronger importance of surface-related processes for runoff generation.

Model sensitivity to changes of saturated hydraulic conductivity of the soil horizons shows a complex pattern (Fig. 5.19e). A decrease of k_s by the factor 0.5 increases runoff up to around 20% for most sub-basins. A larger decrease of k_s by one order of magnitude, which is still in the range of the generally large uncertainty being expected for this parameter, has a very strong effect on runoff simulations, with more than 100% for some sub-basins, particularly for dry conditions. The main reason for runoff increase is the increase of infiltration-excess runoff, induced by the lower soil conductivities (Table 5.12). The exception-

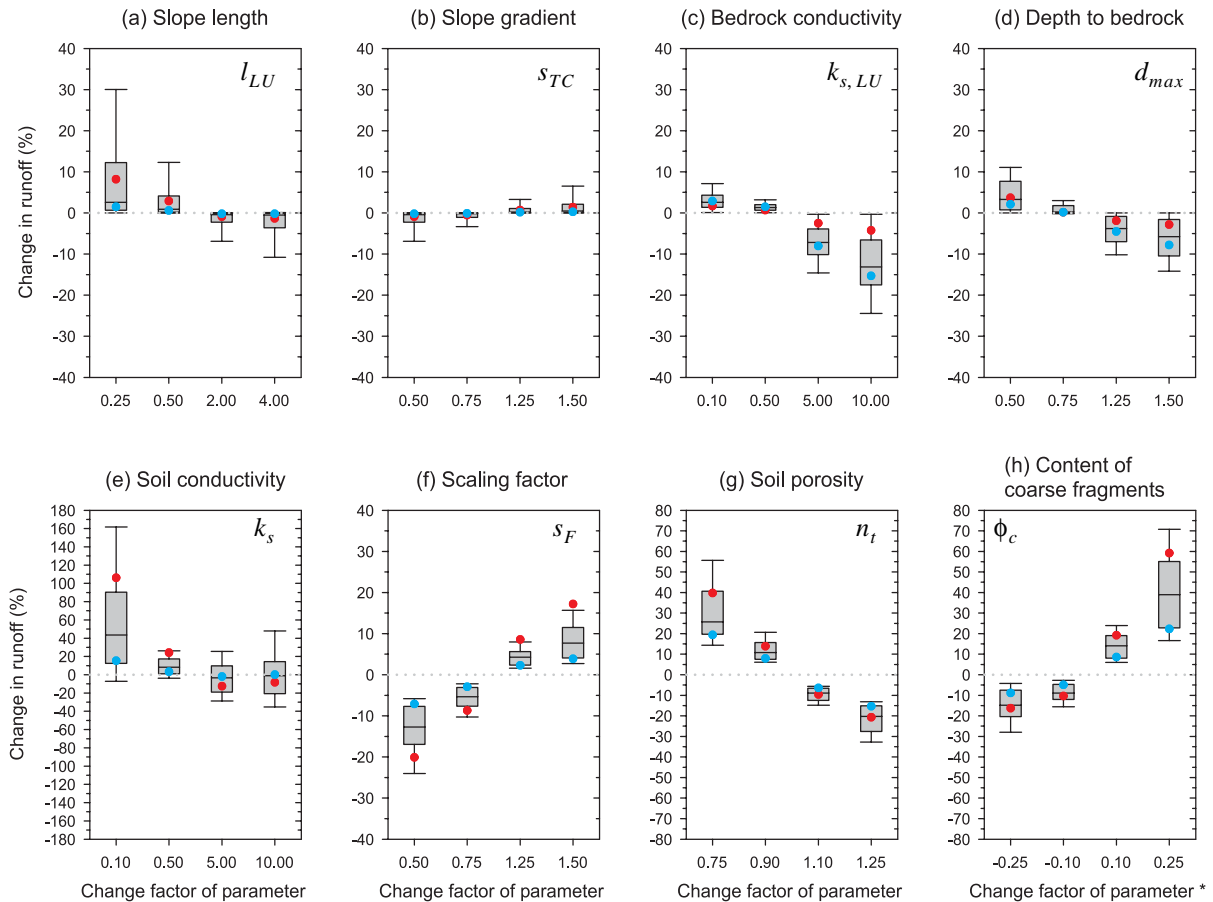


Fig. 5.19 Sensitivity analysis for soil and terrain parameters in WASA. The x-axis indicates the factor by which the parameter is changed multiplicatively (* exception for ϕ_c where the change factor is applied additively); y-axis indicates the percentage change of mean annual runoff (simulation period 1960-98) at the scale of sub-basins as compared to the reference simulation without parameter change; note that the scaling of the y-axis varies between graphs. Box-whisker-plots give the variability of the effect of parameter changes on mean annual runoff among the 107 sub-basins of the study area: Boxes are limited by the 25th and 75th percentiles, black line within box = median, whiskers mark 10th and 90th percentiles. Red points indicate the median change in runoff for all sub-basins for the 10 driest years within 1960-98 only, blue points indicate the median change in runoff for all sub-basins for the 10 wettest years within 1960-98.

ally large effect when changing k_s by the factor 0.1 may point out that soil conductivities for many soils of the study area are then in the range of usual rainfall intensities. Thus, even small changes may have a considerable effect on the infiltration process. On the other hand, when k_s is increased as compared to the reference version of the model, the average effect for the study area on runoff is practically zero, with variability to positive and negative changes among individual sub-basins. This is because k_s does not only influence the infiltration process, but also percolation through the soil profile and lateral flow. Both fluxes are enhanced by a larger value of k_s , so that more water is transported to lower soil horizons or to the river

with the chance of losses to evapotranspiration being reduced. This compensates in average for lower infiltration-excess runoff (Table 5.12). For individual sub-basins, the net effect on total runoff varies with the relative importance of both runoff components (lateral subsurface flow and infiltration-excess runoff) as function of the specific terrain and soil characteristics, which explains the variability in Fig. 5.19e.

In contrary to soil conductivity, the scaling factor, which is introduced to compensate for underestimated rainfall intensities, affects only the infiltration process. A simple type of its sensitivity on runoff volumes is found (Fig. 5.19f, see also discussion in Chapter 5.3.1.1).

Changes in soil porosity have a large sensitivity on runoff volumes, in average for the entire study area in an approximately linear form (Fig. 5.19g). Changes in n_t modify the total storage capacity of the soil and thereby act on the fraction of rainfall which can infiltrate into the soil and which runs off at the surface. This parameter is of considerable uncertainty, as it is based on estimates of the bulk density of soil horizons (Eq. 4.64). These estimates comprise a strong degree of subjectivity when being fixed during the survey of soil profiles in the field, and may vary considerably between locations even for the same soil type.

Table 5.12 Model sensitivity to changes in soil hydraulic conductivity k_s on mean annual runoff, averaged for the study area, period 1960-98, (compare Fig. 5.16e); Q : Total runoff, Q_{hort} : Infiltration-excess runoff, Q_{lat} : Lateral subsurface flow; f_{hort} , f_{lat} : fraction of both runoff components on total runoff.

Change factor		0.1	0.5	1.0	5.0	10.0
Q	mm	181	154	147	142	148
Q_{hort}	mm	142	86	64	33	23
f_{hort}	%	78.5	55.8	43.5	23.2	15.5
Q_{lat}	mm	27	38	42	59	71
f_{lat}	%	14.9	24.7	28.6	41.5	48.0

The content of coarse fragments in the soil profile ϕ_c influences within WASA all soil water retention characteristics (e.g., field capacity, wilting point) and the hydraulic conductivity (see Chapter 4.3.2). The analysis on this parameter thus implies a complex set of processes, including also model sensitivity for water retention characteristics of the soil, which are in practice determined from the parameters of the pedo-transfer-functions but not examined in detail here. Generally, an increase in the coarse fragment content of 10Vol%, which decreases the other above parameters by 10%, results in runoff increasing by about the same percentage (Fig. 5.19). The inverse effect is found for a decrease in ϕ_c . However, the analysis in this direction is limited as the minimum value for ϕ_c is 0. Changes in ϕ_c can be expected to act ϕ_c on runoff generation via the soil storage capacity and infiltration capacity for rainfall.

It should be pointed out that for changes in soil parameters (second row of Fig. 5.19), the model reacts markedly more sensitive in relative terms for dry years as compared to wet years. In dry years, the dominant process which might generate runoff is infiltration-excess, whereas for wet conditions saturation-

excess and subsurface flow gain in importance. Thus, any small change of relevant soil parameters for infiltration-excess in dry years has large implications on the, in absolute terms, low runoff volumes. This differentiated model sensitivity has to be respected in the discussion of uncertainty of model results, particularly for scenario calculations with an assumed future decrease of rainfall.

Table 5.13 Sensitivity analysis for soil and terrain parameters on soil moisture available for plants to a soil depth of 1 m in the period February-May; median values for all sub-basins of the study relative to the reference model version, period 1960-98. Four simulations with different change factors (strong reduction (--) to strong increase (++)) corresponding to the factors given in Fig. 5.16 for each parameter.

Change factor	--	-	+	++
Parameter				
Slope length	-1.1	-0.4	0.1	0.2
Slope gradient	+0.1	+0.1	-0.1	-0.2
Bedrock conductivity	+2.3	+1.1	-6.2	-11.9
Depth to bedrock	-1.6	-0.5	-0.4	-0.7
Soil conductivity	-5.1	+0.2	-3.3	-6.1
Scaling factor	-1.1	-0.3	+0.1	0.0
Soil porosity	-23.1	-9.9	+10.0	+24.3
Soil coarse fragments	+15.3	+7.9	-11.0	-26.2

The sensitivity to changes in terrain parameters on plant-available soil moisture is in general lower in relative terms than the sensitivity on runoff (Table 5.13). This indicates that these parameters (e.g., slope length, gradient, bedrock conductivity) act on processes (lateral subsurface flow) which mainly occur below the relevant soil moisture zone. It has been set for this analysis to a maximum depth of 1 m. In general, parameter changes act in the opposite direction in terms of sensitivity for soil moisture availability as compared to sensitivity for runoff generation. Changes in soil conductivity, however, lead to a decrease in practically all cases, as, on the one hand, a decrease of k_s reduces the infiltration amount, and, on the other hand, an increase in k_s causes a more rapid percolation or lateral outflow from the soil profile, such that soil moisture availability decreases also in this case. The most sensitive parameters with regard to soil moisture are those which directly influence the water retention characteristics of the profile, i.e., soil porosity and the content of coarse fragments. Here, changes of about 20% may occur for the assumed parameter uncertainty.

5.3.3.2 Vegetation parameters

In general for the sensitivity of vegetation parameters (see parameter overview in Table 4.2) on runoff simulations, a larger effect can be seen for wet than for dry conditions (Fig. 5.20). This can be explained by the large evapotranspiration volumes for the type of environment under study, where losses of soil moisture to evapotranspiration occur rapidly after rainfall events. The rate of these losses, which is primarily governed by the values of the vegetation parameters studied here (in contrary to the total evapotranspiration loss volume after a sufficiently long dry period, which will be approximately the same for all parameter values) is of more importance for wetter conditions with a more frequent sequence of rainfall events. In this case, soil moisture pre-conditions for a event are still to a larger

extent influenced by the previous events and, thus, by evapotranspiration rates between these events.

Canopy height (Fig. 5.20a) and albedo of the land surface (Fig. 5.20d) are two parameters which primarily act on the potential of the atmosphere for evapotranspiration, as they govern the ventilation conditions and available energy. The assumed range of uncertainty of these parameters leads to changes in simulated runoff in the range of up to 10% at the sub-basin scale. The same average effect, but a considerably larger variability among sub-basins, can be assigned to changes in the root depth. Here, an extension of the root depth by a factor of 2 may lead to a runoff reduction of up to 30%. The larger variability among sub-basins is explained by the interaction of root depth with the highly variable soil characteris-

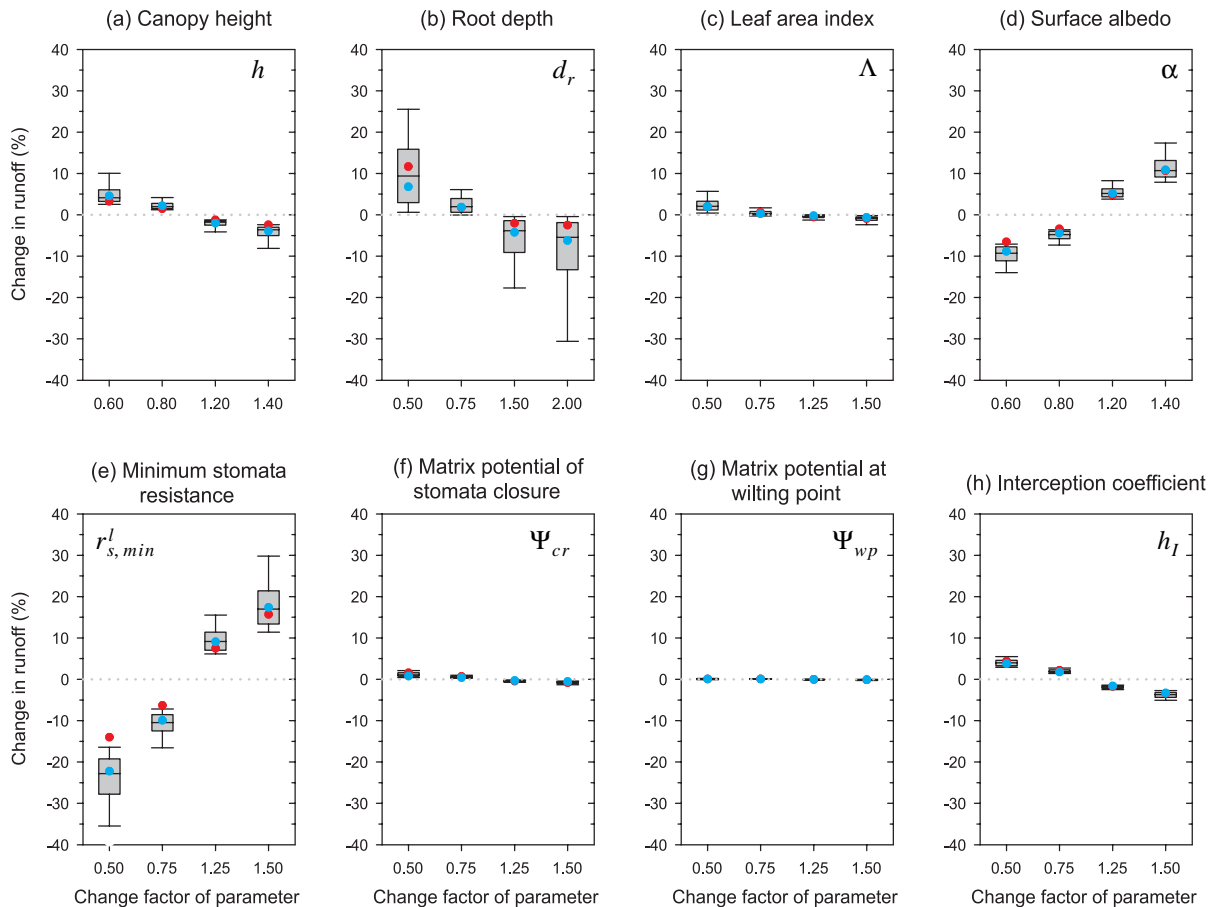


Fig. 5.20 Sensitivity analysis for vegetation parameters in WASA. The x-axis indicates the factor by which the parameter is changed multiplicatively, the y-axis indicates the percentage change of mean annual runoff (simulation period 1960-98) at the scale of sub-basins as compared to the reference simulation without parameter change; for details for the description of box-whisker plots see Fig. 5.16.

tics, also among soil horizons. Thus, whether roots reach a certain horizon or not in the different simulations may considerably change the overall water balance of the soil profile. Root depth is a highly uncertain parameter as it is influenced by a variety of factors related to plant-specific characteristics, soil texture and structure, bedrock conditions, and soil chemistry, for which only very limited information is available.

A small model sensitivity is found for the leaf area index Λ (Fig. 5.20c), although this parameter is used to scale surface resistances for transpiration from the leaf to the canopy scale (Chapter 4.2.2) and an important influence might be expected. However, the scaling relationship (Eq. 4.32), which includes attenuation of radiation within the canopy, results in an approximately constant value of canopy resistance for $\Lambda > 1.5$, depending only on the underlying leaf stomatal resistance r_s^l (Fig. 5.21). Because most vegetation types of the study area are set to $\Lambda > 1.5$ in the rainy period (Table 4.3), the sensitivity to changes in Λ is comparatively low. The clearly more sensitive factor in this context is thus the minimum leaf stomatal resistance $r_{s,min}^l$ for which changes of 25% result in related changes in runoff by in average about 10% (Fig. 5.20e).

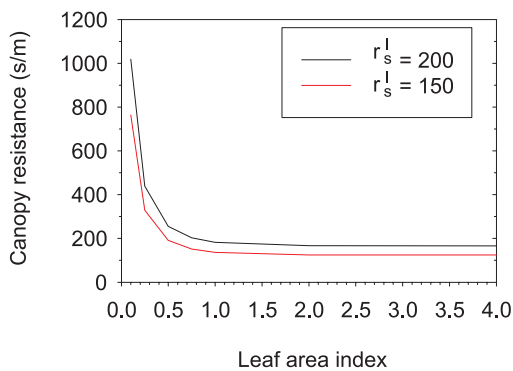


Fig. 5.21 Scaling relationship for surface resistance from the leaf to the canopy scale (Eq. 4.32) for two different values of leaf stomatal resistance r_s^l .

Low sensitivities to runoff simulations are found for the parameters Ψ_{cr} and Ψ_{wp} which govern the reduction of transpiration due to water stress. The reason may be that these parameters, particularly Ψ_{wp} , are relevant only for comparatively large negative soil moisture potentials, which are related due to the non-linearity of the soil moisture-suction-relationship to very low absolute soil moisture values. Changes in model parameterization for such dry conditions do in

consequence not significantly affect runoff generation which occurs mainly during a higher soil moisture status.

Also for the interception coefficient, a comparatively low sensitivity on runoff simulations is found. For interception losses, it is rather the temporal sequence of rainfall events which is of major importance (see Chapter 5.3.1.1).

Changes in the values of the vegetation parameters tested here (particularly $r_{s,min}^l$, d_r and Λ) result in changes of simulated plant transpiration. Simulated total evapotranspiration of the land surface, however, is affected to a lower degree in relative terms. This is due to an opposite change in soil evaporation as compared to changes in transpiration. Both components are simulated simultaneously including their interaction by the approach used in WASA (Chapter 4.2.2). Thus, e.g., a reduction in transpiration may enhance soil evaporation as more energy is available for that component (Table 5.14). The sensitivity to runoff simulations by changing transpiration is consequently dampened to some extent by soil evaporation.

Table 5.14 Model sensitivity to changes in minimum stomatal resistance $r_{s,min}^l$ on mean annual evapotranspiration E and soil evaporation E_S , averaged for the study area, period 1960-98, (compare Fig. 5.17e); f_{E_S} : fraction of E_S on total evapotranspiration.

Change factor		0.50	0.75	1.00	1.25	1.50
E	mm	732	712	695	680	667
E_S	mm	227	244	256	266	274
f_{E_S}	%	31.0	34.3	36.8	39.1	41.1

Finally, for the example of model sensitivity to $r_{s,min}^l$, it should be pointed out that small relative changes in annual evapotranspiration (a maximum of about 10% between the simulations in Table 5.14) have a considerably larger effect on relative changes in runoff (about 40%, Fig. 5.20e) due to the low fraction of runoff on rainfall as compared to evapotranspiration for these semi-arid areas. Thus, deviations in evapotranspiration modelling may heavily influence model performance with regard to runoff simulations.

Model sensitivity of vegetation parameters with regard to plant-available soil moisture is, in general, smaller and of opposite direction than the sensitivity found above with regard to runoff. The only marked exception is the effect of changes in Ψ_{wp} . As this parameter directly defines the soil moisture potential to which plants may extract water from the soil, a decrease of its value by 25%, for instance, increases soil moisture availability by in average 10%.

5.4 Results for the Historical Period at the Regional Scale

5.4.1 General results on runoff and soil moisture

Results of the reference version of WASA (see beginning of Chapter 5.3) for the regional scale of the State of Ceará are presented at in Fig. 5.22. The spatial distribution of generated runoff (Fig. 5.22a) in general reflects the spatial distribution of rainfall (Fig. 2.3). Highest runoff values occur in the coastal zone and the adjacent mountainous area. In the southwestern interior of the study area, runoff is smallest with mean annual values below 100mm. The smaller the annual precipitation, the smaller is usually the runoff ratio (ratio between runoff and precipitation) (Fig. 5.22c), demonstrating the non-linear behaviour of the semi-arid hydrological system. This can be mainly explained by the in general higher actual soil storage capacity at the onset of a rainfall event in are-

as with lower total rainfall, because the time period between events is in average larger and the event volumes themselves are often smaller. Evapotranspiration, which is high in this type of semi-arid environments, reduces the actual soil moisture to a lower level until the onset of the next event than in wetter areas, thus providing more storage volume for the next rainfall input. This in turn leads to a smaller fraction of rainfall being transformed into runoff.

Looking at river discharge at the outlet of the sub-basins (Fig. 5.22b), the spatial pattern stresses the larger volumes in down-stream sub-basins of the larger river basins of the study area. Generally high coefficients of variation of annual runoff are found for most sub-basins of the study area (Fig. 5.22d). Values >1.0 correspond to those reported for other semi-arid areas, e.g. in Australia (CHIEW ET AL., 1995) or in Southern Africa (SMITHERS, 2001, personal communi-

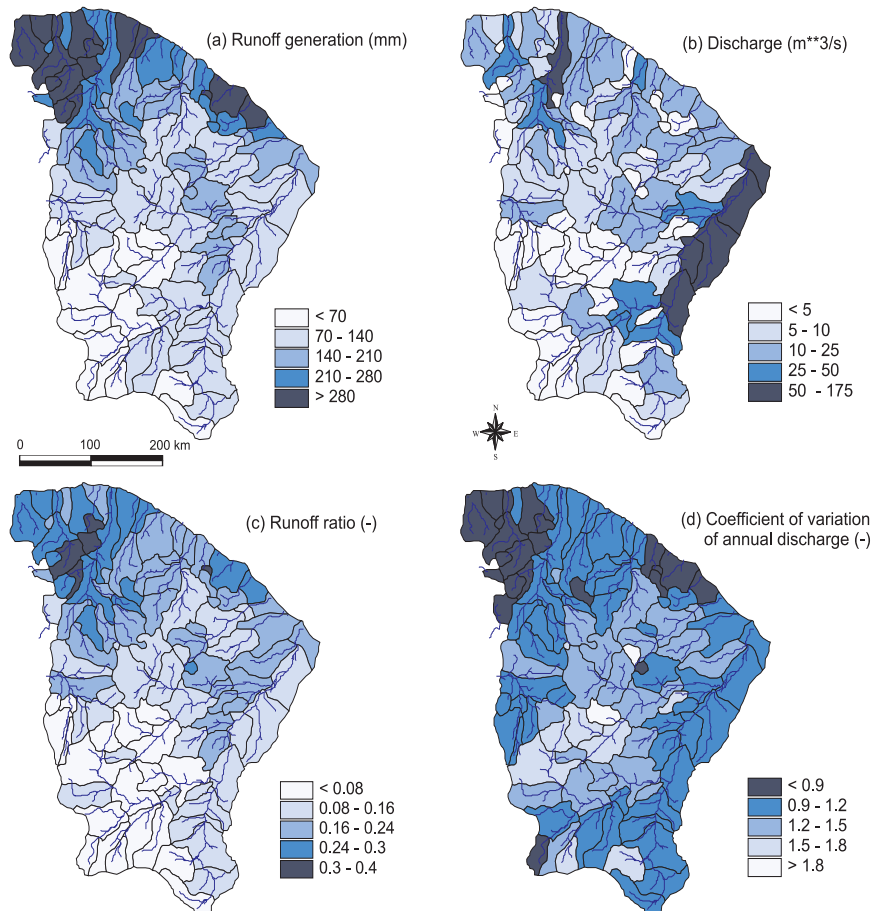


Fig. 5.22 Results of model application for the state of Ceará, mean annual values for the period 1960-1998.

cation). The spatial distribution of the coefficient of variation (CV) of annual discharge, characterizing the interannual variability of discharge, reflects two main features:

- CV tends to be higher in areas with lower runoff ratios, i.e., in the drier areas in the center of the study area. For a given rainfall variability, the resulting runoff variability is larger for these areas with lower total rainfall volumes than for those with larger ones, in line with the above reasoning concerning the runoff ratio. A direct relation of CV of discharge to the spatial pattern of the interannual variability of rainfall input, however, can hardly be recognized (compare Fig. 2.3).
- CV tends to be lower for sub-basins of a more downstream position in river basins. Here, the strong interannual variability of smaller areas due to their specific physio-climatic conditions is smoothed by integrating over larger areas. Additionally, spatial rainfall variability between sub-basins for individual years may be important also in the case that these sub-basins have the same long-term mean annual rainfall. The relative importance of this rainfall variability on its effect on runoff variability is reduced when proceeding to larger areas.

Concerning plant-available soil moisture, no consistent spatial pattern is found throughout the study area for values averaged to the scale of sub-basins (Fig. 5.23). Large spatial variability occurs, caused by the complex interaction of climatic, pedological and land use factors. Additionally, averaging from the level of soil profiles through the various scale levels used in WASA up to the scale of sub-basins seems to prevent any interpretation of the results with regard to the underlying factors at the final coarse resolution.

5.4.2 Effect of reservoirs and water use

The effect of water storage in reservoirs and of water use on water availability is illustrated in Fig. 5.24. The mean annual storage volume in the reservoirs of Ceará at the end of the rainy period (month of June) is $8.1 \cdot 10^9 \text{ m}^3$ in average for the simulation period (1960-1998). It has to be taken into account when looking at mean annual values for the historical time series that there is an increasing trend in water storage in reservoirs due to the construction of several new reservoirs which is dynamically represented in WASA (see Chapter 4.2.7). The spatial pattern of storage volumes in Fig. 5.24a is dominated by several large reservoirs which have a storage capacity of about an order of

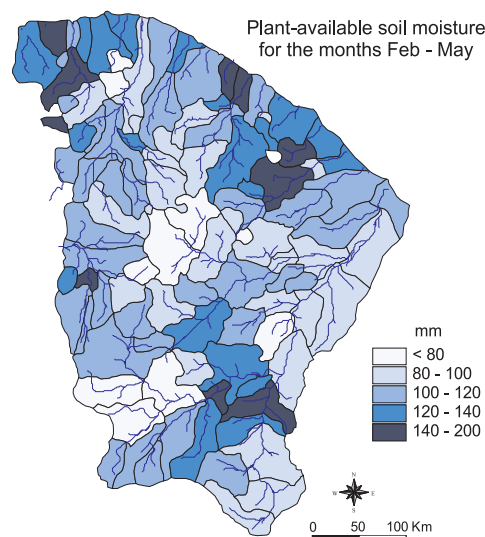


Fig. 5.23 Plant available soil moisture to a depth of 1 m for the months February-May, mean of period 1960-1998.

magnitude larger than the sum of all smaller reservoirs ($< 50 \cdot 10^6 \text{ m}^3$) in the respective sub-basins (compare Fig. 5.24b). Nevertheless, a large amount of runoff is retained also in these small and medium-sized reservoirs, particularly in the Jaguaribe and Banabuiú basin.

Table 5.15 Difference in storage volume for various reservoir classes (grouped by storage capacity in 10^6 m^3 , see Fig. 4.8) between the end of the rainy season (June) and the dry season (December), average for Ceará and the period 1960-1998, in %.

Reservoir class	1	2	3	4	5
Storage capacity	<0.1	0.1-1	1-3	3-10	10-50
Storage difference	51.9	41.7	29.0	18.7	15.2

The comparison of water storage in reservoirs at the end of the rainy period (June) and the dry period (December is taken as an exemplary month) for different reservoir classes (Chapter 4.2.7) illustrates their different storage behaviour (Table 5.15). The smaller reservoirs show a considerably stronger variability, falling to low levels or drying out during the dry season. Larger reservoirs generally have a more balanced behaviour with a smaller relative decline of storage volumes in the dry season. This different behaviour is mainly a consequence of the non-linearity of the relationship between actual storage volume and the water surface area (Chapter 4.2.7), leading to, in relative terms, a weaker susceptibility to evaporation losses for

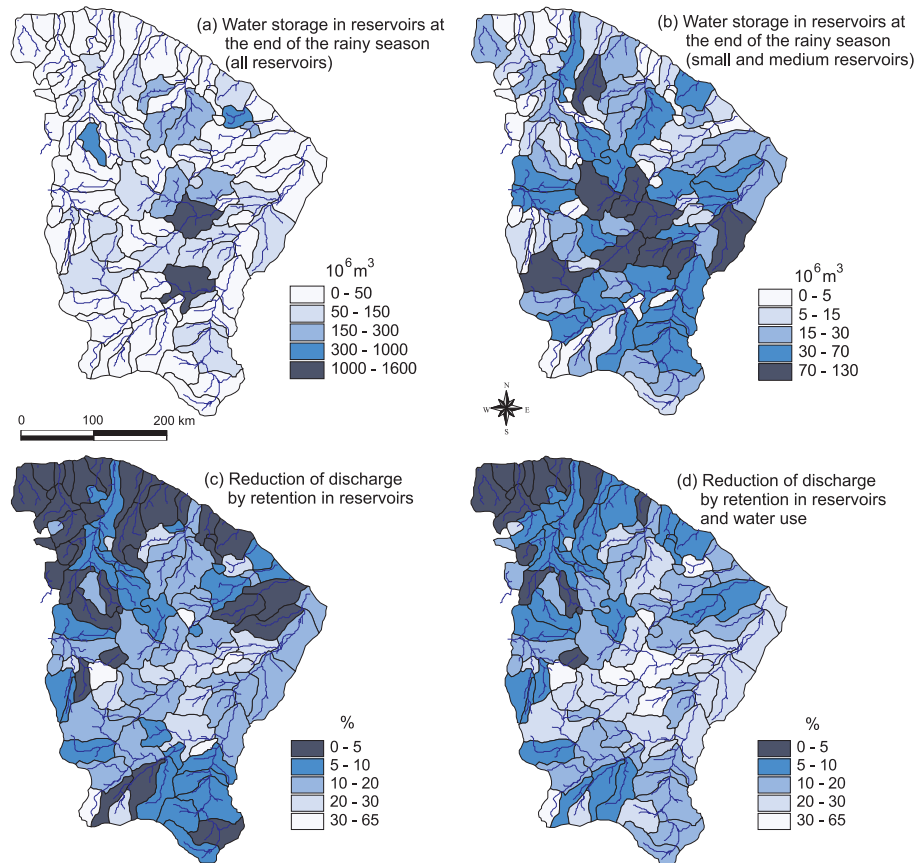


Fig. 5.24 Simulation results for Ceará on the effect of reservoirs and water use on water availability; mean annual values for the period 1960-98. (a)+(b): Storage in reservoirs at the end of the rainy season (June), in (b) only reservoirs with a storage capacity of $<50 \cdot 10^6 \text{ m}^3$ are considered. (c)+(d): Reduction of mean annual discharge (as compared to naturalized flow) at the sub-basin outlet by upstream (c) retention in reservoirs and (d) retention in reservoirs and water use.

larger reservoirs. These provide, thus, more reliability in providing water throughout the entire dry season or during a prolonged drought period.

Water retention in reservoirs and subsequent evaporation reduces markedly the mean annual discharge in downstream sub-basins as compared to naturalized flow (Fig. 5.24c). In areas of a high reservoir density, reduction of downstream discharge is generally up to 20%. If additionally the withdrawal of water from reservoirs and directly from the river is taken into account, downstream discharge reduction often exceeds 20% in the annual mean, for some parts particularly in the Banabuiú basin even more than 30% (Fig. 5.24d). Thus, while providing the potential to reduce the intra- and interannual variability of water availability at downstream positions by a managed release from reservoirs during the dry season or during dry years, the total discharge volumes are considerably reduced in most parts of the study area by upstream retention and

use. This large effect has also been taken into account during model validation (see next chapter).

5.4.3 Model validation

5.4.3.1 General aspects and criteria

The limited quality of the available discharge and reservoir storage data has been discussed in Chapter 2.1.6.3. Measurement errors introduce an additional source of uncertainty in the evaluation of model results. The following quantitative performance criteria were defined for model validation:

- (1) Δ_Q , the difference between simulated mean annual runoff Q_{sim} and observed mean annual runoff Q_{obs} , normalised by the observed runoff and given as a percentage value (Eq. 5.2). Δ_Q is a

criteria to evaluate the accuracy of simulation results in terms of the overall water balance.

$$\Delta_Q = (Q_{sim} - Q_{obs}) / Q_{obs} \cdot 100 \quad (5.2)$$

- (2) Δ_{var} , the difference between the simulated and observed coefficient of variation of annual runoff, normalised by the observed coefficient of variation and given as a percentage value (similar to Eq. 5.2). Δ_{var} assesses the performance of the model to reproduce the observed interannual variability of discharge.
- (3) Δ_{vol} , the mean annual difference between simulated and observed reservoir storage volumes at the end of the rain season (month of June), normalised by the observed storage volume and given as percentage value (similar to Eq. 5.2). Δ_{vol} evaluates model performance with regard to a key variable of water availability in reservoirs, i.e., storage volume to sustain availability during the following dry period.
- (4) R_1 , the coefficient of efficiency according to NASH & SUTCLIFFE (1970), based on mean monthly discharge data (Eq. 5.3). R_1 evaluates the ability of the model to reproduce the mean intra-annual variability of discharge.

$$R_1 = 1 - \frac{\sum_{m=1}^{12} (\overline{Q_{obs,m}} - \overline{Q_{sim,m}})^2}{\sum_{m=1}^{12} (\overline{Q_{obs,m}} - \overline{Q_{ann,obs}})^2} \quad (5.3)$$

- $\overline{Q_{obs,m}}$ Mean observed discharge of month m , averaged for all months m in the validation period
- $\overline{Q_{sim,m}}$ Mean simulated discharge of month m , averaged for all months m in the validation period
- $\overline{Q_{ann,obs}}$ Mean observed annual discharge, averaged for all years in the validation period

- (5) R_2 , the coefficient of efficiency according to NASH & SUTCLIFFE (1970), based on monthly discharge data (Eq. 5.4). R_2 assesses the performance of the model to reproduce the observed hydrograph on a monthly basis.

$$R_2 = 1 - \frac{\sum_{x=1}^t (Q_{obs,x} - Q_{sim,x})^2}{\sum_{x=1}^t (Q_{obs,x} - \overline{Q_{obs}})^2} \quad (5.4)$$

- $\overline{Q_{obs}}$ Observed mean monthly discharge for the validation period of t months duration
- $Q_{obs,x}$ Observed monthly discharge
- $Q_{sim,x}$ Simulated monthly discharge

- (6) R_3 , the coefficient of efficiency according to NASH & SUTCLIFFE (1970), based on monthly reservoir storage volumes (similar to Eq. 5.4). R_3 evaluates model performance to reproduce time series of water availability in large reservoirs.

Additionally, simulated and observed annual runoff was compared separately for particularly dry and wet years. For this purpose, the 10 driest and 10 wettest years in Ceará within the simulation period 1960-1998 were determined, derived from grid-based annual rainfall (Set 2) averaged for the entire study area. For each station, simulation results for these two subsets of very dry and wet years were compared to the observation if available for the respective years.

Based on experiences of model applications for semi-arid regimes in Africa, ANDERSEN ET AL. (2001) give a qualitative description on model performance based on the above criteria Δ_Q and R_2 (Table 5.16).

Table 5.16 Qualitative interpretation of model performance criteria, according to ANDERSEN ET AL. (2001).

Performance	Δ_Q (%)	R_2 (-)
Very good	< 5	> 0.95
Good	5 - 10	0.85 - 0.95
Fair	10 - 20	0.70 - 0.85
Poor	> 20	< 0.70

5.4.3.2 Results for discharge

The model being validated in this chapter is the reference version of WASA (see beginning of Chapter 5.3). Table 5.17 and Fig. 5.25 summarize the results for the comparison of observed and simulated discharge at various stations of different catchment size within the the study area. Simulated mean annual discharge is generally in the right order of magnitude compared to the observations. The performance in terms of Δ_Q , however, varies considerably between the stations, covering the entire range from very good to poor results. Deviations in the worst cases may be up to around $\pm 50\%$, in average they are about $\pm 20\%$. No systematic over- or underestimation can be seen when considering the performance for the entire set of stations throughout the study area (Fig. 5.25a). A larger underestimation of discharge by the model is however

found for all stations in the Banabuiú catchment (stations 8-10). Reasons of primary importance may be:

1. Deficits in the simple conceptualization and parameterization of water retention in reservoirs and of withdrawal by water use, causing a reduction of about 30% of runoff in this basin according to the simulation results, which may be too high (Fig. 5.24).
2. Underestimation of rainfall input because differences between the rainfall data Set 2 and Set 4 due to an effect of elevation are pronounced in some parts of the basin (Fig. A.3), resulting in a net effect on discharge of 10% at the most downstream station 10 (Table 5.10).
3. Deficits in the conceptualization and parameterization of lateral redistribution of water fluxes, which

lead to a large (in parts more than 40%) reduction in runoff within some of the sub-basins of the Banabuiú river (Fig. 5.17), a possibly overestimated effect.

Although being discussed for the example of one specific basin, the above aspects may give reasons for over- or underestimation in simulated mean annual flow for other stations, too. Further reasons are:

4. Deviations in the estimates of terrain, soil or vegetation parameters, of which some are highly sensitive on mean annual runoff (Chapter 5.3.3).
5. Deviations of basin area in the model from the real-world area, which is about $\pm 10\%$ in average, for smaller sub-basins in maximum up to 30% (Table A.1)

Table 5.17 Validation results of WASA for various gauging stations in Ceará (for station number (column 1) see Fig. 2.6 and Table A.1). Mean annual values for n validation years within the period 1960-98; P_{all} : mean annual precipitation for entire period 1960-98, P_{sim} : mean annual precipitation of the validation years only, Q_{obs} : observed discharge, Q_{sim} : simulated discharge. For the definition of wet and dry years and of the performance criteria Δ_Q , Δ_{var} , R_1 , and R_2 , see Chapter 5.5.3.1.

Station	Basin area km ²	P_{all} mm	All validation years								Dry years				Wet years			
			n	Q_{obs} m ³ s ⁻¹	P_{sim} mm	Q_{sim} m ³ s ⁻¹	Δ_Q %	Δ_{var} %	R_1 -	R_2 -	n	P_{sim} mm	Q_{obs} m ³ s ⁻¹	Q_{sim} m ³ s ⁻¹	n	P_{sim} mm	Q_{obs} m ³ s ⁻¹	Q_{sim} m ³ s ⁻¹
1	6036	629	14	6.6	584	5.0	-24.2	18.8	0.91	0.94	3	450	1.9	2.2	2	712	10.4	8.3
2	5327	950	10	9.9	925	9.4	-4.6	-17.6	0.96	0.82	2	711	4.7	7	2	1071	15.2	9.7
3	19250	726	31	32.5	742	37.4	15.0	-8.5	0.97	0.90	7	530	9	17.6	8	998	74.7	79.4
4	3612	873	17	4.0	858	5.7	42.2	21.4	0.69	0.34	5	660	1.5	2.6	4	1175	10.1	15.3
5	1903	995	12	4.1	1030	3.1	-25.3	163.1	0.79	-0.54	2	744	2	1.5	4	1307	6.4	6.8
6	8804	915	10	13.8	858	12.3	-11.2	40.3	0.96	0.70	3	632	6.7	5.2	2	1111	21.1	23.3
7	11891	922	30	28.7	942	33.7	17.3	-1.7	0.87	0.68	7	722	9.1	12.5	9	1202	60.2	68.6
8	4843	764	22	11.3	774	6.5	-42.7	32.7	0.73	0.78	5	536	4.6	1.3	6	1125	26.6	17.7
9	7688	725	13	18.0	731	11.5	-36.1	20.8	0.88	0.90	4	405	5.3	1.7	3	1165	45.2	33.6
10	18271	757	30	39.8	732	26.9	-32.4	-21.8	0.81	0.67	8	493	35.6	11.7	6	1075	83.7	60.8
11	38572	808	13	41.2	726	45.9	11.5	-9.6	0.89	0.83	4	519	14.6	22.3	2	1012	105.5	108.4
12	47308	805	21	120.9	817	109.8	-9.1	-13.5	0.94	0.88	6	620	33.3	56.9	5	1077	260.1	228.6
13	2037	838	26	6.8	854	6.4	-6.5	-9.6	0.98	0.94	6	560	0.7	1.4	7	1278	18.4	16.3
14	3726	912	10	10.4	779	10.7	2.6	2.8	0.94	0.90	4	553	2.9	3.2	2	1282	31.9	33.4
15	440	1102	11	3.1	1206	3.5	12.7	-37.6	0.98	0.82	1	877	0.1	1.8	3	1677	7.6	6.2
16	7330	802	28	21.2	776	19.6	-7.3	-10.1	0.98	0.94	8	466	3.4	5.2	6	1252	66.8	54.9
17	2790	793	26	12.7	823	17.5	38.5	-15.7	0.79	0.76	6	474	3.9	3.8	7	1260	30.3	37.9
18	3786	1150	11	38.9	1189	35.5	-8.8	-16.8	0.97	0.93	3	675	4.4	9.8	3	1810	89.8	73.7
19	1530	777	31	7.7	824	10.5	35.3	-8.9	0.72	0.76	6	424	0.1	0.9	9	1195	17.5	21.5
20	2698	764	28	8.1	781	12.9	58.8	-17.9	0.50	0.72	7	470	1.2	3.2	7	1201	22.3	30.7
21	561	1126	8	6.3	1179	5.7	-9.0	-1.4	0.93	0.90	2	613	1.2	1.2	3	1704	11.4	10.5
22	11210	850	7	76.2	857	76.0	-0.3	-6.7	0.96	0.95	2	407	6.9	9.0	2	1466	201.8	185.1
23	1050	990	15	4.4	1056	4.0	-10.8	-3.3	-1.51	-1.03	3	603	1.2	0.5	5	1407	8.2	7.1

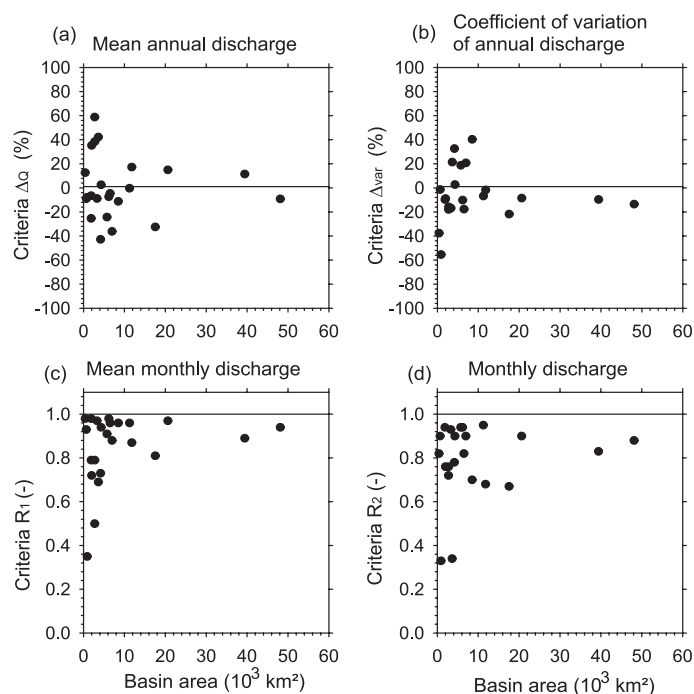


Fig. 5.25 Model performance of WASA, validated against observed discharge at 23 stations in Ceará. For details on the stations and validation criteria, see Table 5.14.

The interannual variability of discharge is generally reasonably represented, with Δ_{var} being in the range of $\pm 30\%$ for most stations. This can also be seen when looking specifically at the driest and wettest years of the simulation period (Table 5.17). Discharge is generally in the right order of magnitude for both dry and wet years, thus reproducing the large differences which occur in the study area between wet and dry years. However, at a closer look, a slight overall underestimation of the interannual variability can be observed, particularly for larger catchments (Fig. 5.25b). This is mainly due to a tendency of overestimation of discharge in dry years. A main reason may be the lack of a routine for transmission losses by infiltration into the river bed in WASA at the scale of sub-basins. WASA accounts for losses in the river network due to evaporation and water use only, and for transmission losses by infiltration at the smaller scale of landscape units only. However, the infiltration losses may be important in the study area also for larger rivers, particularly for dry conditions with low groundwater levels in the surrounding alluvium (e.g., ARAÚJO & RIBEIRO, 1996; MANOEL FILHO, 2000). Another reason for overestimated runoff in dry years may be the application of more strict reservoir operation rules in reality, with regulated outflow being low-

er than in wetter years. In WASA, however, no differences are made between the years as long as the actual storage volume is above the alert volume (see Chapter 4.2.7).

The mean intra-annual runoff regime is well reproduced by the model for most basins (see R_1 in Table 5.17 and examples in Fig. 5.26a-c). One reason are the, in average, clearly defined climatic boundary conditions with a rainfall regime separated into a rainy and a dry season. A lower model performance according to R_1 is often related to lower values of Δ_Q , i.e., larger deviations of the simulated mean annual runoff. Additionally, a worse representation of the intra-annual regime is also found in smaller sub-basin with a flow contribution from deeper groundwater bodies. This long-lasting outflow, continuing during the dry season, cannot be represented with the model without calibration of its time delay (particularly relevant for station 23 influenced by baseflow from sedimentary bedrock (see Fig. 5.26d), and also for stations 4 and 5, see below).

In terms of model performance in representing the observed monthly hydrograph (criteria R_2) fair to good results (see Table 5.16) are obtained for most of the stations in the study area (Table 5.17). Fig. 5.27 gives an example for the most downstream station

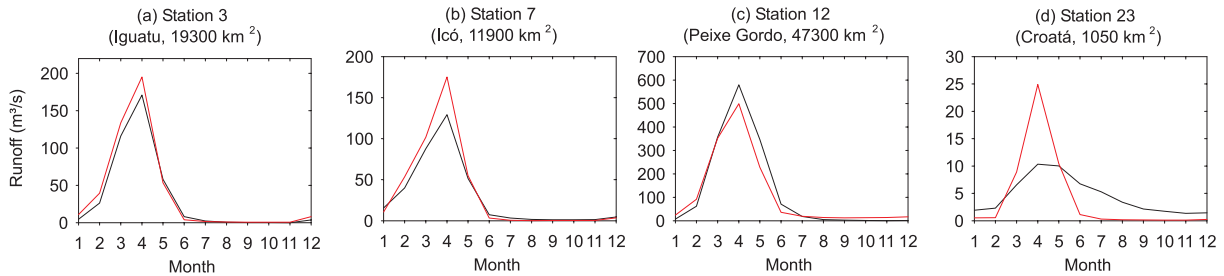


Fig. 5.26 Examples of model validation for mean monthly runoff, black line: observed, red line: simulated. Details on stations and performance criteria see Table 5.14.

with available data in the Jaguaribe basin (Station 12, Peixe Gordo). Lower values of R_2 are, similar to R_1 , often correlated with larger deficiencies in the simulation of mean annual runoff at the respective station. Poor results in terms of R_2 are found for the two smaller basins 4 and 5 in the Cariri region in the south of the study area. The area is characterized by a com-

plex geological setting at the contact zone of crystalline and sedimentary zones. Different deep and shallow groundwater systems are of relevance for river runoff, while surface and sub-surface catchment boundaries may differ (see, e.g., DNPM, 1996). This complex system cannot be well represented in WASA as seen in the model results.

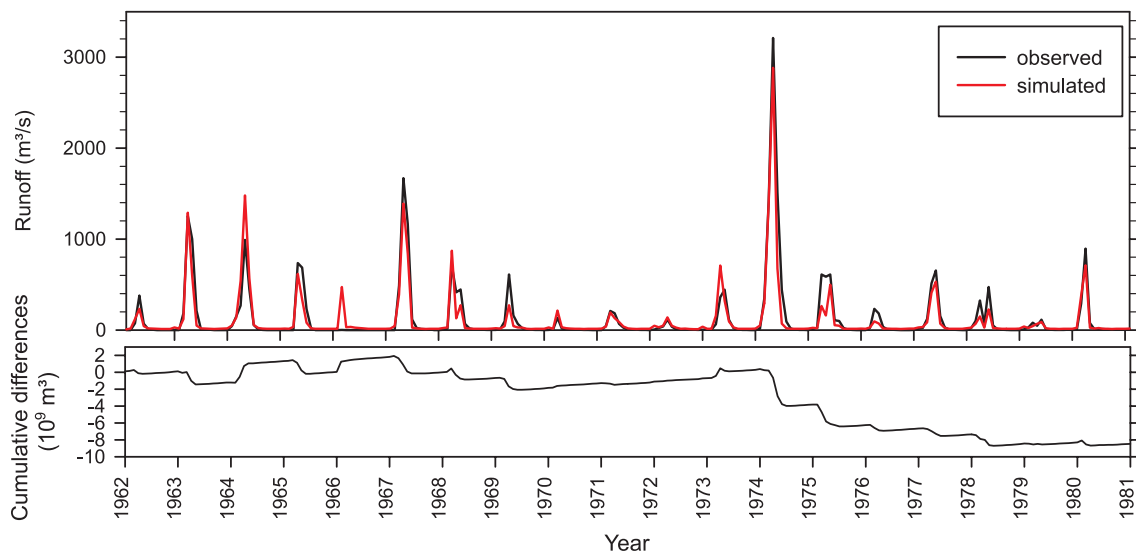


Fig. 5.27 Example of model validation for monthly discharge at station Peixe Gordo, Jaguaribe River, basin area 47300km^2 . Upper graph: simulated and observed discharge, lower graph: cumulative difference between simulation and observation.

The results of model performance found here are in average similar in terms of Δ_Q and R_2 to those of ANDERSEN ET AL. (2001) for the application of an uncalibrated model to a set of basins in semi-arid Africa with, in average, even larger catchment areas. In general, a tendency of better model performance at stations with a larger basin area is found (Fig. 5.25), although this statement is limited by the smaller number of larger sub-basins. It may, however, be rea-

sonable as deviations in discharge from different sub-basins may balance out to some extent when aggregating into larger catchment areas.

5.4.3.3 Results for reservoir storage volumes

Model validation of WASA with regard to reservoir storage volumes shows that model deviations from observations at the end of rainy season in terms of Δ_{vol}

are about $\pm 20\%$ in average for the complete set of reservoirs tested (Table 5.18). Variations in performance between the reservoirs are large. There is, however, no

tendency of a systematic over- or underestimation of the observations (see also Fig. 5.28). Also in terms of criteria R_3 , there is a broad range of good to poor re-

Table 5.18 Validation results of WASA for various large reservoirs in Ceará for n validation years within the period 1960-98; Nbr: Identification number of reservoir, see Fig. 2.6 and Table A.2; V_{obs} : Mean annual observed storage volume in the month of June (end of rainy season); V_{sim} : Mean annual simulated storage volume in the month of June; For performance criteria Δ_{vol} and R_3 see Chapter 5.4.3.1.

Nbr	1	2	3	4	5	6	7	8	9	10	11	12	13	14	15	16	17	18	19	20	21	22
n	34	28	31	20	20	31	8	17	33	24	18	6	6	10	20	27	17	22	14	21	24	16
V_{obs}	51	689	100	823	144	61	166	31	215	53	1530	200	210	63	179	307	22	40	95	51	57	43
V_{sim}	48	609	97	1096	140	99	234	36	223	55	1503	190	269	19	317	270	16	36	115	49	47	43
Δ_{vol}	-7.0	-11.6	-2.8	33.1	-2.9	63.6	41.2	14.8	3.5	3.0	-1.8	-4.7	27.7	-70.5	77.2	-12.1	-24.2	-9.5	20.3	-4.3	-17.5	-0.2
R_3	-2.02	0.45	0.39	-3.35	0.37	-0.72	-1.37	0.60	0.80	0.22	0.94	0.54	0.76	-13.4	-0.34	0.12	0.40	0.39	0.32	0.18	-1.39	0.84

sults. Beside of the variety of factors which introduce uncertainties in river discharge flowing into the reservoirs, there are additional factors which enhance the uncertainty of the simulation results for reservoirs: (1) Accuracy of the area-volume-relationship and of evaporation rates to determine losses by evaporation, (2) possible percolation to bedrock which is neglected in the model, (3) uncertainty in the simplified operation rules of controlled reservoir outflow used in the model (Chapter 4.2.7.2) and of direct withdrawal water use. On the other hand, the variability of simulated storage volumes, and thus uncertainty of the results is bounded by the storage capacity of the reservoir which sets a maximum value.

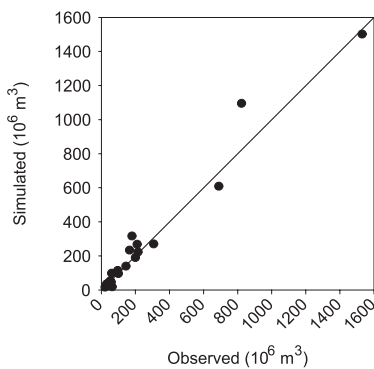


Fig. 5.28 Observed versus simulated mean reservoir storage volume at the end of the rainy period (June) for 22 reservoirs in Ceará (see Table 5.15).

Fig. 5.29 gives examples of storage volume time series for three reservoirs with different model performance. For the largest and most important reservoir of the study area (Açude Orós) very good simulation results are obtained (see also Table 5.18). With regard to runoff inflow volumes, the comparatively large basin

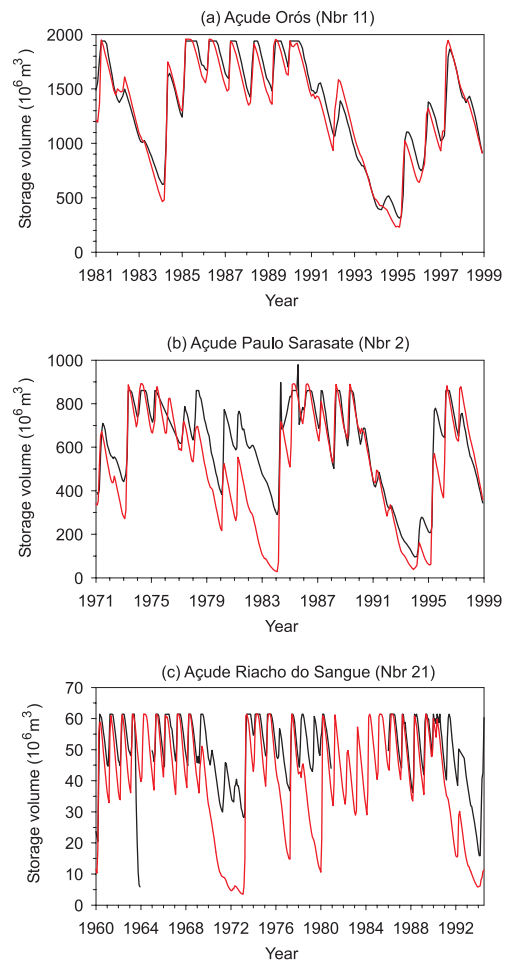


Fig. 5.29 Examples of model validation for monthly storage volumes in large reservoirs (Nbr refers to the first column in Table 5.15, see also Table A.2 and Fig. 2.6). Black line: observed, red line: simulated.

area provides input of larger reliability as argued in the discharge section above. The tendency of storage volumes falling below the maximum storage capacity too early in some wet years in the simulation (e.g., 1985-89), may be the effect of a more flexible outflow control, with reduced outflow volumes during the rainy period, as opposed to constant outflow volumes throughout the year as applied in the model.

Also for the reservoir in Fig. 5.29b, good results are obtained, with the intra- and interannual dynamics well represented by the model. There is primarily one year (1978), however, where reservoir inflow is underestimated by the model. As a consequence, observed and simulated time series run parallel to each other (separated roughly by the missing inflow volume) until the next complete filling of the reservoir in 1984. Although the dynamics are again well represented, this discrepancy considerably degrades the overall quantitative performance criteria for the reservoir. This is to illustrate the possible long-term persistency of singular model deviations on modelling results of

water availability in reservoirs. In this sense, a different, less strict, interpretation of performance criteria like R_3 is advised as compared the similar measure R_2 for discharge. An additional visual inspection of the time series is required.

Finally, as an example for a reservoir where a negative value of R_3 is obtained, see Fig. 5.29c. The time series indicates a too quick emptying of the reservoir in the dry season, but also in a sequence of dry years. This may be a combined effect of an overestimation of evaporation and outflow volumes and, at least in dry years, an underestimated inflow.

In summary, model performance for reservoir storage volumes is in the same range as discharge simulations when looking at mean annual values. On a monthly scale, deviations tend to be higher because of additional factors of uncertainty are comprised in the modelling of storage volumes. Nevertheless, reasonable values of water availability result at the scale of the study area.

5.5 Scenario Simulations

5.5.1 Climate scenarios

Climate data for scenario calculations of water availability with WASA are based on the results of complex physically-based climate models (General Circulation Models, GCMs). GCMs show an increasing ability to simulate climate patterns and historic trends at the global to continental scale (IPCC, 2001). They agree in projecting a significant global warming to take place in the current century (by 1.5° - 5.8° in the period 1990-2100; IPCC, 2001) under the assumption of a continuous increase in atmospheric greenhouse gas concentrations. However, the skill of these models in representing climate at the regional scale of north-eastern Brazil is modest (KROL ET AL., 2002). The comparison of seven GCMs (data of IPCC-DDC, 1999) resulted in only two which were able to fairly represent the semi-arid climate of the study area, i.e., its mean annual precipitation and its seasonal cycle, as well as mean global precipitation. Main reasons for the low performance of the GCMs at the regional scale may be their coarse resolution (300 to 900km) or an imperfect representation of regional important physical processes.

The two GCMs with reasonable results for north-eastern Brazil are ECHAM4 model (Max-Planck-Institute for Meteorology, Germany, ROECKNER ET AL., 1996) and HADCM2 (Hadley Centre, Great Britain,

JOHNS ET AL., 1997). Runs of both models for an assumed future annual increase of greenhouse gases by 1% per year as in 1990 were used as basis for this study. Due to their coarse resolution, cell-based data of the GCMs cannot be used directly as input for the hydrological model, but have to be downscaled to the required resolution. One approach is to use regional climate models with higher spatial resolution being embedded into GCMs. However, such a model is presently not available with sufficient accuracy for the study area (BÖHM, 2002). Alternatively, the regional climate scenario data provided for this study (GERSTENGARBE & WERNER, 2002) were generated by a statistical downscaling method (see also WERNER & GERSTENGARBE, 1997). This method combines historical daily time series of different meteorological variables at the level of climate stations with long-term trends given by the GCM projections. The trend in annual precipitation was taken to be the regional most relevant tendency. It was translated by multivariate procedures, which consistently adjust other meteorological variables to the change in precipitation, into daily scenario time series at the station level for the scenario period 2001-2050. Long-term time series of historical precipitation data are required for this methodology (here the period 1921-1980 was used) which constrained the number of stations to about 25 in and around the study area (see also Chapter 2.1.6.2). Inter-

polation to the scale of municipalities was performed as described in Chapter 2.1.6.2 by the method of SHEPARD (1968). For scenario calculations with WASA at the scale of sub-basins, daily values of all climate elements except precipitation were derived as the area-weighted mean of the values of all contribut-

ing municipalities. In the case of precipitation, the daily value of only one municipality which makes up the largest fraction of area of a sub-basin was used in order to prevent any additional modification of the temporal time series properties by averaging from different spatial units.

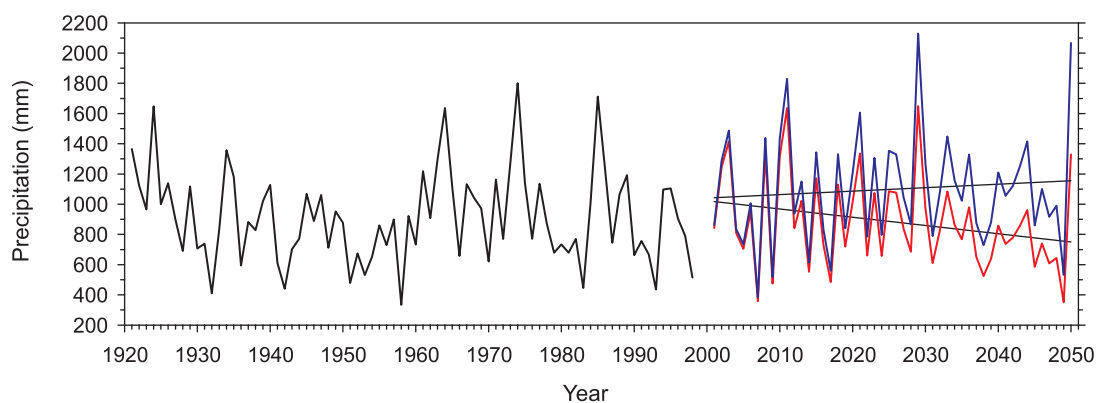


Fig. 5.30 Annual precipitation in Ceará for the historical time series (1921-1998) and the scenario period (2001-2050). Scenarios based on results of ECHAM4 (red line) and HADCM2 (blue line), with trend lines.

The expected future change in precipitation for the study area of Ceará is of opposite direction for the two scenarios. The ECHAM4-based scenario shows a marked decreasing trend and the HADCM2-based scenario a considerable increasing trend of annual precipitation (Table 5.19, Fig. 5.30). This difference among the scenarios illustrates the large uncertainties associated with conclusions on possible future precipitation changes in the study area. Changes in both directions should be considered in this study as plausible scenarios in view of the given information from GCMs. Future changes in other climate variables are low for both scenarios, resulting in very small changes in potential evaporation (calculated according to PENMAN-MONTEITH, Chapter 4.2.2) (Table 5.19). The spatial patterns of precipitation trends are different for the two scenarios (Fig. 5.31a, d), which indicates that the correlations between local and large-scale precipitation amounts which were used for generation of the scenario time series are different for dry as compared to wet years. The expected decrease of rainfall for the ECHAM4 scenario is in general larger in the northern part of Ceará except for some coastal areas. The HADCM2 scenario shows a stronger increasing trend of rainfall in the eastern and north-eastern part of Ceará, comprising large regions in the Jaguaribe basin.

Changes in mean annual precipitation between two 25-year periods at the end of the historical period (1974-1998) and the scenario period (2026-2050), respectively, are different in magnitude and in their spa-

tial pattern as compared to the changes indicated by the trends for the entire scenario period (2001-2050) (Table 5.19). This is due to the fact that the basis for the generation of the scenario time series by GERSTENGARBE & WERNER (2002) were the rainfall characteristics (e.g., interannual variability, spatial patterns, daily characteristics) derived for the period 1921-1980, which differ from those of 1974-98. Thus, the direct evaluation of changes between the latest historical and the future time period is limited by this discrepancy. The presentation of scenario results in the following therefore has its focus on changes within the scenario period 2001-2050, with internally consistent climate data reflecting the future trend given by the GCMs.

5.5.2 Results

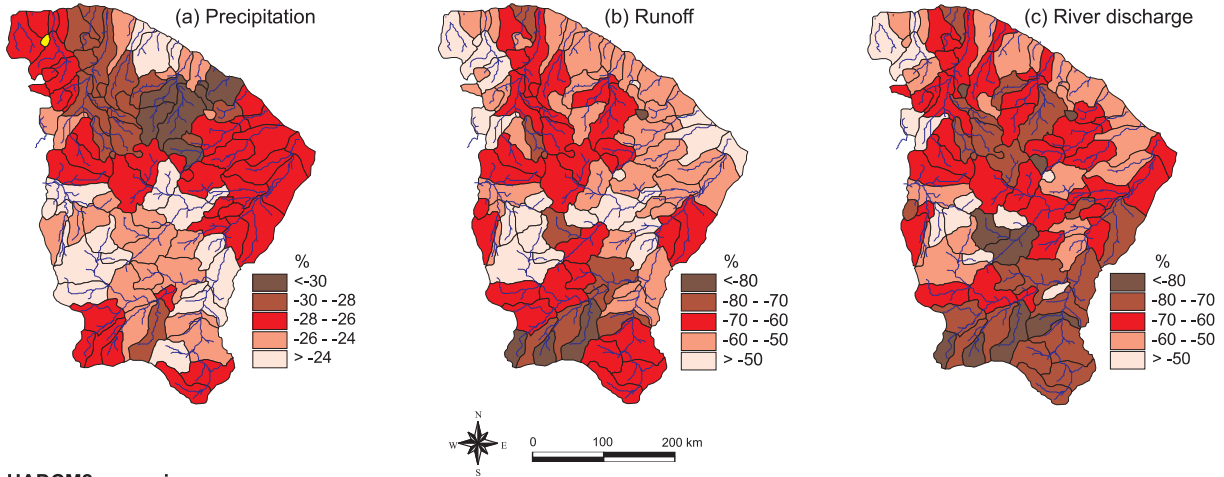
Scenario simulations with WASA were performed for the above two climate change scenarios for 2001-2050. Except for the climate input, all other boundary conditions of the model (i.e., land cover, vegetation characteristics, number of reservoirs and operation rules) were kept constant throughout the scenario period. Water use was calculated based on the demand at the end of the historical time period but can change as a function of climate variability with regard to irrigation water demand (Chapter 4.2.9).

In terms of runoff, the simulations show a highly sensitive response of the study area to the climate

change scenarios (Table 5.19, Fig. 5.31). Runoff trends for 2001-2050 are in average by a factor of 2-3 larger than the underlying trends in precipitation for both scenarios. This large amplification factor is in

line with the results of the sensitivity analysis for rainfall volumes (Chapter 5.3.1.3) and with results of impact analysis in other semi-arid areas (Chapter 3.4.3). In average for Ceará, runoff is expected to decline by

ECHAM4 scenario



HADCM2 scenario

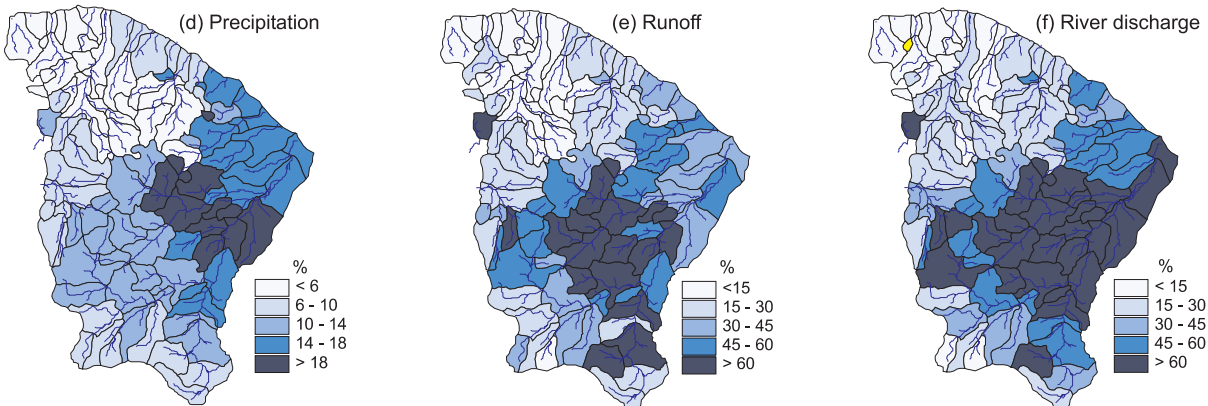


Fig. 5.31 Climate change scenarios for Ceará, trends in precipitation, runoff and discharge for the period 2001-2050.

Table 5.19 Climate scenarios for Ceará and their effects on the water balance (calculated with WASA). Comparison of a historical time period (column a) and scenario time period (25 years each) (columns b and c), and linear trends for the total scenario period (2001-2050) (columns d and e).

	(a) Historical 1974-1998	(b) ECHAM4 2026-2050		(c) HADCM2 2026-2050		(d) ECHAM4 2001-2050	(e) HADCM2 2001-2050
	Mean mm	Mean mm	Change %	Mean mm	Change %	Trend %	Trend %
Precipitation	916	825	-10	1138	+24	-26	+11
Potential evaporation	2062	2042	-1	2028	-2	-3	-3
Actual evapotranspiration	740	669	-10	785	+6	-15	+4
Deep groundwater recharge	15	14	-7	24	+60	-37	+23
Runoff	161	141	-12	329	+104	-56	+33

-56% in the case of the ECHAM4 scenario and to increase by +33% for the HADCM2 scenario between 2001 and 2050. For the ECHAM4 scenario, due to lower availability of soil moisture by decreasing rainfall, actual evapotranspiration and groundwater recharge is expected to decrease, too. For the HADCM2 scenario, the slight decreasing trend of potential evaporation prevents in parts a larger increase of actual evapotranspiration in spite of increasing rainfall. Additionally, the length of the rainy period does in average not increase with increasing annual rainfall for this scenario. Thus, more rainfall can be assumed to be quickly transformed into runoff and groundwater recharge instead of being evaporated or transpired. Plant-available soil moisture (above water content at wilting point) in the uppermost meter of the soil horizons is expected to decline in the main vegetation period (February-May) by in average -15% for the ECHAM4 scenario and to increase by 20% for the HADCM2 scenario.

In contrary to the ECHAM4 trends of rainfall and runoff for 2001-2050 (-26% and -56%, respectively, Table 5.19), the difference between both changes is less pronounced when comparing the historical period 1974-1998 and the scenario period 2026-2050 (-10% and -12%). On the other hand, the percentage increase of runoff relative to rainfall is stronger when comparing 1974-1998 with 2026-2050 (+104% and +24%, amplification factor 4) as for 2001-2050 (+33% and +11%, amplification factor 3). These results indicate for both scenarios a tendency towards enhanced runoff production in the scenario period relative to the historical period, which weakens, on the one hand, the effect of decreasing rainfall in the ECHAM4 case and amplifies, on the other hand, the effect of increasing rainfall in the HADCM2 case, when being compared to the trends within 2001-2050 only. A reason can be differences in the rainfall characteristics at the daily scale between the historical and the scenario time series which are less relevant within the scenario period itself. The scenario time series are in general characterized by larger daily rainfall intensities (i.e., the increasing annual sums in the HADCM2 case are not transferred into more days with rainfall than in the historical time series, but into larger daily volumes; decreasing annual sums in the ECHAM4 case are transferred into a lower number of rainy days while the daily volume are in average higher or the same as in the historical period) (Table 5.20). Additionally, the number of consecutive days with precipitation (the duration of rainfall events) is in average higher in the scenario period than in the historical period. Both time series characteristics tend to increase runoff genera-

tion (see, e.g., Chapter 5.3.1.1) and, thus, they overlay the tendency induced by the annual trends. These scenario results point out that changes in the future water balance due to changes in annual precipitation may additionally be influenced by changes in short-term time series characteristics. Whether the latter are considered as a really possible future change or as a bias caused by the method for scenario generation, in any case an additional source of uncertainty is introduced in the scenario simulations.

Table 5.20 Characteristics of daily precipitation time series of the historical and the scenario period. Events are defined as consecutive days with rainfall >0. Mean values for the 137 sub-basin time series of Ceará.

Scenario Period	ECHAM4			HADCM2	
	1974-1998	2001-2025	2026-2050	2001-2025	2026-2050
Number of rain days per year	141	133	129	141	138
Mean rainfall volume of wet days (mm)	6.9	7.6	6.9	7.8	8.5
Variance of daily volumes	143	149	125	169	205
Event duration (days)	2.7	3.2	3.1	3.4	3.4

Runoff trends for the scenarios show a modified spatial pattern (Fig. 5.31b,e) relative to the pattern of precipitation trends as a consequence of the complex effect of various physiographic conditions in the individual sub-basins. There is a tendency of sub-basins with a lower runoff volume or a smaller runoff ratio in the historical time period to react more sensitive to climate change (compare Fig. 5.22). For instance, this may be a reason for the areas in northern Ceará with the strongest decreasing precipitation trends (ECHAM4 scenario) to stand out to a lesser extent when looking at the pattern of the strongest decreasing runoff trends, which stresses several sub-basins in the centre and south of the study area. Additionally, sub-basins where lateral redistribution and reinfiltration of runoff influences to a large extent total runoff (compare Fig. 5.17) tend to react stronger on precipitation changes in the scenario period. This is in line with the sensitivity analysis in Chapter 5.3.2.2 which indicates a differing relevance of these processes in wet or dry years.

Changes in water availability in terms of river discharge for the climate scenarios (Fig. 5.31c,e) are generally more pronounced at the outlet of sub-basins with a larger water storage capacity in reservoirs (compare Fig. 5.24). For instance, in the case of the

ECHAM4 scenario, the percentage of total river discharge being stored in reservoirs and consequently lost by evaporation increases with decreasing annual discharge volumes and this effect is more important in sub-basins with large storage capacity. Similarly, changes in river discharge are in general more severe at more downstream locations in river basins which are exposed to the aggregate effect of all changes in upstream areas. This can also be seen when looking at the expected storage volumes in reservoirs. Large reservoirs, which usually receive inflow from a large upstream catchment area are relatively more affected by the changing runoff volumes than smaller reservoirs with rather local catchment areas. E.g., the trend in reservoir storage volume at the end of the rainy season for the ECHAM4 scenario is -32% and -16% for large and small reservoirs, respectively (Table 5.21, Fig. 5.32). Reduced (HADCM2) or increased (ECHAM4)

losses by evaporation and water use during the dry season enhance the expected changes of water availability in reservoirs for the two scenarios, as the trends for water storage in December (exemplary taken as a month at the end of the dry season) are slightly stronger than those of June (Table 5.21).

Table 5.21 Trends of water storage in reservoirs in Ceará, simulated with WASA for the period 2001-2050 at the end of the rainy season (June) and the dry season (December) (in %).

Scenario	ECHAM4		HADCM2	
	June	Dec	June	Dec
Large reservoirs (>50·10 ⁶ m ³)	-32	-35	+16	+20
Small and medium-sized reservoirs (<50·10 ⁶ m ³)	-17	-20	+5	+6

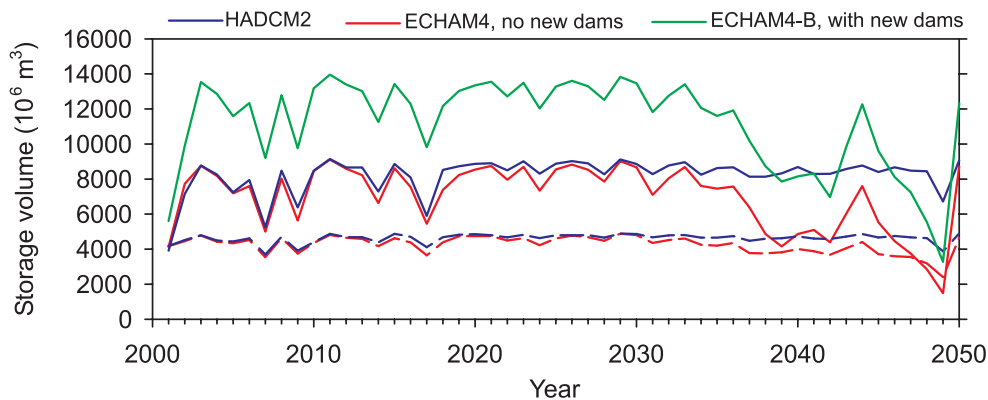


Fig. 5.32 Reservoir storage volume at the end of the rainy season (June) in Ceará, in large reservoirs (storage capacity >50·10⁶m³) (solid lines), small and medium-sized reservoirs (storage capacity <50·10⁶m³) (dashed lines), simulated with WASA for the ECHAM4 scenario without changes in the number of reservoirs (red lines), the ECHAM4-B scenario with new large reservoirs (green line) and the HADCM2 scenario (blue lines).

In other scenario run of WASA (ECHAM4-B and HADCM2-B), the effect of new reservoirs on future water availability was assessed. In these simulations, all large reservoirs (storage capacity >50·10⁶m³) being under construction in 2001 (see Table A.2) were taken into account. The additional storage capacity provided by these new reservoirs is about 4.9·10⁹m³, of which the largest part (4.4·10⁹m³) is attributed to the Castanhão dam in the Jaguaribe basin (see Fig. 2.6). The simulated total storage volume in the reservoirs of Ceará at the end of the rainy period is considerably larger for these scenarios as compared to those without new dams (Fig. 5.32). Mainly due the downstream position of the Castanhão dam, a large

amount of river discharge is retained which would otherwise flow to the ocean. For the HADCM2-B scenario and for wet years of the ECHAM4-B scenario, the efficiency of the new dams, i.e., the ratio between the additionally stored water and the storage capacity of the new dams, is close to 1 which indicates that practically all new storage capacity is used (Fig. 5.33). However, in dry years of ECHAM4-B and particularly in a sequence of dry years as towards the end of the scenario period, the efficiency decreases markedly. This shows that the considerably lower runoff production in the case of a decreasing precipitation trend, amplified by the in relative terms larger amount of retention and use in upstream areas, may reduce river

discharge in downstream locations to a degree such that the full use of additional storage capacity of large reservoirs as the Castanhão dam may not be attained.

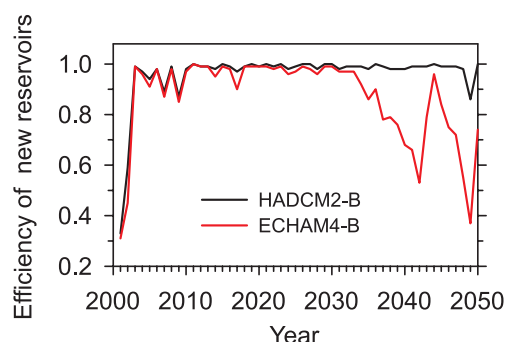


Fig. 5.33 Efficiency (additional storage volume at the end of the rainy season in June relative to storage capacity of new reservoirs) of new large reservoirs in Ceará for simulations with WASA based on two climate scenarios.

Further simulations with WASA were performed to assess the effect of the construction of small reservoirs on future water availability. Using the ECHAM4-based climate scenario and the additional large reservoirs introduced in scenario ECHAM4-B, the number of reservoirs and thus the storage capacity also in the small reservoirs classes 1-4 ($<10 \cdot 10^6 \text{m}^3$) (see Fig. 4.8) was increased for each sub-basin (Table 5.22) For simplic-

Table 5.22 Results of scenario runs with an increase of small reservoir storage capacity (*V*: storage capacity in reservoir classes 1-4; Δ : change in storage capacity as compared to scenario ECHAM4-B; *eff*: efficiency of new reservoirs (see text).

Scenario	<i>V</i>	Δ	<i>eff</i>	
	10^6m^3	%	2001-2025	2026-2050
ECHAM4-C	4502	+25	0.81	0.57
ECHAM4-D	5403	+50	0.79	0.51
ECHAM4-E	6303	+75	0.75	0.46
ECHAM4-F	7204	+100	0.71	0.42

ity, this increase was not realized gradually in time during the scenario period, but it was set at once at the beginning of the scenario period. The results are also interpreted in terms of the reservoir efficiency, which is defined as the additional amount of water being stored at the end of the rainy season (June) in all reservoirs of Ceará as compared to scenario ECHAM4-B without new small reservoirs, divided by the storage capacity of the new dams. The results (Table 5.22,

Fig. 5.34) show in general a substantial increase of water availability in the first part of the scenario period (2001-2030) by in average about 75% of the additional capacity. A full usage of the new reservoirs (efficiency close to 1) is attained only in wet years and for the scenarios ECHAM4-C and ECHAM4-D with a smaller increase of the number of reservoirs. The lower efficiency values for scenarios with a larger number of new reservoirs illustrate the increasingly limiting influence which reservoirs have mutually on each other by the retention of available runoff. Lower storage volumes and efficiencies in dry years as compared to wet years demonstrate that runoff volumes are too low in this case to fill the existing reservoirs. A particularly severe effect occurs in the second half of the scenario period. With the significant decreasing trend in precipitation and runoff, the net effect of additional storage capacity in small upstream reservoirs on total available storage volumes in Ceará declines considerably. The additional water stored in these smaller reservoirs is counteracted by a simultaneous decrease of storage in the large downstream reservoirs as most of the discharge is already retained in upper parts of the basins. This effect is more severe for scenarios with a larger number of new small reservoirs, where the efficiency is close to or even below 0 (see, e.g., ECHAM4-F in Fig. 5.34b). Thus, according to these simulation results, the system of surface water resources in Ceará is in a state where an increase in reservoir storage capacity does not necessarily imply a substantial increase of water availability for the given scenario assumptions with a decreasing precipitation trend.

The simplicity of the scenario assumptions applied here should be taken into account in the interpretation of the results. For instance, changes in water use are a function of the climate variability only, but do not include increasing water demand in the course of, e.g., population growth or industrial development. No land cover changes are taken into account, neither human-induced by regional development nor as a consequence of the adaptation of plant communities to changed climatic conditions. Similarly, the possible effect of increasing atmospheric CO_2 on plant transpiration and thus total evapotranspiration is not considered. Additionally, the availability of only one realisation of each climate scenario in this study enhances the risk of the results being influenced by some stochastic singularities of the scenario time series. Examples of more comprehensive scenario analysis for the study area, including other components beside of the hydrological part, are given in KROL ET AL. (2002).

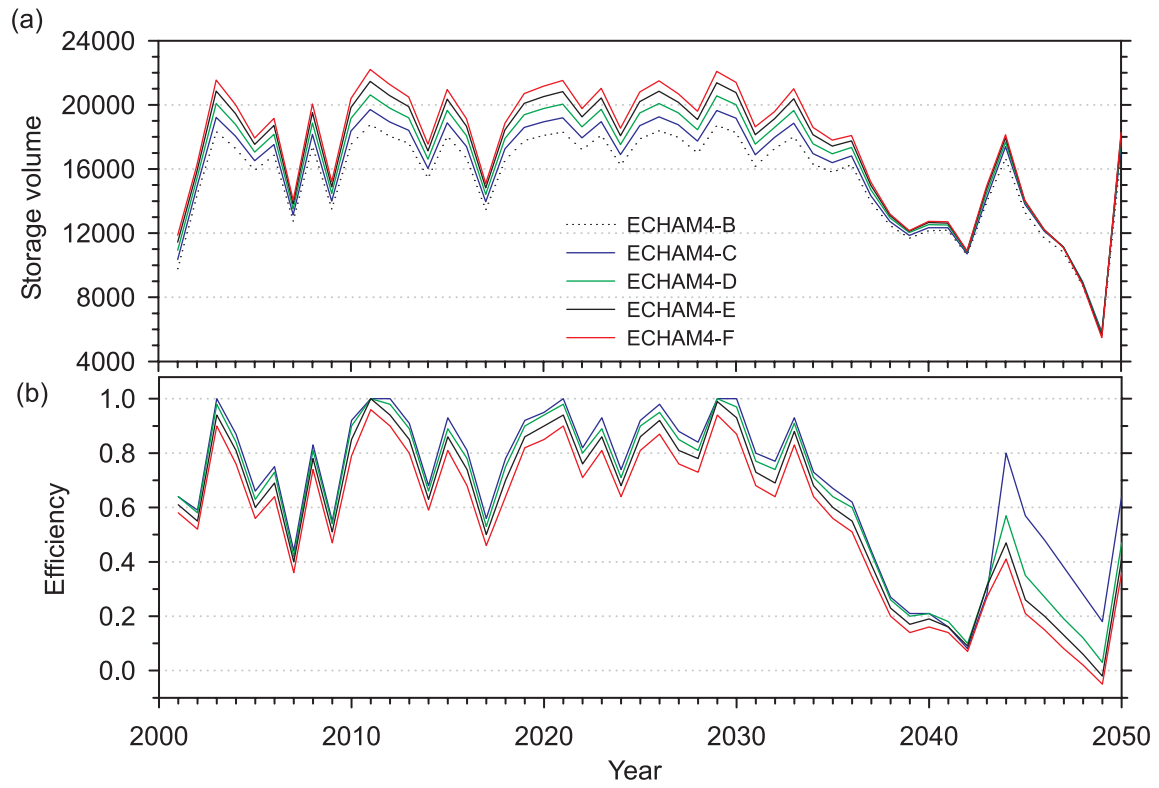


Fig. 5.34 Reservoir storage volumes (in $10^6 m^3$) at the end of the rainy season (June) (a) and efficiency of additional dams (b) for WASA scenario simulations with additional small reservoirs based on the ECHAM4 climate scenario (see Table 5.18 for scenario assumptions on reservoirs).

Conclusions and Perspectives

6.1 General Discussion and Conclusions

6.1.1 Modelling concept

For the development of a hydrological modelling concept in this study, the criteria of primary relevance are its applicability for distinct features of semi-arid environments, for large spatial scales and for environmental change impact analysis. From this follows the general model concept realized in WASA as a dynamic, process-based model, with a multi-scale spatial modelling approach, and basically no need for calibration (Chapter 3.5). Based on the characteristics of the study area and the general features of hydrology in semi-arid environments, an adequate representation of the following processes is emphasized in WASA (Chapter 3.5.3):

- Generation of infiltration-excess surface runoff, in particular with respect to the temporal time series characteristics of the precipitation input.
- Evapotranspiration from a sparse vegetation cover.
- Lateral surface and subsurface water fluxes, including reinfiltration of surface runoff.
- Water balance and storage behaviour of a dense network of artificial reservoirs of various sizes.

A detailed discussion of the contents and grounds for the modelling concept in this study is given in the conclusions of Chapter 3.5 and is not repeated here. In the following, the essentials are taken up again in view of the simulation results.

6.1.2 Spatial structure and lateral fluxes

Essentials of the new concept

The structure of modelling units in WASA (Chapter 3.5.4, Chapter 4.1.2) combines the need in process-based hydrological models to represent the dominant hydrological processes at their specific

scale, while at the same time ensuring to link these process scales with the final scale of interest of the model application. This is realized in WASA by the hierarchical multi-scale concept. Beside of the mainly vertical processes at the scale of profiles or soil-vegetation-components (infiltration, percolation, evapotranspiration), the concept respects lateral fluxes at the hillslope or small-basin scale, i.e., lateral redistribution of soil moisture and reinfiltration of surface runoff. This requires a modelling unit which represents this spatial scale, realized in WASA by the introduction of landscape units. These units are areas of similar hydrological response (hydrotopes). However, they are not areas of quasi-homogeneous characteristics (as in the classical meaning of hydrotopes), but they are similar in terms of their sub-scale variability, i.e., in the distribution of different terrain, soil and land cover characteristics. This includes the association of these sub-scale patches of different characteristics with a specific position in the landscape (toposequence) and, thus, also their location relative to each other. This concept overcomes the problem of defining the lateral connectivity between modelling units that were delineated with regard to similarity in vertical processes only, which usually impedes to take into account processes of lateral redistribution, particularly in large-scale models. Here, in contrary, the aspect of lateral redistribution is respected a priori in the definition of the modelling units by including their topographic position, and thus runoff-runoff relationships. The possibility of using, at some scale level, the distribution of modelling units with statistical flux transition frequencies instead of geographically referenced modelling units is a simplifying but efficient and flexible way to include sub-scale processes in a large-scale model in view of limited data availability and model economy (Chapter 4.2.5).

Relevance of lateral processes

The model results for the study area of Ceará show that lateral fluxes and their interaction among different spatial units at small scales considerably influence the hydrological response at the basin scale, where the runoff response cannot simply be represented as the sum of the contributions of individual sub-areas (Chapter 5.2.2, Chapter 5.3.2.2). The main effect exerts the re-infiltration of surface runoff into areas of larger infiltration capacity, which causes a net decrease of mean annual runoff (by 13% in average, more than 40% for some sub-basins) when compared to simulations without any lateral redistribution. In dry years this effect is more pronounced in relative terms (decrease of 30% in average). Model validation at the small scale roughly confirms the appropriateness to incorporate lateral redistribution in the model in order to explain markedly lower runoff ratios at the basin scale as compared to the hillslope/headwater scale (Chapter 5.2.2). A thorough validation of the approach also at the large scale, however, is restricted by the lack of appropriate data, e.g., on soil moisture patterns (Chapter 6.2). Nevertheless, in spite of the simplicity of the approach used here and the limitations in its reliability due to low data availability, the results indicate that lateral fluxes have to be taken into account in models for this type of semi-arid environments. In particular for climate change impact assessment, the magnitude of change in discharge for a given change in precipitation is influenced by the lateral redistribution effects.

Spatial limitations of the concept

The limits with regard to the spatial scale of representing lateral redistribution effects in WASA are twofold:

- At the large scale, the limit is given by the redistribution within landscape units, i.e., due to structured, topography-related variability at the scale of toposequences up to small basins in the range of up to 10^1 - 10^2 km². Thus, large-scale groundwater flow over longer distances, of small importance in the crystalline part of the study area, is not respected. Additionally, transmission losses in rivers by infiltration are not taken into account beyond the landscape unit scale. A lower model performance at large scales for dry conditions points at this limitation of the present model (Chapter 5.4.3.2), which should be subject of future model improvements (Chapter 6.2).
- At the small scale, the limit is given by redistribution at the scale of soil-vegetation components, i.e., due to variability between patches with different

soil and land cover characteristics in the range of 10^{-2} - 10^{-1} km². About threequarters of the total effect of runoff reduction by lateral redistribution is attributed to this type of variability according to the model results (Chapter 5.3.2.2). Variability at smaller scales (within a land cover and soil patch) is only considered for soil storage capacity, but not with regard to lateral redistribution between, e.g., shrub and inter-shrub areas or crusted and non-crusted areas or due to other stochastic variability over very short distances (meters) of, e.g., soil hydraulic conductivity. In WASA it is assumed that the net effect of this variability with regard to large-scale applications is efficiently represented by applying homogeneous conditions and vertical processes only. Appropriate data at various scales to corroborate this assumption are not available. This simplification may set limitations on the applicability of WASA for land cover change studies or eco-hydrological applications.

Other aspects of the spatial model structure

For the given type and resolution of spatial data on landscape characteristics in the study area, a rough sub-division into the major landscape units at the scale of interest of model applications (sub-basins with an average size in the order of 10^3 km²) is appropriate for simulating river discharge at this scale, as the related loss of information compared to a more detailed model version based on grid cells (10^2 km²) does not result in a significant decrease in the accuracy of simulation results (Chapter 5.3.2.1).

Using administrative units (municipalities with an average size in the order of 10^3 km²) as the largest spatial units instead of sub-basins shows that the loss in accuracy in discharge simulations is small for river basin areas of more than about 15000 km² (Chapter 5.3.2.1). For smaller areas, however, the conceptual advantage of quantifying water availability in an integrated modelling approach at the common administrative scale where most of the other components work, e.g., water use, is at the expense of a considerable lower accuracy in the hydrological part. Differences in mean annual discharge compared to the sub-basin version are in average about $\pm 20\%$ for areas smaller than 15000 km², mainly due to deviations between natural catchment boundaries and administrative boundaries (Chapter 5.3.2.1).

It should be noted that the above conclusions on the influence of the spatial model structure refer to basin and landscape characteristics only and do not include effects of precipitation data, for instance, for which a

higher resolution may be required to capture the essentials of the spatial distribution (Chapter 6.1.3).

6.1.3 Temporal resolution, rainfall characteristics and runoff generation

Relevance of rainfall time series characteristics

Rainfall intensities are one important factor governing the generation of infiltration-excess surface runoff. The simulation results with WASA at various scales demonstrate that the model is very sensitive to the temporal characteristics of rainfall time series (Chapter 5.2, Chapter 5.3.1.1). Of particular relevance are the following two aspects:

- The daily modelling time-step is too coarse to capture the high intensities of predominantly short-term convective precipitation events, typical for the semi-arid climate.
- Interpolation of precipitation from station data to the modelling units is associated with a loss of variance in the input data and a modified temporal structure in the frequency and sequence of wet / dry intervals.

Both aspects cause underestimated rainfall intensities in the rainfall input data sets of the model, leading to an underestimation of infiltration-excess runoff, and thus, marked deviations in simulated total runoff in terms of its distribution and volume when compared to the observations (Chapter 5.2.1, Chapter 5.3.1.1). The differences in long term mean annual runoff of the study area, for instance, amounts to 40% between simulations with the same annual rainfall but with time series characteristics of station data and a interpolated data set, respectively. Another consequence of changes in the rainfall time series characteristics due to interpolation is an overestimation of the number of days with rainfall, leading to an overestimated interception evaporation by in average about 50% (Chapter 5.3.1.1).

Beside of the short-term rainfall characteristics, also differences in the model input in terms of long-term mean annual precipitation is large between data sets derived with different station density and interpolation methods. Such differences which may reach $\pm 40\%$ at the scale of municipalities result in considerably larger percentage differences in simulated runoff volumes, generally by a factor of 2 to 3 (Chapter 5.3.1.3).

In general, the results of WASA applications emphasize that for practical model applications which rely in many studies on interpolated rainfall input data at a daily scale, rainfall characteristics not only in

terms of spatial patterns but also with regard to sub-scale temporal characteristics as a function of the modelling timestep and interpolation effects are essential for an adequate representation of the hydrological response of semi-arid environments.

Scaling approaches

According to the simulation results, the concept in WASA to reduce the soil hydraulic conductivity in the infiltration routine by a scaling factor proves to be an efficient, yet simple, way to compensate for the bias in runoff generation caused by too low rainfall input intensities and can be seen as a first reasonable approximation (Chapter 5.2.1, Chapter 5.3.1.1). This also applies to the application of the scaling factor for interception evaporation by a reduction of the interception storage capacity. Being derived from the ratio of mean rainfall intensities in the model input data to the mean intensities of the original station data and data with high temporal resolution, the scaling factor is physically meaningful and can respect spatial variations in these rainfall time series characteristics. On the other hand, a limitation of the approach is its simplicity of taking into consideration only one mean characteristic of the rainfall time series, which may capture the scaling of intensities in a limited way only. Similarly, it does not address a changed spatial structure of the rainfall time series due to interpolation with regard to the sequence of wet and dry time intervals. Additionally, the approach is limited because in its current form it does not respect variations in the scaling relationship between years, seasons or days. For climate scenario calculations, possible changes in the sub-scale (sub-daily) temporal rainfall distribution including extremes (if given in the scenario) can thus not be respected in their hydrological impact.

More comprehensive concepts include the spatio-temporal simulation of rainfall input data sets and the use of temporal disaggregation methods. A first attempt by adding a stochastic component to interpolated rainfall data resulted in only small improvements (Chapter 5.3.1.1). The adaptation of a disaggregation model to the rainfall characteristics of the study area and its exemplary application for a version of WASA with higher (hourly) temporal resolution to a small area gives good results in terms of various rainfall characteristics at the small temporal scale (Chapter 5.1) as well as in terms of runoff simulations (Chapter 5.2.1) and may serve for future model extensions (Chapter 6.2).

Finally, it should be pointed out that the model timestep is sensitive on runoff generation not only with regard to precipitation effects, but also with re-

gard to evapotranspiration modelling. The separate quantification of a day and night component of evapotranspiration can be considered to be an efficient way to overcome the underestimation of evapotranspiration when using mean daily climate values (Fig. 5.3.2.3).

6.1.4 Model performance and uncertainty

Application of an uncalibrated model

Model validation at different spatial scales (0.7km^2 - 50000km^2) (Chapter 5.2, Chapter 5.4.3) proves that the uncalibrated model WASA is generally well able to represent the hydrological behaviour of the semi-arid study area in terms of discharge and reservoir storage. This includes also the large intra- and interannual variabilities which are key characteristics for the assessment of long-term water availability. Model performance, however, varies considerably between the validation points. From the set of validation results, model uncertainty in terms of mean annual discharge for ungauged locations can be estimated to be about $\pm 20\%$, with a maximum deviation of about $\pm 50\%$. Performance tends to increase with increasing basin area, as deviations at smaller scales balance out to some extent when aggregated into large basins. The applicability of the uncalibrated model is clearly limited in the case of sub-basins with important baseflow contributions from deep groundwater bodies.

Deviations of model results relative to the observations in the historical period may be considered to be large when compared to model performances in humid environments. However, one has to take into account that runoff is usually only a small fraction of precipitation in semi-arid areas. Thus, small absolute deviations are often large in relative terms. Additionally, the deviations found here can be seen to be a reasonable concession to the ability of the model to run in an uncalibrated mode. Just the large model sensitivity to rainfall input in various respects (Chapter 6.1.3), for instance, points out that model calibration, although possibly leading to better values of model performance, does not at all mean that model reliability, e.g. for scenario simulation results, is larger in that case. In contrary, such uncertainties in model input or model structure (the large but uncertain influence of reservoirs and water use on discharge shown in Chapter 5.4.2 is another important example) will probably lead to model calibration at the wrong place and, thus, degrade the prognostic capacity of the model to give a process-adequate representation of environmental change impact. Nevertheless, for model applica-

tions to individual sub-basins, the model should be adjusted to their specific characteristics if additional information is available. Beside of an adequate representation of the spatial and temporal rainfall characteristics (Chapter 6.1.3), the sensitivity analysis shows that the main focus during a calibration procedure should generally be laid on the highly sensitive soil parameters (Chapter 5.3.3). If no other validation variables than river discharge are available, the comparison of simulations and observations separately for dry and wet years may help towards a process-related adjustment of parameters with a varying sensitivity due to the predominance of different processes under dry and wet conditions (Chapter 5.3.3.1, see also below).

Factors of model uncertainty

Uncertainty of the simulation results is generally high, partly due to uncertainties in the model structure to represent adequately the most important hydrological processes. The small-scale model validation (Fig. 5.2) is a valuable way to enhance the confidence in model performance with regard to runoff generation. Nevertheless, large uncertainties remain due to the lack of a broader range of validation data (see also Fig. 6.2). Furthermore, uncertainties of model input data and parameters are of particular relevance in the study area with generally low data availability. Some important aspects as a consequence of parameter uncertainty are the following:

- Model validation for a small basin (roughly corresponding in size to two grid cells of the large-scale model, $\sim 200\text{km}^2$) reveals that the uncertainty of the large-scale model to reproduce the hydrological response at such a small scale is much more dependent on deviations of the large-scale rainfall data in volume and time-series characteristics from the local data than on uncertainties of the large-scale available terrain, soil and vegetation data in representing the local characteristics (Chapter 5.2.2).
- Uncertainty of model results in terms of runoff at the scale of sub-basins due to uncertain parameter values is estimated to be largest for soil parameters given at the profile scale according to the simulation results (Chapter 5.3.3). As an average value for all sub-basins, the effect may amount to $\pm 40\%$ of mean annual runoff for the most sensitive parameters (soil hydraulic conductivity, porosity, content of coarse fragments), but the effect can be even higher for individual sub-basins with specific characteristics. Less sensitive are slope and bedrock parameters ($< \pm 15\%$) and vegetation parameters, of which in turn root depth and stomata resistance are comparatively more sensitive (about $\pm 20\%$). How-

ever, it should be noted that for semi-arid areas, due to the in general low percentage of runoff on rainfall as compared to evapotranspiration, small changes in evapotranspiration cause, in relative terms, considerably larger changes in runoff.

- The parameter sensitivity of WASA, and thus model uncertainty, with regard to plant-available soil moisture is in general lower in relative terms than that for runoff. The most sensitive parameters are water retention characteristics of the profile which directly define the available soil moisture, i.e., soil porosity and soil moisture content at the wilting point (Chapter 5.3.3).
- Model parameter sensitivity with regard to runoff simulations usually differs between wet and dry years (Chapter 5.3.3). For changes in soil parameters, the model reacts markedly more sensitive in relative terms in dry as compared to wet years, whereas for bedrock and vegetation parameters the sensitivity is larger in wet years, with higher soil moisture, percolation reaching the bedrock and higher transpiration rates. This directly affects the reliability of scenario simulation results, as the uncertainty of individual parameters is of different relevance for scenarios with increasing or decreasing precipitation trends, respectively.

Results and reliability of scenario simulations

Concerning the uncertainty of the scenario simulation results, in addition to the uncertainties as discussed above, one can argue that additional uncertainty is in parts limited due to the fact that the climatic conditions of the scenario period will most probably not be outside of the range of those already found in the historical period due its large climate variability. This applies, e.g., for annual precipitation. For these conditions the reliability of the model has been confirmed by model validation. Nevertheless, additional factors remain which may cause a reaction of the system which is beyond those captured by the model, e.g., increase of atmospheric CO₂. These increase uncertainty of the scenario results. In any case, uncertainty of the underlying climate scenarios based on global climate models can be considered to be the most important factor. Trends of annual precipitation at the scale of the entire study area until 2050 are -26% and +11% for the two available scenarios, re-

spectively. Related changes in runoff are larger by a factor of 2 to 3, highlighting the strong non-linear response of semi-arid environments to rainfall changes. The expected change of future runoff for the two scenarios is accordingly in the large range of -56% to +33%, respectively (Chapter 5.5.2). Changes in both orders of magnitude of opposite direction should be considered to be plausible for the study area in view of the given information from global climate models.

Uncertainties of the spatial pattern of future water availability are additionally enhanced by the discrepancies (up to 40%) in the spatial pattern of mean annual precipitation between the optimum data set, using the maximum of available station data, and the data set derived from a smaller number of rainfall stations on which also the scenarios are based (Chapter 2.1.6.2, Chapter 5.3.1.3).

The vulnerability of the study area, expressed by water scarcity in consequence of climate variability already for present-day conditions, will even increase for the climate scenario with a decreasing precipitation trend considered here. The simulation results indicate that future changes in river discharge tend to be larger (1) in sub-basins with basically lower runoff volumes in absolute values, (2) in sub-basins with a larger importance of lateral redistribution effects, and (3) in sub-basins with a larger reservoir storage capacity. Furthermore, in the case of the scenario with a decreasing precipitation trend, an increase of surface water availability provided by the construction of new reservoirs is increasingly less effective, relative to the storage capacity of the new dams, the lower the annual rainfall volumes are and the larger the increase of storage capacity is in absolute values (Chapter 5.5.2). This points to a tendency towards a state of saturation with regard to surface reservoirs in the water resources system in Ceará, where within a dense network of reservoirs the benefit of additional ones can be constrained due to the limiting interaction between them. However, stronger integrated scenario calculations of which the hydrological model developed here is one part, including, e.g., the dynamic representation of water use and water management aspects, are required to support such conclusions on their way to support regional planning for the development of adaptation strategies (Chapter 6.2).

6.2 Perspectives

Model validation

Extended possibilities of model validation are an essential prerequisite for future improvements of the hydrological model developed in this study. Multi-criterial validation methods, including several validation variables at various scales, are required to assess model performance more specifically for individual processes, to realize adequate modifications of process formulations and, in this way, to enhance the overall model reliability. This applies in particular for the newly developed model components. For the new spatial concept of WASA with lateral redistribution of water fluxes, soil moisture data at the hillslope scale and at the larger basin scale are required to evaluate the appropriateness of the concept to represent the essentials of the spatial soil moisture patterns. Additionally, further simultaneous runoff measurements ranging from the plot to the basin scale, including tracer methods for separation of different runoff components, may help to identify more precisely the way of lateral interaction among adjacent spatial units and how to include them efficiently into the large-scale model in extension of the simple approach used so far. An important model component to be added are transmission losses by infiltration in the main river network at scales larger than the landscape units.

Model transfer

The multi-scale spatial concept developed here could also be applied in even larger-scale models, e.g., as sub-grid land surface parameterization in climate models to capture the possible feedbacks of the state of the land surface on the atmosphere. In this respect, testing the approach with even coarser terrain, soil and vegetation data may lead to a closer view of which are the critical landscape features to be indispensably represented in the model. This will be a step towards the generalization and transferability of the approach. The applicability of existing continental-scale data bases which follow the SOTER structure (see FAO (2001) and ISRIC (1999) for examples), which is also the basis of the spatial structure in this model, is to be tested with regard to the coupling with a climate model. Nevertheless, a main restriction for the transfer of the current spatial approach to other study areas may be the lack of combined soil and terrain data, i.e., information that allows to delineate landscape units and to distribute soil and land cover information among the units of different topographic position in WASA. For some areas, detailed maps may allow to derive such

relationships. Generally, to support the modelling approach, further data bases as in this study respecting the standardized SOTER structure have to be built in interdisciplinary work with soil scientists and extended for the hydrological application.

For applications to more humid environments with a larger importance of lateral subsurface flow processes (including, e.g., piston-type flow, preferential flow at the hillslope scale), extensions may be required in the concept of subsurface lateral redistribution, as the simple DARCY-type approach used in WASA might not be sufficient in that case. Similarly, groundwater flow at the regional scale should be included. The existing concept based on landscape units (which are defined also by their geological properties) may serve as a reasonable basis in this respect by extending their function as source areas or receiving areas for large-scale groundwater fluxes.

Erosion modelling

A further model extension, of particular relevance for integrated impact assessment in semi-arid areas, is the incorporation of a module for erosion modelling. Its importance exists not only with regard to the assessment of terrain resources, e.g., for agricultural use, but also directly with regard to the assessment of water resources by changing runoff generation in line with changing characteristics of the erosion surfaces and with regard to the reduction of storage capacity in reservoirs due to subsequent sedimentation of the reservoir volume. With erosion assessment being one basic idea behind the type of data base structure defined in the SOTER concept, the model WASA has the potential to efficiently include an erosion module within its existing spatial structure.

Rainfall data

In view of the results of this study, a focus in any further model application should be given to the rainfall input data, an aspect to which generally too less attention is paid in many hydrological modelling studies. Extended methods for the assimilation of model input data are required, on the one hand, with regard to the spatial interpolation of station data, respecting more detailed information on different rainfall zones with respectively different spatial correlation patterns and different relations between precipitation amounts and altitude (see, e.g., UVO & BERNDTSSON, 1996). On the other hand, methods are to be further developed to capture appropriately the spatial and temporal variability of precipitation also at smaller scales, i.e., by

spatio-temporal simulation of rainfall and/or disaggregation approaches, and by scaling approaches within the hydrological model to compensate for the remaining scale mismatch between the spatial and temporal resolution of the model and the real rainfall characteristics being relevant for the hydrological response. Particularly in view of low rainfall data availability, it has to be tested which of two possible approaches is more appropriate, i.e., perform spatial rainfall interpolation at large time scales where spatial correlation is more obvious (e.g., for 10-day periods) and apply subsequently a disaggregation scheme to higher resolutions, or do interpolation at a small time scale (daily) and add a stochastic component afterwards to compensate for the loss in variance. For the sub-daily scale, a promising approach is to include a temporal rainfall disaggregation scheme dynamically into the hydrological model, like the cascade scheme tested here, allowing for a internally smaller simulation timestep at least for infiltration modelling. In this respect, the relevance of diurnal precipitation patterns

for the type of model application should be tested and the disaggregation scheme adapted accordingly.

Scenarios and uncertainty assessment

Important factors to be respected in integrated scenario simulations of future water availability are land cover / land use changes as well as dynamic water management aspects, like operation rules of reservoirs in dependence on water availability and water demand, or withdrawal water use as a function of water availability. In this respect, decision rules for water allocation, as negotiated among water user groups within recently established basin committees in the study area, for instance (CAMPOS & STUDART, 2000), are to be respected. In general for the interpretation of scenario results, a more comprehensive uncertainty analysis is required which in extension to the single factor analysis done here allows to give bounds of uncertainty resulting from the combination of several sources of uncertainty.

References

- Abbott, M.B., Bathurst, J.C., Cunge, A., O'Connell, P.E. & Rasmussen, J. (1986a): An introduction to the SHE, 1: History and philosophy of a physically-based, distributed modelling system. *Journal of Hydrology*, 87, 49-59.
- Abbott, M.B., Bathurst, J.C., Cunge, A., O'Connell, P.E. & Rasmussen, J. (1986b): An introduction to the SHE, 2: Structure of a physically-based, distributed modelling system. *Journal of Hydrology*, 87, 61-77.
- Abdulla, F.A. & Lettenmaier, D.P. (1997): Application of regional parameter estimation schemes to simulate the waterbalance of a large continental river. *Journal of Hydrology*, 197, 258-285.
- Abrahams, A.D. & Parsons, A.J. (1991): Relation between infiltration and stone cover on a semiarid hillslope, Southern Arizona. *Journal of Hydrology*, 122, 49-59.
- Abrahams, A.D., Parsons, A.J. & Luk, S. (1988): Hydrologic and sediment responses to simulated rainfall on desert hillslopes in southern Arizona. *Catena*, 15, 103-117.
- Abrahams, A.D., Parsons, A.J. & Wainwright, J. (1994): Resistance to overland-flow on semiarid grassland and shrubland hillslopes, Walnut Gulch, Southern Arizona. *Journal of Hydrology*, 156, 431-446.
- Ahuja, L.R. (1983): Modeling infiltration into crusted soils by the Green-Ampt approach. *Soil Sci. Soc. Am. J.*, 47, 412-418.
- Allen, S.J., Wallace, J.S., Gash, J.H.C. & Sivakumar, M.V.K. (1994): Measurements of albedo variation over natural vegetation in the Sahel. *International Journal of Climatology*, 14, 625-636.
- Amundsen, A.J., Ali, A.R. & Belsky, A.J. (1995): Stomatal responsiveness to changing light-intensity increases rain-use efficiency of below-crown vegetation in tropical savannas. *Journal of Arid Environments*, 29(2), 139-153.
- Andersen, J., Refsgaard, J.C. & Jensen, K.H. (2001): Distributed hydrological modelling of the Senegal River Basin - model construction and validation. *Journal of Hydrology*, 247, 200-214.
- Andrade-Lima, D. (1981): The caatinga dominum. *Revista Brasileira de Botanica*, 4, 149-163.
- Araújo Filho, P.F.d., Pereira Cabral, J.J.d.S., Antonio, A.C.D. & Braga, R.A.P. (2000): Modelagem de eventos de cheia para a bacia do Rio Tapacurá: model SMAP horário. *Anais do V Simpósio de Recursos Hídricos do Nordeste*, ABRH (Associação Brasileira de Recursos Hídricos), Natal, Brazil, Vol. 2, 418-428.
- Araújo, J.A. (1990): Barragens no Nordeste do Brasil. DNOCS (Departamento Nacional de Obras contra as Secas), Fortaleza, 328 pp.
- Araújo, J.C., Oliveira, M.R.L., Machado Junior, J.C., Teixeira, L.R. & Akabassi, L. (2000): Medidas de assoreamento em bacias de reservatórios do semi-árido. *Anais do V simpósio de recursos hídricos do nordeste*, ABRH (Associação Brasileira de Recursos Hídricos), Natal, Brazil, Vol.1, 559 - 562.
- Araújo, J.C. & Ribeiro, A.L. (1996): Avaliação de perda d'água em rios no semi-árido. *Proceedings of the III Seminário de Recursos Hídricos do Nordeste*, Salvador, Bahia, Brazil, 215-221.
- Araújo, J.C. (2000): Hydrological aspects of the States of Ceará and Piauí. Technical Report, Universidade Federal do Ceará, Fortaleza, Brazil - Potsdam Institute for Climate Impact Research, Potsdam, Germany, unpublished.
- Arnell, N.W. (1999): A simple water balance model for the simulation of streamflow over a large geographic domain. *Journal of Hydrology*, 217, 314-335.
- Arnell, N.W. (2000): Thresholds and responses to climate change forcing: the water sector. *Climatic Change*, 46, 305-316.
- Arnell, N.W. & Reynard, N.S. (1996): The effects of climate change due to global warming on river flows in Great Britain. *Journal of Hydrology*, 183, 397-424.

- Arnold, J.G. & Williams, J.R. (1995): SWRRB - A watershed scale model for soil and water resources management. In: V.P. Singh (Ed.): Computer models of watershed hydrology. Water Resources Publications, Colorado, U.S.A., 847-908.
- Arnold, J.G., Williams, J.R., Griggs, A.D. & Sammons, N.B. (1990): SWRRB: A basin scale simulation model for soil and water resources management, Texas A&M Univ. Press, College Station, U.S.A.
- Asfora, M.C. & Campello, S. (2000): Bacia hidrográfica representativa de escada - aplicação de um modelo chuva-vazão diário aos dados do Rio Jundiá-Açu. Anais do V Simpósio de Recursos Hídricos do Nordeste. ABRH (Associação Brasileira de Recursos Hídricos), Natal, Brazil, Vol.2, 438-447.
- Austin, R.B., Playan, E. & Gimeno, J. (1998): Water storage in soils during the fallow: prediction of the effects of rainfall pattern and soil conditions in the Ebro valley of Spain. *Agricultural Water Management*, 36(3), 213-231.
- Avissar, R. (1992): Conceptual aspects of a statistical-dynamical approach to represent landscape subgrid-scale heterogeneities in atmospheric models. *Journal Geophysical Research*, 97(D3), 2729-2742.
- Bajracharya, R.M. & Lal, R. (1999): Land use effects on soil crusting and hydraulic response of surface crusts on a tropical Alfisol. *Hydrological Processes*, 13, 59-72.
- Baldocchi, D.D., Luxmore, R.J. & Hatfield, J.L. (1991): Discerning the forest from the trees: an essay on scaling stomatal conductance. *Agricultural and Forest Meteorology*, 54, 197-226.
- Barbosa, J.M.S.G., Barbosa, D.L., Almeida, M.A., Costa, C.F.L., Braga, A.C.F.M. & Figueiredo, E.E. (2000): Calibração e validação do modelo SMAP para uma bacia do semi-árido da Paraíba: Anais do V Simpósio de Recursos Hídricos do Nordeste. ABRH (Associação Brasileira de Recursos Hídricos), Natal, Brazil, Vol.2, 295-304.
- Bárdossy, A. (1993): Stochastische Modelle zur Beschreibung der raum-zeitlichen Variabilität des Niederschlages. *Mitteilungen des Instituts für Hydrologie und Wasserwirtschaft*, Nr. 44, Universität Karlsruhe, Germany.
- Bárdossy, A. (1998): Generating precipitation time series using simulated annealing. *Water Resources Research*, 34(7), 1737-1744.
- Bárdossy, A. (2001): Räumliche Interpolation und zeit-räumliche Simulation des Niederschlages in Nordost Brasilien. Technical Report, Potsdam Institute of Climate Impact Research, Potsdam, Germany, unpublished.
- Baumgartner, A. & Liebscher, H.J. (1990): *Allgemeine Hydrologie - Quantitative Hydrologie*. Lehrbuch der Hydrologie, Band 1. Gebrueder Borntraeger, Berlin, Germany.
- Bazin, F. (1993): Levantamento dos açudes do município de Tauá / CE, SUDENE-DPP-APR, Recife, Brazil, 37 pp.
- Becker, A. (1995): Problems and progress in macroscale hydrological modelling. In: R.A. Feddes (Ed.): *Space and time scale variability and interdependencies in hydrological processes*. Cambridge University Press, Cambridge, UK, 135-143.
- Becker, A. & Braun, P. (1999): Disaggregation, aggregation and spatial scaling in hydrological modelling. *Journal of Hydrology*, 217, 239-252.
- Becker, A., Güntner, A. & Katzenmaier, D. (1999): Required integrated approach to understand runoff generation and flow path dynamics in catchments. In: C. Leibundgut, J. McDonnell & G. Schultz (Eds.): *Integrated methods in catchment hydrology*. IAHS-Publ. 258, Wallingford, UK, 3-9.
- Becker, A. & Nemeč, J. (1987): Macroscale hydrological models in support to climate research. In: Solomon, S.I., Beran M. & Hogg, W. (Eds.): *The influence of climate change and the variability on the hydrologic regime and water resources*, IAHS-Publ. 168, Wallingford, UK, 431-445.
- Becker, A. & Pfützner, B. (1987): EGMO-system approach and subroutines for river basin modeling. *Acta Hydrophys.*, 31(3/4), 125-141.
- Bergström, S. (1992): The HBV model - its structure and applications. Reports RH, No. 4, SMHI, Norrköping, Sweden.
- Beven, K. (1982): On subsurface stormflow: Predictions with simple kinematic theory for saturated and unsaturated flows. *Water Resources Research*, 18, 1627-1633.
- Beven, K. (1989): Changing ideas in hydrology - the case of physically based models. *Journal of Hydrology*, 105, 157-172.
- Beven, K. (1997): TOPMODEL: A critique. *Hydrological Processes*, 11, 1069-1085.
- Beven, K. & Germann, P.F. (1982): Macropores and water flow in soils. *Water Resources Research*, 18(5), 1311-1325.
- Beven, K., Lamb, R., Quinn, P., Romanowicz, R. & Freer, J. (1995): TOPMODEL. In: V.P. Singh (Ed.): *Computer models of watershed hydrology*. Water Resources Publications, Colorado, U.S.A., 626-668.

- Beven, K.J. & Binley, A. (1992): The future of distributed models: model calibration and uncertainty predictions. *Hydrological Processes*, 6, 349-368.
- Beven, K.J., Calver, A. & Morris, E. (1987): The Institute of Hydrology Distributed Model. Institute of Hydrology Report, No. 98, Institute of Hydrology, Oxon, UK.
- Beven, K.J. & Kirkby, M.J. (1979): A physically based, variable contributing area model of basin hydrology. *Hydrological Sciences Bulletin*, 24(1), 43-70.
- Birkeland, P.W. (1999): *Soils and geomorphology*. Oxford University Press, New York, Oxford.
- Blöschl, G. & Sivapalan, M. (1995): Scale issues in hydrological modelling: a review. *Hydrological Processes*, 9, 312-329.
- Blyth, E.M. & Harding, R.J. (1995): Application of aggregation models to surface heat flux from the Sahelian tiger bush. *Agricultural and Forest Meteorology*, 72, 213-235.
- Blyth, E.M., Harding, R.J. & Essery, R. (1999): A coupled dual source GCM SVAT. *Hydrology and Earth System Sciences*, 3(1), 71-84.
- Bo, Z., Islam, S. & Eltahir, E.A.B. (1994): Aggregation-disaggregation properties of a stochastic rainfall model. *Water Resources Research*, 30, 3423-3435.
- Böhm, U. (1999): Eine Methode zur Validierung von Klimamodellen für die Klimawirkungsforschung hinsichtlich der Wiedergabe extremer Ereignisse. Dissertation, Freie Universität Berlin, Fachbereich Geowissenschaften, Berlin, Germany.
- Böhm, U., Gerstengarbe, F.-W., Hauffe, D., Kücken, M., Österle, H. & Werner, P.C. (2002): Dynamical regional climate modelling and sensitivity experiments for the Northeast of Brazil. In: T. Gaiser, M.S. Krol, H. Frischkorn & J.C.d. Araújo (Eds.): *Global change and regional impacts: Water availability and vulnerability of ecosystems and society in the semi-arid Northeast of Brazil*. Springer-Verlag, Berlin, Germany, in print.
- Bonell, M. (1998): Possible impacts of climate variability and change on tropical forest hydrology. *Climatic Change*, 39(2-3), 215-272.
- Boorman, D.B. & Sefton, C.E.M. (1997): Recognising the uncertainty in the quantification of the effects of climate change on hydrological response. *Climatic Change*, 35(4), 415-434.
- Boulet, G., Chehbouni, A., Braud, I. & Vauclin, M. (1999): Mosaic versus dual source approaches for modelling the surface energy balance of a semi-arid land. *Hydrology and Earth System Sciences*, 3(2), 247-258.
- Brakensiek, D.L., Rawls, W.J. & Stephenson, G.R. (1986): Determining the saturated hydraulic conductivity of a soil containing rock fragments. *Soil Society of America Journal*, 50, 834-835.
- Brenner, A.J. & Incoll, L.D. (1997): The effect of clumping and stomatal response on evaporation from sparsely vegetated shrublands. *Agricultural and Forest Meteorology*, 84(3-4), 187-205.
- Brisson, N., Itier, B., L'Hotel, J.C. & Lorendeau, J.Y. (1998): Parameterisation of the Shuttleworth-Wallace model to estimate daily maximum transpiration for use in crop models. *Ecological Modelling*, 107, 159-169.
- Bronstert, A. (1994): Modellierung der Abflussbildung und der Bodenwasserdynamik von Hängen. *Mitteilungen des Instituts für Hydrologie und Wasserwirtschaft*, Nr. 46, Universität Karlsruhe, Germany.
- Bronstert, A. (1999): Capabilities and limitations of detailed hillslope hydrological modelling. *Hydrological Processes*, 13(1), 21-48.
- Bronstert, A., Güntner, A., Jaeger, A., Krol, M. & Krywkow, J. (1999): Großräumige hydrologische Parametrisierung und Modellierung als Teil der integrierten Modellierung. In: Fohrer, N. & Döll, P. (Eds.): *Modellierung des Wasser- und Stofftransports in großen Einzugsgebieten*. Kassel University Press, Kassel, Germany, 31-40.
- Bronstert, A. & Katzenmaier, D. (2001): The role of infiltration conditions on storm runoff generation at the hillslope and lower meso-scale. In: C. Leibundgut, S. Uhlenbrook & J. McDonnell (Eds.): *Runoff generation and implications for river basin modelling*. *Freiburger Schriften zur Hydrologie*, Band 13, Institut für Hydrologie, Universität Freiburg, Germany, 60-67.
- Brunt, D. (1932): Notes on radiation in the atmosphere: I. *Quart. J. Roy. Meteorol. Soc.*, 58, 389-420.
- Burch, G.J., Bath, R.K., Moore, I.D. & O'Loughlin, E.M. (1987): Comparative hydrological behaviour of forested and cleared catchments in Southeastern Australia. *Journal of Hydrology*, 90, 19-42.
- Cadier, E. (1993): *Hydrologie des petits bassins du Nordeste brésilien semi-aride - Transposition à des bassins non étudiés*. ORSTOM, Institut français de recherche scientifique pour le développement en coopération, Collection Études et Thèses, Paris, France, 414 pp.
- Cadier, E. (1996): *Hydrologie des petits bassins du Nordeste Brésilien semi-aride: typologie des bassins et transposition écoulement annuels*. *Journal of Hydrology*, 182, 117-141.

- Cadier, E., Leprun, J.C. & Nouvelot, J.F. (1996): Le comportement des bassins versants représentatifs du Nordeste Brésilien bilan de la collaboration entre hydrologues et pédologues. In: Chevallier, P. & Pouyaud, B (Eds.): L'hydrologie tropicale: géoscience et outil pour le développement. IAHS-Publ. 238, Wallingford, UK, 41-52.
- Camillo, P.J. & Gurney, R.J. (1986): A resistance parameter for bare-soil evaporation models. *Soil. Sci.*, 141, 95-105.
- Campos, J.N.B. & Studart, T.M.C. (2000): An historical perspective on the administration of water in Brazil. *Water International*, 25(1), 148-156.
- Cappus, P. (1960): Étude des lois de l'écoulement. Application au calcul et à la prévision des débits. *La Houille Blanche*, N° A, 493-520.
- Casenave, A. & Valentin, C. (1992): A runoff classification system based on surface features criteria in semi-arid areas of West Africa. *Journal of Hydrology*, 130, 231-249.
- Cavalcante, N.M., Doherty, F.R. & Cadier, E. (1989): Bacia hidrográfica representativa Tauá - relatório final. *Seria hidrologia*, 28, SUDENE, Recife, Brazil.
- Ceará (1992): Plano estadual dos recursos hídricos. Vol. 2, Estudo de Base II, SHR, Secretaria dos recursos hídricos Ceará, Fortaleza, Brazil.
- Ceará, 2002. <http://www.citybrazil.com.br/ce/>.
- Ceballos, A. & Schnabel, S. (1999): Hydrological behaviour of a small catchment in the dehesa landuse system (Extremadura, SW Spain). *Journal of Hydrology*, 210, 146-160.
- Chaubey, I., Haan, C.T., Grunwald, S. & Salisbury, J.M. (1999): Uncertainty in the model parameters due to spatial variability of rainfall. *Journal of Hydrology*, 220, 48-61.
- Chiew, F.H.S., Whetton, P.H., McMahon, T.A. & Pittock, A.B. (1995): Simulation of the impacts of climate change on runoff and soil moisture in Australian catchments. *Journal of Hydrology*, 167, 121-147.
- COGERH (2000): Plano de gerenciamento das águas da bacia do Rio Jaguaribe. COGERH (Companhia de Gestão dos Recursos Hídricos), Fortaleza, Brazil.
- Connolly, R.D., Schirmer, J. & Dunn, P.K. (1998): A daily rainfall disaggregation model. *Agricultural and Forest Meteorology*, 92, 105-117.
- Costa, C.F.L., Braga, A.C.F.M., Almeida, M.A., Barbosa, J.M.S.G., Barbosa, D.L. & Figueiredo, E.E. (2000): Simulação de eventos de cheia da bacia representativa Sumé: Anais do V Simpósio de Recursos Hídricos do Nordeste. ABRH (Associação Brasileira de Recursos Hídricos), Natal, Brazil, Vol. 2, 409-417.
- Cowpertwaite, P.S.P., O'Connell, P.E., Metcalfe, A.V. & Mawdsley, J.A. (1996): Stochastic point process modelling of rainfall. II. Regionalisation and disaggregation. *Journal of Hydrology*, 175, 47-65.
- CPRM (1996): Avaliação da potencialidade hídrica e mineral do médio-baixa Jaguaribe. CPRM, Serviço Geológico do Brasil, Fortaleza, Brazil.
- CPRM (1999): Atlas dos recursos hídricos subterrâneos do Ceará. CPRM, Serviço Geológico do Brasil, CD-ROM, Fortaleza, Brazil.
- Daamen, C.C. & Simmonds, P. (1996): Measurement of evaporation from bare soil and its estimation using surface resistance. *Water Resources Research*, 32(5), 1393-1402.
- Dam, J.C. (1999): Impacts of climate change and climate variability on hydrological regimes. UNESCO International Hydrological Series. Cambridge University Press, Cambridge, UK.
- de Boer, D.H. (1992): Constraints on spatial transference of rainfall-runoff relationships in semiarid basins drained by ephemeral streams. *Hydrological Science Journal*, 37(5), 491-504.
- de Lima, M.I.P. & Grasman, J. (1999): Multifractal analysis of 15-min and daily rainfall from a semi-arid region in Portugal. *Journal of Hydrology*, 220, 1-11.
- Deidda, R., Benzi, R. & Siccaldi, F. (1999): Multifractal modeling of anomalous scaling laws in rainfall. *Water Resources Research*, 35, 1853-1876.
- Desconnets, J.C., Taupin, J.D., Lebel, T. & Leduc, C. (1997): Hydrology of the HAPEX-Sahel Super-Site: surface water drainage and aquifer recharge through the pool system. *Journal of Hydrology*, 188-189, 155-178.
- D'Herbes, J.M. & Valentin, C. (1997): Land surface conditions of the Niamey region: ecological and hydrological implications. *Journal of Hydrology*, 188-189, 18-42.
- Diamantopoulos, J., Pantis, J., Sgardelis, S., Iatrou, G., Pirintzos, S., Papatheodorou, E., Dalaka, A. & Stamou, G.P. (1996): The Petralona and Hortiatís field sites (Thessaloniki, Greece). In: J. Brandt & J.B. Thornes (Eds.): *Mediterranean desertification and land use*. Wiley, London, UK, 229-246.
- Dickinson, R. (1984): Modeling evapotranspiration for three-dimensional global climate models. In: AGU (Ed.). *Climate Processes and Climate Sensitivity*, Geophys. Monogr. No. 29. Amer. Geophys. Union, 58-72.

- DNAEE (1983): Modelo SIMMQE - Concetuação. Ministério das Minas e Energia - Departamento Nacional de Águas e Energia, Rio de Janeiro, Brazil.
- DNPM (1983): Mapa geológico do Estado do Ceará. Ministerio das Minas e Energia, Departamento Nacional da Produção Mineral, Fortaleza, Brazil.
- DNPM (1996): Projeto avaliação hidrogeológica da bacia sedimentar do Araripe, Fase 1 - Texto. Ministério de Minas e Energia, Departamento Nacional de Produção Mineral, Recife, Brazil.
- Dolman, A.J. (1993): A multiple-source land-surface energy-balance model for use in general-circulation models. *Agricultural and Forest Meteorology*, 65(1-2), 21-45.
- Domingo, F., Sanchez, G., Moro, M.J., Brenner, A.J. & Puigdefabregas, J. (1998): Measurement and modelling of rainfall interception by three semi-arid canopies. *Agricultural and Forest Meteorology*, 91(3-4), 275-292.
- Domingo, F., Villagarcia, L., Brenner, A.J. & J., P. (1999): Evapotranspiration model for semi-arid shrub-lands tested against data from SE Spain. *Agricultural and Forest Meteorology*, 95(2), 67-84.
- Dorman, J.L. & Sellers, P.J. (1989): A global climatology of albedo, roughness length and stomatal resistance for atmospheric general circulation models as represented by the simplke biosphere model (SiB). *Journal of Applied Meteorology*, 28, 833-855.
- Dubois, G., Malczewski, J. & De Cort, M. (1998): Spatial interpolation comparison 97. *Journal of Geographic Information and Decision Analysis (Special Issue)*, 2(2).
- Dunkerley, D. (2000): Measuring interception loss and canopy storage in dryland vegetation: a brief review and evaluation of available research strategies. *Hydrological Processes*, 14(4), 669-678.
- Dunkerley, D.L. & Booth, T.L. (1999): Plant canopy interception of rainfall and its significance in a banded landscape, arid western New South Wales, Australia. *Water Resources Research*, 35(5), 1581-1586.
- Dunne, T. & Black, R.D. (1970): An experimental investigation of runoff production in permeable soils. *Water Resources Research*, 6, 478-490.
- DVWK (1996): Ermittlung der Verdunstung von Land- und Wasserflächen. DVWK-Merkblätter zur Wasserwirtschaft, Heft 238, Deutscher Verband für Wasserwirtschaft und Kulturbau, Bonn, Germany.
- Dyck, S. & Peschke, G. (1995): *Grundlagen der Hydrologie*. Verlag für Bauwesen, Berlin, Germany.
- Econopouly, T.W., Davis, D.R. & Woolhiser, D.A. (1990): Parameter transferability for a daily rainfall disaggregation model. *Journal of Hydrology*, 118, 209-228.
- El-Hames, A.S. & Richards, K.S. (1994): Progress in arid-lands rainfall-runoff modelling. *Prog. Phys. Geogr.*, 18(3), 343-365.
- Entekhabi, D. & Eagleson, P.S. (1989): Land surface hydrology parametrization for atmospheric general circulation models including subgrid scale variability. *Journal of Climate*, 2(8), 816-831.
- Ewen, J. (1997): 'Blueprint' for the UP Modelling System for large scale hydrology. *Hydrology and Earth System Sciences*, 1, 55-69.
- Ewen, J., Kilsby, C.G., Sloan, W.T. & O'Connell, P.E. (1999): UP modelling system for large scale hydrology: deriving large-scale physically-based parameters for the Arkansas-Red River basin. *Hydrology and Earth System Sciences*, 3(1), 137-149.
- Ewen, J. & Parkin, G. (1996): Validation of catchment models for predicting land-use and climate change impacts. 1. Method. *Journal of Hydrology*, 175, 583-594.
- Famiglietti, J.S. & Wood, E.F. (1994): Multiscale modelling of spatially variable water and energy balance processes. *Water Resources Research*, 30(11), 3061-3078.
- FAO (1992): CROPWAT - A computer program for irrigation planning and management. FAO Irrigation and drainage paper, No. 46, FAO (Food and Agriculture Organization of the United Nations), Rome, Italy.
- FAO (1993): Global and national soils and terrain digital databases (SOTER). Procedures Manual. World Soil Resources Reports, No. 74., FAO (Food and Agriculture Organization of the United Nations), Rome, Italy.
- FAO, 2001. Global Soil and Terrain Database (WORLD-SOTER). FAO, AGL (Food and Agriculture Organization of the United Nations, Land and Water Development Division), <http://www.fao.org/ag/AGL/agll/soter.htm>.
- Faulkner, H. (1992): Simulation of summer storms of differing recurrence intervals in a semiarid environment using a kinematic routing scheme. *Hydrological Processes*, 6(4), 397-416.
- Faurès, J.-M., Goodrich, D.C., Woolhiser, D.A. & So-rooshian, S. (1995): Impact of small-scale spatial rainfall variability on runoff modeling. *Journal of Hydrology*, 173(1-4), 309-326.
- Feddes, R.A., Kowalik, P.J. & Zaradny, H. (1978): Simulation of field water use and crop yield. *Simulation Monograph.*, PUDOC, Wageningen, Netherlands.

- Federer, C.A., Vörösmarty, C.J. & Fekete, B. (1996): Intercomparison of methods for potential evapotranspiration in regional or global water balance models. *Water Resources Research*, 32, 2315-2321.
- Fennessy, M.J. & Xue, Y. (1997): Impact of USGS vegetation map on GCM simulations over the United States. *Ecological Applications*, 7(1), 22-33.
- Ferraro, R.R., Grody, N.C. & Marks, G.F. (1994): Effects of surface conditions on rain identification using the DMSP-SSM/I. *Remote Sensing Reviews*, 11, 195-209.
- Ferraro, R.R. & Marks, G.F. (1995): The development of SSM/I rain-rate retrieval algorithms using ground-based radar measurements. *Journal of Atmospheric and Oceanic Technology*, 12, 755-770.
- Flerchinger, G.N., Cooley, K.R., Hanson, C.L. & Seyfried, M.S. (1998): A uniform versus an aggregated water balance of a semi-arid watershed. *Hydrological Processes*, 12(2), 331-342.
- Flügel, W.-A. (1995): Delineating hydrological response units by geographical information system analysis for regional hydrological modelling using PRMS/MMS in the drainage basin of the river Bröl/Germany. *Hydrological Processes*, 9(3-4), 423-436.
- Formiga, K.T.M., Góis, R.S.S., Siqueira, M.T. & Alves, L.M. (1999): Avaliação da disponibilidade hídrica no açude Custódia - PE. *Anais do XVIII Simpósio Brasileiro de Recursos Hídricos*. ABRH (Associação Brasileira de Recursos Hídricos), CD-ROM.
- FUNCEME (1998a): GeoView. Versão experimental, Janeiro 1998, CD-ROM. FUNCEME (Fundação Ceasense de Meteorologia e Recursos Hídricos), Fortaleza, Brazil.
- FUNCEME (1998b): Levantamento da biomassa florestal e técnicas de geoprocessamento. Relatório Técnico, FUNCEME (Fundação Ceasense de Meteorologia e Recursos Hídricos), Fortaleza, Brazil.
- Gaiser, T., Krol, M.S., Frischkorn, H. & Araújo, J.C. (2002a): Global change and regional impacts: Water availability and vulnerability of ecosystems and society in the semi-arid Northeast of Brazil. Springer-Verlag, Berlin, Germany, in print.
- Gaiser, T., Graef, F., Hilger, T.H., Ferreira, L.G.R. & Stahr, K. (2002b): An information system for land resources in Piauí and Ceará. In: T. Gaiser, M.S. Krol, H. Frischkorn & J.C. Araújo (Eds.): *Global change and regional impacts: Water availability and vulnerability of ecosystems and society in the semi-arid Northeast of Brazil*. Springer-Verlag, Berlin, Germany, in print.
- Gash, J.H. (1979): An analytical model of rainfall interception by forests. *Quart. J. R. Met. Soc.*, 105, 43-55.
- Gash, J.H.C., Lloyd, C.R. & Lachaud, G. (1995): Estimating sparse forest rainfall interception with an analytical model. *Journal of Hydrology*, 170, 79-86.
- Germann, P.F. (1986): Rapid drainage response to precipitation. *Hydrological Processes*, 1, 3-13.
- Gerstengarbe, F.-W. & Werner, P.C. (1999): Estimation of the beginning and end of recurrent events within a climate regime. *Climate Research*, 11(2), 97-107.
- Gerstengarbe, F.-W. & Werner, P.C. (2002): Climate scenarios and climate modelling. In: T. Gaiser, M.S. Krol, H. Frischkorn & J.C. Araújo (Eds.): *Global change and regional impacts: Water availability and vulnerability of ecosystems and society in the semi-arid Northeast of Brazil*. Springer-Verlag, Berlin, Germany, in print.
- Giesen, N.C.v.d., Stomph, T.J. & de Ridder, N. (2000): Scale effects of Hortonian overland flow and rainfall-runoff dynamics in a West African catena landscape. *Hydrological Processes*, 14, 165-175.
- Glasbey, C.A., Cooper, G. & McGechan, M.B. (1995): Disaggregation of daily rainfall by conditional simulation from a point-process model. *Journal of Hydrology*, 165, 1-9.
- Gleick, P.H. (1986): Methods for evaluating the regional hydrologic impacts of global climate changes. *Journal of Hydrology*, 88, 97.
- Goodrich, D.C., Faures, J.M., Woolhiser, D.A., Lane, L.J. & Sorooshian, S. (1995): Measurement and analysis of small-scale convective storm rainfall variability. *Journal of Hydrology*, 173(1-4), 283-308.
- Goodrich, D.C., Lane, L.J., Shillito, R.M., Miller, S.N., Syed, K.H. & Woolhiser, D.A. (1997): Linearity of basin response as a function of scale in a semiarid watershed. *Water Resources Research*, 33(12), 2951-2965.
- Görgens, A.H.M. (1983): Reliability of calibration of a monthly rainfall-runoff model: the semiarid case. *Hydrological Science Journal*, 28(4), 485-498.
- Grayson, R.B., Blöschl, G. & Moore, I.D. (1995): Distributed parameter hydrologic modelling using vector elevation data: THALES and TAPES-C. In: V.P. Singh (Ed.): *Computer models of watershed hydrology*. Water Resources Publications, Colorado, U.S.A., 669-696.
- Grayson, R.B., Moore, I.D. & McMahon, T.A. (1992): Physically based hydrologic modeling 1. A

- terrain-based model for investigative purposes. *Water Resources Research*, 28(10), 2639-2658.
- Grayson, R.B., Western, A.W., Chiew, F.H. & Blöschl, G. (1997): Preferred states in spatial soil moisture patterns: local and nonlocal controls. *Water Resources Research*, 33(12), 2897-2908.
- Green, W.H. & Ampt, G.A. (1911): Studies on soil physics: 1. Flow of water and air through soils. *J. Agric. Sci.*, 4, 1-24.
- Grimes, D.I.F., Pardo-Igúzquiza, E. & Bonifacio (1999): Optimal areal rainfall estimation using rain-gauges and satellite data. *Journal of Hydrology*, 222, 93-108.
- Grody, N.C. (1991): Classification of snow cover and precipitation using the SSM/I. *Journal of Geophysical Research*, 96(D4), 7423-7435.
- Güntner, A., Olsson, J., Calver, A. & Gannon, B. (2001): Cascade-based disaggregation of continuous rainfall time series: the influence of climate. *Hydrology and Earth System Sciences*, 5(2), 145-164.
- Güntner, A., Uhlenbrook, S., Seibert, J. & Leibundgut, C. (1999): Multi-criterial validation of TOPMODEL in a mountainous catchment. *Hydrological Processes*, 13, 1603-1620.
- Haberlandt, U. & Kite, G.W. (1998): Estimation of daily space-time precipitation series for macroscale hydrological modelling. *Hydrological Processes*, 12(9), 1419-1432.
- Halm, D. (2000): Soil water balance in the semiarid Northeast of Brazil - characterisation, simulation, evaluation, and comparison of hydrological properties and processes in representative soils of the Picos region, Piauí. *Hohenheimer Bodenkundliche Hefte*, Heft 55. Universität Hohenheim, Institut für Bodenkunde und Standortslehre, Stuttgart, Germany, 205 pp.
- Hamon, W.R. (1963): Computation of direct runoff amounts from storm rainfall. *Int. Assoc. Sci. Hydrol. Publ.*, 63, 52-62.
- Hanan, N.P. & Prince, S.D. (1997): Stomatal conductance of West-Central Supersite vegetation in HAPEX-Sahel: measurements and empirical models. *Hydrological Processes*, 11, 188-189, 536-562.
- Hargreaves, G.H. (1974): Estimation of potential and crop evapotranspiration. *Trans. of the ASAE*, 17, 701-704.
- Hargreaves, G.H. & Samani, Z.A. (1985): Reference crop evapotranspiration from temperature. *Applied Engineering in Agriculture*, 1(2), 96-99.
- Hastenrath, S. & Greischar, L. (1993): Further work on northeast Brazil rainfall anomalies. *Journal of Climate*, 6, 743-758.
- Hauschild, M. & Döll, P. (2000): Water use in semi-arid northeastern Brazil - modeling and scenario analysis. *Kassel World Water Series*, Report No. 3, Center for Environmental Systems Research, University of Kassel, Germany.
- Hayashi, I. (1995): Changing aspects of drought-deciduous vegetation in the semi-arid region of North-East Brazil. In: T. Nishizawa & J. Uitto (Eds.): *The fragile tropics of Latin America - Sustainable management of changing environment*. United Nations University Press, Tokyo, Japan, 268-279.
- Hershendorff, J. & Woolhiser, D.A. (1987): Disaggregation of daily rainfall. *Journal of Hydrology*, 95, 299-322.
- Hilger, T., Gaiser, T., Herfort, J., Ferreira, L.G.R. & Leihner, D.E. (2000): Calibration of EPIC for crop growth in NE-Brazil. *Proceedings of Deutscher Tropentag 1999*, Humboldt Universität zu Berlin, Germany, CD-ROM.
- Holbrook, N.M., Whitbeck, J.L. & Mooney, H.A. (1995): Drought response of neotropical dry forest trees. In: S.H. Bullock, H.A. Mooney & E. Medina (Eds.): *Seasonally dry tropical forests*. Cambridge University Press, Cambridge, UK, 64-92.
- Holtan, H.N. (1961): A concept for infiltration estimates in watershed engineering. *USDA Tech. Bull.*, 41-51.
- Horton, R.E. (1933): The role of infiltration in the hydrologic cycle. *Geophysical Union Transactions*, 14, 446-460.
- Horton, R.E. (1940): An approach toward a physical interpretation of infiltration capacity. *Soil Sci. Soc. Am. J.*, 5, 399-417.
- Hubert, P., Tessier, Y., Lovejoy, S., Schertzer, D., Schmitt, F., Ladoy, P., Carbonell, J.P., Violette, S. & Desrosiers, I. (1993): Multifractals and extreme rainfall events. *Geophys. Res. Lett.*, 20, 931-934.
- Hughes, D.A. (1995): Monthly rainfall-runoff models applied to arid and semiarid catchments for water resource estimation purposes. *Hydrological Science Journal*, 40(6), 751-769.
- Hughes, D.A. & Sami, K. (1992): Transmission losses to alluvium and associated moisture dynamics in a semiarid ephemeral channel system in southern Africa. *Hydrological Processes*, 6, 45-53.
- Hughes, D.A. & Sami, K. (1994): A semi-distributed, variable time interval model of catchment hydrology - structure and parameter estimation procedure. *Journal of Hydrology*, 155, 265-291.
- Huntingford, C., Allen, S.J. & Harding, R.J. (1995): An intercomparison of single and dual-source vegetation-atmosphere transfer models applied to tran-

- spiration from Sahelian savannah. *Boundary-Layer Meteorology*, 74, 397-418.
- Huntingford, C., Verhoef, A. & Stewart, J. (2000): Dual versus single source models for estimating surface temperature of African savannah. *Hydrology and Earth System Sciences*, 4(1), 185-191.
- IBGE (1998): Censos economicos de 1995-1996. Censo Agropecuário Ceará, No. 11, IBGE (Instituto Brasileiro de Geografia e Estatística), Rio de Janeiro, Brazil.
- IPCC (2001): Climate change 2001 - Impacts, adaptation and vulnerability. 3rd assessment report of the intergovernmental panel on climate change, Cambridge University Press, Cambridge, UK.
- IPCC-DDC (1999): GCM climate change scenarios and observed climate datasets. <http://ipcc-ddc.cru.uea.ac.uk>.
- ISRIC, 1999. Global and National Soils and Terrain Digital Databases (SOTER). International soil reference and information centre, <http://www.isric.nl/SOTER.htm>.
- Jacomine, P.K.T., Almeida, J.C. & Medeiros, L.A.R. (1973): Levantamento exploratorio - Reconhecimento de solos do Estado do Ceará. Boletim Técnico No. 28 / Série Pedologia No. 16, DNPEA / SUDENE, Recife, Brazil.
- Jarvis, P.G. (1976): The interpretation of leaf water potential and stomata conductance found in canopies in the field. *Philos. Trans. R. Soc. London, Ser. B*, 273, 593-610.
- Johns, T.C., Carnell, R.E., Crossley, J.F., Gregory, J.M., Mitchell, J.F.B., Senior, C.A., Tett, S.F.B. & Wood, R.A. (1997): The Second Hadley Centre coupled ocean-atmosphere GCM: model description, spinup and validation. *Climate Dynamics*, 13, 103-134.
- Kabat, P., Hutjes, R.W.A. & Feddes, R.A. (1997): The scaling characteristics of soil parameters: From plot scale heterogeneity to subgrid parameterization. *Journal of Hydrology*, 190, 363-396.
- Kelliher, F.M., Leuning, R., Raupach, M.R. & Schulze, E.D. (1995): Maximum conductances for evaporation from global vegetation types. *Agricultural and Forest Meteorology*, 73, 1-16.
- Kidwell, M.R., Weltz, M.A. & Guertin, D.P. (1997): Estimation of Green-Ampt effective hydraulic conductivity for rangelands. *Journal of Range Management*, 50(3), 290-299.
- Kilsby, C.G., Ewen, J., Sloan, W.T., Burton, A., Fallows, C.S.I. & O'Connell, P.E. (1999): The UP modelling system for large scale hydrology: simulation of the Arkansas-Red River basin. *Hydrology and Earth System Sciences*, 3(1), 137-149.
- Kite, G.W. (1978): Development of a hydrologic model for a canadian watershed. *Canadian Journal of Civil Engineering*, 5(1), 126-134.
- Klemes, V. (1985): Sensitivity of water-resource systems to climate variations. WCP-Report No. 98, WMO, Geneva, Switzerland.
- Klemes, V. (1986): Operational testing of hydrological simulation models. *Hydrol. Sci. J.*, 31, 13-24.
- Knudsen, J.A., Thomsen, A. & Refsgaard, J.C. (1986): A semi-distributed, physically based hydrological modelling system. *Nordic Hydrology*, 17, 347-362.
- Körner, C. (1994): Leaf diffusive conductances in the major vegetation types of the globe. In: E.-D. Schulze & M.M. Caldwell (Eds.): *Ecophysiology of Photosynthesis*. Ecological Studies, Vol. 100., Springer, Berlin, Germany, 463-490.
- Kousky, V.E. (1979): Frontal influences on Northeast Brazil. *Mon. Weather. Rev.*, 107, 1140-1153.
- Kousky, V.E. (1980): Diurnal rainfall variation in Northeast Brazil. *Mon. Weather. Rev.*, 108, 488-498.
- Kousky, V.E. & Gan, M.A. (1981): Upper tropospheric cyclonic vortices in the tropical South Atlantic. *Tellus*, 33, 539-551.
- Krol, M., Jaeger, A., Bronstert, A. & Kryukow, J. (2001): The Semi-arid Integrated Model SIM, regional integrated model assessing water availability, vulnerability of ecosystems and society in NE-Brazil. *Physics and Chemistry of the Earth. Part B: Hydrology, Oceans and Atmosphere*, 26(7-8), 529-534.
- Krol, M.S., Jaeger, A. & Bronstert, A. (2002): Integrated modelling of climate change impacts in Northeastern Brazil. In: T. Gaiser, M.S. Krol, H. Frischkorn & J.C. Araújo (Eds.): *Global change and regional impacts: Water availability and vulnerability of ecosystems and society in the semi-arid Northeast of Brazil*. Springer-Verlag, Berlin, Germany, in print.
- Kundzewicz, Z.W., Budhakooncharoen, S., Bronstert, A., Hoff, H., Lettenmaier, D., Menzel, L. & Schulze, R. (2001): Floods and droughts: coping with variability and climate change. *International Conference on Freshwater*, Bonn, Germany, http://www.water-2001.de/co_doc/Floods.pdf.
- Kustas, W.P., Stannard, D.I. & Allwine, K.J. (1996): Variability in surface energy flux partitioning during Washita '92: Resulting effects on Penman-Monteith and Priestley-Taylor parameters. *Agricultural and Forest Meteorology*, 82(1-4), 171-193.
- Lane, L.J. (1982): Distributed model for small semi-arid watersheds. *Journal Hydraulics Division*. Pro-

- ceedings of the American Society of Civil Engineers, 108, 1114-1131.
- Lane, L.J. (1983): Transmission losses: National engineering handbook. U.S. Printing Office, U.S. Department of of Agriculture, Soil Conservation Service, Washington DC, U.S.A.
- Lange, J., Leibundgut, C., Greenbaum, N. & Schick, A.P. (1999): A noncalibrated rainfall-runoff model for large, arid catchments. *Water Resources Research*, 35(7), 2161-2172.
- Lanna, A.E. & Schwarzbach, M. (1989): MODHAC - Modelo hidrológico auro-calibrável. Pós-Graduação em Recursos Hídricos e Saneamento, Publicação 21, Universidade Federal do Rio Grande do Sul, Porto Alegre, Brazil.
- Larcher, W. (1984): *Ökologie der Pflanzen auf physiologischer Grundlage*. Ulmer, Stuttgart, Germany.
- Leavesley, G.H. (1994): Modeling the effects of climate change on water resources - a review. *Climatic Change*, 28, 159-177.
- Leavesley, G.H., Lichty, B.M., Troutman, L.G. & Saindon, L.G. (1983): Precipitation-runoff modeling system: user's manual. USGS Water-Resources Investigations Report, 83-4238, USGS, Denver, U.S.A.
- Lebel, T., Braud, I. & Creutin, J.-D. (1998): A space-time rainfall disaggregation model adapted to Sahelian mesoscale convective complexes. *Water Resources Research*, 34(7), 1711-1726.
- Lebel, T.T., J.D.; D'Amato, N. (1997): Rainfall monitoring during HAPEX-Sahel. 1. General rainfall conditions and climatology. *Journal of Hydrology*, 188-189, 74-96.
- Leopold, L.B. (1994): *A view of the river*. Harvard University Press, Cambridge, UK, 298 pp.
- Lhomme, J.-P. (1997): An examination of the Priestley-Taylor equation using a convective boundary layer model. *Water Resources Research*, 33(11), 2571-2578.
- Lhomme, J.-P., Elguero, E., Chehbouni, A. & Boulet, G. (1998): Stomatal control of transpiration: Examination of Monteith's formulation of canopy resistance. *Water Resources Research*, 34(9), 2301-2308.
- Liang, X., Lettenmaier, D.P., Wood, E.F. & Burges, S.J. (1994): A simple hydrologically based model of land surface and energy fluxes for general circulation models. *Journal of Geophysical Research*, 99(D7), 14415-14428.
- Lloyd, C.R., Gash, J.H.C. & Sivakumar, M.V.K. (1992): Derivation of the aerodynamic roughness parameters for a Sahelian savanna site using the eddy correlation technique. *Boundary-Layer Meteorology*, 58, 261-271.
- Lopes, J.E.G. (1981): Simulação hidrológica: aplicações de um modelo simplificado. *Anais do IV Simpósio Brasileiro de Hidrologia e Recursos Hídricos*, Fortaleza, Brazil, Vol. 2.
- Magalhães, A.R., Filho, H.C., Garagorry, F.L., Gasques, J.G., Molion, L.C.B., Neto, M.d.S.A., Nobre, C.A., Porto, E.R. & Reboucas, O.E. (1988): The effects of climatic variations on agriculture in Northeast Brazil. In: M.L. Parry, T.R. Carter & N.T. Konjin (Eds.): *The impacts of climatic variations on agriculture*, Vol.2, Assessments in semi-arid regions. Kluwer Academic, Norwell, Mass., U.S.A., 273-382.
- Mahouf, J.F. & Noilhan, J. (1991): Comparative study of various formulations of evaporation from bare soil using in situ data. *Journal of Applied Meteorology*, 30, 1354-1365.
- Manoel Filho, J. (2000): Recarga fluvial dos aquíferos nas bacias hidrográficas receptoras da transposição do Rio São Francisco. *Anais do V Simpósio de Recursos Hídricos do Nordeste*. ABRH (Associação Brasileira de Recursos Hídricos), Natal, Vol. 1, 112-121.
- Martin, P.H. (1998): Land-surface characterization in climate models: biome-based parameter inference is not equivalent to local direct estimation. *Journal of Hydrology*, 212/213, 287-303.
- Martinez-Mena, M., Albaladejo, J. & Castillo, V.M. (1998): Factors influencing surface runoff generation in a Mediterranean semi-arid environment: Chicamo watershed, SE Spain. *Hydrological Processes*, 12, 741-754.
- Marwell Filho, P. (1995): Análise de sustentabilidade do Estado do Piauí quanto aos recursos hídricos. Projeto Áridas, Tema 7, Governo do Estado do Piauí, Secretaria de Planejamento, Grupo Recursos Hídricos, Teresina, Brazil.
- Maurer, T. (1997): Physikalisch begründete, zeitkontinuierliche Modellierung des Wassertransportes in kleinen ländlichen Einzugsgebieten. *Mitteilungen des Instituts für Hydrologie und Wasserwirtschaft*, Nr. 61, Universität Karlsruhe, Germany.
- McCabe, G.R. & Hay, L.E. (1995): Hydrological effects of hypothetical climate change in the East River basin, Colorado, USA. *Hydrological Science Journal*, 40(3), 303-318.
- MDME (1981a): Levantamento de recursos naturais - Projeto Radambrasil. Volume 21, Folhas SA 24 (Fortaleza), Ministerio das Minas e Energia, Secretaria Geral, Rio de Janeiro, Brazil.
- MDME (1981b): Levantamento de recursos naturais - Projeto Radambrasil. Volume 23, Folhas SB 24/25

- (Jaguaribe / Natal), Ministerio das Minas e Energia, Secretaria Geral, Rio de Janeiro, Brazil.
- Menabde, M., Harris, D., Seed, A., Austin, G. & Stow, D. (1997): Multiscaling properties of rainfall and bounded random cascades. *Water Resources Research*, 33, 2823-2830.
- Menabde, M., Seed, A., Harris, D. & Austin, G. (1999): Multiaffine random field model of rainfall. *Water Resources Research*, 35, 509-514.
- Menaut, J.C., Lepage, M. & Abbadie, L. (1995): Savannas, woodlands and dry forests in Africa. In: S.H. Bullock, H.A. Mooney & E. Medina (Eds.): *Seasonally dry tropical forests*. Cambridge University Press, Cambridge, UK, 64-92.
- Menzel, L. (1997): Modellierung der Evapotranspiration im System Boden-Pflanze-Atmosphäre. *Zürcher Geographische Schriften*, Band 67, Geographisches Institut, Eidgenössische Technische Hochschule, Zürich, Switzerland, 128 pp.
- Merz, B. (1996): Modellierung des Niederschlag-Abfluss-Vorgangs in kleinen Einzugsgebieten unter Berücksichtigung der natürlichen Variabilität. *Mitteilungen des Instituts für Hydrologie und Wasserwirtschaft*, Nr. 56, Universität Karlsruhe, Germany.
- Michaud, J. & Sorooshian, S. (1994): Comparison of simple versus complex distributed runoff models on a semiarid watershed. *Water Resources Research*, 30(3), 593-605.
- Milly, P.C.D. & Eagleson, P.S. (1988): Effect of storm scale on surface runoff volume. *Water Resources Research*, 24(4), 620-624.
- Milne, G. (1935): Composite units for the mapping of complex soil associations. *Trans. 3rd Int. Cong. Soil Sci.*, 1, 345-347.
- Milne, G. (1935): Some suggested units for classification and mapping, particularly for East African soils. *Soil Res.*, Berlin 4, 183-198.
- Molle, F. (1989): Perdas por evaporação e infiltração em pequenos açudes. *Serie Hydrologia*, 25, SUDENE / ORSTOM, Recife, Brazil.
- Molle, F. & Cadier, E. (1992): *Manual do pequeno açude*. SUDENE / ORSTOM, Recife, Brazil, 523 pp.
- Monteith, J.L. (1965): Evaporation and environment. *Symo. Soc. Exp. Biology*, 19, 205-234.
- Moore, I.D. & Burch, G.J. (1986): Sediment transport capacity of sheet and rill flow: application of unit stream power theory. *Water Resources Research*, 22, 1350-1360.
- Moore, R.J. & Clarke, R.T. (1981): A distribution function approach to rainfall-runoff modelling. *Water Resources Research*, 17, 1367-1382.
- Mroczkowski, M., Raper, P. & Kuczera, G. (1997): The quest for more powerful validation of conceptual catchment models. *Water Resources Research*, 33(10), 2325-2335.
- Nash, J.E. & Sutcliffe, J.V. (1970): River flow forecasting through conceptual models. Part I - A discussion of principles. *Journal of Hydrology*, 10, 282-290.
- Nash, L.L. & Gleick, P.H. (1991): Sensitivity of streamflow in the Colorado basin to climate changes. *Journal of Hydrology*, 125, 221-241.
- Niehoff, D. (2002): Modellierung des Einflusses der Landnutzung auf die Hochwasserentstehung in der Mesoskala. *Brandenburgische Umweltberichte*, Band 11. Mathematisch-Naturwissenschaftliche Fakultät, Universität Potsdam, Germany.
- Nobre, C.A. & Molion, L.B.C. (1988): The climatology of droughts and drought prediction. In: M. Parry, T.R. Carter & N.T. Konijn (Eds.): *The impact of climatic variations on agriculture*, Vol.2, Assessments in semi-arid regions. Kluwer Academic, Norwell, Mass., U.S.A., 305-324.
- Norman, J.M., Kustas, W.P. & Humes, K.S. (1995): Source approach for estimating soil and vegetation energy fluxes in observations of directional radiometric surface temperature. *Agricultural and Forest Meteorology*, 77, 263-293.
- O'Connell, P.E. & Todini, E. (1996): Modelling of rainfall, flow and mass transport in hydrological systems: an overview. *Journal of Hydrology*, 175, 3-16.
- Oliveira, C.W., de Souza, F., Yoder, R.E., da Ribeiro, R.S. & de Miranda, F.R. (1998): Estimating reference evapotranspiration in Northeastern Brazil. *ASAE Annual International Meeting*, July 1998, Orlando, Florida, U.S.A., Paper No. 982184.
- Olsson, J. (1998): Evaluation of a scaling model for temporal rainfall disaggregation. *Hydrology and Earth System Sciences*, 2, 19-30.
- Olsson, J., Niemczynowicz, J. & Berndtsson, R. (1993): Fractal analysis of high-resolution rainfall time series. *Nonlin. Proc. Geophys.*, 2, 23-29.
- Owe, M. & van der Griend, A.A. (1990): Daily surface moisture model for large scale semiarid land application with limited climate data. *Journal of Hydrology*, 121, 119-132.
- Paiva, A.E.D.B., Passerat de Silans, A.M.B., Albuquerque, D.J.S.d. & Almeida, C.d.N. (1999): Aplicação do modelo hidrológico distribuído Açumod à bacia hidrográfica do Rio Taperoá - Estado do Paraíba. *Anais do XVIII Simpósio Brasileiro de Recursos Hídricos*, ABRH (Associação Brasileira de Recursos Hídricos), 305-315.

- Parsons, A.J., Wainwright, J., Stone, P.M. & Abrahams, A.D. (1999): Transmission losses in rills on dryland hillslopes. *Hydrological Processes*, 13, 2897-2905.
- Passerat de Silans, A.M.B., Almeida, C.d.N., Albuquerque, D.J.S.d. & Paiva, A.E.D.B. (2000): Aplicação do modelo hidrológico distribuído Açumod à bacia hidrográfica do Rio do Peixe - Estado do Paraíba. *Revista Brasileira de Recursos Hídricos*, 5(3), 5-19.
- Penman, H.L. (1948): Natural evaporation from open water, bare soil and grass. *Proceedings Royal Society London*, A 193, 120-145.
- Perroll, K. & Sandström, K. (1995): Correlating landscape characteristics and infiltration - A study of surface sealing and subsoil conditions in semi-arid Botswana and Tanzania. *Geografiska Annaler Series A - Physical Geography*, 77A(3), 119-133.
- Peschke, G. (1977): Ein zweistufiges Modell der Infiltration von Regen in geschichtete Böden. *Acta hydrophysica*, 22(1), 39-48.
- Peschke, G. (1987): Soil moisture and runoff components from a physically founded approach. *Acta hydrophysica*, 31(3/4), 39-48.
- Peugeot, C., Esteves, M., Galle, S., Rajot, J.L. & Vandervaere, J.P. (1997): Runoff generation processes: results and analysis of field data collected at the East Central Supersite of the HAPEX-Sahel experiment. *Journal of Hydrology*, 188/189, 179-202.
- Pfister, J.A. & Malachek, J.C. (1986): Dietary selection by goats and sheep in a deciduous woodland of Northeastern Brazil. *Pesquisa Agropecuária Brasileira*, 18, 1037-1043.
- Pilgrim, D.H., Chapman, T.G. & Doran, D.G. (1988): Problems of rainfall-runoff modelling in arid and semiarid regions. *Hydrological Science Journal*, 33(4), 379-400.
- Pinol, J., Beven, K. & Freer, J. (1997): Modelling the hydrological response of mediterranean catchments, Prades, Catalonia. The use of distributed models as aid to hypothesis formulation. *Hydrological Processes*, 11, 1287-1306.
- Pitman, W.V. (1973): A mathematical model for generating monthly river flows from meteorological data in South Africa, Report no. 2/73, Hydrological Reserch Unit, Univ. of Witwatersrand, Johannesburg, South Africa.
- Poesen, J. & Bunte, K. (1996): The effects of rock fragments on desertification processes in Mediterranean environments. In: J. Brandt & J.B. Thornes (Eds.): *Mediterranean desertification and land use*. Wiley, London, UK, 247-270.
- Priestley, C.H.B. & Taylor, R.J. (1972): On the assessment of surface heat flux and evaporation using large-scale parameters. *Mon. Weather Rev.*, 100, 81-92.
- Puigdefabregas, J., Aguilera, C., Alonso, J.M., Brenner, A.J., Clark, S.C., Cueto, M., Delgado, L., Domingo, F., Gutierrez, L., Incoll, L.D., Lazaro, R., Nicolau, J.M., Sanchez, G., Sole, A. & Vidal, S. (1996): The Rambla Honda field site: Interactions of soil and vegetation along a catena in semi-arid SE Spain. In: J. Brandt & J.B. Thornes (Eds.): *Mediterranean desertification and land use*. Wiley, London, UK, 137-168.
- Puigdefabregas, J., del Barrio, G., Boer, M.M., Gutierrez, L. & Sole, A. (1998): Differential responses of hillslope and channel elements to rainfall events in a semi-arid area. *Geomorphology*, 23(2-4), 337-351.
- Puigdefabregas, J., Sole, A., Gutierrez, L., del Barrio, G. & Boer, M. (1999): Scales and processes of water and sediment redistribution in drylands: results from the Rambla Honda field site in Southeast Spain. *Earth-Science Reviews*, 48(1-2), 39-70.
- Ramos, R.P.L. (1975): Precipitation characteristics in the Northeast Brazil dry region. *Journal of Geophysical Research*, 80(1665-1678).
- Rana, G., Katerji, N. & Mastrorilli, M. (1997): Environmental and soil-plant parameters for modelling actual crop evapotranspiration under water stress conditions. *Ecological Modelling*, 101(2-3), 363-371.
- Raupach, M.R. (1992): Drag and drag partition on rough surfaces. *Agric. Forest Meteorol.*, 77, 263-293.
- Rawls, W.J., Ahuja, L.A., Brakensiek, D.L. & Shirmohammadi, A. (1992): Infiltration and soil water movement. In: D.R. Maidment (Ed.): *Handbook of Hydrology*. McGraw-Hill, Inc., New York, U.S.A., 5.1-5.51.
- Rawls, W.J. & Brakensiek, D.L. (1983): A procedure to predict Green Ampt infiltration parameters. *Adv. Infiltration*, *Am. Soc. Agric. Eng.*, 102-112.
- Rawls, W.J. & Brakensiek, D.L. (1985): Prediction of soil water properties for hydrologic modeling. *Watershed Management in the Eighties*, ASCE, 293-299.
- Refsgaard, J.C. (1997): Parametrisation, calibration and validation of distributed hydrological models. *Journal of Hydrology*, 198, 69-97.
- Refsgaard, J.C. & Knudsen, J. (1996): Operational validation and intercomparison of different types of hydrological models. *Water Resources Research*, 32(7), 2189-2202.

- Refsgaard, J.C. & Storm, B. (1996): Construction, calibration and validation of hydrological models. In: M.B. Abbott & J.C. Refsgaard (Eds.): Distributed hydrological modelling. Kluwer Academic, Dordrecht, 41-54.
- Reimers, W. (1990): Estimating hydrological parameters from basin characteristics for large semiarid catchments. In: M.A. Beran, M. Brilly, A. Becker & O. Bonacci (Eds.): Regionalization in Hydrology. IAHS-Publ. 191, IAHS-Press, Wallingford, UK, 187-194.
- Renard, K.G., Lane, L.J., Simanton, J.R., Emmerich, W.E., Stone, J.J., Wertz, M.A., Goodrich, D.C. & Yakowitz, D.S. (1993): Agricultural impacts in an arid environment: Walnut Gulch case study. *Hydro. Sci. Technol.*, 9(1-4), 145-190.
- Richards, L.A. (1931): Capillary conduction of liquids through porous medium. *Physics*, 1, 318-333.
- Ritchie, J.T. (1972): A model for predicting evaporation from a row crop with incomplete cover. *Water Resources Research*, 8(5), 1204-1213.
- Rockström, J., Jansson, P.E. & Barron, J. (1998): Seasonal rainfall partitioning under runoff and runoff conditions on sandy soil in Niger. On-farm measurements and water balance modelling. *Journal of Hydrology*, 210(1-4), 68-92.
- Rodriguez-Iturbe, I., Cox, D.R. & Isham, V. (1987): Some models for rainfall based on stochastic point processes. *Proc. Roy. Soc. Lond. A*, 410, 269-288.
- Rodriguez-Iturbe, I., Cox, D.R. & Isham, V. (1988): A point process model for rainfall: further developments. *Proc. Roy. Soc. Lond. A*, 417, 283-298.
- Roeckner, E., Arpe, K., Bengtsson, L., Christoph, M., Claussen, M., Dümenil, L., Esch, M., Girotta, M., Schlese, U. & Schulzweida, U. (1996): The atmospheric general circulation model ECHAM-4: model description and simulation of present-day climate. Report No. 218, Max-Planck Institute for Meteorology (MPI), Hamburg, Germany.
- Rosso, R. (1994): An introduction to spatially distributed modelling of basin response. In: R. Rosso, A. Peano, I. Becchi & G.A. Bemporad (Eds.): Advances in distributed hydrology. Water Resources Publications, Highlands Ranch, Colorado, U.S.A., 3-30.
- Russell, G. & J., M. (1990): Global river runoff calculated from a global atmospheric general circulation model. *Journal of Hydrology*, 29, 243-249.
- Rutter, A.J., Kershaw, K.A., Robins, P.C. & Morton, A.J. (1971): A predictive model of rainfall interception in forests. I. Derivation of the model from observations in a plantation of Corsican Pine. *Agric. Meteorology*, 9, 367-384.
- Rutter, A.J. & Morton, A.J. (1977): A predictive model of rainfall interception in forest. III. Sensitivity of the model to stand parameters and meteorological variables. *J. Appl. Ecology*, 14, 567-588.
- Rutter, A.J., Morton, A.J. & Robins, P.C. (1975): A predictive model of rainfall interception in forest. II. Generalisation of the model and comparison with observations in some coniferous and hardwood stands. *J. Appl. Ecology*, 12, 367-380.
- Sampaio, E.V.S.B. (1995): Overview of the Brazilian caatinga. In: S.H. Bullock, H.A. Mooney & E. Medina (Eds.): Seasonally dry tropical forests. Cambridge University Press, Cambridge, UK, 35-63.
- Sampaio, E.V.S.B., Araújo, E.L., Salcedo, I.H. & Tiessen, H. (1998): Regeneração da vegetação de caatinga após corte e queima, em Serra Talhada, PE. *Pesquisa Agropecuária Brasileira*, 33(5), 621-632.
- Sandström, K. (1995): Modelling the effects of rainfall variability on groundwater recharge in semi-arid Tanzania. *Nordic Hydrology*, 26(4/5), 313-330.
- SARA (1987): Mapa de solo. Zoneamento agrícola do Estado do Ceará, Governo do Estado do Ceará, SARA (Secretaria de agricultura e reforma agrária), Volume - II/IV, Fortaleza, Brazil.
- Saugier, B. & Katerji, N. (1991): Some plant factors controlling evapotranspiration. *Agricultural and Forest Meteorology*, 54, 263-277.
- Schertzer, D. & Lovejoy, S. (1987): Physical modeling and analysis of rain and clouds by anisotropic scaling multiplicative processes. *Journal of Geophysical Research*, 92, 9693-9714.
- Schrodin, R. (1995): Dokumentation des EM/DM-Systemes. Dokumentationen des DWD, Deutscher Wetterdienst, Abteilung Forschung, Offenbach, Germany.
- Schulla, J. (1997): Hydrologische Modellierung von Flussgebieten zur Abschätzung der Folgen von Klimaänderungen. Zürcher Geographische Schriften, Band 69, Geographisches Institut, Eidgenössische Technische Hochschule, Zürich, Switzerland, 161 pp.
- Schulze, E.D., Kelliher, F.M., Körner, C., Lloyd, J. & Leuning, R. (1994): Relationships among maximum stomatal conductance, ecosystem surface conductance, carbon assimilation rate and plant nitrogen nutrition: A global ecology scaling exercise. *Annual Reviews Ecol. Syst.*, 25, 629-660.
- Schulze, R.E. (1995): Hydrology and agrohydrology: A text to accompany the ACRU 3.00 Agrohydrological Modelling System. Report TT69/95, Water Research Commission, Pretoria, Republic of South Africa.

- Schulze, R.E. (1997): Impacts of global climate change in a hydrologically vulnerable region: challenges to South African hydrologists. *Progress in Physical Geography*, 21, 113-136.
- Schumann, A.H. & Funke, R. (1996): GIS-based components for rainfall-runoff models. In: K. Kovar & H.P. Nachtnebel (Eds.): *Application of Geographic Information Systems in hydrology and water resources management*. IAHS-Publ. 235, IAHS Press, Wallingford, UK, 477-484.
- Schumann, A.H., Funke, R. & Schultz, G.A. (2000): Application of a geographic information system for conceptual rainfall-runoff modelling. *Journal of Hydrology*, 240, 45-61.
- Scogging, H.M. & Thornes, J.B. (1979): Infiltration characteristics in a semi-arid environment. In: IAHS (Ed.): *Hydrology of Areas of Low Precipitation*. IAHS-Publ. 128, IAHS Press, Wallingford, UK, 159-168.
- SCS (1972): *Soil Conservation Service National Engineering Handbook*, Sec. 4, Hydrology, USDA, U.S.A.
- Sellers, P.J., Los, O., Tucker, C.J., Justice, C.O., Dalziel, D.A., Collatz, G.J. & Randall, D.A. (1996): A revised land surface parameterization (SiB2) for atmospheric GCMs, II, The generation of global fields of terrestrial biophysical parameters from NVDI. *Journal of Climatology*, 9, 706-737.
- Seyfried, M.S. & Wilcox, B.P. (1995): Scale and the nature of spatial variability - field examples having implications for hydrologic modeling. *Water Resources Research*, 31(1), 173-184.
- Shah, S.M.S., O'Connell & Hosking, J.M.R. (1996): Modelling the effects of spatial variability in rainfall on catchment response. 2. Experiments with distributed and lumped models. *Journal of Hydrology*, 175, 89-111.
- Sharma, K.D. & Murthy, J.S.R. (1994): Estimating transmission losses in an arid region - a realistic approach. *Journal of Arid Environments*, 27, 107-112.
- Sharma, K.D., Murthy, J.S.R. & Dhir, R.P. (1994): Streamflow routing in the Indian arid zone. *Hydrological Processes*, 8, 27-43.
- Shepard, D. (1968): A two-dimensional interpolation function for irregularly spaced data. *ACM National Conference Proceedings*, Harvard College, Cambridge, Massachusetts, U.S.A.
- Shuttleworth, W.J. (1992): Evaporation. In: D.R. Maidment (Ed.): *Handbook of hydrology*. McGraw-Hill Inc., New York, U.S.A., 5.1-5.51.
- Shuttleworth, W.J. & Gurney, R.J. (1990): The theoretical relationship between foliage temperature and canopy resistance in sparse crops. *Q.J.R. Meteorol. Soc.*, 116, 497-519.
- Shuttleworth, W.J. & Wallace, J.S. (1985): Evaporation from sparse crops-an energy combination theory. *Quart. J. Roy. Meteorol. Soc.*, 111, 839-855.
- Silva Junior, A.N.d., Paiva, A.E.D.B. & Passerat de Silans, A.M.B. (2000): Aplicação do modelo hidrológico distribuído Açumod à bacia hidrográfica do Rio Gramame - Estado do Paraíba. *Anais do V Simpósio de Recursos Hídricos do Nordeste, ABRH (Associação Brasileira de Recursos Hídricos)*, Natal, Brazil, Vol. 2, 305-315.
- Sloan, P.G., Morre, I.D., Coltharp, G.B. & Eigel, J.D. (1983): Modeling surface and subsurface stormflow on steeply-sloping forested watersheds. *Water Resources Inst. Report*, 142, University of Kentucky, Lexington.
- Smith, R.E., Goodrich, D.C., Woolhiser, D.A. & Unkirk, C.L. (1995): KINEROS - A kinematic runoff and erosion model. In: V.P. Singh (Ed.): *Computer models of watershed hydrology*. Water Resources Publications, Colorado, U.S.A., 697-732.
- Stannard, D.I. (1993): Comparison of Penman-Monteith, Shuttleworth-Wallace, and modified Priestley-Taylor evapotranspiration models for woodland vegetation in semiarid rangeland. *Water Resources Research*, 29(5), 1379-1392.
- Stewart, J.B. (1988): Modelling surface conductance of pine forest. *Agricultural and Forest Meteorology*, 43, 19-37.
- Taupin, J.D. (1997): Characterization of rainfall spatial variability at a scale smaller than 1 km in a semiarid area (region of Niamey, Niger). *Comptes Rendues de la Academie des Sciences, Serie II Fascicule A: Sciences de la Terre et des Planetes*, 325(4), 251-256.
- Taupin, J.D., Bonaf, E. & Robin, J. (1996): EPSAT-NIGER suivi à long terme. *Rapport de Campagne 1995, ORSTOM-DMN*.
- Taylor, C.M. (2000): The influence of antecedent rainfall on Sahelian surface evaporation. *Hydrological Processes*, 14, 1245-1259.
- Tessier, Y., Lovejoy, S., Hubert, P., Schertzer, D. & Pecknold, S. (1996): Multifractal analysis and modeling of rainfall and river flows and scaling, causal transfer functions. *Journal of Geophysical Research*, 101, 26427-26440.
- Tessier, Y., Lovejoy, S. & Schertzer, D. (1993): Universal multifractals: theory and observations for rain and clouds. *Journal of Applied Meteorology*, 32, 223-250.
- Thornes, J.B. (1996): Introduction. In: C.J. Brandt & J.B. Thornes (Eds.): *Mediterranean desertification*

- and land use. John Wiley & Sons, Chichester, UK, 1-12.
- Thorsen, M., Refsgaard, J.C., Hansen, S., Pebesma, E., Jensen, J.B. & Kleesculte, S. (2001): Assessment of uncertainty in simulation of nitrate leaching to aquifers at the catchment scale. *Journal of Hydrology*, 242, 210-227.
- Tiessen, H., Feller, C., Sampaio, E.V.S.B. & Garin, P. (1998): Carbon sequestration and turnover in semi-arid savannas and dry forest. *Climate Change*, 40, 105-117.
- Todini, E. (1996): The ARNO rainfall-runoff model. *Journal of Hydrology*, 175(339-382).
- Tomasella, J. & Hodnett, M.G. (1997): Estimating unsaturated hydraulic conductivity of Brazilian soils using soil-water retention data. *Soil Science*, 162(10), 703-712.
- Uhlenbrook, S. (1999): Untersuchung und Modellierung der Abflussbildung in einem mesoskaligen Einzugsgebiet. *Freiburger Schriften zur Hydrologie*, Band 10, Institut für Hydrologie, Universität Freiburg, Germany.
- UNESCO (1979): Map of the world distribution of arid regions. MAB Technical Notes, 7, UNESCO, Paris, France.
- USGS (1999): Global 30 Arc Second Elevation Data Set, USGS Eros Data Center, <http://edcdaac.usgs.gov/topo30/topo30.html>.
- Uvo, C. & Berndtsson, R. (1996): Regionalization and spatial properties of Ceará state rainfall in northeast Brazil. *Journal of Geophysical Research*, 101(D2), 4221-4233.
- Valentin, C. & Bresson, L.M. (1992): Morphology, genesis and classification of surface crusts in loamy and sandy soils. *Geoderma*, 55(3-4), 225-245.
- Valentin, C. & Casenave, A. (1992): Infiltration into sealed soils as influenced by gravel cover. *Soil Sci. Soc. Am. J.*, 56, 1667-1673.
- Valentini, R., Scarascia Mugnozza, G.E., De Angelis, P. & Bimbi, R. (1991): An experimental test of the eddy correlation technique over a mediterranean macchia canopy. *Plant, Cell and Environment*, 14, 987-994.
- Van Genuchten, M.T. (1980): A closed-form equation for predicting the hydraulic conductivity of unsaturated soils. *Soil Sci. Soc. Am. J.*, 44, 892-898.
- Vertessy, R.A., Hatton, T.J., O'Shaughnessy, P.J.O. & Jayasuriya, M.D.A. (1993): Predicting water yield from a mountain ash forest catchment using a terrain analysis based catchment model. *Journal of Hydrology*, 150, 665-700.
- Vörösmarty, C.J., Federer, C.A. & Schloss, A.L. (1998): Potential evaporation functions compared on US watersheds: Possible implications for global-scale water balance and terrestrial ecosystem modeling. *Journal of Hydrology*, 207, 147-169.
- Walker, B.H. & Langridge, J.L. (1996): Modelling plant and soil water dynamics in semi-arid ecosystems with limited site data. *Ecological Modelling*, 87, 153-167.
- Wallace, J.S. & Holwill, C.J. (1997): Soil evaporation from tiger-bush in Niger. *Journal of Hydrology*, 188-189, 426-442.
- Walter, H. & Breckle, S.-W. (1991): *Spezielle Ökologie der tropischen und subtropischen Zonen. Ökologie der Erde, Band 2, UTB für Wissenschaft, Große Reihe, G. Fischer, Stuttgart, Germany.*
- Walters, M.O. (1990): Transmission losses in arid regions. *J. Hydr. Engineering*, 116(1), 129-138.
- Wang, Q.X. & Takahashi, H. (1999): A land surface water deficit model for an arid and semiarid region: Impact of desertification on the water deficit status in the Loess Plateau, China. *Journal of Climate*, 12(1), 244-257.
- Werner, P.C. & Gerstengarbe, F.-W. (1997): Proposal for the development of climate scenarios. *Climate Research*, 8, 171-182.
- Werner, P.C. & Gerstengarbe, F.-W. (2002): The climate of Piauí and Ceará. In: T. Gaiser, M.S. Krol, H. Frischkorn & J.C. Araújo (Eds.): *Global change and regional impacts: Water availability and vulnerability of ecosystems and society in the semi-arid Northeast of Brazil*. Margraf Verlag, Springer-Verlag, Berlin, in print.
- Western, A.W., Grayson, R.B., Blöschl, G., Willgoose, G.R. & McMahon, T.A. (1999): Observed spatial organization of soil moisture and its relation to terrain indices. *Water Resources Research*, 35(3), 797-810.
- Wheater, H.S., Woods Ballard, B. & Jolley, T.J. (1997): An integrated model of arid zone water resources. In: D. Rosbjerg, N.-E. Boutayeb, A. Gustard, Z.W. Kundzewicz & P.F. Rasmussen: *Sustainability of water resources under increasing uncertainty*. IAHS-Publ. 240, IAHS Press, Wallingford, UK, 395-405.
- Wilby, R. & Wigley, T.M.L. (1997): Downscaling general circulation model output: a review of methods and limitations. *Progress in Physical Geography*, 29, 321-344.
- Wilcox, B.P., Newman, B.D., Brandes, D., Davenport, D.W. & Reid, K. (1997): Runoff from a semiarid ponderosa pine hillslope in New Mexico. *Water Resources Research*, 33(10), 2301-2314.
- Williams, J. & Bonell, M. (1988): The influence of scale of measurement on the spatial and temporal

- variability of the Philip infiltration parameters - an experimental study in an Australian savannah woodland. *Journal of Hydrology*, 104, 33-51.
- Williams, J.R., Jones, C.A. & Dyke, P.T. (1984): The EPIC model and its application. In: ICRISAT-IBSNAT-SYS (Ed.): Proc. ICRISAT-IBSNAT-SYS Symp. on minimum data sets for agrotechnology transfer, Hyderabad, India, March 1983, 111-121.
- Wood, E.F., Lettenmaier, D.P. & Zartarian, V.G. (1992): A land-surface hydrology parameterization with subgrid variability for general circulation models. *Journal of Geophysical Research*, 97(D3), 2717-2728.
- Wood, E.F., Sivapalan, K.J., Beven, K.J. & Band, L. (1988): Effects of spatial variability and scale with implications to hydrologic modeling. *Journal of Hydrology*, 102, 29-47.
- Woolhiser, D.A., Goodrich, D.C., Emmerich, W.E. & Keefer, T.O. (1990): KINEROS, a kinematic runoff and erosion model: documentation and user manual. Agricultural Research Service, ARS-77, USDA.
- Xu, C.-Y. (1998): From GCMs to river flow - A review of downscaling methods and hydrologic modeling approaches. Report Series A, No. 54, Uppsala University, Department of Earth Sciences, Hydrology, Uppsala, Sweden.
- Yair, A. & Lavee, H. (1985): Runoff generation in arid and semi-arid zones. In: M.G. Anderson & T.P. Burt (Eds.): *Hydrological Forecasting*. John Wiley, New York, U.S.A., 183-220.
- Ye, W., Bates, B.C., Viney, N.R., Sivapalan, M. & Jakeman, A.J. (1997): Performance of conceptual rainfall-runoff models in low-yielding ephemeral catchments. *Water Resources Research*, 33(1), 153-166.
- Zhao, R.-J. (1992): The Xinanjiang model applied in China. *Journal of Hydrology*, 134, 371-381.
- Zhu, T.X., Band, L.E. & Vertessy, R.A. (1999): Continuous modeling of intermittent stormflows on a semi-arid agricultural catchment. *Journal of Hydrology*, 226, 11-29.
- Zhu, T.X., Cai, Q.G. & Zeng, B.Q. (1997): Runoff generation on a semi-arid agricultural catchment: field and experimental studies. *Journal of Hydrology*, 196, 99-118.

Publications by the Author of this Study

- Becker, A., Güntner, A. & Katzenmaier, D. (1999): Required integrated approach to understand runoff generation and flow path dynamics in catchments. In: C. Leibundgut, J. McDonnell & G. Schultz (Eds.): *Integrated methods in catchment hydrology*. IAHS-Publ. 258, IAHS Press, Wallingford, UK, 3-9.
- Bronstert, A., Güntner, A., Jaeger, A., Krol, M. & Krywkow, J. (1999): Großräumige hydrologische Parametrisierung und Modellierung als Teil der integrierten Modellierung. In: Fohrer, N. & Döll, P. (Eds.): *Modellierung des Wasser- und Stofftransports in großen Einzugsgebieten*. Kassel University Press, Kassel, Germany, 31-40.
- Bronstert, A., Jaeger, A., Güntner, A., Hauschild, M., Döll, P. & Krol, M. (2000): Integrated modelling of water availability and water use in the semi-arid Northeast of Brazil. *Physics and Chemistry of the Earth*, 25(3), 227-232.
- Güntner, A. & Bronstert, A. (1999): A large-scale hydrological model for the semi-arid tropics of northeastern Brazil. In: HiBAm (Ed.): *Manaus'99 - Hydrological and Geochemical Processes in Large Scale River Basins, Manaus, Brazil*, CD-ROM.
- Güntner, A. & Bronstert, A. (2001): Modelling the effects of climate change on water availability in the semi-arid North-East of Brazil. In: J. Suttmöller & E. Raschke (Eds.): *Modellierung in meso- bis makroskaligen Flußeinzugsgebieten*. GKSS Forschungszentrum, Geesthacht, Germany, 76-85.
- Güntner, A. & Bronstert, A. (2001): WAVES - Water Availability, Vulnerability of Ecosystems and Society in the Northeast of Brazil - Sub-project large-scale hydrological modelling. In: M.E. McClain & M. Zalewski (Eds.): *Ecohydrology - Hydrological and geochemical processes in large scale river basins*. IHP-V, Technical Documents in Hydrology, UNESCO, Paris, p. 26.
- Güntner, A. & Bronstert, A. (2002): Large-scale hydrological modelling of a semi-arid environment: model development, validation and application. In: T. Gaiser, M.S. Krol, H. Frischkorn & J.C. Araújo (Eds.): *Global change and regional impacts: Water availability and vulnerability of ecosystems and society in the semi-arid Northeast of Brazil*. Springer-Verlag, Berlin, Germany, in print.
- Güntner, A., Bronstert, A. & Gaiser, T. (1999): Parameterization of lateral hydrological processes based on geomorphologic units. IUGG 99, XXII General Assembly of the International Union of Geodesy and Geophysics, Birmingham, Workshop HW4 Regionalization of parameters of hydrological and atmospheric land surface models, Book of abstract II, p. B 317.
- Güntner, A., Olsson, J., Calver, A. & Gannon, B. (2001): Cascade-based disaggregation of continuous rainfall time series: the influence of climate. *Hydrology and Earth System Sciences*, 5(2), 145-164.
- Güntner, A., Seibert, J. & Uhlenbrook, S. (2000): Modeling spatial patterns of saturated areas - an evaluation of different terrain indices. *Eos Trans. AGU*, 81 (48), Fall Meet. Suppl., Abstract H11B-02.
- Güntner, A., Uhlenbrook, S., Seibert, J. & Leibundgut, C. (1999): Estimation of saturation excess overland flow areas - comparison of topographic index calculations with field mapping. In: B. Diekkrüger, M. J. Kirkby & U. Schröder: *Regionalization in Hydrology*, IAHS Publ. 254, IAHS Press, Wallingford, 203-210.
- Güntner, A., Uhlenbrook, S., Seibert, J. & Leibundgut, C. (1999): Multi-criterial validation of TOPMODEL in a mountainous catchment. *Hydrological Processes*, 13, 1603-1620.

Appendix

Table A.1 Characteristics of gauging stations with available discharge data in Ceará (location see numbers in Fig. 2.3); (A1: Basin area according to CEARÁ (1992), A2: Basin area as derived from DTM and maps and as shown in Fig. 2.3; A3: Basin area according to upstream municipalites, n: number of complete years with data in the period 1960-98).

Number	Name	River	A1 (km ²)	A2 (km ²)	A3 (km ²)	n	Period
1	Arneiroz	Jaguaribe	6036	5730	4880	14	60-61, 65-71, 76-80
2	Carius	Carius	5327	6493	-	10	84, 87-90, 92-96
3	Iguatu	Jaguaribe	19250	20615	20446	31	60-63, 67-82, 84-93, 96
4	Podimirim	Rch. dos Porcos	3612	3639	3746	17	78-79, 82-96
5	Sítio Lapinha	Salgado	1903	1875	2335	12	85-96
6	Lavras da Mangabeira	Salgado	8804	8521	-	10	82, 88-96
7	Ícó	Salgado	11891	11794	9449	30	60-62, 64-77, 79, 82-92, 96
8	Senador Pompeu	Banabuiú	4843	4183	5007	22	60-61, 74-92, 95
9	Quixeramobim	Quixeramobim	7688	6979	-	13	82-86, 88-93, 95-96
10	Morada Nova	Banabuiú	18271	17558	17492	30	62-63, 65-72, 75-80, 82-96
11	Jaguaribe	Jaguaribe	38572	39415	38482	13	82-84, 87-96
12	Peixe Gordo	Jaguaribe	47308	48111	50330	21	62-82
13	Cristais	Pirangi	2037	1858	-	26	70-92, 94-97
14	Chorozinho	Choro	3726	4309	3019	10	82-83, 86-93
15	Umarituba Nova	São Gonçalo	440	407	-	11	85-92, 95-97
16	São Luis	Curu	7330	6190	7370	28	68-93, 95, 97
17	Amontada	Aracatiaçu	2790	2773	-	26	71-92, 94-97
18	Granja	Coreaú	3786	3308	-	11	82-92
19	Cajazeiras	Acaraú	1530	2003	-	31	63-77, 80, 82-91, 93-97
20	Groeiras	Groeiras	2698	2740	-	28	69-82, 84-97
21	Ararius	Jaibas	561	682	-	8	85, 88-94
22	Sobral	Acaraú	11210	11261	-	7	60-61, 82-83, 85, 87-88
23	Croatá	Macambira	1050	905	534	15	63, 65-75, 87, 89-90

Table A.2 Parameters of large reservoirs in Ceará (storage capacity $>50 \cdot 10^6 \text{m}^3$) with explicit representation in WASA. (Nbr: For reservoirs with observation data, reservoir number in Fig. 2.6. Year: year of inauguration (u.c.: under construction). n: number of complete years with data in the period 1960-1998. A1: Catchment area according to CEARÁ (1992) or ARAÚJO (2000). A2: Catchment area in WASA as derived from DTM and maps and as shown in Fig. 2.6. For explanations of other variables, see Chapter 4.2.7.)

Nbr	Name of reservoir	Location (Municipality)	Year	n	V_{max}	Q_{90}	f_Q	V_{al}	V_{min}	A1	A2	c_{LR}	d_{LR}
				-	10^6m^3	m s^{-1}	-	10^6m^3	10^6m^3	km^2	km^2	-	-
1	Acara Mirim	Massapê	1907	34	52	0.9	0.9	20.1	9.5	460	639	76.22	0.59
-	Angicos	Coreaú	?	0	56	0.7	0.9	0.0	0.0	-	313	74.95	0.70
2	Araras	Varjota	1958	28	891	9.0	0.8	170.4	17.5	3520	3265	102.98	0.63
-	Atalho	Brejo Santo	1991	0	108	0.6	0.9	0.0	0.0	2064	1586	82.39	0.53
3	Ayres de Sousa	Sobral	1936	31	104	2.1	0.9	32.9	9.0	1100	1213	85.60	0.57
4	Banabuiú	Banabuiú	1966	20	1800	12.9	0.8	243.6	12.0	13500	13727	7.76	0.97
-	Barra Velha	Independencia	u.c.	0	100	0.5	0.9	0.0	0.0	-	735	68.02	0.74
-	Canoas	Assaré	u.c.	0	69	0.2	0.9	0.0	0.0	-	1027	22.06	0.62
-	Carnaubal	Crateús	?	0	88	0.7	0.9	0.0	0.0	2061	2449	74.95	0.70
-	Castanhão	Alto Santo	u.c.	0	4451	21.8	0.9	0.0	0.0	-	44704	74.95	0.70
-	Castro	Itapiúna	?	0	64	0.6	0.9	0.0	0.0	360	390	40.27	0.74
5	Caxitoré	Pentecoste	1962	20	202	2.3	0.9	51.3	7.5	1450	1150	190.33	0.60
6	Cedro	Quixadá	1906	31	126	0.5	0.9	10.2	1.0	224	222	0.09	0.90
-	Cipoada	Morada Nova	1800	0	86	0.2	0.9	0.0	0.0	356	565	74.95	0.70
7	Edson Queiroz	Santa Quitéria	1987	8	251	0.2	0.8	38.0	6.0	1765	1837	88.97	0.63
-	Favelas	Tauá	1988	0	30	0.3	0.9	0.0	0.0	678	640	74.95	0.70
-	Flor do Campo	Novo Oriente	u.c.	0	111	1.0	0.9	0.0	0.0	-	475	98.51	0.62
-	Fogareiro	Quixeramobim	1996	0	119	0.8	0.9	0.0	0.0	-	4871	63.70	0.70
8	Forquilha	Forquilha	1921	17	50	0.3	0.9	17.5	8.0	176	203	80.41	0.62
-	Frios	Umirim	1989	0	33	0.6	0.9	7.2	0.9	240	301	74.95	0.70
-	Gangorra	Granja	1995	0	63	0.5	0.9	0.0	0.0	-	153	100.53	0.56
9	General Sampaio	General Sampaio	1935	33	322	3.2	0.8	63.4	8.5	1720	1702	57.81	0.70
-	Jaburu I	Tianguá	?	0	210	5.0	0.9	29.1	0.0	-	902	74.95	0.70
-	Jaburu II	Independência	?	0	128	0.6	0.9	17.1	0.0	-	659	74.95	0.70
10	Lima Campos	Icó	1932	24	64	0.5	0.9	6.1	2.5	340	486	99.09	1.00
11	Orós	Orós	1961	18	1956	20.4	0.8	656.7	30.0	25000	24597	52.22	0.78
12	Pacajus	Pacajus	?	6	240	2.8	0.8	0.0	0.0	-	4636	74.95	0.70
13	Pacoti	Horizonte	?	6	380	2.9	0.8	0.0	0.0	1110	1110	74.95	0.70
14	Patu	Senador Pompeu	1987	10	72	0.7	0.9	12.4	3.4	1016	1061	44.47	0.70
15	Pedras Brancas	Banabuiú	1978	20	434	3.2	0.8	68.0	12.8	1787	2092	49.83	0.82
16	Pereira de Miranda	Pentecoste	1965	27	396	4.3	0.8	93.9	18.5	2840	3022	141.76	0.63
17	Poço da Pedra	Campos Sales	1958	17	50	0.5	0.9	8.7	2.3	800	970	60.40	0.66
18	Poço do Barro	Morada Nova	1956	22	52	0.6	0.9	7.4	1.0	356	536	72.39	0.68
19	Pompeu Sobrinho	Quixadá/Choro	1934	14	143	0.1	0.9	63.6	16.0	322	413	80.43	0.65
20	Quixeramobim	Quixeramobim	1960	21	54	1.8	0.9	11.0	0.5	8300	6979	62.89	0.72
21	Riacho do Sangue	Solonópole	1918	24	61	0.6	0.9	21.7	5.0	1209	1487	53.47	0.70
-	Serafim Dias	Mombaça	1985	0	43	8.1	0.9	3.0	0.4	1533	1060	74.95	0.70
-	Sítios Novos	Caucaia	u.c.	0	123	1.1	0.9	0.0	0.0	-	508	187.04	0.62
-	Trussu	Iguatu	1996	0	261	1.6	0.9	0.0	0.0	-	1189	74.56	0.63
-	Tucunduba	Senador Sá	1919	0	40	1.3	0.9	30.0	16.0	335	443	74.95	0.70
22	Várzea do Boi	Tauá	1954	16	52	0.2	0.9	5.9	1.2	1209	1401	29.35	0.91



Fig. A.1 Landscape units in Ceará (based on JACOMINE ET AL., 1973). (The same colour may be attributed to different landscape units in the figure, blue: rivers and reservoirs).

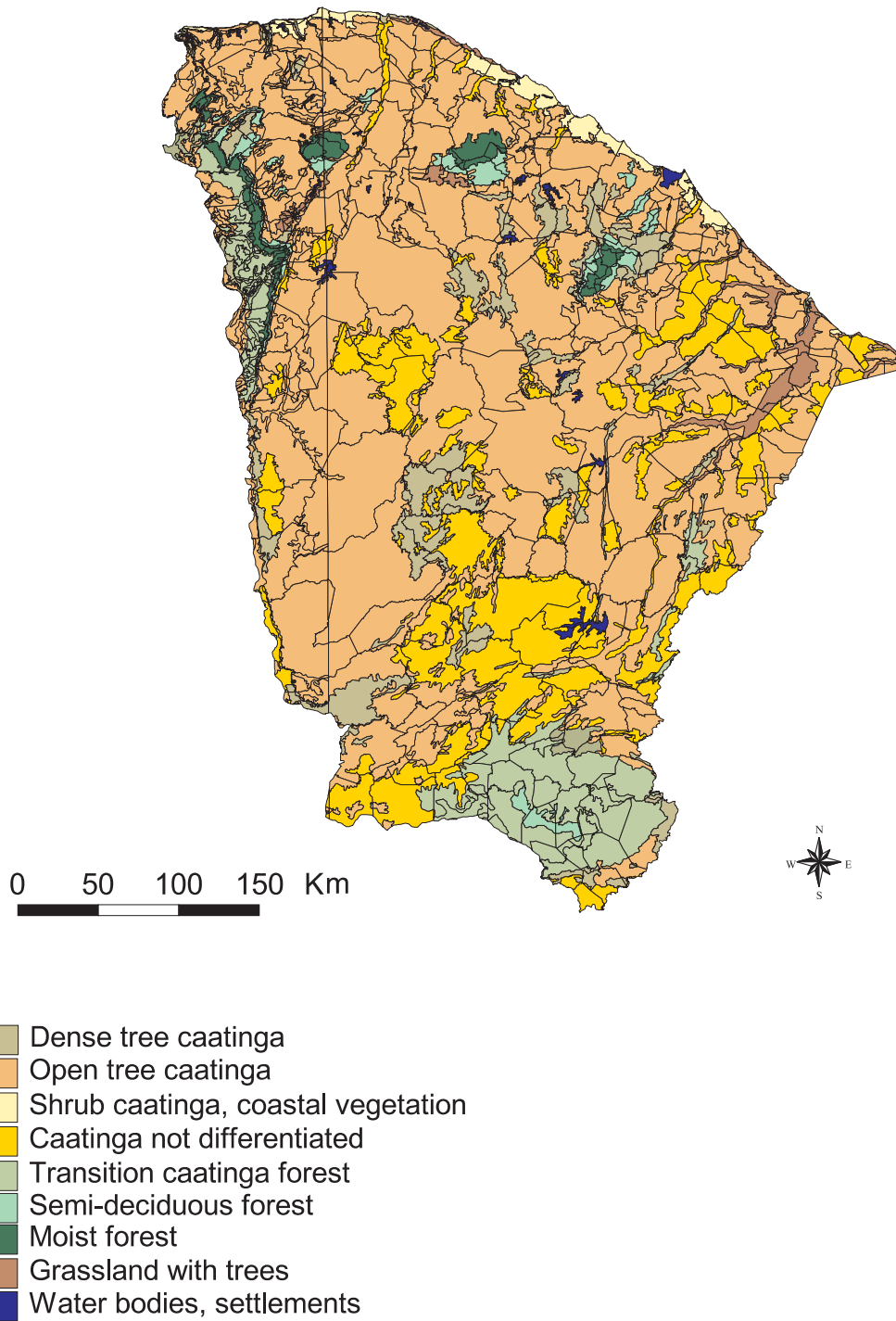


Fig. A.2 Spatial pattern of natural vegetation in Ceará (reclassification based on MDME (1981A,B)), see also Chapter 2.1.6.1, Chapter 4.3.1 and Table 4.3)

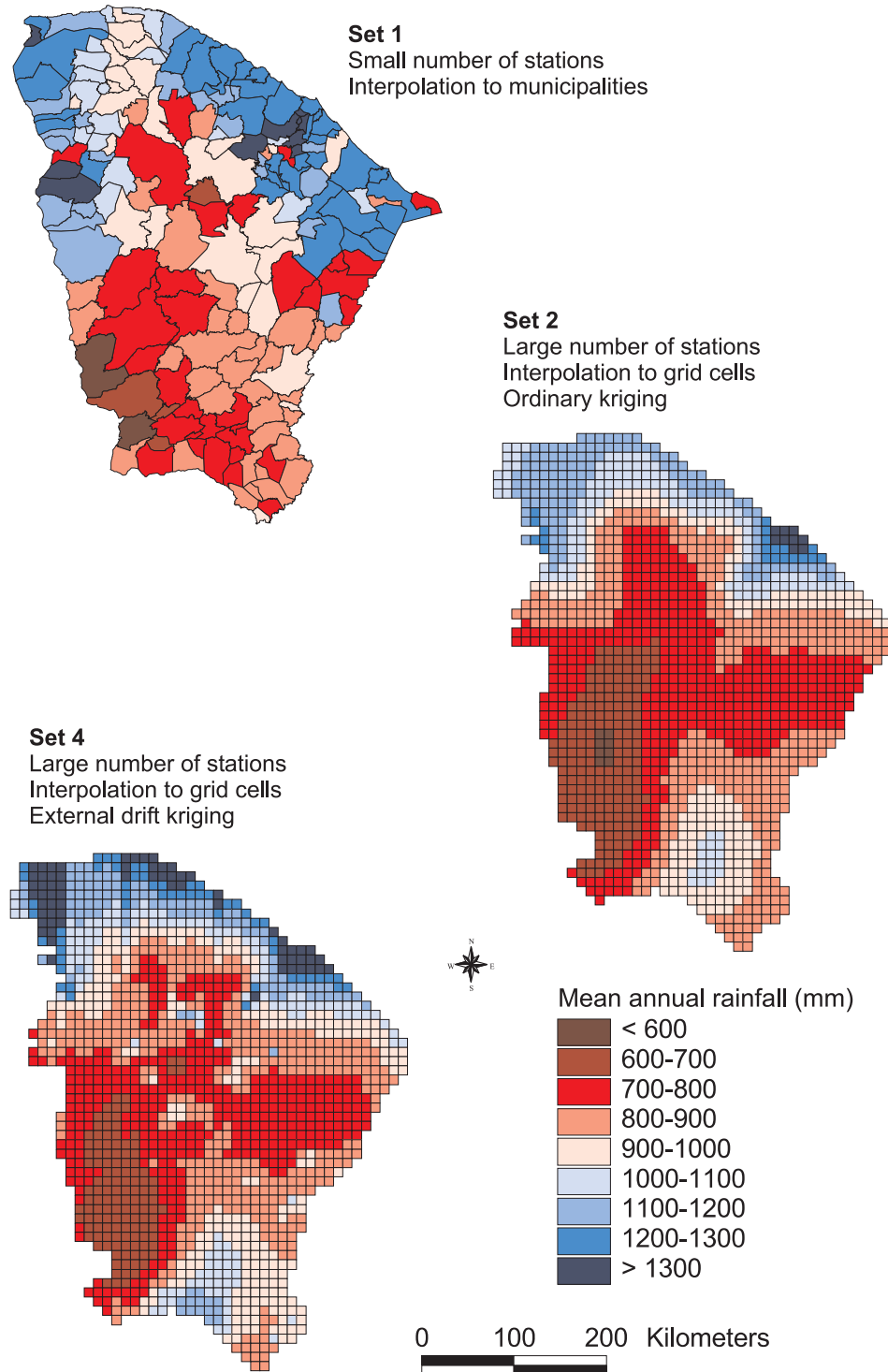


Fig. A.3 Spatial pattern of mean annual precipitation, period 1960-1998, for the State of Ceará, according to different rainfall data sets used in this study (see Chapter 2.1.6.2 for details).

PIK Report-Reference:

- No. 1 3. Deutsche Klimatagung, Potsdam 11.-14. April 1994
Tagungsband der Vorträge und Poster (April 1994)
- No. 2 Extremer Nordsommer '92
Meteorologische Ausprägung, Wirkungen auf naturnahe und vom Menschen beeinflusste Ökosysteme, gesellschaftliche Perzeption und situationsbezogene politisch-administrative bzw. individuelle Maßnahmen (Vol. 1 - Vol. 4)
H.-J. Schellnhuber, W. Enke, M. Flechsig (Mai 1994)
- No. 3 Using Plant Functional Types in a Global Vegetation Model
W. Cramer (September 1994)
- No. 4 Interannual variability of Central European climate parameters and their relation to the large-scale circulation
P. C. Werner (Oktober 1994)
- No. 5 Coupling Global Models of Vegetation Structure and Ecosystem Processes - An Example from Arctic and Boreal Ecosystems
M. Plöchl, W. Cramer (Oktober 1994)
- No. 6 The use of a European forest model in North America: A study of ecosystem response to climate gradients
H. Bugmann, A. Solomon (Mai 1995)
- No. 7 A comparison of forest gap models: Model structure and behaviour
H. Bugmann, Y. Xiaodong, M. T. Sykes, Ph. Martin, M. Lindner, P. V. Desanker, S. G. Cumming (Mai 1995)
- No. 8 Simulating forest dynamics in complex topography using gridded climatic data
H. Bugmann, A. Fischlin (Mai 1995)
- No. 9 Application of two forest succession models at sites in Northeast Germany
P. Lasch, M. Lindner (Juni 1995)
- No. 10 Application of a forest succession model to a continentality gradient through Central Europe
M. Lindner, P. Lasch, W. Cramer (Juni 1995)
- No. 11 Possible Impacts of global warming on tundra and boreal forest ecosystems - Comparison of some biogeochemical models
M. Plöchl, W. Cramer (Juni 1995)
- No. 12 Wirkung von Klimaveränderungen auf Waldökosysteme
P. Lasch, M. Lindner (August 1995)
- No. 13 MOSES - Modellierung und Simulation ökologischer Systeme - Eine Sprachbeschreibung mit Anwendungsbeispielen
V. Wenzel, M. Kücken, M. Flechsig (Dezember 1995)
- No. 14 TOYS - Materials to the Brandenburg biosphere model / GAIA
Part 1 - Simple models of the "Climate + Biosphere" system
Yu. Svirezhev (ed.), A. Block, W. v. Bloh, V. Brovkin, A. Ganopolski, V. Petoukhov, V. Razzhevaikin (Januar 1996)
- No. 15 Änderung von Hochwassercharakteristiken im Zusammenhang mit Klimaänderungen - Stand der Forschung
A. Bronstert (April 1996)
- No. 16 Entwicklung eines Instruments zur Unterstützung der klimapolitischen Entscheidungsfindung
M. Leimbach (Mai 1996)
- No. 17 Hochwasser in Deutschland unter Aspekten globaler Veränderungen - Bericht über das DFG-Rundgespräch am 9. Oktober 1995 in Potsdam
A. Bronstert (ed.) (Juni 1996)
- No. 18 Integrated modelling of hydrology and water quality in mesoscale watersheds
V. Krysanova, D.-I. Müller-Wohlfeil, A. Becker (Juli 1996)
- No. 19 Identification of vulnerable subregions in the Elbe drainage basin under global change impact
V. Krysanova, D.-I. Müller-Wohlfeil, W. Cramer, A. Becker (Juli 1996)
- No. 20 Simulation of soil moisture patterns using a topography-based model at different scales
D.-I. Müller-Wohlfeil, W. Lahmer, W. Cramer, V. Krysanova (Juli 1996)
- No. 21 International relations and global climate change
D. Sprinz, U. Luterbacher (1st ed. July, 2nd ed. December 1996)
- No. 22 Modelling the possible impact of climate change on broad-scale vegetation structure - examples from Northern Europe
W. Cramer (August 1996)

- No. 23 A method to estimate the statistical security for cluster separation
F.-W. Gerstengarbe, P.C. Werner (Oktober 1996)
- No. 24 Improving the behaviour of forest gap models along drought gradients
H. Bugmann, W. Cramer (Januar 1997)
- No. 25 The development of climate scenarios
P.C. Werner, F.-W. Gerstengarbe (Januar 1997)
- No. 26 On the Influence of Southern Hemisphere Winds on North Atlantic Deep Water Flow
S. Rahmstorf, M. H. England (Januar 1977)
- No. 27 Integrated systems analysis at PIK: A brief epistemology
A. Bronstert, V. Brovkin, M. Krol, M. Lüdeke, G. Petschel-Held, Yu. Svirezhev, V. Wenzel (März 1997)
- No. 28 Implementing carbon mitigation measures in the forestry sector - A review
M. Lindner (Mai 1997)
- No. 29 Implementation of a Parallel Version of a Regional Climate Model
M. Kücken, U. Schättler (Oktober 1997)
- No. 30 Comparing global models of terrestrial net primary productivity (NPP): Overview and key results
W. Cramer, D. W. Kicklighter, A. Bondeau, B. Moore III, G. Churkina, A. Ruimy, A. Schloss, participants of "Potsdam '95" (Oktober 1997)
- No. 31 Comparing global models of terrestrial net primary productivity (NPP): Analysis of the seasonal behaviour of NPP, LAI, FPAR along climatic gradients across ecotones
A. Bondeau, J. Kaduk, D. W. Kicklighter, participants of "Potsdam '95" (Oktober 1997)
- No. 32 Evaluation of the physiologically-based forest growth model FORSANA
R. Grote, M. Erhard, F. Suckow (November 1997)
- No. 33 Modelling the Global Carbon Cycle for the Past and Future Evolution of the Earth System
S. Franck, K. Kossacki, Ch. Bounama (Dezember 1997)
- No. 34 Simulation of the global bio-geophysical interactions during the Last Glacial Maximum
C. Kubatzki, M. Claussen (Januar 1998)
- No. 35 CLIMBER-2: A climate system model of intermediate complexity. Part I: Model description and performance for present climate
V. Petoukhov, A. Ganopolski, V. Brovkin, M. Claussen, A. Eliseev, C. Kubatzki, S. Rahmstorf (Februar 1998)
- No. 36 Geocybernetics: Controlling a rather complex dynamical system under uncertainty
H.-J. Schellnhuber, J. Kropp (Februar 1998)
- No. 37 Untersuchung der Auswirkungen erhöhter atmosphärischer CO₂-Konzentrationen auf Weizenbestände des Free-Air Carbon dioxide Enrichment (FACE) - Experimentes Maricopa (USA)
Th. Kartschall, S. Grossman, P. Michaelis, F. Wechsung, J. Gräfe, K. Waloszczyk, G. Wechsung, E. Blum, M. Blum (Februar 1998)
- No. 38 Die Berücksichtigung natürlicher Störungen in der Vegetationsdynamik verschiedener Klimagebiete
K. Thonicke (Februar 1998)
- No. 39 Decadal Variability of the Thermohaline Ocean Circulation
S. Rahmstorf (März 1998)
- No. 40 SANA-Project results and PIK contributions
K. Bellmann, M. Erhard, M. Flechsig, R. Grote, F. Suckow (März 1998)
- No. 41 Umwelt und Sicherheit: Die Rolle von Umweltschwellenwerten in der empirisch-quantitativen Modellierung
D. F. Sprinz (März 1998)
- No. 42 Reversing Course: Germany's Response to the Challenge of Transboundary Air Pollution
D. F. Sprinz, A. Wahl (März 1998)
- No. 43 Modellierung des Wasser- und Stofftransportes in großen Einzugsgebieten. Zusammenstellung der Beiträge des Workshops am 15. Dezember 1997 in Potsdam
A. Bronstert, V. Krysanova, A. Schröder, A. Becker, H.-R. Bork (eds.) (April 1998)
- No. 44 Capabilities and Limitations of Physically Based Hydrological Modelling on the Hillslope Scale
A. Bronstert (April 1998)
- No. 45 Sensitivity Analysis of a Forest Gap Model Concerning Current and Future Climate Variability
P. Lasch, F. Suckow, G. Bürger, M. Lindner (Juli 1998)

- No. 46 Wirkung von Klimaveränderungen in mitteleuropäischen Wirtschaftswäldern
M. Lindner (Juli 1998)
- No. 47 SPRINT-S: A Parallelization Tool for Experiments with Simulation Models
M. Flechsig (Juli 1998)
- No. 48 The Odra/Oder Flood in Summer 1997: Proceedings of the European Expert Meeting in
Potsdam, 18 May 1998
A. Bronstert, A. Ghazi, J. Hladny, Z. Kundzewicz, L. Menzel (eds.) (September 1998)
- No. 49 Struktur, Aufbau und statistische Programmbibliothek der meteorologischen Datenbank am
Potsdam-Institut für Klimafolgenforschung
H. Österle, J. Glauer, M. Denhard (Januar 1999)
- No. 50 The complete non-hierarchical cluster analysis
F.-W. Gerstengarbe, P. C. Werner (Januar 1999)
- No. 51 Struktur der Amplitudengleichung des Klimas
A. Hauschild (April 1999)
- No. 52 Measuring the Effectiveness of International Environmental Regimes
C. Helm, D. F. Sprinz (Mai 1999)
- No. 53 Untersuchung der Auswirkungen erhöhter atmosphärischer CO₂-Konzentrationen innerhalb des
Free-Air Carbon Dioxide Enrichment-Experimentes: Ableitung allgemeiner Modellösungen
Th. Kartschall, J. Gräfe, P. Michaelis, K. Waloszczyk, S. Grossman-Clarke (Juni 1999)
- No. 54 Flächenhafte Modellierung der Evapotranspiration mit TRAIN
L. Menzel (August 1999)
- No. 55 Dry atmosphere asymptotics
N. Botta, R. Klein, A. Almgren (September 1999)
- No. 56 Wachstum von Kiefern-Ökosystemen in Abhängigkeit von Klima und Stoffeintrag - Eine
regionale Fallstudie auf Landschaftsebene
M. Erhard (Dezember 1999)
- No. 57 Response of a River Catchment to Climatic Change: Application of Expanded Downscaling to
Northern Germany
D.-I. Müller-Wohlfel, G. Bürger, W. Lahmer (Januar 2000)
- No. 58 Der "Index of Sustainable Economic Welfare" und die Neuen Bundesländer in der
Übergangsphase
V. Wenzel, N. Herrmann (Februar 2000)
- No. 59 Weather Impacts on Natural, Social and Economic Systems (WISE, ENV4-CT97-0448)
German report
M. Flechsig, K. Gerlinger, N. Herrmann, R. J. T. Klein, M. Schneider, H. Sterr, H.-J. Schellnhuber
(Mai 2000)
- No. 60 The Need for De-Aliasing in a Chebyshev Pseudo-Spectral Method
M. Uhlmann (Juni 2000)
- No. 61 National and Regional Climate Change Impact Assessments in the Forestry Sector
- Workshop Summary and Abstracts of Oral and Poster Presentations
M. Lindner (ed.) (Juli 2000)
- No. 62 Bewertung ausgewählter Waldfunktionen unter Klimaänderung in Brandenburg
A. Wenzel (August 2000)
- No. 63 Eine Methode zur Validierung von Klimamodellen für die Klimawirkungsforschung hinsichtlich
der Wiedergabe extremer Ereignisse
U. Böhm (September 2000)
- No. 64 Die Wirkung von erhöhten atmosphärischen CO₂-Konzentrationen auf die Transpiration eines
Weizenbestandes unter Berücksichtigung von Wasser- und Stickstofflimitierung
S. Grossman-Clarke (September 2000)
- No. 65 European Conference on Advances in Flood Research, Proceedings, (Vol. 1 - Vol. 2)
A. Bronstert, Ch. Bismuth, L. Menzel (eds.) (November 2000)
- No. 66 The Rising Tide of Green Unilateralism in World Trade Law - Options for Reconciling the
Emerging North-South Conflict
F. Biermann (Dezember 2000)
- No. 67 Coupling Distributed Fortran Applications Using C++ Wrappers and the CORBA Sequence
Type
Th. Slawig (Dezember 2000)
- No. 68 A Parallel Algorithm for the Discrete Orthogonal Wavelet Transform
M. Uhlmann (Dezember 2000)

- No. 69 SWIM (Soil and Water Integrated Model), User Manual
V. Krysanova, F. Wechsung, J. Arnold, R. Srinivasan, J. Williams (Dezember 2000)
- No. 70 Stakeholder Successes in Global Environmental Management, Report of Workshop,
Potsdam, 8 December 2000
M. Welp (ed.) (April 2001)
- No. 71 GIS-gestützte Analyse globaler Muster anthropogener Waldschädigung - Eine sektorale
Anwendung des Syndromkonzepts
M. Cassel-Gintz (Juni 2001)
- No. 72 Wavelets Based on Legendre Polynomials
J. Fröhlich, M. Uhlmann (Juli 2001)
- No. 73 Der Einfluß der Landnutzung auf Verdunstung und Grundwasserneubildung - Modellierungen
und Folgerungen für das Einzugsgebiet des Glan
D. Reichert (Juli 2001)
- No. 74 Weltumweltpolitik - Global Change als Herausforderung für die deutsche Politikwissenschaft
F. Biermann, K. Dingwerth (Dezember 2001)
- No. 75 Angewandte Statistik - PIK-Weiterbildungsseminar 2000/2001
F.-W. Gerstengarbe (Hrsg.) (März 2002)
- No. 76 Zur Klimatologie der Station Jena
B. Orlowsky (September 2002)
- No. 77 Large-Scale Hydrological Modelling in the Semi-Arid North-East of Brazil
A. Güntner (September 2002)